# Ontogenetic allometry of the postcranial skeleton of the giraffe (*Giraffa camelopardalis*), with application to giraffe life history, evolution and palaeontology

By

**Sybrand Jacobus van Sittert**

Submitted in partial fulfilment of the requirements for the degree of

Doctor of Philosophy (PhD)

in the

Department of Production Animal Studies

Faculty of Veterinary Science

University of Pretoria

Supervisor: Prof Graham Mitchell

Former supervisor (deceased): Prof John D Skinner

Date submitted: October 2015

# Declaration

I, Sybrand Jacobus van Sittert, declare that the thesis, which I hereby submit for the degree Doctor of Philosophy at the University of Pretoria is my own work and has not previously been submitted by me for a degree at this or any other tertiary institution.

October 2015

# Acknowledgements

Including a list of people to whom I am grateful to in the acknowledgement section hardly does justice to the respective persons: A thesis is, in all honestly, only comprehensively read by very few people. Nevertheless, it occurred to me that even when I roughly skim through a thesis or dissertation for bits of information, I am always drawn into the acknowledgements. I suppose it is the only section where one can get a glimpse into the life of the researcher in an otherwise rather 'cold' academic work. Therefore, although not a large platform to say 'thank you', I wish to convey to everyone listed here that you are in the warmest part of my heart … and probably the most read part of my thesis.

- Prof Graham Mitchell for his patience with me, his guidance, enthusiasm and confidence. I consider myself lucky and honoured to have had you as a supervisor. Many thanks to Prof Mitchell's family for their hospitality during my visit to England.
- The late Prof John Skinner who started all of this. We still miss you.
- The departmental administrators, Ms Marie Watson and Ms Daleen Anderson, whose help always came with a smile.
- Mr Blondie Leathem and all involved at the Bubye Valley Conservancy for making the specimens and labour needed available to us. Many thanks to Messrs. Kenneth Manyangadze, Mark Brewer and Blake Wilhelmi for their professionalism, friendliness and patience. Your hospitality is still fondly remembered. Without the Bubye Valley Conservancy, this project would have been but a dream.
- Technical field support was provided by (now) Drs. Nicky Buys, Andrew Henning, Lauren Leathem, Carl-Heinz Moeller, Struan Muirhead and David Roberts.
- The Eastern Cape Department of Agriculture granted me study leave on various occasions to collect field data.
- Mr. Colin Geekie for his assistance with the Maberly Memorial Scholarship.
- I thank the following people who assisted me during my visits to various institutions: Dr Virgini Volpato and Ms. Katrin Krohman for assistance at the Senckenberg Naturmuseum, Frankfurt; Ms. Emma Bernard for assistance at the Natural History Museum, London; Mr. Tarik Afoukati from the Muséum national d'Histoire naturelle, Paris and to the staff of the Ditsong Museum of Natural History, Pretoria, South Africa.
- Ms Antoinette Lourens for helping me find some very old manuscripts. In general thank you to the Jotella F Soga Library at Onderstepoort for their professionalism and excellent resources they offer freely to students.
- Ms. Gina Viglietti for her enthusiasm and professionalism while designing the *G. sivalensis* palaeoart.

- Friends and family who kept on enquiring on how my thesis is going and asking the dreaded 'When are you going to finish?' It motivated me again and again to complete this project. In particular, to our neighbours, Johann and Alexa, who proved that a postgrad study group is possible even in the remotest parts of South Africa.
- My wife Tessa who, without complaining, shared me with this project for so long. By ignoring my pleas to be left alone with my thesis, your occasional check-ins at my desk with coffee, stories of the day and encouragement did help me stay relatively sane through all of this. Especially towards the end you were managing the household and practice almost single-handedly, for which I am truly indebted to you.

Financial support

- During this study I was in receipt of a University of Pretoria Bursary as well as the Maberly Memorial Scholarship.
- Additional funds were provided by the Don Craib Trust (John Skinner), from a personal research grant (John Skinner), and the University of Wyoming (Graham Mitchell).

# Ethics statement

The author, whose name appears on the title page of this thesis, has obtained, for the research described in this work, the applicable research ethics approval from the Animal Ethics Committee of the University of Pretoria. The project approval was granted under project number: V043-08.

The author declares that he has observed the ethical standards required in terms of the University of Pretoria's Code of ethics for researchers and the policy guidelines for responsible research.

# Summary

Ontogenetic allometry of the postcranial skeleton of the giraffe (*Giraffa camelopardalis*), with application to giraffe life history, evolution and palaeontology

By

Sybrand Jacobus van Sittert

Supervisor: Prof Graham Mitchell

Co-Supervisor: Prof John Skinner (deceased)

Department: Production Animal Studies

Degree: Doctor of Philosophy

Giraffes (*Giraffa camelopardalis*) have evolved into a unique and extreme shape. The principle determinant of its shape is the skeleton and the overarching theme of the study was to describe how this shape is achieved throughout ontogeny. Accordingly, the study had three main objectives: 1) To describe the growth of the giraffe postcranial skeleton allometrically, 2) To interpret the allometric patterns described in an evolutionary and functional sense and 3) To reconstruct the size and shape of the extinct *Giraffa sivalensis* using, if feasible, allometric equations obtained in this study. Secondary objectives were to a) establish if sexual dimorphism was evident in *G. camelopardalis* and b) determine if growth patterns in the foetus differed from those in postnatal *G. camelopardalis*.

Data were collected from giraffes culled as part of conservancy management in Zimbabwe. The sample included 59 animals from which vertebral dimensions were taken in 48 animals and long bone dimensions in 47 animals. Body masses ranged from 21 kg to 77 kg in foetuses and 147 kg to 1412 kg postnatally, representing 29 males and 30 females. In addition to body mass, external body dimensions were recorded from each animal. Each vertebra and unilateral long bone was dissected from the carcasses and cleaned, after which dimensions were measured with a vernier calliper, measuring board or measuring tape. Vertebral dimensions measured included body (centrum) length, height and width as well as vertebral spinous process length. Long bone dimensions included length, two midshaft diameters and circumference. Allometric equations ($y=bx^k$) were constructed from the data, with special interest in the scaling exponent ($k$) to illustrate regions of positively allometric, isometric or negatively allometric growth.

In the first series of analyses the growth patterns of the components of the postcranial axial skeleton were analysed. The adaptations in vertebral growth to create and maintain extraordinary shape were identified as disproportionate elongation of the cervical vertebrae after birth, increasing cross sectional diameters of the cervical vertebrae from cranial to caudal and positively allometric spinal process growth. The theory of sexual selection as a driver for neck elongation in giraffes was brought into question by showing that male and female vertebral elongation rates are similar relative to increases in body mass.

The second series of analyses described the growth pattern of the long bones of the appendicular skeleton. The allometric exponents seemed unremarkable compared to the few species described previously, and it was shown that the giraffe appendicular skeleton does not elongate in the dramatic way the neck does. Limbs at birth, after lengthening with positive allometry in utero, are already elongated and slender in shape and a further increase in the gracility of the bones is either not possible or not desirable. This result implies that it is neck elongation rather than leg elongation that is the dominant factor in the evolution of the giraffe shape. Nevertheless, the front limb bones and especially the humerus may show responsiveness to increasing high loads and/ or bending moments, which may be caused by the neck mass which increases with positive allometry, or with behaviours such as splaying the forelegs during drinking.

In the third component of the study ontogenetic allometric equations in extant giraffes were applied to the remains of an extinct giraffid, *G. sivalensis*. The procedure was unusual as it employed ontogenetic regressions instead of the more commonly used interspecific regressions. The appropriateness of each equation to estimate body mass was evaluated by calculating the prediction error incurred in both extant giraffes and okapis (*Okapia johnstoni*). It was concluded that, due to body shape, ontogenetic equations were adequate and perhaps preferable to interspecific equations to estimate proportions in *Giraffa* species. This analysis showed that *G sivalensis* was smaller than extant giraffes and weighed around 400 kg (range 228 kg–575 kg), with a neck length of about 147 cm and a height of 390 cm. There may be evidence of sexual dimorphism in this species, with males being about twice the body weight of females. However, if sexual dimorphism was not present and all the bones were correctly attributed to this species, then *G. sivalensis* had a slender neck with a relatively stocky body.

In conclusion, this study established ontogenetic regression equations for the skeleton of an animal of which the body shape seems to be at the extreme limits of mammalian possibility. The value of the current study lies especially in its sample size and quality, which included an unprecedented number of giraffe body masses, vertebral and long bone dimensions. This dataset had applications in the giraffe's evolutionary biology, palaeontology and even ecology. Future studies still need to compare the findings from giraffe growth with similar data from other taxa, especially those with long legs and necks. Specifically, it would interesting to determine if positively allometric neck growth combined with isometric leg growth is found in other mammalian species. In addition, the strength of giraffe long bones

and vertebrae needs to be investigated with more accuracy using parameters like second moment of area. Lastly, further palaeontological studies on other giraffid sizes are necessary to validate the current and future interpretations of fossil giraffid findings.

# Contents

**Declaration** ..... **ii**

**Acknowledgements** ..... **iii**

**Ethics statement** ..... **v**

**Summary** ..... **vi**

**Contents** ..... **ix**

**List of figures** ..... **xii**

**List of tables** ..... **xiii**

**List of abbreviations** ..... **xiv**

**List of publications arising from work related to this thesis** ..... **xvi**

**Chapter 1 Introduction** ..... **1**

1.1 On the biology of giraffes ..... 1

1.1.1 Phylogeny and Classification ..... 1

1.1.2 Distribution and morphotypes ..... 2

1.1.3 Giraffe general morphology ..... 3

1.1.4 The physiological and anatomical adaptations of being tall ..... 4

1.1.5 Skeletal anatomy and physiology ..... 6

1.1.6 Drives for a long neck ..... 11

1.2 On bone biology ..... 13

1.2.1 Scaling of bone ..... 14

1.3 Objectives, research questions and hypotheses ..... 23

1.4 General materials and methods ..... 25

1.4.1 Experimental/ observational design ..... 25

1.4.2 Obtaining samples ..... 25

1.4.3 Measurements taken ..... 25

1.4.4 Data analyses ..... 26

1.5 Outline of thesis ..... 29

**Chapter 2 On the scaling of the vertebral column of *Giraffa camelopardalis*** ..... **30**

2.1 Introduction ..... 31

2.2 Materials and methods ..... 34

2.2.1 Preparation and measurement ..... 34

2.2.2 Data analysis ..... 35

2.3 Results ..... 36

2.3.1 Description of study sample ..... 36
2.3.2 Sexual dimorphism ..... 36
2.3.3 Scaling of exponents of vertebral lengths with regard to body mass ..... 39
2.3.4 Scaling exponents of vertebral widths, heights and spinous processes vs. body mass ..... 40
2.3.5 Comparison of Lengths, widths and heights at different body masses ..... 42
2.4 Discussion ..... 47
2.4.1 The scaling of vertebrae ..... 47
2.4.2 The cervicothoracic delineation ..... 49
2.4.3 Sexual dimorphism in scaling ..... 50
2.5 Conclusion ..... 50
**Chapter 3 On the scaling of the appendicular skeleton of *Giraffa camelopardalis* ..... 51**
3.1 Introduction ..... 52
3.2 Materials and methods ..... 54
3.2.1 Sampling ..... 54
3.2.2 Body mass ..... 54
3.2.3 Bone preparation ..... 54
3.2.4 Bone measurements ..... 54
3.2.5 Scaling model ..... 56
3.2.6 Statistics ..... 56
3.3 Results ..... 58
3.3.1 Sample description ..... 58
3.3.2 Sexual dimorphism ..... 59
3.3.3 Growth patterns ..... 59
3.4 Discussion ..... 73
3.4.1 Pre- and postnatal growth differences ..... 73
3.4.2 Sexual dimorphism ..... 73
3.4.3 Long bone length vs. body mass ..... 73
3.4.4 Increase in diameter and circumference with regard to body mass ..... 76
3.4.5 Diameter and circumference vs. length ..... 77
3.4.6 Cross sectional area ..... 78
3.4.7 Practical application of giraffe allometric equations ..... 79
3.5 Conclusion ..... 79
**Chapter 4 On reconstructing *Giraffa sivalensis*, an extinct giraffid from the Siwalik Hills, India ..... 80**
4.1 Introduction ..... 81

4.2 Materials and methods ..... 85
4.2.1 Studied material and dimensions measured ..... 85
4.2.2 Statistical analyses ..... 92
4.2.3 Assumptions made ..... 92
4.3 Results ..... 95
4.3.1 Dimensions measured ..... 95
4.3.2 Predictions based on vertebra OR39747 ..... 95
4.3.3 Predictions based on long bone dimensions ..... 96
4.3.4 Predictions based on dental dimensions ..... 100
4.4 Discussion ..... 101
4.4.1 Vertebral identity of OR39747 ..... 101
4.4.2 Ontogenetic and interspecific scaling models ..... 102
4.4.3 Neck length and reaching height ..... 103
4.4.4 Body mass ..... 103
4.4.5 *G. sivalensis* palaeoart— notes on palaeoenvironment, body shape and skin colour ..... 109
4.5 Conclusion ..... 114
**Chapter 5 General discussion ..... 116**
5.1 Introduction and salient findings ..... 116
5.2 Research questions ..... 117
5.3 Value of study ..... 119
5.3.1 Perspective on the evolution of the giraffe ..... 119
5.3.2 Size estimates for *G. sivalensis* ..... 119
5.3.3 Determining the population structure of giraffes that succumbed during a drought ..... 120
5.4 Limitations of study ..... 121
5.4.1 Small foetal sample sizes ..... 121
5.4.2 Lack of data on other taxa ..... 121
5.4.3 Lack of certainty regarding the origin of fossil specimens of *G. sivalensis* ..... 121
5.4.4 Cross sectional areas ..... 121
5.4.5 The effect of soft tissues or cartilage loss ..... 121
5.5 Possible avenues for future research ..... 121
**References ..... 123**
**Appendices ..... 138**

# List of figures

Figure 1.1 Giraffa camelopardalis (left) and Okapia johnstoni (right), the only extant giraffids. 1
Figure 1.2 Giraffe metapodial (left) and buffalo metapodial (right) in cross section 10
Figure 2.1 The giraffe cervical vertebra 7 and thoracic vertebra 1 33
Figure 2.2 Custom-made measuring board used for the length measurement of the larger cervical vertebrae 34
Figure 2.3 The scaling of vertebral body lengths 39
Figure 2.4 The caudal vertebral body dorsoventral (A, height) and transverse (B, width) growth 41
Figure 2.5 The growth of the spinous processes. 42
Figure 2.6 The individual vertebral body lengths, widths, and heights at different body mass intervals 45
Figure 2.7 The spinous process lengths as a proportion of trunk lengths 46
Figure 2.8 The cervicothoracic junction in the giraffe compared with the okapi, redrawn from Solounias (1999) 48
Figure 3.1 Long bones of the giraffe 55
Figure 3.2 Growth of limb bone length relative to body mass in postnatal animals 60
Figure 3.3 Diameters of the long bones of the postnatal appendicular skeleton with regard to body mass 66
Figure 3.4 Diameter versus length plots in post natal animals 69
Figure 3.5 Growth in CSA with regard to body mass and bone length 72
Figure 3.6 Length and diameter vs body mass ontogenetic exponents of previously described mammalian species 75
Figure 4.1 A map indicating the probable vicinity of G. sivalensis fossil discoveries 82
Figure 4.2 Giraffa sivalensis holotype, specimen OR39747 85
Figure 4.3 Specimen OR39749 86
Figure 4.4 Specimen OR17136 87
Figure 4.5 The C3's (centre of image) of different size giraffes. 101
Figure 4.6 The C4's (centre of image) of different sized giraffes. 102
Figure 4.7 The relationship between neck length and C3 vertebral length throughout ontogeny in giraffes and okapis 105
Figure 4.8 Body mass predictions for G. sivalensis based on various fossil specimens 106
Figure 4.9 The body mass prediction errors (absolute values) associated with various dimensions in Okapia johnstoni and Giraffa camelopardalis 107
Figure 4.10 G. sivalensis outline and proportions 110
Figure 4.11 Trouessart's (1908) depiction of polygonal shapes in the giraffe's background environment. 110
Figure 4.12 G. sivalensis coat pattern 112
Figure 4.13 G. sivalensis' palaeoenvironment 114
Figure 4.14 The final palaeoart in colour 115

# List of tables

Table 2.1 The gender, weight and length of individual giraffes. ..... 37
Table 2.2 Allometric equations for the determination of vertebral body length (in mm) for foetal and postnatal giraffe. ..... 38
Table 2.3 Summary of common slope values in postnatal vertebral diameter and spinous process dimensions ..... 40
Table 2.4 The different section lengths of the vertebral column as a proportion of total length. ..... 43
Table 2.5 The different section lengths of the vertebral column as a proportion of trunk (thoracic plus lumbar) length ..... 43
Table 3.1 Summary of the various allometric patterns ..... 56
Table 3.2 Summary of the bone length versus body mass slopes ..... 59
Table 3.3 Bone lengths at different life stages predicted from allometric equations presented in this study ..... 62
Table 3.4 Mean bone diameters (average CC and ML) and circumferences at different life stages of the giraffe ..... 63
Table 3.5 Allometric equations describing growth in diameter (CC and ML) and circumference with regard to body mass. . 64
Table 4.1 Previous size estimates of G sivalensis ..... 84
Table 4.2 Dimensions for the G sivalensis holotype; a well preserved C3 cervical vertebra (specimen OR39747) ..... 88
Table 4.3 Dimensions for long bone specimens marked as belonging to G. sivalensis. All values in mm ..... 88
Table 4.4 Summary of fossil teeth assigned to G affinis by Falconer and Cautley (1843) ..... 89
Table 4.5 The studied okapi specimens and their dimensions used in determining the appropriateness of allometric equations in determining body size and shape estimates in G. sivalensis ..... 94
Table 4.6 Power functions, their origin and predicted values for linear dimensions of G. sivalensis ..... 96
Table 4.7 Functions for the prediction of body mass based on various G. sivalensis specimens ..... 97

# List of abbreviations

| | |
|---|---|
| %PE | Percentage prediction error |
| Art. proc. | Articular facet on the caudal articular process |
| Circ | Midshaft circumference |
| CC | Craniocaudal diameter |
| Cd | Caudal |
| CdDv | Caudal dorsoventral diameter |
| CdTr | Caudal transverse diameter |
| Circ | Midshaft circumference |
| Cr | Cranial |
| CrCd | Craniocaudal midshaft diameter |
| CrDV | Cranial dorsoventral diameter |
| CrTr | Cranial transverse diameter |
| CSA | Cross sectional area |
| C*x* | Cervical vertebra number *x* |
| D | Diameter |
| df | Degrees of freedom |
| DMNH | Ditsong National Museum of Natural History |
| $F_m$ | Muscle force |
| H | Humerus |
| I | Second moment of area |
| Inters | Interspecific sample |
| *k* | Allometric exponent, from the power formula $y = bx^k$ |
| $k_t$ | The number of tests used by which the *P*-level should be adjusted in the sequential Bonferroni method |
| L | Length |
| L*x* | Lumber vertebra number *x* |
| MA | Major axis |
| Mc | Metacarpus |
| $M_b$ | Body mass |
| ML | Mediolateral diameter |
| MNHN | Museum National d'Histoire Naturelle, Paris |
| N: FL | Neck length to foreleg ratio |
| Ont | Ontogenetic sample |
| OFL | Observed front limb long bone lengths |
| OHL | Observed hind limb long bone lengths |
| OLS | Ordinary least squares |
| ONL | Observed neck length |
| ONL-1 | Observed neck length minus C1 |
| OTL | Observed trunk length |
| OTVL | Observed total vertebral length |
| PNL | Predicted neck length |

| | |
|---|---|
| R | Radius |
| SD | Sample standard deviation |
| SM | Senckenberg Naturmuseum, Frankfurt |
| SMA | Standardised major axis |
| SUMW | Second upper molar width |
| SUPL | Second upper premolar length |
| SUPW | Second upper premolar width |
| T. for. | Transverse foramen |
| T. proc. | Transverse process |
| Tr | Transverse midshaft diameter |
| TLML | Third lower molar length |
| TLMW | Third lower molar width |
| TLPL | Third lower premolar length |
| TLPW | Third lower premolar width |
| TUML | Third upper molar length |
| TUMW | Third upper molar width |
| T*x* | Thoracic vertebra number *x* |
| Vert | Vertebral body |

# List of publications arising from work related to this thesis

- Van Sittert, S.J., Skinner, J.D. & Mitchell, G., 2010, 'From fetus to adult—an allometric analysis of the giraffe vertebral column', *Journal of Experimental Zoology Part B: Molecular and Developmental Evolution* 314(6), 469-479

- Van Sittert, S.J., Skinner,J.D., & Mitchel, G., 2015, 'Scaling of the appendicular skeleton of the giraffe (Giraffa camelopardalis)', *Journal of Morphology* 276(5), 503-516.

- Van Sittert, S.J. & Mitchell, G., 2015, 'On reconstructing Giraffa sivalensis, an extinct giraffid from the Siwalik hills, India' *PeerJ* 3:e1135; DOI 10.7717/peerj.1135

- Mitchell, G., Van Sittert, S.J. & Skinner, J.D., 2009, 'Sexual selection is not the origin of long necks in giraffes', *Journal of Zoology* 278 (4), 281-286

- Mitchell, G., Van Sittert, S.J. & Skinner, J.D, 2009, 'The structure and function of giraffe jugular vein valves', *South African Journal of Wildlife Research* 39(2), 175-180

- Mitchell, G., Van Sittert, S.J., & Skinner, J.D., 2010, 'The demography of giraffe deaths in a drought', *Transactions of the Royal Society of South Africa* 65(3), 165-168

- Mitchell, G; Roberts, D.G., Van Sittert, S.J. & Skinner, J.D., 2013, 'Growth patterns and masses of the heads and necks of male and female giraffes' *Journal of Zoology* 290(1), 49-57

- Mitchell, G., Roberts, D.G., Van Sittert, S.J., & Skinner, J.D., 2013, 'Orbit orientation and eye morphometrics in giraffes (*Giraffa camelopardalis*)', *African Zoology* 48(2), 333-339

- Mitchell, G., Roberts, D.G. & Van Sittert, S.J., 2015, 'The digestive morphophysiology of wild, free-living, giraffes', *Comparative Biochemistry and Physiology Part A: Molecular & Integrative Physiology* 187, 119-129

# Chapter 1
# Introduction

The introduction is broadly divided into four parts. It starts with a general discussion on the biology of giraffes, on the biology of bone and on principles of scaling. It is followed by a statement of objectives for the study, an outline of the thesis contents and finally a general introduction into materials and methods used.

## 1.1 On the biology of giraffes

### 1.1.1 Phylogeny and Classification

Giraffes belong to the class Mammalia (Linnaeus 1758), order Artiodactyla (Owen 1848) or alternatively Cetartiodactyla (Montgelard *et al.* 1997), suborder Ruminantia (Scopoli 1777), superfamily Giraffoidea (Gray 1821), family Giraffidae (Gray 1821), subfamily Giraffinae (Gray 1821), genus *Giraffa* (Brunnich 1771) species *camelopardalis* (Schreber 1784). The only other extant giraffid is the much smaller, shorter necked okapi (*Okapia johnstoni*), which is confined to the forests of Central Africa (Figure 1.1).

***Figure 1.1 Giraffa camelopardalis (left) and Okapia johnstoni (right), the only extant giraffids***

The true phylogenetic position of the giraffe has been uncertain until recently. After dissecting a giraffe Owen (1838) argued that giraffes are modified cervids, a view followed by later workers as well (for instance Simpson 1945). Giraffe horns, like that of the Cervidae, are covered in skin; although unlike the Cervidae, the horns are permanent and not shed—a

characteristic which is more akin to the Bovidae. Therefore, giraffes had been placed in both the superfamilies Cervoidea as well as the Bovoidea (Hernández Fernández & Vrba 2005), while other researchers have argued that giraffes should be classified as a sister group to both the cervids and bovids (Janis & Scott 1987, 1988). Current consensus is that giraffes belong to the superfamily Giraffoidea (Skinner & Chimimba 2005).

The evolutionary history of the Giraffidae—and other pecoran families—is still uncertain, judging by the incongruence between molecular and morphological phylogenetic analyses (Janis & Theodor 2014). Nevertheless, Mitchell and Skinner (2003) presented an extensive review of known giraffid phylogenetics which is still upheld and is briefly summarised here. The Gelocidae represent some of the most basal ruminant artiodactyls from which the Giraffidae and other Pecora arose (although technically 'Gelocidae' might not be a monophyletic group but rather a polyphyletic assemblage of similar animals during the late Oligocene to Early Miocene, Janis & Scott 1987). One of the families arising out of the gelocid type animals was the Palaeomerycidae, which in turn gave rise to the Climacoceratidae and Canthumerycidae around the middle Miocene. The Climacoceratidae was to become the ancestor of the sivatheres, some of which were the heaviest giraffoids ever to exist. The Canthumerycidae, on the other hand, gave rise to the palaeotragines during the middle to late Miocene. Palaeotraginae probably encompassed the genera *Palaeotragus*, *Giraffokeryx,* and *Samotherium.* From *Palaeotragus,* through the genus *Samotherium,* arose *Bohlinia attica* from which the *Giraffa* genera would emerge throughout the Pliocene and Pleistocene. It is currently held that the genus *Giraffa* emerged in Asia, and then radiated into Africa. All the Asian genera were extinct by the late Pleistocene.

Molecular data has shown the Giraffidae as one of the basal ruminant groups, diverging during the early Miocene together with the Antilocapridae (pronghorns of America) through the family Palaeomerycidae. The Bovidae, Moschidae and Cervidae are therefore the more derived pecorans (Janis & Theodor 2014). Giraffoids have two distinguishing characteristics: a bilobed lower canine and an elongated and flat cubonavicular facet on the metatarsal bone (Janis & Scott 1987). Amongst the Giraffoidea, the Giraffidae can be recognised by characteristics of premolar four, although these characteristics may also be found in other superfamilies. Currently, the palaeaomericine *Teruelia* is upheld as the first giraffoid, whereas within the Giraffidae, *Palaeotragus* is the earliest genus (Janis & Scott 1987). It was through *Teruelia* that the Climacoceratidae and Canthumerycidae arose.

### 1.1.2 Distribution and morphotypes

Giraffes only occur in Africa, although their distribution is widespread within the continent. Their range is not continuous however and certain subpopulations have become geographically isolated. Accordingly, they exhibit regional polymorphism, leading some authors to propose that the different forms might in actual fact be subspecies or even species. Most noticeably, the coat pattern differs among morphotypes—as a gross

generalisation one can describe the pattern change from a blotchier brown-red pattern on pale skin in the Southern giraffes to a more reticulated pattern of well-defined blotches in the more northern giraffes. Lydekker extensively reviewed the giraffe patterns and cranial shapes from available specimens and paintings in 1904 and recognised 11 polymorphs, which he interpreted to represent two species (*G. camelopardalis* and *G. reticulata*), of which *G. camelopardalis* contained 10 subspecies. Lydekker would add two subspecies in 1911: One to *G. camelopardalis* and one to *G. reticulata* (Seymour 2012). However, about half a century later, the multi-species idea in giraffes was beginning to dwindle. In 1962 Dagg argued for only one species of giraffe (*G. camelopardalis*), judging by the ability of different morphotypes to breed. In the same report she also casted doubt on the usage of coat patterns alone as an indicator of subspeciation, as coat patterns were then known to vary to different degrees even within populations. Indeed, the coat pattern is not always diagnostic to the race of the giraffe and even an expert has reported a 25% error rate in identifying morphotypes on skin blotches alone (Dagg 2014, citing personal communication with Russell Seymour). Recently though, there has been a renewed drive for establishment of different giraffe species rather than races or subspecies. Using mitochondrial DNA sequence analyses of different morphotypes (Brown *et al.* 2007; Hassanin *et al.* 2007; Seymour 2001), some researchers suggested that certain morphotypes should be elevated to the level of species. Notwithstanding the molecular findings, suggestions of different species of giraffes ultimately depend 'wholly on the species concept used' (Seymour 2012). In this thesis, different morphotypes will be considered different races of giraffes. The study will describe the morphology of the Southern giraffes, and will assume it a reasonable approximation for all races of giraffes.

### 1.1.3 Giraffe general morphology

Giraffes are the world's tallest extant animals and represent the largest browsers as well as the largest true ruminants in existence today. They reach heights of 4.9 m to 5.2 m and 4.3 m to 4.6 m in males and females respectively (Skinner & Chimimba 2005), although some researchers have found giraffes to grow even as tall as 5.5 m to 5.8 m (Dagg 2014; Shortridge 1934). The body mass of this megaherbivore is on average 1192 kg (range 973 kg–1395 kg) in adult males and 828 kg in adult females (range 703 kg–950 kg, Mitchell & Skinner 2003). On first observation, it appears as though the tall shape is brought about through an elongated and slender neck and limbs, while the thorax and abdomen do not immediately strike as remarkable for the size of the animal.

Dagg (2014) lists the advantages of being large, in the case of giraffes, as: Increased browse availability (matched only by the elephant), ability to cover greater larger distances in search of food or water, increased vigilance, increased feed utilisation and increased lifespan. Although not strictly related to size, the slender shape of the giraffe is apparently also an exceptionally efficient aid to thermoregulation during hot weather.

### 1.1.4 The physiological and anatomical adaptations[1] of being tall

The known physiological adaptations in giraffes will be briefly reviewed in order to highlight that the evolutionary drive for being tall is, in this sense, costly.

Mitchell and Skinner (1993) summarised various adaptations in giraffes that enable them to 'survive' the tall shape. They identified three physiologic-anatomical system adaptations needed in the long necked animal: Cardiovascular system, respiratory system and thermoregulatory system. In 2003 they also pointed out that significant adaptations to musculoskeletal and to a lesser extent gastrointestinal physiology would play a role in giraffe survival.

#### 1.1.4.1 Cardiovascular physiology

Arguably, the most famous physiological adaptation of the giraffe is cardiovascular. A fully grown giraffe has to maintain a high blood pressure at the level of the heart in order to maintain 'normal' blood pressure at brain level. Subsequently, the systolic blood pressure of the giraffe is about 185.7 mmHg (Mitchell & Skinner 1993), the highest known normal blood pressure in a mammal. High blood pressure could create the following complications in an unadapted animal:

- Excessively high intracranial pressure when lowering the head—blood pressure at the level of the head changes from around 145/55 mmHg when the head is held high to 330/240 mmHg when lowered to the ground.
- Sudden loss of intracranial pressure and fainting when suddenly raising the head after drinking water, and
- Organ failure and oedema formation (Hargens *et al.* 1987; Van Citters *et al.* 1968, 1969).

Mitchell and Skinner (2009) highlighted the cardiovascular adaptations which circumvent these complications. To prevent fainting during head raising, blood is diverted from the carotid arteries into the cerebral perfusion through an anastomosis between the carotid and vertebral arteries. Additionally, intracranial pressure is maintained through drainage of cerebral venous blood into a vertebral venous plexus.

High intracranial pressure is averted through jugular veins that prevent excessive backflow of blood to the head (Mitchell *et al.* 2009b) and oedema is prevented through specialised venous return mechanisms and properties of the skin. In addition, a multibranched vascular

[1] *Throughout this text, unless mentioned otherwise or when used in a non-biological sense, the term 'adaptive'(or its variants) will refer to adaptation in an interspecific evolutionary sense or, in other words, adaptation by means of natural selection. This is opposed to acclimatisation or responsiveness, which is a more immediate and dynamic adjustment, within the life history of an individual. Where adaptation is used in context of ontogenetic growth, it will mean that the growth strategy itself is an evolutionary adaptation.*

network or *Rete mirabile*[2] in the cranium may play an important role in the reduction of cranial pressure in giraffes. The network, referred to as the carotid rete, arises from the external carotid artery and has been fundamental in artiodactyl success (Mitchell & Lust 2008). Goetz & Keen (1957) illustrated that the giraffe's rete does not have elastic walls and, by implication, that mitigation in cranial blood pressure is achieved through a large cross sectional area which develops as a result of the rete's branching. Recently however, O'Brien & Bourke (2015) modelled the giraffe rete from the domestic goat, and argued for mechanisms other than the carotid rete in reduction of intracranial pressure. These mechanisms may include shunts away from the cranium or a non-collapsible venous plexus.

Giraffe kidneys cope with being exposed to chronic hypertension through a valve like structure between the renal vein and the caval vein as well as a strong renal capsule (Damkjær *et al.* 2015). These renal structures in effect reduce glomerular filtration rate, renal plasma flow, renal artery resistance index and net filtration pressure.

Initially, it was thought that the giraffe's hypertension was due to an unusually large heart. However, in a seminal study Mitchell and Skinner (2009) showed that giraffe hearts are as large as expected for their body size, and that blood pressure is increased through narrowing of arterial lumens.

#### 1.1.4.2 Respiratory adaptations

With the longest trachea amongst extant animals, tracheal dead space presents a challenge to efficient ventilation. Giraffes overcome this problem partially by having smaller tracheal diameters expected for their body size. Ultimately however, the giraffe's dead space problem is solved through an increased tidal volume which, in turn, creates a similar dead space to tidal volume ratio as is found in other mammals (Mitchell & Skinner 2011).

#### 1.1.4.3 Neurological adaptations

Although the corticospinal tract of the giraffe is longer than the typical ungulate, Badlangana *et al.* (2007) did not find the organisation of the giraffe corticospinal tract to be unique. Similarly, the recurrent laryngeal nerve follows the same path in giraffes as that of all other mammals and therefore constitutes for a long and counterintuitive route to innervate the muscles of the larynx. Nevertheless, the recurrent laryngeal nerve functions normally in giraffes despite its length. In terms of neurology therefore, the giraffe do not seem to require adaptations to an increase in length.

[2] *As with other wildlife species, standardised anatomical nomenclature for the giraffe has not been published. However, terms from the Nomina Anatomica Veterinaria or NAV (International Committee on Veterinary Gross Anatomical Nomenclature 2012) were assumed to be acceptable for use in the giraffe as well. Where a structure with an anglicised name was mentioned for the first time, its NAV equivalent was included in brackets in italics.*

#### 1.1.4.4 Water balance

Water conservation may be particularly important in giraffes, where drinking water is an awkward procedure and may pose a serious predatory risk. It was therefore perhaps not surprising that giraffe kidneys were indeed found to be specially adapted towards this cause (Maluf 2002). Giraffe kidneys have the ability to hyperconcentrate urine, which is facilitated through extensions of the renal pelvis into the corticomedullary area, which in turn facilitates exchange of urea into the interstitium.

#### 1.1.4.5 Skin

It has been proposed that the skin blotch pattern might have thermoregulatory (Mitchell & Skinner 2004; Sathar *et al.* 2010) or camouflage function (Dagg 2014; Trouessart 1908), reflecting the different hide morphotypes. The skin is of various thicknesses throughout the body and is thought by some to contribute to the maintenance of high blood pressure (Hargens *et al.* 1987; Pedley 1987; Sathar *et al.* 2010) and to prevent damage from intraspecies combat, predation (Dagg 2014) or ticks and biting insects (own observation). The thickest skin areas are around the trunk, approaching 20 mm.

### 1.1.5 Skeletal anatomy and physiology

#### 1.1.5.1 Skull

During Owen's (1838) description of the giraffe skull he singled out the extensive development of the frontal sinuses, which extends as far as occipital crest. This finding was later confirmed through Computed Tomography scanning and it was subsequently postulated that giraffes have a frontal sinus that is relatively more developed than any other artiodactyl (Badlangana *et al.* 2011).

The horns (or ossicones) of the giraffe are situated caudolaterally on the parietal and frontal bones of the skull. These horns are remarkable as they are bone covered by skin as in the cervids—except in the males where the most dorsal horn portion is exposed—while they are also more like bovids in that the horns are not deciduous. Giraffe horns start as flexible cartilaginous outgrows covered by skin in the foetus and neonate, which then later ossifies and fuses with the skull. Owen (1838) noted that the ossicones articulated via a synchondrosis to the skull, making the horns in his opinion epiphyses rather than apophyses (although technically apophyses can also be attached to the underlying bone via physeal line and there does not seem to be consensus regarding the definitions of a apophyses and epiphyses). In males the dorsal ossicone can protrude from the underlying skin, which is remarkable considering that the dorsal part of the horn then represents living, uncovered bone, which is a rare occurrence in mammals (Solounias 2007). Owen (1838, 1850) noted marked sexual differences in the ossicones. A ‘third’ median horn develops rostrally later in life to a greater and lesser extent in different morphotypes, particularly in males. In addition to the parietal and median horns, certain older giraffes may also display two ‘occipital horns’ (Thomas 1901; Trouessart 1908), which is in actual fact two bony exostoses. Initially,

there was controversy regarding the formation of the median horn (Murie 1872; Solounias & Tang 1990), but the issue was settled through the work of Spinage (1993) who showed that the median horn forms in a similar fashion to that of the two main ossicones. The ossicones of males are popularly asserted (Dagg 2014; Simmons & Scheepers 1996) to be exposed due to frequent fighting and sparring. However, this interpretation fails to explain why most—if not all—males have a lack of hair on the dorsal ossicones, even ones not regularly engaged in sparring. It also fails to take into account that there are possible differences in the thickness of ossicones between males and females.

#### 1.1.5.2 Vertebral column

Considering that the neck is arguably the most outstanding feature of the giraffe, the musculoskeletal anatomy of the neck has been studied relatively little. One of the earlier, more detailed publications was that of Owen (1838) who described neck circumferences, leg length, neck muscles and some aspects of the gross superficial structure of the *Ligamentum nuchae*. Other significant contributions to neck muscle anatomy in the giraffe include the work of Murie (1872) and more recently Angermeyer (1966), Endo *et al.* (1997) and Dzemski (2005).

The normal vertebral formula of the giraffe is seven cervicals, fourteen thoracic, five lumbar, four sacral and twenty caudal vertebrae (Owen 1838). The most striking feature of the cervical vertebrae is their length, but they are also notably wide and articulate with deep convex and concave cranial and caudal extremities into one another. In these respects giraffe cervicals do resemble the cervical vertebrae of the Camelidae (Owen 1838). In addition, Owen highlighted the following giraffe vertebral characteristics:

- The length of the cervical vertebrae decreased caudally while the width gradually increased. The width of the thoracic vertebrae thereafter decreased up to ninth vertebra, after which width increased again up to the sacrum.
- The cervicals exhibited a thickened portion caudally which was noted to represent the ‘superior transverse process’.
- The *Foramen transversarium* enters at the seventh cervical vertebra and not from the sixth as is the case in many other mammals.
- In general a more ‘pecoran type’ cervical, as opposed to the more ‘camelid type’. This conclusion was reached because the vertebral artery passes through the *For. transversarium* and does not proceed cranially through the *For. vertebrale* as is the case in the Camelidae.
- The spinous processes of the cervical vertebrae were described as ‘thin triangular laminae’ while the seventh cervical’s spinous process were more elongated. The spinous processes after the cervicals continued to elongate up to the fourth thoracic vertebra, after which it declined caudally. Even at this early stage of research on

giraffe anatomy (and biomechanics), Owen proposed that the length of the thoracic spinous processes are related to the length of the neck.

- The greater development of the tail was found to be more in agreement with the Bovidae than with the Cervidae.

It was Lankester (1908) however who first and foremost truly recognised the remarkable adaptations in the cervical vertebral morphology of the giraffe. He compared the caudal cervical and cranial thoracic vertebral series of the giraffe with various mammalian taxa, notably that of the okapi, domestic ox (*Bos taurus*), camel (species not stated) and rhino (*Dicerorhinus sumatrensis*). Giraffes differ from okapis in that giraffes have:

- Proportionately shorter cervical spinous processes (*Processus spinosi*).
- Proportionately smaller ventral transverse processes (*Processus transversi*).
- A lack of a *Lamina ventralis* on the *Proc. transversus* in C6.
- The presence of a ventral *Proc. transversus* on C7.
- A general 'cervical' appearance of C7 whereas in okapis C7 is said to be 'dorsalised' or thoracic in character[3]. C7 is further said to be more 'cervical' in character in giraffes by the orientation of the articular facets of the caudal articular processes (*Proc. articularis caudalis*). However, the 'cervical' nature of C7's articular processes is not unique to giraffes and occurs in at least one species of rhino as well. The okapi's caudal cervical and cranial thoracic vertebral morphology tends to be in agreement with most other artiodactyls.

Lankester concluded his study by recognising that the giraffe cervical vertebrae represented specialised or derived features and were not primitive in nature.

It would be short of a century before another in-depth study on giraffe vertebral morphology would appear again. Using the bone morphology pointed out by Lankester (1908) and by noting the muscle origins and insertions and the location of the brachial plexus, Solounias (1999) proposed that a 'vertebra has been added in the neck of the giraffe between cervical 2 and 6, and that some type of structural blending has occurred in the region of the first rib.' Mitchell & Skinner (2003) and Badlangana *et al.* (2009) refuted this idea. They argued that there are seven cervical vertebrae in the giraffe, based on the presence of transverse foramina, elongated vertebral bodies, short spinous and transverse processes in all C2 to C7 vertebrae and the fact that the eighth postcranial vertebra supports a rib. Measuring the length of vertebral bodies in the vertebral column of 11 ungulates and the length of fossil giraffid vertebrae published previously, Badlangana *et al.* (2009) also demonstrated that elongation of the neck took place within the constraints of seven cervical vertebrae and provided an evolutionary time frame within which the elongation occurred.

[3] *Note that what Lankester designates as an inferior transverse process is considered as a ventral transverse process in this thesis.*

Moreover, they showed that the proportional elongation of each vertebra was not atypical and that the cervical vertebrae in the giraffe scaled similarly to any other ungulate that would have a long neck. In other words, they concluded that the giraffe did not only elongate its neck within the constraints of seven cervical vertebrae, but also with the constraint of similar relative elongation in each individual vertebra.

Biomechanical aspects of the giraffe's neck and its vertebrae have not been studied in much detail. Slijper (1946) published some measurements on giraffe vertebrae and calculated estimated second moment of area from these. Dzemski (2005) did measurements on the range of motion and position of the neck as a whole, while Sakamoto *et al.* (2011) presented brief biomechanical considerations on the estimated hourglass shape of giraffe cervical vertebrae.

#### 1.1.5.3 Limbs

The front limb long bones of giraffes consists of a humerus (*Humerus*), radius / ulna (*Radius / Ulna*) and a fused metacarpal III and IV (*Os metacarpale III et IV*). Hind limb long bones consist of a Femur (*Femur*), Tibia / Fibula (*Tibia* / *Fibula*) and a fused metatarsal III and IV (*Os metatarsale III et IV*). The distal part of the ulna becomes confluent with the radius, appearing again on the distal radius, but this feature does not seem to be consistent (Owen 1838). Owen also noted that the femur was relatively larger in proportion to the distal extremity than any other mammal which he has observed. Vestigial metatarsal II bones may sometimes be noted in giraffes, while in the okapi (which in general has less derived traits than giraffes), vestigial metacarpals II and V and metatarsals II and V may be present (Fraser 1951). Like other artiodactyls, the limb bones of giraffe are specialised towards terrestrial locomotion, i.e. there is reduction of digits and elongation of metacarpals. However, giraffe limb bones (and perhaps all giraffids) also seem specialised towards further limb elongation, especially so in the more distal long bones (Solounias 2007). The humerus of the giraffe has a double groove for the biceps muscle rather than the single groove that is usually the case in ruminants (Owen 1838). Dagg (2014) notes that the front hooves are slightly wider than the hind hooves, which may be a reflection of the greater weight supported by the front limbs.

Various authors have described the proportions of giraffe limbs. D'Arcy Thompson (1917), using his famous system of coordinates, quantified the slender appearance of the giraffe limbs. He showed that the giraffe metacarpus is proportional in thickness to a third that of the ox, despite its much larger body size. McMahon (1975); Alexander *et al.* (1979); Biewener (1983); Anderson *et al.* (1985); Christiansen (1999 & 2002) and Campione & Evans (2012) quantified giraffe limb bone proportions in more depth. Researchers and artists realised early on that the front legs were longer than the hind legs, although it was not sure whether this observation was apparent or real (Colbert 1938). For example, Owen (1838) casted doubt over the true relative length of the legs, stating that the legs appear long because of the depth of the chest, the length of the thoracic spinous processes and the

nearly vertical position of the *Scapula* on the thorax. In addition to its length, the slender limb bones of giraffes intrigued researchers as it went against the general observation that heavier animals have relatively thicker and shorter limbs.

There has been no study on the ontogeny of giraffe limb bones. In fact, studies on the scaling of limb bones in larger non-primate mammals and especially ungulates during postnatal ontogeny are exceptionally scarce—to date only the elephant (Miller *et al.* 2008), goat (Main 2007; Main & Biewener 2004), domestic pig (Liu *et al.* 1999), polar bear (Brear *et al.* 1990) and muskoxen (Heinrich *et al.* 1999) have been described (see below).

#### 1.1.5.4 Skeletal adaptations

Because of their relative and perhaps unexpected slenderness, Van Schalkwyk *et al.* (2004) set out to determine if giraffe limb bones were perhaps denser than would be expected from a similar sized mammal. They measured bone density through water displacement using vertebrae, ribs, pelvic bones, carpal bones, metacarpals and femora collected from giraffe and buffalo carcasses in the Kruger National Park, South Africa. In addition, the cross sectional shape of the femora and metacarpal midshafts were recorded. They found, surprisingly, that there were no significant differences in the density of bones between buffaloes and giraffes. However, they also noted that the giraffe cortical thicknesses were significantly greater than the buffalo equivalents. Therefore, midshaft limb bone strength in the giraffe seems to be related partially to greater relative cortical thicknesses as well as relatively straighter limb bones, as noted by Biewener (1983). In addition to the finding of thicker cortical thicknesses, Van Schalkwyk (2004) proposed that the cross sectional shape of metapodial bones (the thicker 'caudal columns') were another adaptation to metapodial strength in the giraffe. However, this proposal fails to explain why the thickened caudal cortical thicknesses in metapodial bones are not unique to the giraffe, and can be found in many members of the Giraffidae, even those much lighter than okapi (Solounias 2007).

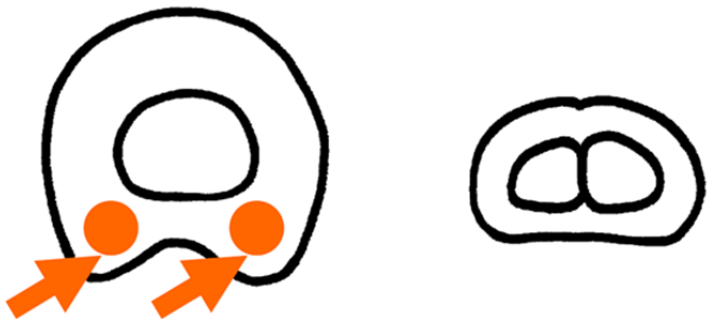

***Figure 1.2 Giraffe metapodial (left) and buffalo metapodial (right) in cross section, showing greater thickness especially in the caudal part of the bones (orange arrows and dots). Image from Van Schalkwyk (2004).***

Unfortunately, because body mass had not been available previously, it has not been possible to relate limb bone diameter, cortical thickness and cross sectional areas to body mass. It also follows that questions regarding sexual dimorphism and immature animals still remain unanswered.

Bredin *et al.* (2008), recognising that by the sheer size of the skeleton, calcium and phosphorus requirements of the giraffe must be high, investigated whether osteophagia might provide necessary supplementation of these minerals to the diet. Osteophagia is often observed in giraffes, and has also previously been recognised as a sign of phosphorus deficiency in cattle. It was found that, with regard to rumen fluid and saliva at least, bones will not be digested to sizes small enough to pass to the abomasum nor will bones in the rumenoreticulum provide additional calcium and phosphorus. What still needs to be investigated, however, is to what extent the chewing of bones and rumination can reduce bone fragments to sizes that are able to pass to the abomasum where digestion is more likely.

### 1.1.6 Drives for a long neck

Given the physiological costs mentioned, it begs the question as to why such a long neck will evolve in the first place. Arguably, the most well known theory is the feeding advantage that long necks confer by allowing access to browsing strata that no other ungulate has access to: The only other extant contender in the topmost browsing strata of the giraffe is the elephant, a non-obligate browser. However, this explanation has not been without criticism (Simmons & Scheepers 1996) and even Darwin (1888), who proposed the idea, seemed hesitant about it. The neck of the giraffe was mentioned only by the sixth edition of the Origin of Species, and while the former editions of the Origin of Species did discuss the giraffe, it was only concerned with the animal's tail.

A second theory that has recently become very popular is that sexual selection was the drive for the long neck. Already in the early studies on giraffe it was noted that the horns of the giraffe is a sexual adaptation (Owen 1838, 1850). It was Simmons & Scheepers (1996) however who first popularised the 'necks for sex' theory. They noted that females often preferred males with the larger necks and that males are known to establish dominance through necking contests. They therefore argued that it was through necking contests that males with longer and larger necks would be selected at each generation to gradually contribute to the elongation of the longer neck.

A third possible drive for a long neck might be increased vigilance against predators (Brownlee 1963). Complementing the long neck, giraffes are furthermore thought to possess excellent sight. Mitchell *et al.* (2013) investigated gross anatomical aspects of the giraffe head that might have an influence on the quality of sight, and concluded that giraffes do indeed have the conformational adaptations to support good vision.

Long slender necks also serve to increase the surface of the body with regard to body mass. Subsequently, it is reasonable to speculate their dolichomorphic shape as an evolutionary adaptation for heat loss with a large body. Compared to other large bodied mammals, giraffes do not possess traditional heat radiating organs like the ear of elephants nor are they known to make use of swimming to cool down (Henderson & Naish 2010). Giraffe skin may however have a thermoregulatory function, judging by the association of blood vessels

with the patches and the presence of sweat glands (Mitchell & Skinner 2004), in which case a long dolichomorphic body shape would make sense.

Finally, a more fluid scenario could also be considered where two or more of the above hypotheses might have influenced giraffe shape—simultaneously or in succession. For instance, a factor that might have cause elongation of shape a few million years ago might not be present any more and further elongation (or maintenance) of the long neck is currently caused by a different selective pressure. More intricately, evolution of height might have been advantageous in two or more aspects simultaneously. For instance, greater browse availability in conjunction with the doligomorphic shape and vigilance advantages might have been much a much stronger evolutionary driver than any one these factors alone.

## 1.2 On bone biology

Bone has two principal functions: to be stiff and to be strong (Currey 2002). It must be strong enough not to yield, to fail by fatigue or fracture. Furthermore, bones should be strong enough both in bending, impact loading or torsion (Currey & Alexander 1985). Sub functions of bones include acting as a mechanical framework to enable locomotion through the action of muscles and tendons, to protect vital organs, to transmit energy (e.g. inner ear), to act as armour (e.g. horns) and for housing haemapoietic cell lines. In order to be stiff bone tissue is therefore highly mineralised (≈66%), primarily through calcium and phosphate based crystals. The mineral constitution of bone highlights another sub function of bone, which is to act as a storage depot for minerals, primarily calcium and phosphorus, and participating in the body's mineral homeostasis. In addition to its mineralised nature, the remaining proportion of bone is composed of organic material and water. The organic proportion of bone is primarily in the form of a collagenous matrix which imposes some degree of flexibility to the tissue and prevents bones from becoming overly brittle.

Bones have been classified according to various criteria, including density, anatomical location, method of formation and shape. In terms of density, cortical (compact/ lamellar) and cancellous (trabecular/ woven/ spongy) bone can be discerned. At a microscopic level, cortical bone consists of a system of cylindrical elements or osteons with relatively few 'boneless' areas in between. Cancellous bone on the other hand consists of a network of bony spicules or strands between which other connective tissue such as adipose tissue or blood forming elements can be found. Although both cortical and cancellous bone participate in load bearing, cortical bone is the most significant contributor in this regard—this is the case even in bones where cancellous bone constitutes the majority of bony tissue (Currey 2003; Leppänen 2009). In terms anatomical location or position, bones can be grouped into those comprising the skull (cranium) and postcranium. Alternatively, the skeleton can also be subdivided into axial (skull, vertebral column and ribs), appendicular (limb bone) and visceral (e.g. *Os penis* in dogs) elements. Two types of bone can be recognised when classified according to their method of formation. In the foetus, most of the bones develop via endochondral ossification, a process by which a cartilage framework is gradually replaced by bone from centres of ossification. However, certain bones, like the flatbones of the skull, develop without a cartilage framework therefore forms via intramembranous ossification. When categorising bone according to shape, four general bone morphologies are recognised: Long bones, flat bones, short bones and irregular bones. Long bones are typified, as their name suggests, by the long bones of the appendicular skeleton which are primarily involved in locomotion. These bones can be further subdivided into stylopod (humerus and femur), zeugopod (radius, ulna, tibia and fibula) and metapod (metacarpus and metatarsus) elements. Long bones develop from three or more centres of ossification. A typical long bone consists of a shaft (diaphysis) and two expanded ends (metaphyses and epiphyses), and may also contain other protrusions for muscle attachments (apophyses). The shaft has an outer cortex, which consists of cortical bone, and

an inner boneless area (marrow cavity) consisting of haemapoietic tissue in a young animal and fat in older animals. The outer cortex of the shaft is surrounded by a membranous sheet called the periosteum, and is therefore referred to as the periosteal surface. The inner cortex is covered by an endosteum and is referred to as an endosteal surface. Metaphyses and epiphyses are typified by a predominantly cancellous bone constitution and in the case of epiphyses are covered by hyaline cartilage where they participate in joint formations. Flat bones generally occur in areas where organ protection is necessary such as the cranium or ribs. These bones consist of two thin sheets of cortical bone between which is a layer of cancellous bone. Short bones, as is typically encountered in the carpus and tarsus, develops from a single centre of ossification and consist of cancellous bone covered by a thin layer of cortical bone. They primarily function as compressive load bearers (Currey 2002). Irregular bones such as vertebrae have a varied shape but in constitution are similar to short and flat bones. Other irregular bones include sesamoid bones (present in tendons) and visceral bones.

Bone is not static. A skeleton constantly maintains the balance between being as strong as possible while being as light as possible—it does this by continuously modelling according to the stresses and strains experienced. Bone shape is therefore the sum total of its genetic makeup, hormonal regulation as well as its loading history. This can be seen in the cross sectional shape of the diaphysis of a newborn which is circular, whereas an older individual's cross sectional shape assumes a more elliptical character (Leppänen 2009). In addition to shape change, maturing bone also becomes increasingly mineralised and stiff. Bone modelling is also not limited to ontogeny or certain life stages. Modelling takes place even in mature bone, albeit at a different rate, and differences in size, loading regimens and body postures also lead to differences in bone morphology (Slijper 1946). The end result of bone tissue's ability to model is that it maintains economical yet acceptable safety factors against fracture.

### 1.2.1 Scaling of bone

#### 1.2.1.1 Early history of the allometric method and scaling

The mathematical description of shape change is a relatively new discipline in biology. D'Arcy Thompson's (1917) famous work, 'On growth and form', established that the adaption of form between closely related species could be described through the consistent deformation of a Cartesian sketch of the image. At about the same time as Thompson's work however, another approach to the description of shape emerged. Allometry, which literally means 'by different measure', referred to the realisation that two organs (or body parts or systems or even processes) could grow at different rates, but that the ratio of these rates remained constant. This phenomenon was first described by workers such as Snell in 1891 (cited by Gould 1971), Dubois in 1897, Lapicque in 1898, Pézard in 1918 and Champy in 1924 (citations from Gayon 2000). At the heart of these researchers' quest was a way to describe common biological 'laws' in scaling and physiology applicable to most animals or at

least a subset of taxa. The most famous contribution to the field of allometry was however still to come from Julian Huxley and his law of heterogonic growth in 1924, which culminated in his book *Problems of relative growth* (1932). Huxley and Teisser introduced the term allometry in a work simultaneously published in English and French in 1936 (Gayon 2000). The allometric method makes use of the algebraic formula of $y=bx^k$ , the so-called power function or allometric equation, to describe the change of one variable *y* (which can be a body part, system or whole organism) with regard to another body part, system or whole organism, *x.* Although not without problems or criticism, power or allometric functions have since been used extensively throughout biology because of its ease of use, its ease of interpretation and a reasonable fit to many data sets (Gould 1966).

#### 1.2.1.2 Principles of size increase

Size increase is perhaps best explained from the perspective of a cube of which the sides are of length L (McGowan 1999). The surface area of one side of the cube is therefore $L^2$, while the total surface area is $6.L^2$. The volume of the cube is $L^3$. Suppose the cube increases in size in a geometrically similar fashion by increasing the lengths of the sides to 2L. In this case the surface of one side of the cube would be $(2L)^2 = 4L^2$, the total surface area would be $6.(2L)^2 = 24L^2$, and the volume would be $(2L)^3 = 8L^3$. If the sides of the cube were made 3L, then one side's surface area would be $(3L)^2 = 9L^2$, total surface area would be $6.(9L)^2 = 54L^2$, and volume would be $(3L)^3 = 27L^3$. Therefore, when the length of a structure doubles, surface area would increase by a factor of 24/6 = 4 and volume by 8/1 = 8. When length increases by a factor of 3/2=1.5 again, surface area increases by a factor of 54/24 = 2.25 and volume by a factor of 27/8 = 3.38. From another point of view, for a structure to increase in a geometrically similar fashion the proportionate increase in length should be the same as the third power of the proportionate increase in volume.

In certain cases however, a structure might not increase in size in a geometrically similar fashion. For example, although the length of the structure might increase by a factor of 2, volume might increase less or more than the expected proportionate increase of $2^{(1/3)} = 1.26$. In such a case the increase in length is referred to as displaying negative (i.e. $L \propto volume^{<0.333}$) or positive (i.e. $L \propto volume^{>0.333}$) allometry[4].

Because surface area decreases relative to volume as the size of an organism increases, there is less surface area to absorb, secrete, diffuse and dissipate substances or energy relative to body size. Generally, animals would 'cope' with decreasing area to volume ratios through three mechanisms: 1.) by increasing the area through folding and branching, 2.) by changing shape (e.g. flattening) or 3.) by incorporating parts of inactive organic material within the body (Gould 1966). Strength of structures also change with size increases that remain geometrically similar. As the strength of a support structure is related to its cross

[4] *In this text body weight, body size and body volume implies similar concepts because of the close association between body volume and body weight in living organisms.*

sectional area, an increase in overall size usually necessitates relatively thicker limbs in order to maintain relative strength in breaking (bones) or contraction (muscles). This principle has been found in interspecific, ontogenetic and static allometry in animals and even within the plant kingdom (Gould 1966). Nevertheless, Gould also highlights that this differential size increase cannot continue indefinitely before proportions would become absurd. Animals therefore employ additional measures to compensate for size increase, like differing behaviours, stances and limb angularity (Biewener 1983, 1989). If this constellation of mechanisms is not feasible or too costly to an organism, it will ultimately remain limited in its size increase. In the case of ontogenetic size increases, additional measures may also include changes in the stiffness of bones (Torzilli *et al.* 1982).

#### 1.2.1.3 Types of allometry

Size can change between and within organisms. Subsequently, allometric descriptions can be applied to four scenarios of 'growth': 1) Ontogenetic allometry, 2) Phylogenetic allometry (or evolutionary allometry, Gould 1966), 3) Intraspecific allometry and 4) Interspecific allometry (Gayon 2000).

- *Ontogenetic allometry*

  Ontogenetic allometry describes growth throughout the life history of a single species. In studying this type of allometry, the researcher can collect data in two ways: By examining an individual animal throughout its growth (longitudinal), or by examining different individuals of different growth stages (cross sectional or transversal). Cross sectional studies are perhaps less desirable than longitudinal studies as it introduce inter-individual variation into a dataset that was supposed to highlight only individual growth. Nevertheless, longitudinal data are more difficult to obtain, especially in wild animals or animals with longer life histories. Ontogenetic allometry is therefore often estimated from cross sectional data, which will be the approach followed in this thesis as well.

- *Phylogenetic (evolutionary) allometry*

  Phylogenetic allometry describes differences in body size amongst related animals (usually of adult stage) across an evolutionary lineage.

- *Intraspecific allometry*

  Intraspecific allometry describes size changes across members of the same population but of differing size. A single growth stage is decided upon—usually adults. In Gould's (1966) definition, intraspecific allometry can be subdivided further into size changes across a single species of differing size but of the same growth stage (individual allomorphosis) or across races or subspecies of the same species (race allomorphosis). The distinction from ontogenetic allometry is arguably arbitrary with limited biological meaning. On the other hand, intraspecific allometry may be considered as valid independent category as it does not have a temporal dimension

to it in the way ontogenetic allometry has—it considers only interindividual variation without temporal growth. In this thesis, 'ontogenetic' will mainly be used in the temporal growth sense, whereas 'interspecific' will not have a growth aspect associated with it—for example, when talking about 'interspecific communication'.

- *Interspecific allometry*

  Through interspecific allometry, size changes are explained across related species of the same taxonomic group (i.e. across a genus, a family, class etc.). The distinction between interspecific and phylogenetic/ evolutionary allometry presents little, if any, biological value. Nevertheless, it may be argued that evolutionary allometry has a temporal aspect connected to it whilst interspecific allometry is static in nature (Gayon 2000). In this thesis, the distinction between interspecific and evolutionary allometry will not be entertained and interspecific allometry will refer to both types of allometry.

#### 1.2.1.4 The power function

In the allometric equation ($y = bx^k$), the *y* and *x* variables represent two body parts, regions or systems that change in size at different rates. The ratio of these rates, in the case of simple allometry, remains constant and is indicated with the allometric (or scaling) exponent, *k*. The allometric exponent is usually of most interest as it provides information on the relative growth rate of the two variables, or 'a criterion for the intensity of differential increase' (Gould 1966). If the exponent is greater than the expected exponent for geometric similarity (isometry), it is said to be positively allometric or hyperallometric. Oppositely, if the exponent is less than isometry, it is referred to negatively allometric or hypoallometric.

The interpretation of the coefficient *b* has been much less certain than the allometric exponent. Some authors have argued for deeper investigation into its significance, whilst others have declared it devoid of meaning. In its simplest form, *b* can be understood purely as the value of *y* at $x = 1$, which also carries zero biological meaning. In a more complex analyses, White & Gould (1965) showed that when the value of *k* is equal between two slopes, the value of *b* can be explained in the context of a 'scale ratio' ($s_2/s_1$)—which is equal to $(b_2/b_1)^{(1/(1-k)}$. This ratio indicates the ratio of *x*-values at which both slopes will have the same *y/x* value (Gould 1966), but it is important to keep in mind that this meaning of *b* is only valid when *k* is the same between slopes.

Allometric parameters (*b* and *k*) are not necessarily the same across different types of allometry. In other words, an exponent in interspecific allometry is not readily applicable to ontogenetic allometry. Gould (1966) summarised this principle perfectly: 'Since ontogeny does not recapitulate phylogeny and since smaller adults of a population are not merely arrested ontogenetic stages of larger adults, this lack of correspondence is not unexpected.' Interestingly however, in the same paper Gould (perhaps hesitantly) suggests that differential increases in leg thickness could have similar parameters in ontogeny and

phylogeny as legs perform the same function throughout an animal's life history. Gould was right in his caution about this statement, as others would subsequently show this assertion to be invalid (Carrier 1983; Kilbourne & Makovicky 2012; Lammers & German 2002; Main & Biewener 2004).

#### 1.2.1.5 Interspecific scaling

Bone has been found to have similar material qualities among vertebrates. Therefore, as adult animals change in size, both between and within species, relative bone dimensions are expected to differ in order to safely continue carrying weight. Indeed, it has been found that safety factors in bones are size independent (Biewener 1982; Garcia & da Silva 2006). Nevertheless, although differential scaling of limb bone proportions plays a role in the maintenance of safety factors, this may not always be adequate and additional compensatory mechanisms like alterations in limb bone posture, bone curvature and locomotory behaviour are employed. In this section, as in this thesis, the differential scaling of limb bone dimensions will be the main focus.

Garcia & da Silva (2006) presented one of the best recent reviews on the subject of interspecific scaling in long bones, and their approach will be followed closely in the following paragraphs. Galileo in his 'Dialogues concerning two new sciences' was probably one of the first researchers to propose that limb bones would need to scale differentially in order to support increasing body weight (Galilei 1638). Much more recently Thompson (1917) also devoted a section of his book to differential limb bone scaling across different sizes. It was McMahon's (1973, 1975) papers however that intensified research into interspecific limb bone scaling. McMahon proposed that limb bones scale in a way so as to prevent Euler buckling, and as such would scale as Length (L) $\propto$ Body mass (Mb)$^{0.25}$ and Diameter (D) $\propto$ Mb$^{0.38}$. Although experimental support for this proposal was initially found by him and other researchers (Alexander 1977), it was ultimately shown to be invalid across all mammals as more and more data became available (Alexander *et al.* 1979; Biewener 1983). In addition to general buckling, local buckling also did not seem to be a concern in mammalian bones as their midradius to wall thickness ratios were found to be around 2, which is far below the critical level of 14 (Currey & Alexander 1985).

After the elastic similarity theorem lost support for use in taxa outside of the Bovidae, it was becoming apparent that a single interspecific allometric exponent was probably not able to explain scaling in both small and large mammals (Bertram & Biewener 1990; Bou *et al.* 1987; Christiansen 1999; Economos 1983). In 1989 Selker & Carter proposed a new approach by linking bone allometry to muscle force allometry. Kokshenev *et al.* (2003) also argued that instead of static loads, muscle force is the principle determinant of bone allometry. Muscle force ($F_m$) can be described through body mass by the relationship of $F_m = M_b^{\alpha}$. The exponent $\alpha$ is related to the diameter and length of the bone through the formula $\alpha = 3D\text{-}L$ where $D$ and $L$ is the diameter and length of bones respectively. They found that $3D\text{-}L$ in previous data was approximately equal to 0.8, which is the exponent that muscle force

scales with body mass. This finding was supported by Garcia & da Silva (2004) across large and small body masses and seems to indicate that mammalian bones incorporate mainly bending and compression in their scaling.

#### 1.2.1.6 On the ontogeny of the appendicular skeleton

To achieve its principal functions (to be stiff and not to break), bones should be adapted to the animals' lifestyle, locomotor habits and body weight. However, during ontogeny many of these factors can change: Bones become more mineralised, therefore stiffer, and have to respond to new loading regimes. Loading regimens change because of changing behaviours such as predator avoidance strategies, hunting strategies and in distances travelled. Most significantly however, body mass also increases during ontogeny and could, within a single lifetime, demand changes in locomotor habits, bone shape or posture.

Studies on the changes and responses of long bones throughout ontogeny in quadrupeds are very limited. Some of the first studies on the properties of immature bone were done on canines (Torzilli *et al.* 1981, 1982). It was found that rapidly growing bones had fewer osteons, lower density and lower mineral content, and were therefore relatively weaker. It was also found that long bone structural and material properties increased over two phases—a rapid phase over the first 6 months and then a slower phase for another 6 months. The only bone property not to show this biphasic increase was tissue strain to failure, which remained similar throughout growth. Shortly after these findings Carrier (1983) published a seminal study on the ontogenetic allometry of the musculoskeletal system of black-tailed jack rabbits (*Lepus californicus*). The bone and muscle morphometrics in a broad range of animals (n=58) were interpreted to show that new-born hares have relatively short limbs, weak muscles and weak bone tissues. Growth in length in hind limb bones was shown to be positively allometric. Younger hares therefore have a larger lever advantage over the tibiotarsal joint and a larger second moment of area in the metatarsal bones. This allows younger hares to be efficient in escape from predation despite their small size. Interestingly, this is one of the few studies that also interprets ontogenetic allometry of limb bones in the context of interspecific allometry and phylogenetics. Interspecific mechanical similarity is maintained by increasing the relative mechanical advantage of muscles (which become relatively weaker with increasing size). Mechanical similarity during ontogeny, on the other hand, is maintained through relative increase in muscle strength but with a relative decrease in mechanical advantage and bone diameter (Currey 2002). Therefore, the slopes and trajectories of ontogenetic and interspecific allometry of limb bones are often dissimilar. A question that naturally followed this observation was: In what way do ontogenetic growth trajectories change throughout phylogeny? Carrier, assuming that growth trajectories of small and large animals are essentially similar, proposed that allometric rates may not be constant throughout growth—which would explain differences across phylogeny. However, at the time relatively few animals' limb bone allometry had been studied, and the question was not addressed fully until Kilbourne & Makovicky's (2012) paper, which extensively reviewed ontogenetic scaling across mammals (see below).

In order to compare the ontogenetic changes in morphology of limb bones in relation to locomotor function, Carrier & Leon (1990) described skeletal growth in gulls (*Larus californicus*). Gulls were chosen for the study as they are already using their hind limbs from a day after hatching, while their wings are only functional at fully-grown body mass, around 42 to 48 days post hatching. It was shown that bone stiffness increases throughout growth, and that relatively thicker hind limb bones in juveniles are probably a compensation for weaker skeletal tissue. In gulls there was also a notable difference between the strength of wing and hind limb long bones throughout growth, reflecting the role those bones play in locomotion throughout the gull's life history. Because of the relatively weaker strength of immature bones, Carrier & Leon predicted that negative allometry of long bones is likely present in the ontogeny of all rapidly growing animals. However, more recently Main *et al.* (2010) challenged a widely held view that changes in long bone morphology during ontogeny are to a great deal due to changes in mineral density in bone. By studying the tibial stiffness in growing mice they demonstrated that bone mineral density is a relatively low influencer of bone stiffness, compared to changes in bone morphology such as longitudinal curvature and cross sectional properties.

Welcome additions to the database of long bone skeletal ontogenetic allometry came from two artiodactyls: Muskoxen (*Ovibos moschatus*) (Heinrich *et al.* 1999) and pigs (*Sus scrofa*) (Liu *et al.* 1999). Heinrich *et al.* measured the femora of 33 muskoxen from three weeks to 4.5 years of age and from 9 kg to 215 kg. They found that mineralisation was complete by 18 months of age and that bone length and section modulus scale negatively allometric with body mass which was, interestingly, a scenario different from that seen in *Lepus californicus*. They too proposed different growth trajectories of bones during different periods of ontogeny. Liu *et al.* (1999) determined the ontogenetic increase in length and diameter in 30 pigs slaughtered from birth to 84 days, at which time they weighed around 31 kg. In pigs, bones lengthened relatively slower than body mass and relatively slower in front limbs than in hind limbs. Diameters increased relatively faster than lengths, although exponents differed between bones: the humerus widened with negative allometry, radius isometrically, femur positively allometric and tibia isometrically. Brear *et al.* (1990) investigated the mechanical properties of the femur in polar bears (*Ursus maritimus*) and compared it with that in humans and in axis deer. They confirmed the change in mechanical properties of this long bone in all three species, but emphasised that the magnitude and timing of these changes are significantly different. Again the stresses in all bones studied were found to be relatively constant throughout growth. Elephants represent the upper extreme of extant terrestrial body masses. Miller *et al.* (2008) were therefore interested in how the elephant (*Elephas maximus* and *Loxodonta africana*) foot responds to these high loads throughout growth. Interestingly, this study also investigated whether principles proposed for interspecific skeletal allometry (e.g. elastic and static stress similarity) are also applicable to ontogenetic allometry. This approach was also the study's weakness however, as ontogenetic and interspecific allometries were pooled and not teased apart properly in the discussion. Nevertheless, valuable information on the ontogeny of a large animal was

provided. With regard to body mass increases, elephant metapodials lengthened isometrically (except for metacarpal 5 and metatarsal 1), while metapodial diameter growth was negatively allometric, except again for the most medial and/or lateral bones. Lammers & German 2002 revisited small mammals, this time making measurements through serial radiographs and weighing. The aim of this study was to identify skeletal differences in growth between half-bounding mammals (*Chinchilla lanigera* and *Oryctolagus caniculus*) and those not employing this mode of locomotion (*Rattus norvegicus* and *Monodelphis domestica*). All the species considered had hind limb lengths that grew faster than front limbs and proximal bone elements which grew faster than the more distal elements. They concluded that because of similarities observed in growth patterns, the small mammals under study had the same constraints on relative growth. These animals may have been subjected to similar selective pressures during growth, although selective pressures differs between adults and juveniles. In his thesis on the limb kinematics of squirrel monkeys, Young (2008) added the possibility that behavioural and postural changes, as described in interspecific scaling studies, may also be employed as a response to a growing body even during ontogeny.

In order to correlate the now known changes in limb bone proportions during growth with limb loading, stresses and strains, Main & Biewener (2004) set out to measure bone strain and morphology throughout different speeds and gaits and throughout ontogeny in the domestic goat (*Capra hircus*) radius. They noted an increase in bone strain through ontogeny, brought about mainly through negative allometry for the cross sectional area ($M_b^{0.53}$), mediolateral ($I_{ML}^{1.03}$) and craniocaudal ($I_{cc}^{0.84}$) second moments of area. Nevertheless, Main & Biewener argued that strains were small enough in juvenile goats not to adversely affect safety factors, and that the more robust design of the radius might be beneficial when considering that limb loading is more variable in these animals than in adults. Main and Biewener reaffirmed their findings in (2006) after comparing goat data with that of the emu (*Dromaius novaehollandie*). Differences in especially cross sectional area scaling between goats and emus were reasoned to be due to differences in predator avoidance strategies in the two taxa. The same reasons were also reflected in Carrier's (1996) paper in which predator avoidance strategies were said to shape the bones of juveniles through ontogeny, perhaps even to the point of influencing adult phenotype. In 2007 Main revisited the goat radius, this time to correlate changes in strains and morphology with histomorphology. He found that thicker cortical regions were related to higher strain levels, but strangely that strain was not necessarily related to bone histomorphology.

Kilbourne and Makovicky identified the hole in the literature on ontogenetic allometry of limb bones by pointing out that, from the relatively few studies that have been conducted, most have been on the smaller mammals. From previous studies it has been postulated that length generally increases relatively faster than circumference (positive allometry). However, when Kilbourne and Makovicky extended the sample base to 22 taxa which

encompassed three orders in magnitude of adult body mass, they found that negative allometry does indeed occur, but largely within the Cetartiodactyla. Furthermore, it was isometry—not increasing gracility of long bones—that was the predominant pattern through ontogeny in mammals. Although Kilbourne and Makovicky's study was unprecedented, it could unfortunately not present measured body masses with the data.

#### 1.2.1.7 On the ontogeny of the vertebrae

Descriptions on the ontogeny of vertebrae in mammals are exceedingly scarce. Ghazi & Gholami (1994) presented an interesting study on growth of the vertebral column in relation to the spinal cord, but unfortunately not in relation to body mass. They showed that the vertebral column grows relatively faster than the spinal cord, especially in the lumbar areas, resulting in the cranial displacement of the *Conus medullaris* throughout growth. Nishida *et al.* (2014) recently examined the changes in vertebral canal (*Foramen vertebrale*) size in juveniles and aged rats, but not with regard to body mass, nor with a continuous age range nor with regard to vertebral body changes. They showed that from an early age, the vertebral column develops to an adequate size to accommodate the future spinal cord.

## 1.3 Objectives, research questions and hypotheses

The overarching theme of this study is to describe the growth patterns of the giraffe's post cranial skeleton. Three main objectives were addressed. Firstly, to describe the growth of the postcranial skeleton allometrically; secondly, to interpret the allometric patterns described in an evolutionary and functional sense and thirdly to reconstruct the size and shape of *Giraffa sivalensis* using, if feasible, allometric equations obtained in this study.

These objectives were approached through the following research questions and, where applicable, hypotheses:

1. What are the patterns of ontogenetic allometry in the vertebral column of the giraffe? Hypotheses tested:
    a. The growth rates of the different sections of the vertebral skeleton are independent of sex, therefore:
    $H_0$: $k_{(\text{vertebral linear dimension vs body mass males})} = k_{(\text{vertebral linear dimension vs body mass females})}$
    b. The growth rates (linear dimensions) of the different vertebral regions (cervical, thoracic and lumbar) are isometric/ geometrically similar, therefore:
    $H_0$: $k_{(\text{vertebral region linear dimension vs body mass})} = 0.333$
    c. The lengthening rates of vertebrae are similar pre-and postnatally, therefore:
    $H_0$: $k_{(\text{vertebral region lengthening foetus})} = k_{(\text{vertebral region lengthening postnatal})}$
2. What are the patterns of ontogenetic allometry in the appendicular skeleton of the giraffe? Hypotheses tested:
    a. The elongation rates of giraffe long bones are independent of sex, therefore:
    $H_0$: $k_{(\text{long bone length vs body mass males})} = k_{(\text{long bone length vs body mass females})}$
    b. The long bones elongate and widen in a geometrically similar or isometric fashion with regard to body mass, therefore:
        i. $H_0$: $k_{(\text{long bone length vs body mass})} = 0.333$
        ii. $H_0$: $k_{(\text{long bone circumference vs body mass})} = 0.333$. For purposes of this hypothesis the circumference will be regarded as inclusive of the effects of both craniocaudal and mediolateral diameter increases.
    c. The long bone thicknesses remain geometrically similar with regard to length, therefore: $H_0$: $k_{(\text{long bone circumference vs length})} = 1.00$
    d. The growth rates of long bone linear dimensions remain similar pre- and postnatally, therefore:
    $H_0$: $k_{(\text{long bone dimension vs body mass foetuses})} = k_{(\text{long bone dimension vs body mass postnatally})}$
3. How does the vertebral patterns of growth compare with those of the appendicular skeleton?

4. What are the implications of the ontogenetic allometric patterns observed on the understanding of giraffe evolution?
5. Are growth patterns observed that defy expected artiodactyl form and function? In other words, are growth patterns observed which contribute to the unique shape of the giraffe rather than typical ungulate shape and responses to stress and strain?
6. Is it feasible to reconstruct body size and shape of *G. sivalensis* from fossil remains using giraffe ontogenetic allometry? If, so, what did this animal look like?

## 1.4 General materials and methods

### 1.4.1 Experimental/ observational design

In this study, the growth of the giraffe vertebral and appendicular skeleton will be described and quantified from foetus to adult. The growth rate of specific vertebrae will be compared with growth rates of vertebrae of similar and other sectional identities (e.g. C3 vs C4 or C3 vs T2), in order to identify unique regions of vertebral growth which might point towards adaptation of shape. Similarly and with the same purpose, vertebral growth rates will be compared to that of the appendicular skeleton. Finally, the data obtained will be applied towards the skeletal reconstruction of the extinct *G. sivalensis*. This will be done by measuring dimensions on available fossil specimens, and estimating body proportions using *G. camelopardalis* ontogenetic allometry. The validity of this method will be tested by comparing prediction errors incurred when *G. camelopardalis* ontogenetic allometric and interspecific regression equations are used to predict the dimensions of the two only extant graffiti species—modern giraffes and okapis (*O. johnstoni*).

### 1.4.2 Obtaining samples

As part of their routine management, the Bubye Valley Conservancy, Matabeleland, Zimbabwe (21°42'S, 29°54'E) has to cull a certain number of giraffes every year. The management of Bubye Valley Conservancy has kindly agreed to make these carcasses and the labour needed available for this project. Culling was done by a professional hunter employed by Bubye Valley Conservancy. Animal specimens were selected from the dry season and the growing season.

### 1.4.3 Measurements taken

After being shot, the external dimensions and body mass were recorded in the field.

The following dimensions were recorded with a flexible measuring tape:

- Total body length from tip of nose to tip of tail along the dorsomedian body outline, as described in (Hall-Martin 1975). Submeasurements included:
    - Tip of nose to occipital crest.
    - Occipital crest to withers.
    - Withers to caudal sacrum.
    - Caudal sacrum to last caudal vertebra.
- Neck length comprised two measurements:
    - Occipital crest to withers.
    - Angle of jaw to the *Acromion*.

- Shoulder height (sole of hoof along the line of the leg to the highest point of the spine of the third thoracic vertebra / withers) and rump height (sole of hoof along the line of the leg to the highest point of the rump).
- Chest girth at the level of the third thoracic vertebra.

After the external dimensions, body mass were measured piecemeal using a Salter suspended spring balance with a capacity of 200 kg. Subsequent to body mass measurement, the relevant bones were freed through sharp dissection and boiling to facilitate measurements of relevant dimensions. A thorough description of bones measured, dimensions measured and the instruments used will be presented in the relevant chapters.

### 1.4.4 Data analyses

Data were recorded on raw data sheets, after which it was entered on a Microsoft® Access database. Statistical inferences about the allometric slope were performed with the SMATR software program (Standardised Major Axis Tests and Routines, Falster *et al.* 2006) and Microsoft® Excel. P-values of less than 0.05 were considered significant unless, where stated, corrections to the P-values were applied in order to compensate for multiple comparisons.

#### 1.4.4.1 Establishing allometric parameters from data

Simple allometry relates a variable $y$ from the variable $x$ through the formula $y = bx^k$. When such data are plotted on an $x$-$y$ (scatter) chart it can be approximated with a curvilinear or 'power function' line (except in the case of isometry, where it will be a straight line). When the same allometric data are plotted on a log-log scale, the data will approximate a straight line, summarised by the algebraic formula of $y = kx + c$. In this equation, $k$ indicates the slope of a line-of-best-fit through the data, and c indicates the point where the straight line crosses the $y$ axis at $x = 0$ ($y$-intercept).

There are various approaches to determine a linear line-of-best-fit through scattered data. Arguably the most popular methods are ordinary least squares (OLS), standardised major axis (SMA) and major axis (MA) regression. Although OLS has been the method of choice for early researchers, later researchers would increasingly implement SMA and MA, the so called model type II regression methods, for certain tests of allometry. The principle difference between OLS, SMA and MA lies in the direction in which the residual (the distance from the observed data point to the line of best fit) is calculated. In OLS the magnitude of residuals are calculated parallel to the y-axis, in MA the direction of residuals are perpendicular to the line of best fit and in SMA the residuals are parallel to a line which is a reflection of the line of best fit about the y-axis. Model type 1 regression (OLS) is sometimes criticised as it tends to underestimate the regression slope, especially if the correlation between $y$ and $x$ is poor (Eberhard 2009). However, when correlations approach 1.00 the difference in slope between OLS and SMA becomes increasingly negligible and either method may be appropriate (Currey 2002: 2002; Warton *et al.* 2006).

Warton *et al.* (2006) summarised the scenarios for which each regression method is appropriate as follows:

- OLS:
    - When one wishes to use to parameters so obtained to predict y from x
    - When one wishes to determine if there is an association between y and x
- MA or SMA:
    - When one wishes to estimate a line that best describes the bivariate scatter of y and x, or the bivariate scatter of y + measurement error and x + measurement error.
    - When one wishes to test whether the slope of such a line equates a certain value or is similar to the slope of another line.

In this study, only the OLS and SMA equations will be implemented. For calculating the slope from the line of best fit, the following formulae were used (Warton *et al.* 2006):

- OLS: $k = \frac{\sum xy}{\sum x^2} = \frac{\sum(X_i - \bar{X})(Y_i - \bar{Y})}{\sum(X_i - \bar{X})^2}$

- RMA: $k = \text{Sign}\,(\sum xy) \times \frac{\sum y}{\sum x}$

Two of the assumptions of regression analysis are homogeneity and normality of variances in the population. In this thesis however, homogeneity and normality of variances were not explicitly tested, as it was not considered critical. Regression statistics tend to be robust against such deviations, provided the deviations are not too grotesque (Zar 2010). In addition, log transformation (as our data are—see below) can also improve homoscedasticity of data.

#### 1.4.4.2 Logarithmic transformation of data

Already in 1907, Lapicque recognised that a power equation could be drawn as straight line when drawn onto logarithmic coordinates (Gayon 2000). This makes sense when one observes that a power equation ($y = bx^k$) becomes linear when log transformed ($\log y = k.\log x + \log b$). Parameters of the allometric equation ($k$ and $b$) can subsequently be established with relative ease through OLS, SMA or some other appropriate technique. Another advantage of log transforming power functions is that statistical inferences regarding linear slopes are less complex than those involving non-linear slopes. The convenience of this method has therefore led to its widespread use.

Recently however, there have been debates over the validity of log transformation in allometry. In a series of papers Packard (2009), Packard & Birchard (2008) and Packard & Boardman (2008) argued that log transformation was inaccurate because:

1.) It often failed to comply with the assumptions necessary for the analysis to be valid.

2.) Back transformation of an allometric equation from log transformed data often resulted in an underestimate of the variable obtained.

3.) Logarithmic transformation conceals outliers

4.) Logarithmic transformation results in multiplicative error and

5.) After minimising the sum of squares, small values for the dependant variable have a greater effect on the parameters of the allometric equation (*k* and *b* above), which can lead to inaccuracies when a large body size ranges is analysed.

Kerkhoff & Enquist (2009) directly responded to and disagreed with Packard (2009), arguing that his criticism of log transformation fails to take into account that biological processes like growth are mostly multiplicative, not additive. They advocated that a major benefit of the log-transformed allometric method, as also highlighted by Glazier (2013), is that it provided a standard approach to analyses which enabled comparison across many studies, and has expanded our concept of growth significantly as a result of it. Furthermore, the method of log-transforming data is relatively simpler to employ, simpler to comprehend (although not always adequately, Zar 1968), and can be used without specialised software or understanding of such software. Logarithmic transformation is also employed to ensure homoscedasticity of data (for example Christiansen 2007). Other authors also joined in the debate for the continuing use of the log-transforming method (Mascaro *et al*, 2011, Xiao *et al*, 2011, White *et al*, 2012) while Packard and others maintained that other methods should be used on a case by case basis (references from Glazier 2013). In this study, especially to enable comparison of growth data amongst similar studies in other forms of allometry and species, the classical log-transformation of data method was chosen.

## 1.5 Outline of thesis

Chapter 2 encompasses the first series of analyses, and addresses research questions 1, 4 and 5. An allometric description of the giraffe vertebral column in length, width and height is provided, across sexes and across pre- and postnatal life stages. Comparisons were also made amongst individual vertebrae and vertebral regions. The aim of this study was identify unique patterns of growth amongst vertebral regions and to determine whether sexual dimorphism, and therefore sexual selection, is present in giraffe vertebrae.

The second series of analyses are covered in Chapter 3, in which research questions 2, 3, 4, and 5 are addressed. This chapter presents the growth of the giraffe appendicular skeleton, with comparisons amongst individual bones, life stages, sexes and with the allometric exponents of the vertebrae. Basic biomechanical consequences of ontogenetic growth patterns are suggested. Once again the overall aim of these analyses was to identify unique patterns of growth in total leg length and regional leg length and to determine whether sexual dimorphism is present in giraffe long bone growth.

Chapter 4 addresses research question 6. It explores the feasibility of using the data obtained during this study to reconstruct an extinct giraffid, *Giraffa sivalensis*. Linear dimensions from a fossil cervical vertebra as well as fossilised *Humeri*, a radius and *Metacarpi* are presented. From these dimensions body size and proportions are estimated using interspecific as well as, unusually, ontogenetic giraffe allometry. The estimations and methods best suited for *G. sivalensis* body reconstructions were evaluated through prediction errors incurred in both of the extant giraffids.

Chapter 5 presents a general discussion of the studies in chapters 2 to 4. Limitations of the study are highlighted, as well as further research questions to be investigated.

# Chapter 2
# On the scaling of the vertebral column of *Giraffa camelopardalis*

*This chapter is adapted from the publication by SJ van Sittert, JD Skinner and G Mitchell entitled: 'From fetus to adult, an allometric analysis of the giraffe vertebral column', published in the Journal of Experimental Zoology part B: Molecular and Developmental Evolution 2010; 314B: 469-479.*

**Abstract**

As mammalian cervical vertebral count is usually limited to seven, the vertebral column of the giraffe (*Giraffa camelopardalis*) provides an interesting study on scaling and adaptation to shape in light of these constraints. In this study the growth rates of the lengths, widths and heights of the vertebrae from foetus through neonatal life to maturity are described. It was found that the disproportionate elongation of the cervical vertebrae is not a foetal process but occurs after birth, and that each cervical (C2-C7) vertebrae elongates at the same rate. C7 is able to specialise toward elongation as its function has been shifted to T1. Support is given for the view that T1 is a transitional vertebra whose scaling exponent and length is between that of the cervical and thoracic series. The importance of the thoracic spinous processes in supporting the head and neck is emphasised.

## 2.1 Introduction

The extraordinary size and shape of the giraffe (*Giraffa camelopardalis*) invites study as to the specialisation of its cardiovascular, respiratory, thermoregulatory, nervous and musculoskeletal systems (Badlangana *et al.* 2007; McMahon 1975; Mitchell & Skinner 2003, 2009; Thompson 1917; Van Schalkwyk *et al.* 2004). Additionally, because of the huge functional demands such a long neck places on these systems, the giraffe is often used when describing evolutionary processes, although there is still no consensus on the long neck's adaptive advantages (Brownlee 1963; Darwin 1888; Mitchell *et al.* 2009a; Pincher 1949; Simmons & Scheepers 1996). Considering the long neck's functional and evolutionary interest, there are still very few studies on the giraffe vertebral column.

The first published description of the skeleton of giraffes was by Vosmaer in 1787, followed by contributions from Pander and D'Alton in 1823 and Owen in 1838 (Citations from Mitchell 2009). It was Lankester (1908) however who was the first to mention cervical homeosis of vertebral characters in the giraffe (especially the articular facets of the cranial and caudal articular processes) of the first thoracic vertebra (T1). He made this observation after comparing the morphology of caudal cervical and cranial thoracic vertebrae of the giraffe with that of the okapi (*Okapia johnstoni*), the giraffe's only extant relative. T1 was still regarded as a 'dorsal' or thoracic vertebra however. Solounias (1999) reinvestigated Lankester' s observation by comparing bone morphology, muscle origins and insertions and the sizes of the roots of the brachial plexus with the okapi and concluded that the eighth post cranial vertebra was in actual fact a cervical vertebra, and that an extra vertebra had been added between C2 and C6. However, some of the criteria used by Solounias to define vertebral identity of the caudal most cervical vertebrae and first thoracic vertebra do vary amongst mammals. The criteria include: The presence of transverse foramina in cervical vertebrae (Badlangana *et al.* 2009; Turner 1847), on the length, position and shape of the spinous and transverse processes (Badlangana *et al.* 2009; Solounias 1999) and on the position and orientation of the articular facets on the articular processes (Lankester 1908; Solounias 1999) (Figure 2.1). However, the major criterion for delineating the first mammalian thoracic vertebra is taken as the first vertebra articulating with a rib that attaches directly with the sternum (Flower 1885). A second criterion is the origins of the roots of the brachial plexus (Burke *et al.* 1995; Giffin & Gillett 1996). Because the eighth post cranial vertebra of the giraffe articulates with a rib and is attached to the sternum, Solounias' view has been contested by Badlangana *et al.* (2009) and Mitchell & Skinner (2003). Furthermore, there seems to be developmental constraints that fix the number of cervical vertebrae at seven in mammals (with exception of the manatee (*Trichechus*) and sloths (*Bradypus and Choloepus*)) (Galis 1999; Narita & Kuratani 2005). The giraffe vertebral column thus presents an excellent case study for scaling and adaption in shape in the light of these constraints.

Conclusions about skeletal growth patterns and scaling require that measurable changes in the skeleton be compared to changes in another measure of growth. Typically the measure

of growth has been body mass, although vertebral column length has also been used (Badlangana *et al.* 2009). The study of these relationships is known as allometry (Huxley 1932). Badlangana *et al.* (2009) compared the giraffe allometrically to other ungulates and concluded that the long neck is a result of the elongation of the entire cervical series, independent of the rest of the vertebral column, thereby supporting Lankester's (1908) view. They also proposed a punctuated evolutionary scenario by which the long neck in modern giraffes could have developed over a brief period in geological time through the caudal shifting of specific *Hox* genes in the presomatic mesoderm.

Despite the importance of body mass on scaling and form (Calder 1984), there is still no study on the scaling of giraffe vertebrae based on body mass. Therefore, this study reports an allometric description of giraffe vertebral growth from foetus to adult with body mass as the covariate. The aim of this study was to define, describe and characterise the growth patterns of the giraffe axial skeleton and evaluate it against recent suggestions with regard to its developmental biology and constraints. Additionally, it was determined whether findings of previous analyses of the vertebral column of giraffes are gender specific and are valid over a large range of body masses.

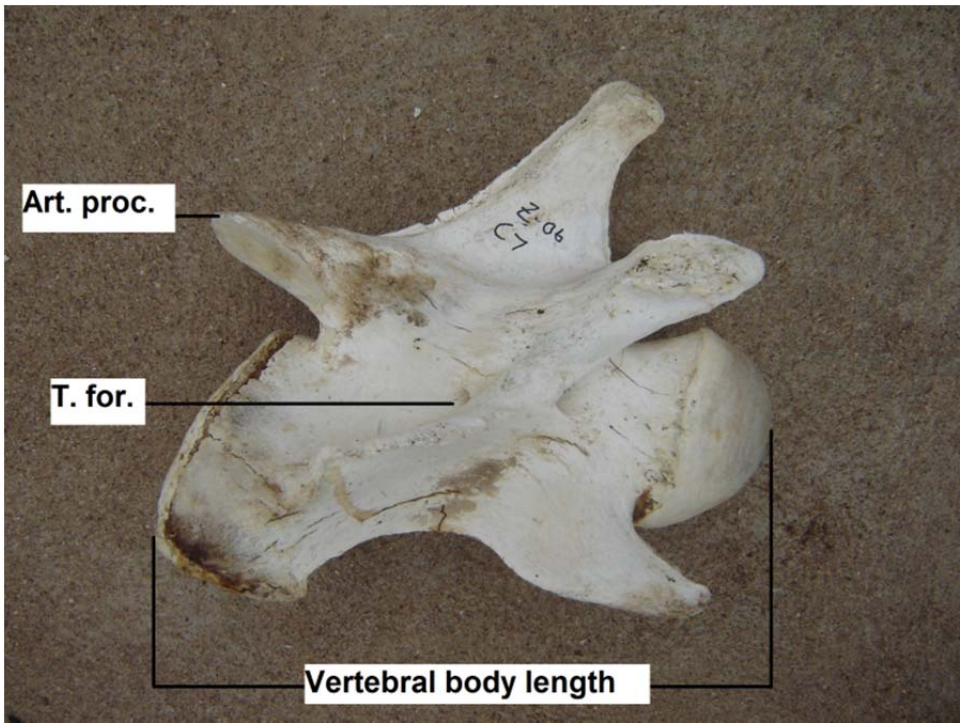


A

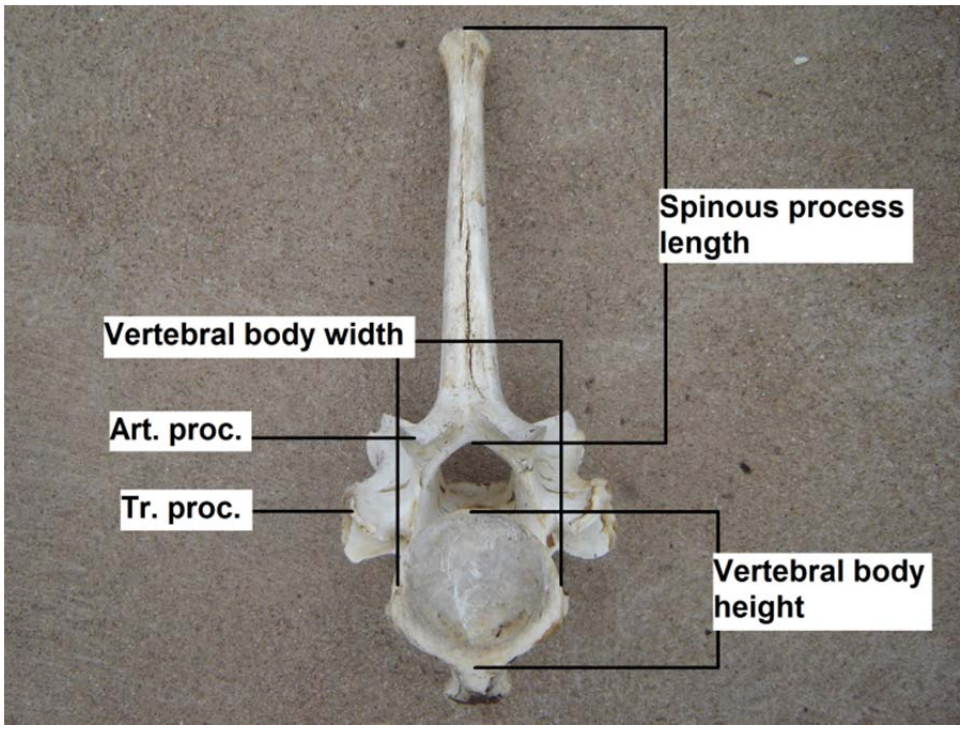


B

***Figure 2.1 The giraffe cervical vertebra 7 and thoracic vertebra 1. Part A depicts C7 in lateral view with the demarcations for vertebral body length measurement, as well as the articular facet on the caudal articular process and the transverse foramen. Part B depicts T1 in caudal view with the demarcations for vertebral body width and height as well as spinous process length. The articular facet on the caudal articular process and the transverse process is also indicated. Art. proc., Articular facet on the caudal articular process; T. for., Transverse foramen; T. proc., Transverse process.***

## 2.2 Materials and methods

Skeletons were obtained from 48 giraffes that were culled for purposes of population management in a conservancy in south eastern Zimbabwe (21°42S, 29°54E). Animals were shot by a professional hunter, and this process stretched over a period of 2 years (April 2007, November 2007, April 2008, November 2008 and April 2009).

### 2.2.1 Preparation and measurement

Body mass was determined by piecemeal weighing using a Salter suspended spring balance with a capacity of 200 kg. Four percent of the piecemeal carcass weight was added to the measured mass to account for sources of mass loss such as blood loss, evaporation and small pieces of tissue that may have been lost during the slaughtering process (Hall-Martin 1975). Mass of foetuses was measured *in toto*. Vertebrae were cleaned by dissection, and/ or boiling to facilitate measurements. Measurements were done with a vernier calliper (Mitutoyo- 18cm). In addition, to facilitate more accurate measurement of the large cervical vertebral bodies, a custom-made measuring board was used (Figure 2.2).

***Figure 2.2 Custom-made measuring board used for the length measurement of the larger cervical vertebrae***

On each vertebra the vertebral body (*corpus vertebrae*) length, width, and height as well as the spinous process (*Processus spinosus*) length were measured. The vertebral body length was measured parallel along the longitudinal axis of the vertebral body, from the most cranial curvature of the cranial extremity (*Extremitas cranialis* [*caput vertebrae*]) to the most caudal part of the caudal extremity (*Extremitas caudalis* [*fossa vertebrae*], Figure 2.1). The vertebral body length of the first cervical vertebra (C1 or atlas) was measured medially along the ventral arch (*Archus ventralis*). For the second cervical vertebra (C2 or axis) the odontoid process (*Dens*) was not included in the vertebral body length. Vertebral body width and height were the longest lengths laterally (width) and dorsoventrally (height) of

the caudal extremity of the vertebral body. Spinous process length was measured at the mid dorsal line as the length from the roof of the vertebral foramen (*Foramen vertebrale*) to the highest point of the spinous process, perpendicular to the long axis of the vertebral body (Figure 2.1B).

### 2.2.2 Data analysis

Data were plotted on an x-y scatterplot and power functions were deemed adequate approximations of the data on visual inspection. Data were log transformed to base $e$ and SMA regression analyses performed. Allometric analysis were performed according to the recommendations of Warton *et al.* (2006) using the SMATR executable software program (Falster *et al.* 2006), available at http://www.bio.mq.edu.au/ecology/SMATR/. Briefly, to test if two data groups have the same allometric exponent, a likelihood ratio test for a common slope was used and compared to a chi squared distribution. Secondly, to test whether or not a slope equals some hypothesised value of *b*, a test for correlation between residual and fitted axis scores were conducted, using the hypothesised value as slope. In addition to an F-test comparing a slope to a hypothesised value, one might also consider the slope's confidence interval and whether or not it includes a hypothesised value. The latter approach might be advantageous when one wishes to get an idea of the magnitude of deviation from a hypothesised slope. Note however that in those cases where the significance value have been adjusted (Bonferroni adjustment), the confidence interval reported will be narrower than required to determine significant departures from a hypothesised slope.

For purposes of illustrating common slopes (of two or more constituent data groups) in graphs, an intercept for each common slope had to be created. This was done by averaging the intercepts obtained from each group when the common slope was applied to the group's data. In other words, for each group a new intercept was obtained by fitting the common slope to its data: $y = Intercept_{new} + k_{common} \times x$ (Falster *et al.* 2006). All the data groups' new intercepts were then averaged and used in conjunction with the common slope. The resultant intercept is somewhat artificial, but the effect is not critical as the new intercept's purpose is merely to aid illustration of the relevant common slope.

## 2.3 Results

### 2.3.1 Description of study sample

Foetal body masses ranged from 18 kg to 77 kg in males (n = 6) and from 21 kg to 59 kg in females (n = 3), with birth mass around 100 kg (Skinner & Hall-Martin 1975). Postnatal body masses ranged from 184 kg to 1 413 kg in males (n = 18) and from 147 kg to 1 028 kg in females (n = 21) (Table 2.1). All animals measured had seven cervical (C1–C7), fourteen thoracic (T1–T14) and five lumbar (L1–L5) vertebrae. In one adult female of 849 kg however, the 11th and 12th thoracic vertebrae were fused. Sacral and caudal vertebrae were not measured. Power functions for the various dimensions measured are presented in (Table 2.2 and Appendix 1).

### 2.3.2 Sexual dimorphism

Each dimension vs. body mass slope was tested for sexual dimorphism. Regarding vertebral length, no significant differences between sexes were detected in any of the vertebrae. Regarding vertebral cross sectional properties however, there were significant sexual dimorphism detected in many of the vertebrae. Relative growth was significantly greater in males in dorsoventral diameter in most of the cervical (83%) and thoracic (64%) vertebrae. Transverse diameter growth was similarly greater in males in the cervical (67%) and thoracic (71%) vertebrae. Cervical vertebrae differed mostly in the cranial region with C7 (dorsoventral) and C6–C7 (transverse) not significantly different. In the lumbar region only vertebra five were significantly dimorphic, both in the dorsoventral and transverse direction. The spinous processes on the other hand showed very few differences between males and females—only T1 and T2 were significantly different ($p<0.01$).

*Table 2.1 The gender, weight and length of individual giraffes.*

| Giraffe nr | Gender | Body mass (kg) | Total length (cm) |
|---|---|---|---|
| **z-01** | M | 1205 | 479 |
| **z-02** | F | 466 | 332 |
| **z-03** | F | 892 | 455 |
| **z-04** | M | 1379 | 489 |
| **z-05** | M | 468 | 347 |
| **z-06** | M | 1409 | 519 |
| **z-07** | F | 850 | 450 |
| **z-08** | F | 1028 | 464 |
| **z-09** | F | 978 | 449 |
| **z-10** | M | 70 | 181 |
| **z-11** | M | 43 | 158 |
| **z-12** | F | 689 | 413 |
| **z-13** | M | 1161 | 496 |
| **z-14** | F | 849 | 437 |
| **z-15** | M | 1413 | 525 |
| **z-16** | M | 780 | 443 |
| **z-17** | F | 565 | 398 |
| **z-18** | M | 227 | 269 |
| **z-19** | M | 184 | 255 |
| **z-20** | F | 936 | 465 |
| **z-21** | M | 38 | 157 |
| **z-22** | F | 1022 | 472 |
| **z-24** | F | 605 | 404 |
| **z-25** | F | 231 | 284 |
| **z-26** | F | 961 | 460 |
| **z-27** | M | 77 | 193 |
| **z-28** | M | 643 | 395 |
| **z-31** | M | 967 | 475 |
| **z-32** | M | 1006 | 506 |
| **z-33** | F | 675 | 416 |
| **z-34** | F | 698 | 419 |
| **z-35** | M | 18 | 117 |
| **z-36** | M | 309 | 318 |
| **z-37** | F | 425 | 325 |
| **z-38** | F | 288 | 320 |
| **z-39** | F | 355 | 311 |
| **z-40** | M | 520 | 370 |
| **z-41** | F | 401 | 347 |
| **z-42** | F | 561 | 382 |
| **z-43** | M | 518 | 373 |
| **z-44** | M | 1308 | 521 |
| **z-45** | M | 30 | 159 |
| **z-46** | F | 21 | 130 |
| **z-47** | M | 1015 | 482 |
| **z-48** | F | 147 | 231 |
| **z-51** | M | 823 | 450 |
| **z-54** | F | 59 | 172 |
| **z-56** | F | 25 | 139 |

*Note: The length of the animal included head and tail and was measured according to Hall-Martin (1975)*

***Table 2.2 Allometric equations for the determination of vertebral body length (in mm) for foetal and postnatal giraffe.***

| Vertebra | n† | Allometric equation†§ | $r^2$† | n‡ | Allometric equation‡§ | $r^2$‡ |
|---|---|---|---|---|---|---|
| C1 | **39** | **$4.74 \times M_b^{0.436\ (0.389\text{-}0.488)}$** | 0.88 | 9 | $11.91 \times M_b^{0.238\ (0.130\text{-}0.434)}$ | 0.49 |
| C2 | **39** | **$13.03 \times M_b^{0.439\ (0.405\text{-}0.477)}$** | 0.94 | 9 | $17.58 \times M_b^{0.381\ (0.284\text{-}0.513)}$ | 0.89 |
| C3 | **39** | **$8.58 \times M_b^{0.496\ (0.448\text{-}0.549)}$** | 0.91 | 9 | $20.41 \times M_b^{0.317\ (0.237\text{-}0.423)}$ | 0.89 |
| C4 | **39** | **$11.18 \times M_b^{0.454\ (0.41\text{-}0.504)}$** | 0.9 | 9 | $17.78 \times M_b^{0.365\ (0.283\text{-}0.471)}$ | 0.92 |
| C5 | **39** | **$12.21 \times M_b^{0.439\ (0.396\text{-}0.488)}$** | 0.9 | 9 | $20.19 \times M_b^{0.328\ (0.227\text{-}0.472)}$ | 0.83 |
| C6 | **39** | **$12.97 \times M_b^{0.430\ (0.384\text{-}0.481)}$** | 0.89 | 9 | $18.28 \times M_b^{0.352\ (0.247\text{-}0.503)}$ | 0.83 |
| C7 | **39** | **$8.59 \times M_b^{0.483\ (0.431\text{-}0.542)}$** | 0.88 | 9 | $11.48 \times M_b^{0.458\ (0.284\text{-}0.74)}$ | 0.69 |
| T1 | **39** | **$4.74 \times M_b^{0.436\ (0.389\text{-}0.488)}$** | 0.88 | 9 | $11.91 \times M_b^{0.238\ (0.130\text{-}0.434)}$ | 0.49 |
| T2 | 35 | $7.58 \times M_b^{0.356\ (0.305\text{-}0.414)}$ | 0.81 | 7 | $6.79 \times M_b^{0.369\ (0.187\text{-}0.730)}$ | 0.59 |
| T3 | 31 | $6.99 \times M_b^{0.336\ (0.274\text{-}0.412)}$ | 0.71 | 7 | $5.57 \times M_b^{0.399\ (0.244\text{-}0.652)}$ | 0.8 |
| T4 | 30 | $6.31 \times M_b^{0.338\ (0.269\text{-}0.426)}$ | 0.64 | 7 | $5.53 \times M_b^{0.377\ (0.235\text{-}0.605)}$ | 0.82 |
| T5 | 31 | $8.58 \times M_b^{0.279\ (0.215\text{-}0.361)}$ | 0.53 | 7 | $3.04 \times M_b^{0.505\ (0.317\text{-}0.806)}$ | 0.82 |
| T6 | 31 | $6.59 \times M_b^{0.307\ (0.249\text{-}0.378)}$ | 0.69 | 7 | $5.16 \times M_b^{0.351\ (0.214\text{-}0.576)}$ | 0.8 |
| T7 | 31 | $6.51 \times M_b^{0.303\ (0.251\text{-}0.365)}$ | 0.75 | 7 | $6.33 \times M_b^{0.274\ (0.176\text{-}0.426)}$ | 0.84 |
| T8 | 31 | $5.60 \times M_b^{0.323\ (0.269\text{-}0.387)}$ | 0.77 | 7 | $5.25 \times M_b^{0.326\ (0.224\text{-}0.473)}$ | 0.89 |
| T9 | 31 | $6.52 \times M_b^{0.300\ (0.255\text{-}0.354)}$ | 0.81 | 7 | $5.38 \times M_b^{0.307\ (0.188\text{-}0.501)}$ | 0.8 |
| T10 | 31 | $7.32 \times M_b^{0.281\ (0.238\text{-}0.331)}$ | 0.81 | 7 | $4.8 \times M_b^{0.350\ (0.194\text{-}0.634)}$ | 0.7 |
| T11 | 31 | $7.25 \times M_b^{0.283\ (0.245\text{-}0.327)}$ | 0.85 | 7 | $3.7 \times M_b^{0.404\ (0.291\text{-}0.560)}$ | 0.92 |
| T12 | 31 | $7.11 \times M_b^{0.286\ (0.244\text{-}0.336)}$ | 0.82 | 7 | $4.64 \times M_b^{0.355\ (0.230\text{-}0.548)}$ | 0.85 |
| T13 | 31 | $6.68 \times M_b^{0.298\ (0.254\text{-}0.35)}$ | 0.82 | 7 | $4.41 \times M_b^{0.367\ (0.247\text{-}0.545)}$ | 0.88 |
| T14 | 31 | $7.36 \times M_b^{0.289\ (0.242\text{-}0.345)}$ | 0.78 | 7 | $5.85 \times M_b^{0.293\ (0.184\text{-}0.467)}$ | 0.83 |
| L1 | 31 | $6.74 \times M_b^{0.308\ (0.263\text{-}0.360)}$ | 0.83 | 7 | $5.23 \times M_b^{0.336\ (0.244\text{-}0.463)}$ | 0.92 |
| L2 | 31 | $7.00 \times M_b^{0.307\ (0.263\text{-}0.357)}$ | 0.84 | 7 | $6.32 \times M_b^{0.302\ (0.197\text{-}0.461)}$ | 0.86 |
| L3 | 31 | $7.79 \times M_b^{0.295\ (0.25\text{-}0.349)}$ | 0.8 | 7 | $4.77 \times M_b^{0.402\ (0.261\text{-}0.620)}$ | 0.85 |
| L4 | 31 | $7.49 \times M_b^{0.304\ (0.258\text{-}0.357)}$ | 0.82 | 7 | $5.62 \times M_b^{0.348\ (0.270\text{-}0.450)}$ | 0.95 |
| L5 | 30 | $6.78 \times M_b^{0.318\ (0.267\text{-}0.379)}$ | 0.79 | 6 | $3.87 \times M_b^{0.446\ (0.256\text{-}0.779)}$ | 0.82 |

*Note: † Postnatal data. ‡ Foetal data. §Mb = Body mass (kg). The brackets contain the upper and lower 95% confidence interval for the scaling exponent.* ***Bold*** *equations indicate positive allometry. In all cases the underlying regressions were significant (i.e. p<0.05).*

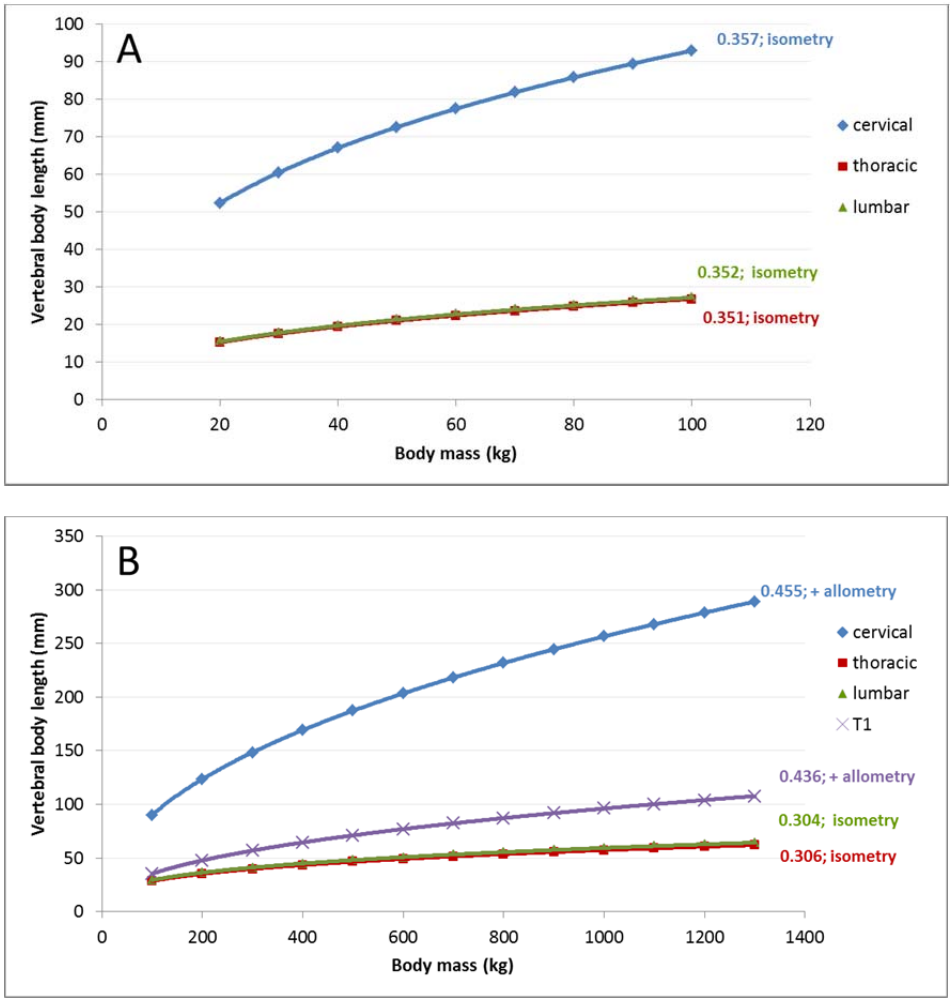


***Figure 2.3 The scaling of vertebral body lengths. Note that the graphs do not indicate the dimensions of any specific vertebra but represents a common slope within a vertebral region. (A) The foetal scaling of vertebral body lengths. The cervical series are clearly longer, but the difference in growth rate is not clearly different from the other vertebrae. (B) The postnatal growth of vertebral body lengths. The cervical vertebrae are clearly longer and grow faster than the succeeding vertebra. Thoracic vertebra 1 also scales with positive allometry and in this respect also adopts 'cervical' behaviour.***

### 2.3.3 Scaling of exponents of vertebral lengths with regard to body mass

For vertebral body lengths, separate allometric equations were calculated for the foetal and postnatal data. The vertebral exponents were compared amongst each other within the cervical, thoracic and lumbar regions. Cervical vertebra 1 was not included in the cervical comparisons as its shape is atypical compared to the other vertebrae. In the foetus there were no significant differences between vertebrae within each of the vertebral regions. Subsequently, a common exponent of 0.357, 0.351 and 0.352 could be drawn for the foetal cervical, thoracic and lumbar regions respectively (Figure 2.3).

Postnatally, cervical vertebrae lengthened at the same rate and a common slope/ exponent of 0.445 was found to be reasonably applicable to all vertebrae in this region ($P_{\text{common slope}} = 0.30$). The common slope for cervical vertebrae scales with significant positive allometry ($P_{(H0:\ k=0.333)}<0.001$). There was however a significant difference in the elevation of cervical

slopes on the y-axis (Wald statistic = 51.6; df = 5; $P$<0.001). Significant differences in lengthening rates were detected amongst thoracic vertebrae ($P_{(\text{common slope})}$ = 0.002). Post-hoc multiple comparisons on these slopes singled out T1 as the main contributor to differences detected: T1's lengthening exponent was significantly different from all the other thoracic vertebra ($P$ = 0.04 , 0.03, 0.01 and 0.01 in T2–T5 comparisons, and $P$≤0.002 in all other comparisons). In T1 the slope is positively allometric ($P_{(\text{H0: } k=0.333)}$<0.001), while the slopes of the rest of the thoracic series displayed isometric or slight negatively allometric lengthening. Lumbar slopes were not significantly different amongst each other ($P_{(\text{common slope})}$ = 0.99). The common slope relevant to all lumbar vertebrae was calculated as 0.306, which is just below isometry ($P_{(\text{H0: k=0.333})}$ = 0.02, Figure 2.3).

Thus, in summary, the postnatal cervical series lengthened faster (with positive allometry) than the cervical series of the foetus (isometry). The postnatal T1 lengthening rate was also positively allometric, while the rest of the thoracic and lumbar as well as the foetal cervical–lumbar series were isometric. However, because of the small foetal sample size, their isometric scaling result will remain unconvincing until larger sample sizes are obtained (Brown & Vavrek 2015).

### 2.3.4 Scaling exponents of vertebral widths, heights and spinous processes vs. body mass

The allometric equations for cross sectional diameters and spinous process lengths with regard to body mass are presented in Appendix 1. A summary of common slope values within vertebral series' is presented in Table 2.3.

***Table 2.3 Summary of common slope values in postnatal vertebral diameter and spinous process dimensions with regard to body mass***

| Vertebral series | Dimension | P(common slope) | Common slope value | P(H0: *k*=0.333) | Type of allometry |
|---|---|---|---|---|---|
| C2-C7 | CdDV | 0.97 | 0.273 | <0.001 | negative allometry |
| | CdTr | 0.52 | 0.299 | 0.014 | negative allometry |
| | Spine | 0.001 | n/a | n/a | n/a |
| T1-T14 | CdDV | 0.64 | 0.267 | <0.001 | negative allometry |
| | CdTr | 0.99 | 0.263 | <0.001 | negative allometry |
| | Spine | 0.003 | n/a | n/a | n/a |
| L1-L5 | CdDV | 0.82 | 0.245 | <0.001 | negative allometry |
| | CdTr | 0.59 | 0.275 | 0.001 | negative allometry |
| | Spine | 0.19 | 0.472 | <0.001 | Positive allometry |

*Note: CdDv = Caudal dorsoventral diameter; CdTr = Caudal transverse diameter; Spine = Spinous process; n/a = Not applicable, which indicates instances where there were significant probability of at least one slope within the vertebral segment being different from a common slope. In other words if P(common slope) < 0.05, then a common slope cannot be fitted and, subsequently, there will be no common slope to classify according to the 'type of allometry' (column 6)*

Common slopes for cross sectional diameters could be drawn for each vertebral region, both in foetuses and postnatal animals. Foetal dorsoventral diameters tended to be isometric (height vs. body mass exponent not different from 0.333), whereas the transverse

diameter growth tended to be significantly greater than isometry. In postnatal animals, vertebral body width and height scaled with significant negative allometry in all segments of the vertebral column (i.e. exponents for vertebral body width or height vs. body mass were significantly less than 0.333; Table 2.3, Figure 2.4).

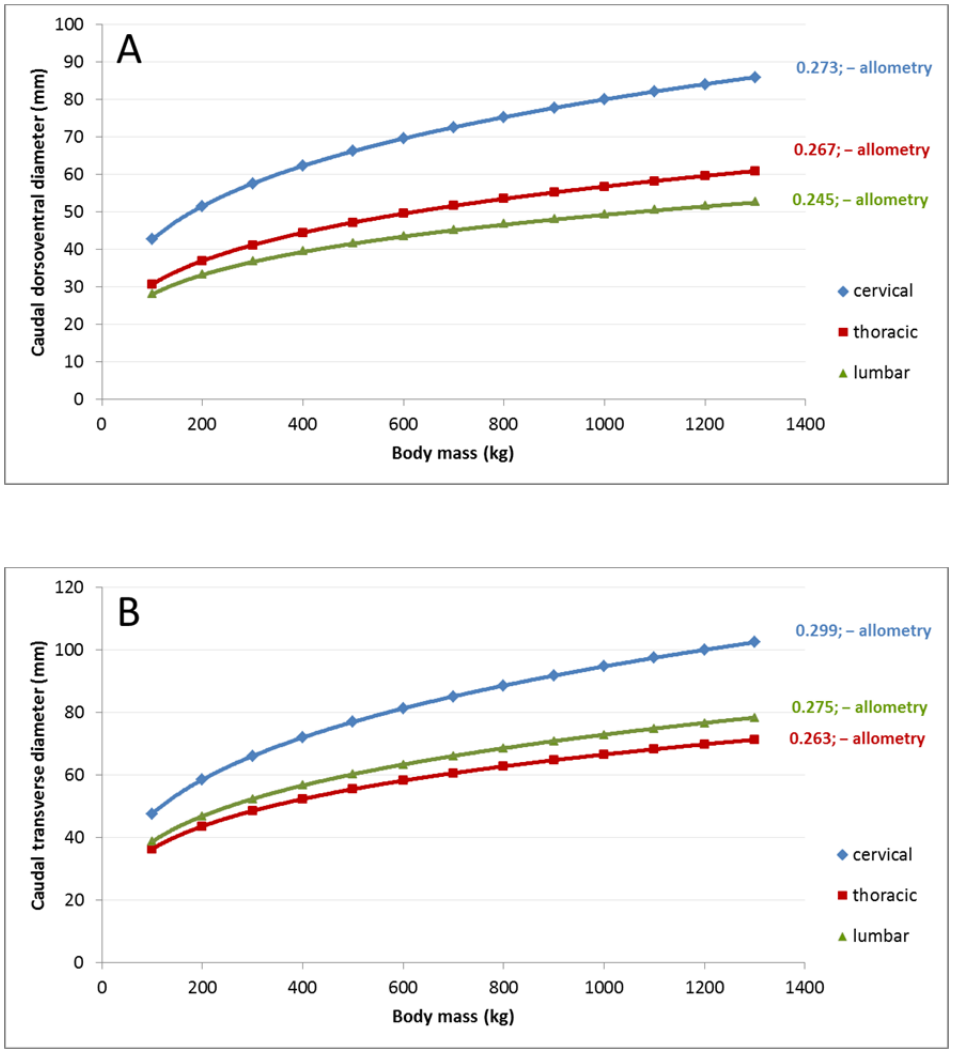


***Figure 2.4 The caudal vertebral body dorsoventral (A, height) and transverse (B, width) growth during postnatal ontogeny. Both of these cross-sectional diameters scale with negative allometry throughout the vertebral column. Note that the graphs do not indicate the dimensions of any specific vertebra but rather the growth of a typical vertebra within a vertebral section.***

In the foetus, significant proportions of the spinous processes were still cartilaginous, and exact dissection from the surrounding tissues was not always successful; thus, the foetal spinous process lengths were omitted from the analysis. Postnatal spinous processes could not be summarised with a common slope for the cervical as well as the thoracic region (Table 2.3). Post-hoc multiple comparisons revealed vertebrae that scaled differently from the rest of the regional vertebrae, and vertebrae were subsequently grouped so that each group could be summarised with a common slope. Groupings that allowed for common slope determination included C2–C5, C6–T3, T4–T14 and the lumbar vertebrae. The common slopes for each of these groups are indicated in Figure 2.5. All the spinous process groupings scaled with positive allometry, although for cervical processes only barely so ($k_{(C2–}$

$_{C5)}$ = 0.370; lower confidence limit = 0.335; upper confidence limit = 0.408; $P_{(common\ slope)}$ = 0.06).

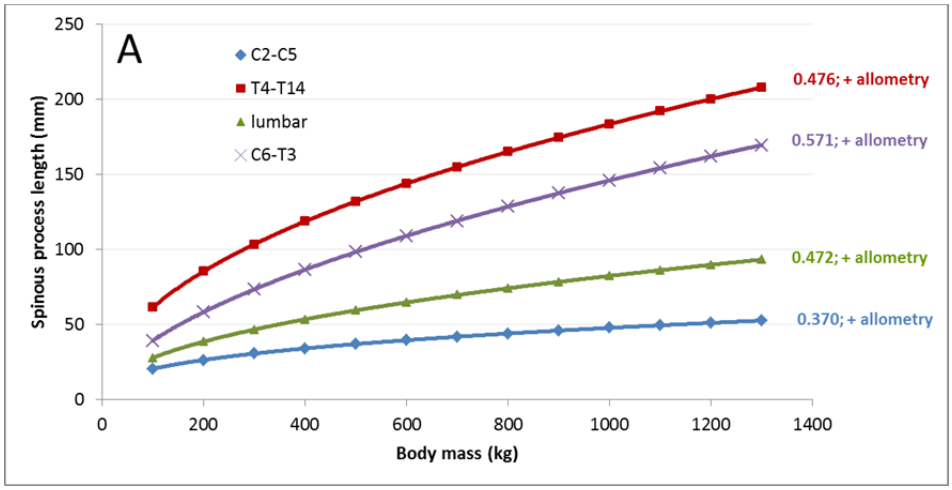


***Figure 2.5 The growth of the spinous processes during postnatal ontogeny. Spinous processes C6–C7 and T1–T3 differs in scaling from the rest cervical and thoracic series respectively. Note that the graphs do not indicate the dimensions of any specific vertebra but rather the growth of a typical spinous process within a vertebral section.***

### 2.3.5 Comparison of Lengths, widths and heights at different body masses

Vertebral body lengths were compared at specific body mass intervals, using allometric equations derived through OLS regression. Ordinary least squares regression was more appropriate than SMA regression in this case as the objective was to use the equation to predict a value for y from x (Warton *et al.* 2006). The body mass intervals were foetal (20 kg–90 kg), neonate (100 kg–200 kg), and mature adult (1200 kg–1300 kg; Figure 2.6). In the foetus, the length of C2-C7 did not differ significantly, whereas the average C1 ($F_{(6,49)}$ = 17.7; P<0.001) and T1 ($F_{(6,49)}$ = 10.1; P<0.001) lengths were significantly shorter than C2-C7. Furthermore, there was a significant decrease in length from T2 to T5 ($F_{(3,28)}$ < 3.006; P<0.05). Similarly, the lengths of neonatal giraffes' C2-C7 did not differ significantly, although a decreasing trend was noticeable. In the neonatal thoracic series T1 ($F_{(1,24)}$ = 11.03, P<0.01) and T2 ($F_{(1,24)}$ < 4.75, P<0.05) were significantly longer than their succeeding vertebrae and shorter than cervical vertebrae ($F_{(7,8)}$ = 4.22, P<0.05), whereas the lengths of T4-L5 did not differ significantly from each other. At 1200 kg–1300 kg, the decreasing trend from C2 to C7 becomes significant ($F_{(5,6)}$ = 6.27; P<0.05), whereas the lengths of T4-L5 did not differ significantly, as was the case in the neonate.

***Table 2.4 The different section lengths of the vertebral column as a proportion of total length.***

| Body mass (kg) | 20 | 90 | 200 | 400 | 600 | 800 | 1000 | 1200 | 1400 |
|---|---|---|---|---|---|---|---|---|---|
| Cervical | 0.53 | 0.53 | 0.55 | 0.56 | 0.57 | 0.57 | 0.58 | 0.58 | 0.58 |
| Thoracic | 0.35 | 0.35 | 0.34 | 0.33 | 0.32 | 0.32 | 0.32 | 0.31 | 0.31 |
| Lumbar | 0.12 | 0.12 | 0.11 | 0.11 | 0.11 | 0.11 | 0.11 | 0.11 | 0.11 |

*Note: Total vertebral column length in this case constitutes cervical plus thoracic plus lumbar vertebral body lengths.*

Table 2.4 and Table 2.5 illustrate the changing proportions of the vertebral sections throughout growth. From 20 kg to full term, the foetal cervical region was consistently ca. 53% of total (cervical to lumbar) spine length, whereas the thoracic and lumbar spines formed 35% and 12%, respectively. When the cervical, thoracic and lumbar vertebral lengths were expressed as percentages of trunk length, the proportions stayed almost constant in the foetus (ca. 113%, 74%, and 26% respectively, Table 2.5). In contrast, the neonatal cervical spine increases markedly in the first 6 months of life from ca. 116% (100 kg) to 122% (200 kg). This pattern continues throughout life and the cervical spine reached 138% of trunk length in the mature adult, whereas an asymptote of 58% of total spine length is reached at 1000 kg body mass. The increase in the cervical proportion of total spine length was associated with a decrease in thoracic proportion from 34% in neonates to 31% in adults, whereas the lumbar proportion remained relatively constant at 11% (Table 2.4).

***Table 2.5 The different section lengths of the vertebral column as a proportion of trunk (thoracic plus lumbar) length***

| Body mass (kg) | 20 | 90 | 200 | 400 | 600 | 800 | 1000 | 1200 | 1400 |
|---|---|---|---|---|---|---|---|---|---|
| Cervical | 1.14 | 1.12 | 1.22 | 1.28 | 1.31 | 1.34 | 1.36 | 1.38 | 1.39 |
| Thoracic | 0.74 | 0.74 | 0.75 | 0.75 | 0.75 | 0.75 | 0.75 | 0.75 | 0.75 |
| Lumbar | 0.26 | 0.26 | 0.25 | 0.25 | 0.25 | 0.25 | 0.25 | 0.25 | 0.25 |

Analysis of the widths (Figure 2.6) at specific body masses showed that in the foetus there were no significant differences in widths between C2 and L4. In animals of 100 kg–200 kg, the differences in width from C2 to C6 were not significant, neither were T3-L3, but width decreased significantly from C7 to T3 ($F_{(3,8)} = 8.8$, $P<0.05$). In adults of 1200 kg–1300 kg body mass, average width increased from C2 to C6 ($F_{(4,5)} = 78.3$, $P<0.001$), decreased from C7 to T3 ($F_{(3,4)} = 175.5$, $P<0.001$), were the same from T4 to L3, but increased in L4 and L5 ($F_{(1,2)} = 121$, $P<0.001$). Analysis of the heights (Figure 2.6 C) revealed that the foetal vertebral heights increased significantly from C2 to C7 ($F_{(5,48)} = 2.04$, $P<0.05$), declined significantly from C7 to T2 ($F_{(2,24)} = 4.09$, $P<0.05$), but thereafter were the same. The vertebral body

heights in neonates followed the same pattern as foetuses, except that heights declined significantly from C7 to T5 ($F_{(5,12)} = 6.82$, $P<0.01$). Adult heights increased from C2 to C6 ($F_{(4,5)} = 240.1$, $P<0.001$), decreased from C7 to T9 ($F_{(9,10)} = 444.05$, $P<0.001$), but remained the same from T10 onwards. Thus, the giraffe exhibits increased differentiation in the width and height of the vertebrae as body mass increases.

Allometric predictions of spinous process length at specific body masses showed that there were no significant differences for C2-C6 and L1-L5 throughout growth, but the lumbar spinous process heights were significantly higher ($t = 2.45$, $P<0.01$) than were the cervical spinous process heights (at 1300 kg, the mean cervical spinous process height = 51.6 ± 4 mm and the mean lumbar spinous process height = 92.5 ± 4 mm). Thoracic spinous process lengths varied significantly ($F_{(13,168)} = 16.4$, $P<0.001$), with the longest spinous processes those of T3-T6 (at 1200 kg, the T3-T6 mean = 304 ± 10 mm), of which T4 was the longest (at 1200 kg = 311 mm). When the spinous process lengths were expressed as a percentage of trunk length (Figure 2.7), the cervical (C2-C5) spinous processes did not increase in length relative to trunk length throughout growth. From C6 to L5, however, spinous process length increased as a percentage of trunk length as the animal grew.

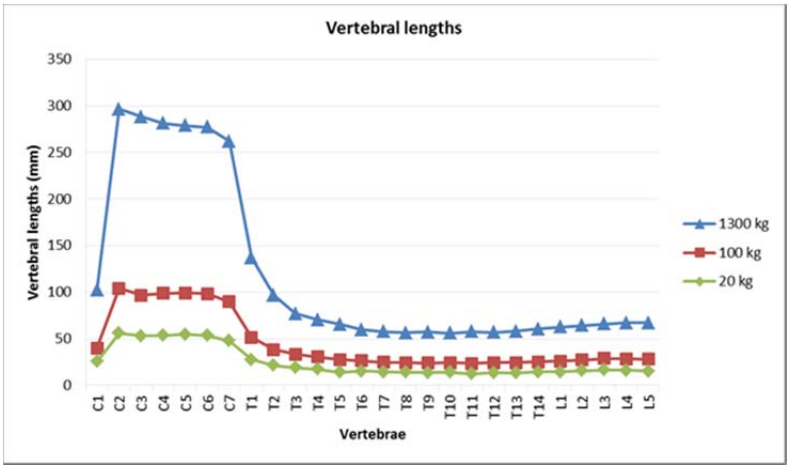


A

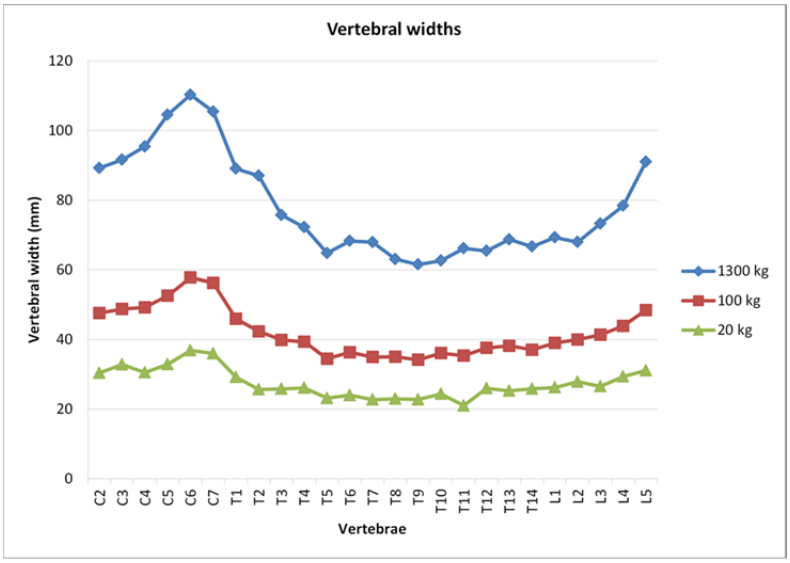


B

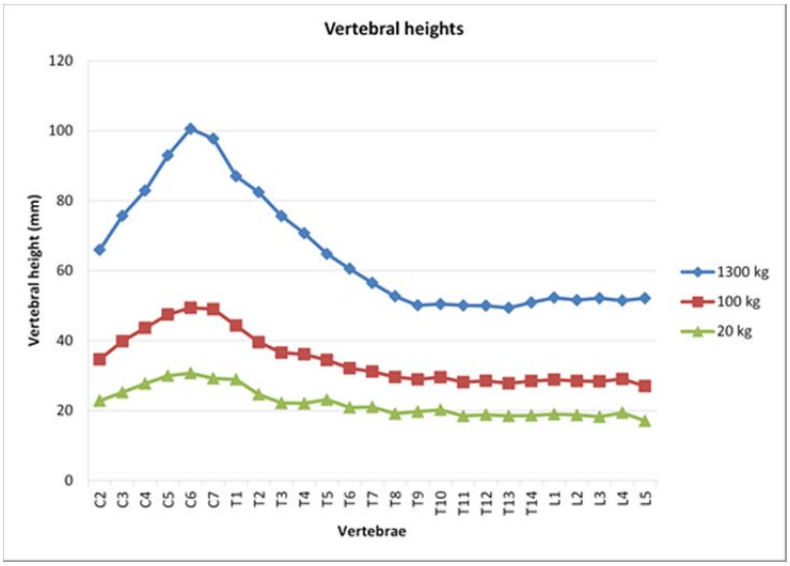


C

***Figure 2.6 The individual vertebral body lengths, widths, and heights at different body mass intervals. (A) The lengths of vertebral bodies at various body mass intervals. Note the disproportionate increase in cervical length. (B) The lateral growth of the vertebral bodies at various body mass intervals. Note the increased differentiation seen in widths as the animal matures. (C) The dorsoventral growth of the vertebral bodies at various body mass intervals. The increased differentiation is even more marked than with the lateral (width) growth.***

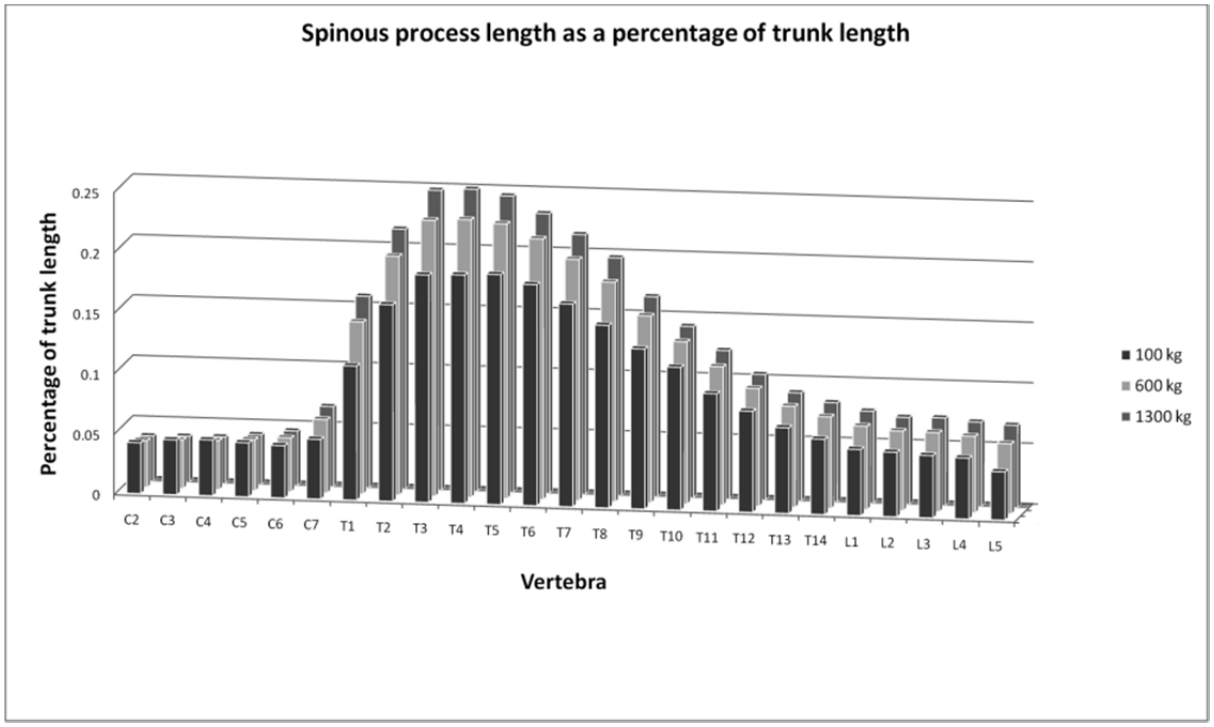


***Figure 2.7 The spinous process lengths as a proportion of trunk lengths. Note the difference in relative growth of the cervical (C2-C6) spinous processes compared with the relative growth from C7 onwards.***

## 2.4 Discussion

In this study the classic definition of T1 was used, i.e. the first vertebra articulating with a rib that attaches to a sternum (Buchholtz & Stepien 2009; Flower 1885). In addition, the origins of the roots of the brachial plexus are similar to those found in the okapi (although the sizes of the branches may differ, as noted by Owen (1838) and illustrated by Solounias (1999). Giraffes, thus, have seven cervical vertebrae as do virtually all other mammals.

Other morphometric studies on giraffe skeletons were often limited in sample size and variation, making a description of growth and scaling with regard to body mass and between genders against the constraint of seven cervical vertebrae difficult. In this study the limitation is overcome through the availability of an unprecedented sample size of giraffe vertebrae. The description of vertebral growth was approached, firstly, by comparing the scaling exponents of foetal data with postnatal data and secondly, by making comparisons within and among the different sections of the vertebral column.

### 2.4.1 The scaling of vertebrae

The lengths of the vertebral bodies from T2 to L5 scaled similarly from foetus to adult. In contrast, a significant increase in the elongation rate occurs in the C2–C7 vertebrae as well as in the first thoracic vertebra after birth. This postnatal elongation rate is similar from C2 to C7. However, it should be borne in mind that foetal exponents, due to the small foetal sample size, have rather wide confidence intervals. Therefore, smaller deviations from isometry might be hidden especially in the foetal sample.

The remarkable postnatal elongation of cervical vertebrae is well illustrated when it is expressed as a percentage of trunk length: Although actually decreasing in the last trimester foetus to ca. 112%, once born, it increased to 122% after 6 months (Table 2.5). An advantage of an increased postnatal elongation rate may be linked to the mechanics of normal parturition. Giraffes, similar to other ungulates, are born in cranial presentation, dorsal position, and unbent head and legs with the forelegs extended cranial to the head (Dagg & Foster 1976). If the foetal giraffe had a neck length to foreleg length ratio of that of the adult animal (which is ca. 1.09 compared with ca. 0.72 in the foetus; (Mitchell *et al.* 2009a), the neck and head would extend beyond the forelegs during parturition, which may pose an increased risk of elbow flexion and ultimately dystocia. The mechanism that triggers differential elongation of the cervical vertebrae postnatally is unknown and needs further investigation.

Previous authors (Lankester 1908; Solounias 1999) alluded to T1 being adapted to the giraffe body form. Building on their findings, the scaling of T1 was shown in this study to scale with positive allometry (0.436), similar to the common slope of the cervical vertebrae (0.455). Therefore, because there is: a) Lack of significant difference between the scaling of T1 vs. cervical vertebrae and b) A significant difference between T1 and the T2–T14 thoracic series, it is suggest T1 is ‘‘cervicalised’’ with regards to its scaling exponent. In terms of

scaling, therefore, T1 is a transitional vertebrae and Lankester's (1908) finding of cervical homeosis is supported. Nevertheless, T1 starts out shorter than cervical vertebrae and never reaches the remarkable length of the cervical vertebrae (Figure 2.6). Because, in giraffes, the point of articulation between the cervical and thoracic vertebrae has shifted caudally to lie between T1 and T2 rather than between C7 and T1, which is the typical ruminant pattern, all seven cervical vertebrae contribute to neck length, whereas in other ruminant species only six do (Solounias 1999, Figure 2.8). However, given positive allometry of T1 length, it can perhaps be argued that even T1 indirectly contributes to neck length by increasingly shifting the C1–C7 vertebrae cranially. T1 does however never reach the remarkable length of the cervicals, and also does not contribute to neck length on the cervical axis but rather from the thoracic axis (Figure 2.8).

Therefore, this study showed that the giraffe evolved an elongated neck within the constraints of seven cervical vertebrae, thereby confirming the stance of Badlangana *et al.* (2009) and Mitchell & Skinner (2003) but disagreeing with Solounias (1999). The elongation is brought about by increasing the rate of elongation in the cervical (C2-C7) vertebrae postnatally and by shifting the function of C7 to T1.

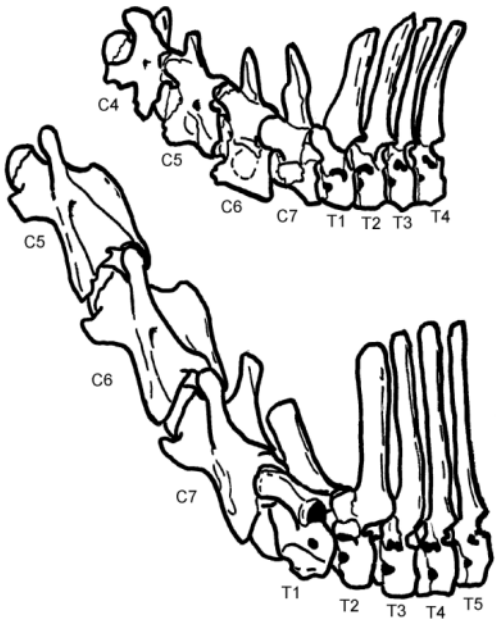


***Figure 2.8 The cervicothoracic junction in the giraffe compared with the okapi, redrawn from Solounias (1999). Okapis (top) are often chosen for comparisons of the sort as they represent the closest extant relative of the giraffe (bottom). The dark areas on the thoracic vertebrae denote attachment areas for the ribs. A change in articulatory facets between vertebrae occurs between C7 and T1 in the okapi and between T1 and T2 in the giraffe (Not illustrated—see Lankester 1908). The caudal shifting in facet morphology allows C7 to contribute to neck elongation in the giraffe (Mitchell & Skinner 2003).***

In addition to lengths, the allometry of vertebral widths, heights and spinous processes were analysed. Giraffes follow the general mammalian pattern, in that the vertebral body width exceeds height (Slijper 1946). There is increased differentiation of these dimensions in the caudal cervical and cranial thoracic vertebrae as the animal matures (Figure 2.6).

Interestingly, none of the vertebrae's cross-sectional diameters scaled with positive allometry or even isometry indicating, perhaps, a greater than needed relative robusticity in younger giraffe vertebrae. In turn, greater relative robusticity might be an adaption to maintain mechanical similarity in younger animals—as Carrier (1983, 1996) proposed to be the case for limb bone ontogeny in certain mammals.

For the first time, the great elongation of the spinous processes of the thoracic vertebrae (Mitchell & Skinner 2003; Owen 1838; Thompson 1917) and shorter cervical spinous processes (Lankester 1908) were quantified. Spinous processes act as lever arms, which transmit muscular force to the vertebral bodies, in addition to providing stability and anchorage to the neck via the *Ligamentum nuchae* (Mitchell 2009; Mitchell & Skinner 2003). Because muscular strength decreases relative to increases in body size of an animal, the absolute size of the animal should determine the height of the spinous processes (Slijper 1946). In this study, although all the spinous processes groups increased with positive allometry (Figure 2.5) and therefore seem important in the stability of the neck, certain spinous processes (C6-T3) grew relatively faster than other groupings. Furthermore, the spinous processes of cervical vertebrae do not seem to increase as a proportion of the trunk length with increased body mass, whereas those of thoracic and lumbar vertebrae do (Figure 2.7). Judging by their size and elongation rates, the function of cranial cervical spinous processes in stabilising and supporting the increasing neck and head mass does not seem to be critical, whereas cranial thoracic spinous processes certainly appears integral to this function. Further analyses on the association between spinous process growth and neck mass growth will provide further clues as to the relative load responses in different groups of vertebrae.

### 2.4.2 The cervicothoracic delineation

The study of the giraffe's fascinating shape has recently started to incorporate genetic and molecular models to solve controversy over its evolutionary process, developmental constraints, and segmental identity of vertebrae (Badlangana *et al.* 2009). It has been suggested that the extraordinary length of the cervical vertebrae could be explained by the caudal shifting of *Hox* gene expression in the presomatic mesoderm during embryonic development. This would then result in a larger proportion of axial skeleton being devoted to cervical vertebrae, in turn leading to seven elongated cervical vertebrae (Badlangana *et al.* 2009). However, if somite (embryonic segments containing the pre- cursors of vertebrae) sizes remain similar to those of other mammals, a caudal shift in the expression boundaries of *Hox* genes expressing thoracic delineation (e.g. the *Hoxc-6* gene; (Burke *et al.* 1995; Gaunt 1994) would lead to an increased number of cervical vertebrae, and not increased vertebral length. Somites are formed periodically from the presomatic mesoderm by the processes of a segmentation clock interacting with a maturation wave or wavefront (Dequéant & Pourquié 2008). The somite sizes are determined by the interaction of these two parameters, which vary during axis production. It is possible that, in the giraffe, these parameters may interact differently to other mammals to produce larger somites anteriorly

(Pourquié, 2010, personal communication). If not, then differential elongation of the cervical vertebrae must occur very early after the vertebrae formed, with similar growth to other vertebrae during the rest of the foetal period, and again differential growth postnatally. Indeed, in this study it has been shown that the disproportionate elongation of the neck occurs mostly postnatally, long after determination of somite sizes and the *Hox* genes have exerted their effect on the identity of the somites.

### 2.4.3 Sexual dimorphism in scaling

The finding that sex did not play a role in the scaling of vertebral body length supports the recent finding that sexual selection is not the origin of the long neck of the giraffe (Mitchell *et al.* 2009a). Although the spinous processes of T1 and T2 of all the males above 1000 kg were longer than would be predicted by our allometric equations, this is probably a biomechanical response resulting from a need to support the significantly heavier heads in male giraffes (Mitchell *et al.* 2009a, 2013a), as the thoracic spinous processes are integral in supporting the neck and head. Further proof of this hypothesis would come from the investigation of whether the angles of incline of thoracic spinous processes differ between male and female giraffes.

In contrast to the vertebral body length and spinous process growth in general, dimorphism was detected in cross sectional scaling of vertebral bodies. It is proposed, as with the dimorphism shown in the T1 and T2 spinous processes, that the cross sectional scaling differences might reflect sexual dimorphism in body or neck mass. However, apart from a tendency to detect dimorphism in the more cranial cervical vertebrae, dimorphism seemed to occur haphazardly especially along the thoracic region. This might indicate both a lack of sensitivity in detecting differences (type II error) or, alternatively, that differences are chance occurrences due to the large number of comparisons (type I error). Indeed, if a sequential Bonferroni adjustment were applied to the p-values (Rice 1989, see also Chapter 3), none of the differences would have been significant. There are thus further studies needed in the biomechanics of the giraffe vertebral spine in order to validate, refute or explain the current study's findings regarding vertebral cross sectional growth.

## 2.5 Conclusion

This study on the scaling of giraffe vertebral lengths, diameters, and spinous processes sheds light on how the axial skeleton responds to support the weight and elongation of the long neck without increasing the number of cervical vertebrae. The elongation rates were similar for the C2-C7 vertebrae, as the functional role of C7 has shifted to T1. The remarkable elongation of these vertebrae occurs after birth. Vertebral diameters are relatively robust at birth but decreases in robusticity during growth. Spinous process length may reflect the stress and strain imposed by the long neck, although further study would be needed to confirm this.

# Chapter 3
# On the scaling of the appendicular skeleton of *Giraffa camelopardalis*

*This chapter is adapted from the publication by SJ van Sittert, JD Skinner and G Mitchell entitled: 'Scaling of the appendicular skeleton of the giraffe (Giraffa camelopardalis)', published in the Journal of Morphology 2015; 276: 503-516.*

**Abstract**

Giraffes have remarkably long and slender limb bones, but it is unknown how they grow with regard to body mass, sex, and neck length. In this study, the length, mediolateral (ML) diameter, craniocaudal (CC) diameter and circumference of the humerus, radius, metacarpus, femur, tibia, and metatarsus in 10 foetuses, 20 postnatal females, and 17 postnatal males of known body masses were measured. Allometric exponents were determined and compared. It was found that the average bone length increased from 340±50 mm at birth to 700±120 mm at maturity, while average diameters increased from 30±3 to 70±11 mm. Foetal bones increased with positive allometry in length (relative to body mass) and in diameter (relative to body mass and length). In postnatal giraffes bone lengths and diameters increased isometrically or negatively allometrically relative to increases in body mass, except for the humerus CC diameter which increased with positive allometry. Humerus circumference also increased with positive allometry, that of the radius and tibia isometrically and the femur and metapodials with negative allometry. Relative to increases in bone length, both the humerus and femur widened with positive allometry. In the distal limb bones, ML diameters increased isometrically (radius, metacarpus) or positively allometrically (tibia, metatarsus) while the corresponding CC widths increased with negative allometry and isometrically, respectively. Except for the humerus and femur, exponents were not significantly different between corresponding front and hind limb segments. It was concluded that the patterns of bone growth in males and females are identical. In foetuses, the growth of the appendicular skeleton is faster than it is after birth which is a pattern opposite to that reported for the neck. Allometric exponents seemed unremarkable compared to the few species described previously, and pointed to the importance of neck elongation rather than leg elongation during evolution. Nevertheless, the front limb bones and especially the humerus may show responsiveness to behaviours such as drinking posture.

## 3.1 Introduction

The scaling of long bones is not fully understood. As animals become bigger, more robust bones are expected in order to keep bone strains along the bone diaphyses similar (Galilei 1638). McMahon (McMahon 1973, 1975) postulated that bones increased in size in a way not to retain similar bone strain levels across body masses but rather to prevent buckling, which became known as the elastic similarity model. If this model is correct, then bone length (L) should be proportional to ($\propto$) diameter (D) to the power 0.67, Body mass $(Mb)^{0.25}$, $D \propto Mb^{0.38}$ and cross sectional area$\propto Mb^{0.75}$. McMahon confirmed his idea by measuring the long bone diameter and length of 72 species of artiodactyls, including giraffes. However, when Alexander *et al.* (1979) retested the elastic similarity model on a broader range of species (not including giraffes) they found, perplexingly, that bones tend to scale closer to isometry (or geometric similarity) across taxa, and that elastic similarity applied mainly to bovids. So far, no single model has emerged that adequately describes regular distortions in bone shape across different adult body sizes (Biewener 1983; Currey 2002; Economos 1983; Garcia & da Silva 2006; Kokshenev *et al.* 2003; Norberg & Aldrin 2010; Selker & Carter 1989).

Most of the research into limb bone allometry has been on interspecific samples, with few devoted to ontogenetic scaling. As the relationship between interspecific and ontogenetic bone allometry has not been elucidated yet, it is also uncommon to apply interspecific models, such as elastic similarity, to ontogenetic data (e.g., Miller *et al.* 2008). Accordingly, limb bone ontogenies have mostly been interpreted in terms of deviations from geometric similarity. A further limitation regarding studies on limb bone ontogeny is that smaller mammals are very much overrepresented, with artiodactyls and other large animals receiving little attention.

Initially it seemed, save for a few exceptions, that increasingly gracile bones throughout growth was the prevailing pattern in mammals (Carrier 1983; Heinrich *et al.* 1999; Lammers & German 2002; Main & Biewener 2004; Miller *et al.* 2008). However, when Kilbourne & Makovicky (2012) investigated a larger sample base including larger animals, they showed that increasingly gracile bones were a feature of animals below 20 kg adult body mass, while increasingly robust bones were mainly confined to the artiodactyla. Interestingly the okapi (*Okapia johnstoni*), the only giraffid to be included in their study sample, was an exception as its bones became increasingly gracile throughout ontogeny.

Giraffes are the tallest extant animals. Tallness has been accomplished through the evolution of a compact thorax and elongated neck and legs. The ontogenetic allometry of the vertebral column have been described previously (Van Sittert *et al.* 2010) where it was found, briefly, that neck elongation occurs at the fastest relative rate after birth, that the C2-C7 vertebrae elongate at equal rates and that neck elongation is accompanied by enlargement of the spines of the thoracic vertebrae to provide attachment of the nuchal ligament. It has also been reported how giraffe limb bones develop strength to support the large body mass. The density of the giraffe's limb bones is approximately 50% more than its

other postcranial bones, its limb bones are straighter than in other artiodactyls, the wall thickness is significantly thicker than in equivalent mass artiodactyls and the metapodials have a unique columned structure (Biewener 1983; Van Schalkwyk *et al.* 2004). The ontogeny of giraffe limb bones is, however, still unknown.

Giraffe limb bones are of particular interest as they are exceptionally gracile and do not seem to conform to mammalian scaling patterns. In 1917 D'Arcy Thompson pointed out that giraffe metatarsals are relatively and absolutely longer than they are in the far less heavy ox, confounding the general observation that heavier animals have relatively stockier and shorter limbs in order to support body mass. Similarly, McMahon (1975) also found it difficult to reconcile giraffe distal limb bones with his elastic similarity model. In this chapter the results of an ontogenetic study of the appendicular skeleton of giraffes ranging in body mass from a foetus weighing 18 kg to a mature (>1400 kg) animal is reported. Giraffe ontogeny was related to known ontogenetic trends in other species (Kilbourne & Makovicky 2012), as well as to known growth data on its long neck (Van Sittert *et al.* 2010) in order to test if increasingly robust bones during ontogeny will also apply to large animals with an extreme shape. As with other ontogenetic allometric studies, limb bone growth was evaluated in terms of deviations from geometric similarity. In addition, giraffe scaling patterns was also compared to the theory of elastic similarity to see if protection against buckling may have an influence in the ontogeny of long slender limbs.

As giraffe tallness is brought about by elongation of neck and limbs, it was expected that similar scaling patterns with regard to length will be present in both these body regions. Therefore, it was anticipated that giraffe leg elongation exponents will be higher postnatally than in the foetus and that there will be a lack of sexual dimorphism in lengthening, as sexual selection did not seem to play a major role in the evolution neck length in this animal (Mitchell *et al.* 2009a; Van Sittert *et al.* 2010). Because of the relative slenderness and length of the giraffe limbs bones (and similar to the okapi data presented by Kilbourne and Makovicky, 2012), it was expected that limb bones would become increasingly gracile throughout ontogeny. This would also mean non-compliance with the principle of elastic similarity, especially in the distal bones. Lastly, it was hypothesized that the greatest bone lengthening rates would occur in the metapodial bones given the great interspecific variation in this region (McMahon 1975; Miller *et al.* 2008; Thompson 1917).

## 3.2 Materials and methods

### 3.2.1 Sampling

A cross-sectional sample of giraffe specimens was obtained from animals culled as part of the routine management of a conservancy in south eastern Zimbabwe (21°42' S, 29°54' E). Samples were collected from April 2007 until December 2010 from 10 foetuses, 21 females, and 23 males. The study was approved by the research and ethics committee of the University of Pretoria (protocol ref V043.08).

### 3.2.2 Body mass

The body mass for each animal was determined by piecemeal weighing using a Salter suspended spring balance with a capacity of 200 kg. The whole carcass, including gastrointestinal and reproductive contents, was measured in this way. Following Hall-Martin (1975), 4% was added to measured body mass as a reasonable approximation for the mass lost by evaporation, blood loss, and the loss of small pieces of tissue during the slaughtering process. The body masses of foetuses were, however, measured *in toto* and no corrections were made to their measured body masses.

### 3.2.3 Bone preparation

Foreleg bones prepared for study were the humerus, radius, fused metacarpal bones 3 and 4 (= metacarpus), femur, tibia, and fused metatarsal bones 3 and 4 (= metatarsus).

After the carcasses were weighed, the muscles and ligaments were removed by dissection and boiling in mature giraffes. In the case of foetuses or immature animals the bones were not boiled but only dissected so as to avoid dislodgement of the epiphyses.

### 3.2.4 Bone measurements

On each bone, length was measured in a straight line parallel to the long axis of the bone between the borders of the most proximal to most caudal part, which included processes, tubercles, condyles or heads of bones. The radial and tibial lengths did not include the ulna or fibula. Craniocaudal (CC) and mediolateral (ML) diameter as well as circumference were measured at the bone midshaft, perpendicular to the long axis of the bone. In addition, after sectioning bones at their midshaft, cross sectional cortical thicknesses were also measured using a vernier caliper at cranial, caudal, lateral and medial positions (Figure 3.1). The radial and tibial diameters and circumferences included the ulna and fibula respectively due to the very intimate association of these bones with each other in the giraffe. For the metapodial bones, the CC diameter included the caudal 'pillars' as described by van Schalkwyk *et al.* (2004). The cross sectional area (CSA) of each bone at midshaft was estimated by assuming its shape approximates an ellipse and using the following formula for the area of an ellipse: $\text{Area} = \times r_1 \times r_2$, where $r_1$ and $r_2$ constitute the CC and ML radii.

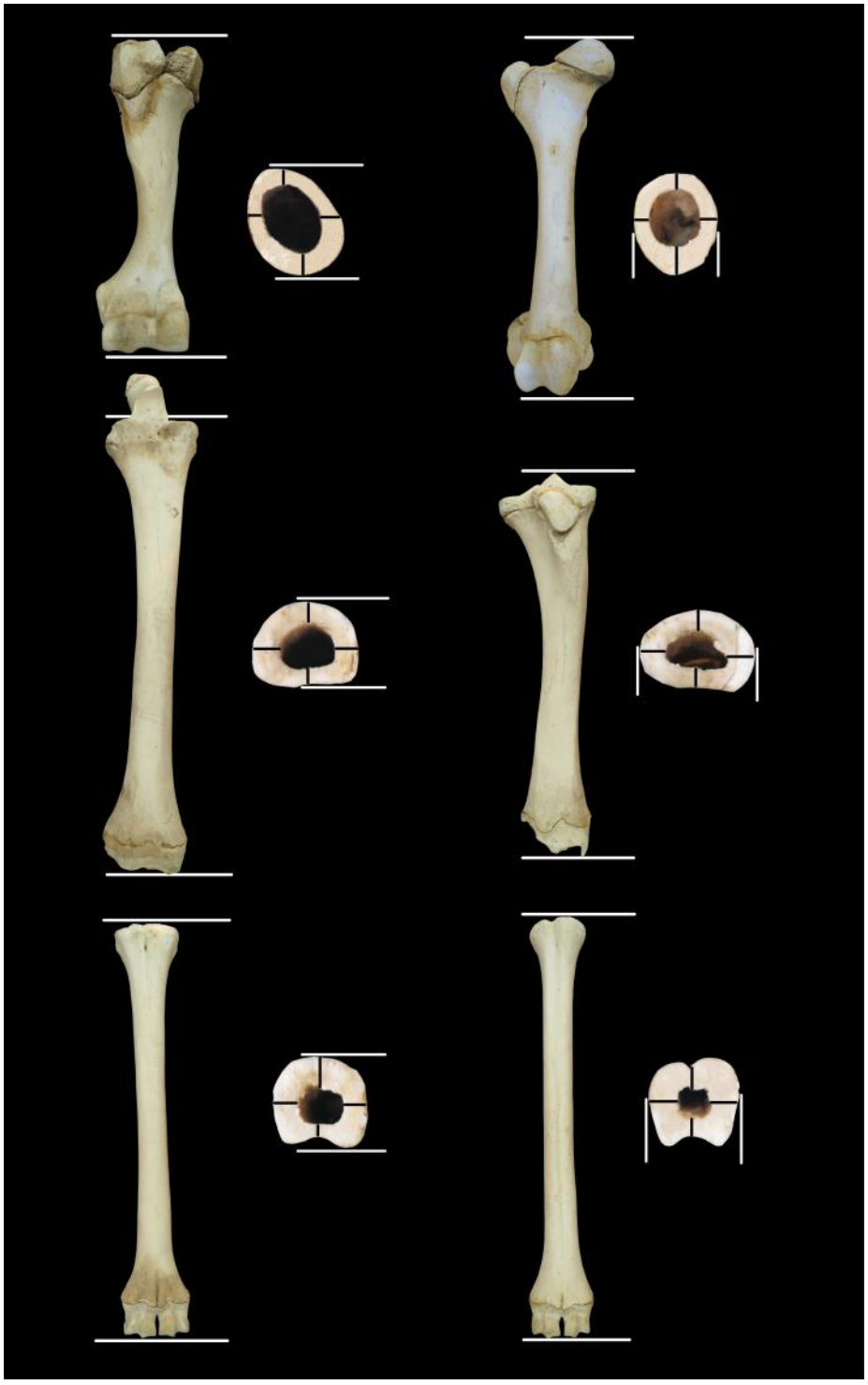

*Figure 3.1 Long bones of the giraffe. The bones are presented in cranial view and in cross section (not to scale). The cross-sectional view is positioned so that the cranial side faces to the top the page. The white lines illustrate length measurements, as well as the CC and ML measurements (indicated on the front and hind limb cross sections, respectively). Black lines denote cortical thickness measurements. Anatomical landmarks for the length measurements were as follows: Humerus, Tuberculum majus to distal surface of Capitulum humeri; Radius, Caput radii to Processus styloideus lateralis; Metapodials, Articular surface of head to articular surface of base; Femur, Proximal Caput ossis femoris to distal surface of Condylus lateralis; Tibia, Eminentia intercondylaris to Malleolus medialis.*

### 3.2.5 Scaling model

Growth data were plotted on bivariate charts. One of the methods available to assess growth patterns is the study of relative bone growth, or allometry. In this study the allometric equation ($y=bx^k$) was the most convenient and easily manageable method to describe growth. When the allometric equation is log transformed it forms a linear relationship between *y* and *x*: $\ln(y) = \ln(b) + k.\ln(x)$, which were used to estimate *b* and *k* using standardised major axis (model II) regression (Warton *et al.* 2006). Two hypotheses were tested regarding the allometric exponent: firstly whether or not two data groups have the same exponent (e.g. foetal vs. postnatal exponents), and secondly if an exponent equalled a specific value (e.g. isometry = 1). Table 3.1 shows the values for exponents complying with geometric or elastic similarity, as well as for increasingly gracile or robust bones.

***Table 3.1 Summary of the various allometric patterns***

| Type of allometry | Length vs. Body mass | Diameter and circumference vs. Body mass | Cross sectional area vs. Body mass | Diameter and circumference vs. Bone length | Cross sectional area vs. Bone length |
|---|---|---|---|---|---|
| Isometric/ geometric similarity | 0.333 | 0.333 | 0.666 | 1.00 | 2.00 |
| Increasingly gracile bones | | <0.333 | <0.666 | <1.00 | <2.00 |
| Increasingly robust bones | <0.333 | >0.333 | >0.666 | >1.00 | >2.00 |
| Elastic similarity | 0.25 | 0.375 | 0.75 | 1.5 | 2.25 |

*Note: For each scenario, the expected scaling exponent (k) for the equation $y=bx^k$ is given*

### 3.2.6 Statistics

Allometric analysis were performed according to the recommendations of Warton *et al.* (2006) using the SMATR executable software program (Falster *et al.* 2006), available at http://www.bio.mq.edu.au/ecology/SMATR/. Briefly, to test if two data groups have the same allometric exponent, a likelihood ratio test for a common slope was used and compared to a chi squared distribution. Secondly, to test whether or not a slope equals some hypothesised value of *b*, a test for correlation between residual and fitted axis scores were conducted, using the hypothesised value as slope. In addition to an F-test comparing a slope to a hypothesised value, one might also consider the slope's confidence interval and whether or not it includes a hypothesised value. The latter approach might be advantageous when one wishes to get an idea of the magnitude of deviation from a hypothesised slope. Note however that in those cases where the significance value have been adjusted (Bonferroni adjustment), the confidence intervals reported will be narrower than required to determine significant departures from a hypothesised slope.

Wherever a group of two or more slopes were simultaneously considered to be significantly different from a hypothesized value, the significance level for each test in the group was adjusted according to the sequential Bonferroni method (Rice 1989). In this way the group-wise significance level ($\alpha$) was kept at 0.05. The number of tests ($k_t$) in each group was determined by the hypothesis to be tested. For example: 'giraffe long bones grow in length to body mass according to geometric similarity postnatally' will have 6 bone's exponents to test simultaneously, and each sequential test ($i$) will have to be $p_i \leq \alpha \div (1 + k_t - i)$, in order to be considered significantly different from geometric similarity.

## 3.3 Results

### 3.3.1 Sample description

Body masses of the animals in the study (*n*=47) ranged from 18 kg to 1409 kg in males and from 21 kg to 1028 kg in females. Foetal (*n*=10) weights ranged from 18 kg to 77 kg (a full term foetus is estimated at *ca.* 100 kg (Skinner & Hall-Martin 1975). The body mass of postnatal animals ranged from 147 kg to 1028 kg in females (*n*=20) and from 184 kg to 1409 kg in males (*n*=17).The size range within this study thus differed by a factor of 4 from youngest to oldest foetus, 78 from foetus to adult and by a factor of 14 from neonate to adult. Although the total number of animals sampled was 47, all dimensions could not be measured in each case, and the number of animals sampled for each dimension is shown in the tables or figures where relevant. As the postnatal dataset was much larger than the foetal dataset it had more power for detecting significant differences between allometric exponents (Brown & Vavrek 2015). Therefore, foetal data were not analysed to the extent of postnatal data.

***Table 3.2 Summary of the bone length versus body mass slopes***

| | Group | n | $r^2$ | Exponent | 95% CI | Intercept | P (H0: foetal- = postnatal slope) | P(H0: k = 0.333) (geometric) | P(H0: b=0.25) (elastic) |
|---|---|---|---|---|---|---|---|---|---|
| **Front leg total** | F | 7 | 0.98 | 0.376 | 0.324 to 0.435 | 174.2 | | 0.09 | <0.01 |
| **— / ▭** | PN | 14 | 0.93 | 0.295 | 0.249 to 0.350 | 225.9 | 0.02 | 0.15 | 0.05 |
| **Hind leg total** | F | 7 | 0.99 | 0.351 | 0.313 to 0.395 | 203.6 | | 0.29 | <0.01 |
| **▼ / ▭** | PN | 16 | 0.95 | 0.276 | 0.243 to 0.312 | 276.7 | <0.01 | 0.01 | 0.11 |
| **Humerus** | F | 7 | 0.98 | 0.373 | 0.313 to 0.445 | 48.7 | | 0.16 | <0.01 |
| **—** | PN | 16 | 0.96 | 0.304 | 0.269 to 0.343 | 63.2 | 0.06 | 0.13 | <0.01 |
| **Radius** | F | 7 | 0.99 | 0.340 | 0.302 to 0.383 | 75.7 | | 0.66 | <0.01 |
| **—** | PN | 15 | 0.97 | 0.346 | 0.310 to 0.386 | 70.1 | 0.80 | 0.47 | <0.01 |
| **Metacarpus** | F | 10 | 0.97 | 0.390 | 0.337 to 0.451 | 73.9 | | 0.04 | <0.01 |
| **—** | PN | 36 | 0.91 | 0.300 | 0.271 to 0.333 | 89.5 | <0.01 | 0.05 | <0.01 |
| **Femur** | F | 7 | 0.98 | 0.409 | 0.342 to 0.490 | 46.3 | | 0.03 | <0.01 |
| **▼ / ▭** | PN | 16 | 0.96 | 0.249 | 0.221 to 0.281 | 94.9 | <0.01 | <0.01 | 0.96 |
| **Tibia** | F | 7 | 0.98 | 0.369 | 0.314 to 0.434 | 57.9 | | 0.16 | <0.01 |
| **—** | PN | 16 | 0.96 | 0.302 | 0.269 to 0.340 | 77.9 | 0.04 | 0.1 | <0.01 |
| **Metatarsus** | F | 10 | 0.95 | 0.315 | 0.265 to 0.375 | 96.5 | | 0.49 | 0.02 |
| **—** | PN | 37 | 0.9 | 0.300 | 0.270 to 0.334 | 88.6 | 0.62 | 0.06 | <0.01 |

*Note: Data were subdivided into foetal and postnatal data. In all cases the underlying regressions were significant (i.e. p<0.05). The last two columns indicate the probability of the exponent (b) being geometrically similar (0.333) or elastically similar (0.25). The significance level was adjusted according to the sequential Bonferroni technique (Rice, 1989). Postnatal bone growth patterns are highlighted with a key: — geometric similarity, ▱ elastic similarity, ▲ positive allometry, ▼ negative allometry. In cases where growth could not be distinguished from either geometric similarity or elastic similarity, or where allometries were both negative and elastically similar, two keys are shown [were indicated]. n = number of animals sampled, CI = confidence interval, F = foetus, PN = postnatal animal.*

### 3.3.2 Sexual dimorphism

Sexual dimorphism was not present in any of the limb bone growth patterns studied ($P_{(H0:\text{male exponent} = \text{female exponent})} \geq 0.05$ for all bone dimension vs. body mass slopes as well as for all bone cross sectional dimension vs. bone length slopes). Data from both sexes were therefore pooled.

### 3.3.3 Growth patterns

#### 3.3.3.1 Growth in length with regard to body mass

The exponents, correlation coefficients and significance values for bone lengthening in foetuses and postnatal giraffes are summarised in Table 3.2 and the growth curves for postnatal giraffes are shown in Figure 3.2.

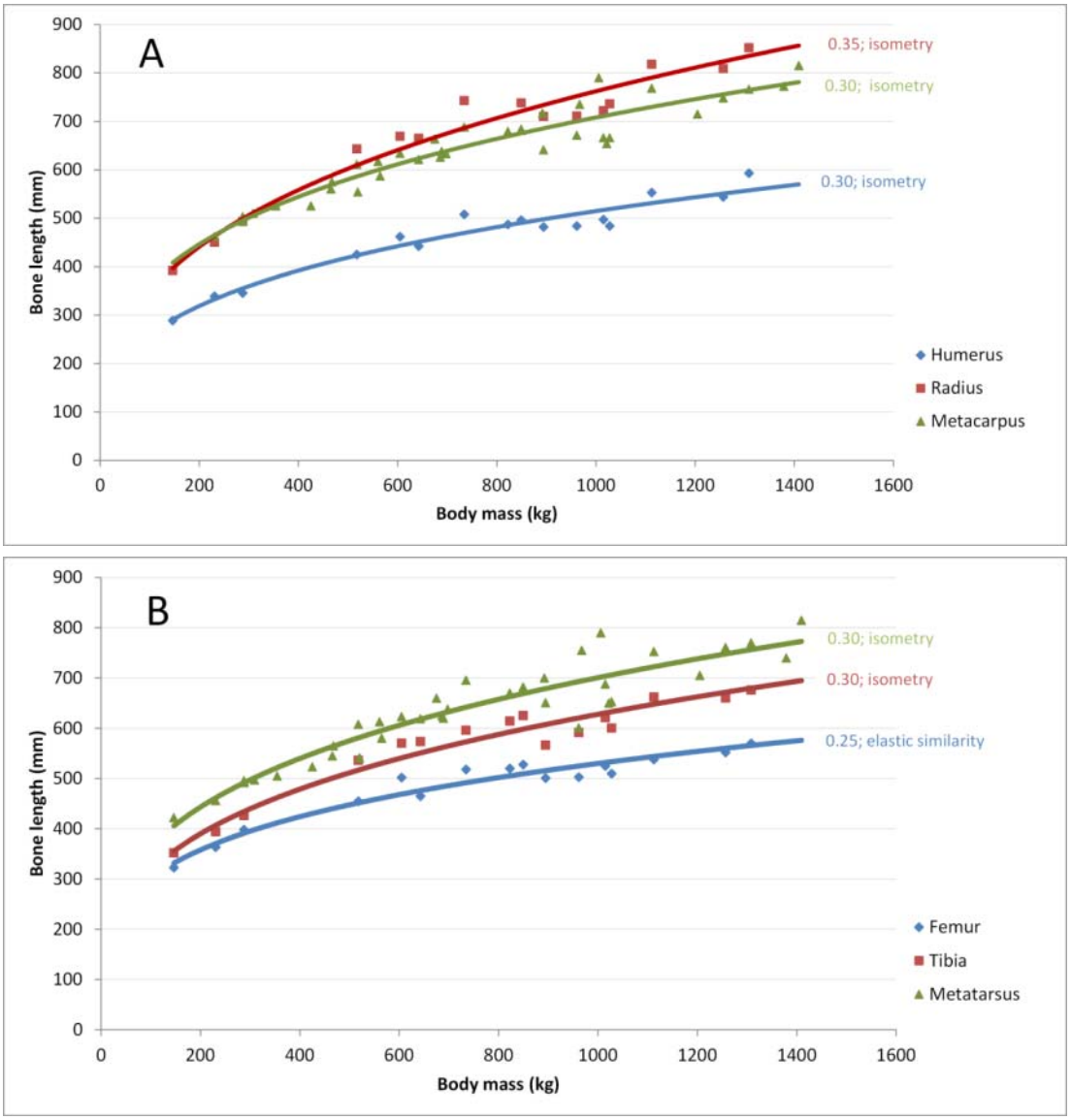


***Figure 3.2 Growth of limb bone length relative to body mass in postnatal animals. (A) Depicts front limb and (B) hind limb bones. Note that curves with the same exponent will differ in presentation because of different allometric coefficients. All exponents except the femur were significantly greater than elastic similarity, but not different from geometric similarity/isometry. The allometric exponent and its classification are indicated next to each curve.***

Foetal limbs grew relatively faster than postnatal limbs: Exponents of total leg length (lengths of constituent bones summated) vs. body mass were significantly greater in the foetus than in postnatal animals ($P_{(H0:\ Foetal\ frontlimb\ =\ postnatal\ frontlimb)} = 0.023$; $P_{(H0:\ foetal\ hindlimb\ =\ postnatal\ hindlimb)} = 0.006$). Considering individual bones, the metacarpus ($P_{(H0:\ foetal\ =\ postnatal\ exponent)} = 0.004$) and femur ($p_{(H0:\ foetal\ =\ postnatal\ exponent)} = 0.001$) grew faster in the foetus than postnatally. On the other hand there were no significant pre- and postnatal differences in the humerus ($P_{(H0:\ foetal\ =\ postnatal\ exponent} = 0.06$), radius ($P_{H0:\ foetal\ =\ postnatal\ exponent} = 0.80$), tibia ($P_{(H0:\ foetal\ =\ postnatal\ exponent)} = 0.03$; sequential Bonferroni adjusted significance level = 0.01) and metatarsus ($P_{(H0:\ foetal\ =\ postnatal\ exponent)} = 0.62$).

In the postnatal animal, total front- and hind limb growth could be summarised with a common negatively allometric exponent of 0.28 (95% confidence interval = 0.26-0.31;

$P_{(H0:\ front\ limb\ exponent\ =\ hind\ limb\ exponent)}$ = 0.50). Testing this common against both the elastic similarity model as well as the geometric similarity model fails to reject either one ($P_{(H0:\ b\ =\ 0.25)}$ = 0.02; $P_{(H0:\ k\ =\ 0.333)}$ = 0.002). The constituent front and hind limb zeugopodial (radius and tibia) and metapodial (metacarpus and metatarsus) limb bones could be summarised with common slopes (0.33 and 0.30 respectively), but the humerus and femur had significantly different slopes ($P_{(H0:\ humerus\ slope\ =\ femur\ slope)}$ = 0.015; Table 3.2).

The individual foetal exponents were significantly greater than the elastic similarity exponent in all cases ($P_{(H0:\ k\ =\ 0.25)}$ ≤ 0.002). Similarly, all the individual postnatal bone exponents except the femur were significantly greater than elastic similarity ($P_{(H0:\ exponent\ =\ 0.25)}$ = ≤ 0.004), but not significantly different to geometric similarity. Thus, none of the individual postnatal limb bones grew disproportionately faster in length relative to increases in body mass.

Table 3.3 shows the absolute lengths and proportions of the bones in foetal (50 kg) and postnatal giraffes (100 kg–1300 kg). The sum of the lengths of the front limb bones was longer than the total length of the hind limb bones throughout ontogeny (from about 19 mm longer in a neonate to about 160 mm longer in an adult 1300 kg giraffe). The humerus and femur were always the shortest of the bones: In the front limb, the proportional contribution of the humerus to the total was relatively constant at 25.7 ± 0.5% while the femur's decreased from 30.2% to 28.2% of the hind limb. The proportion of total length formed by the radius and tibia increased from 34.7% and 31.5% to 38.7% and 33.8% of limb length, respectively. Conversely, the proportion of leg length contributed by the metacarpus decreased from 39.4% to about 35.5%, while that of the metatarsus remained about 38%. In the forelimb, the radius started shorter and ended longer than the metacarpus, overtaking the metacarpus in the first year of life while in the hind limb the tibia was always shorter than the metatarsus (a one-year-old giraffe weighs between 260 kg and 300 kg; G. Mitchell, unpublished data, personal communication). As final metapodial lengths are similar, the final difference of 160 mm between forelimb and hind limb total bone length is almost completely a consequence of the difference in lengths of the tibia and radius (159 mm).

***Table 3.3 Bone lengths at different life stages predicted from allometric equations presented in this study***

| Length measurement | 50 kg | 100 kg | 500 kg | 1000 kg | 1300 kg |
|---|---|---|---|---|---|
| Humerus | 210 (25%) | 264 (26%) | 418 (26%) | 516 (26%) | 559 (26%) |
| Radius | 286 (34%) | 354 (35%) | 602 (38%) | 765 (38%) | 838 (39%) |
| Metacarpus | 340 (41%) | 401 (39%) | 577 (36%) | 711 (36%) | 769 (36%) |
| Total front limb | 836 | 1018 | 1597 | 1992 | 2166 |
| Femur | 229 (28%) | 302 (30%) | 446 (29%) | 530 (28%) | 566 (28%) |
| Tibia | 245 (30%) | 315 (32%) | 509 (33%) | 627 (34%) | 679 (34%) |
| Metatarsus | 331 (41%) | 382 (38%) | 572 (37%) | 704 (38%) | 761 (38%) |
| Total hind limb | 805 | 999 | 1527 | 1861 | 2006 |

*Note: The 100 kg predictions displayed here are the average of foetal and post natal equations for 100 kg. Predictions in mm, with the percentage the bone contributes to the respective limb noted in brackets.*

### 3.3.3.2 Cross sectional properties

#### *3.3.3.2.1 Increase in diameter and circumference with body mass as the covariate*

Table 3.4, Table 3.5 and Figure 3.3 summarise changes in diameter as body mass increases. A one way ANOVA was conducted to test for differences in the mean diameter versus body mass slopes of foetal and postnatal samples along CC and ML dimensions. Slopes were significantly different among the four groups ($F_{(3,\ 20)} = 23.76,\ P<0.001$). Post hoc tests indicated that mean foetal diameter exponents were significantly higher ($P<0.01$) than postnatal animals (mean CC slope foetus = 0.46 ± 0.04, mean ML slope foetus = 0.45 ± 0.03, mean CC slope postnatal = 0.32 ± 0.05, mean ML slope postnatal = 0.35 ± 0.03). The 95% confidence intervals for mean foetal diameters were higher than both isometry (viz., 0.33) and elastic similarity (viz., 0.38), whereas the confidence intervals for mean postnatal growth were not different from isometry.

The same general pattern was seen when individual bone diameters were evaluated. The growth rate of foetal diameters with regard to body mass was not different to elastic similarity and thus greater than geometric similarity. In certain cases however (femur and tibia CC and ML), the exponents were not significantly different from either geometric or elastic similarity due to wide confidence intervals.

*Table 3.4 Mean bone diameters (average CC and ML) and circumferences at different life stages of the giraffe*

| Body mass | 50 kg | 100 kg | 500 kg | 1000 kg | 1300 kg |
|---|---|---|---|---|---|
| | | | **Average diameter** | | |
| **Humerus** | 30 | 35 | 59 | 77 | 85 |
| **Radius** | 26 | 31 | 50 | 63 | 69 |
| **Metacarpus** | 24 | 30 | 44 | 54 | 58 |
| **Femur** | 28 | 35 | 52 | 64 | 69 |
| **Tibia** | 26 | 33 | 50 | 62 | 67 |
| **Metatarsus** | 23 | 28 | 42 | 52 | 56 |
| | | | **Average circumference** | | |
| **Humerus** | 92 | 109 | 179 | 234 | 259 |
| **Radius** | 86 | 103 | 163 | 205 | 224 |
| **Metacarpus** | 83 | 101 | 148 | 182 | 197 |
| **Femur** | 91 | 109 | 159 | 195 | 211 |
| **Tibia** | 90 | 106 | 163 | 202 | 219 |
| **Metatarsus** | 80 | 97 | 144 | 177 | 191 |

*Note: The 100 kg predictions are the average of foetal and postnatal equations for 100 kg. Predictions in mm.*

***Table 3.5 Allometric equations describing growth in diameter (CC and ML) and circumference with regard to body mass.***

| | Age group | n | r2 | Slope | 95% CI | Intercept | p(H0: k=0.333) (geometric) | P(H0: b= 0.375) (elastic) |
|---|---|---|---|---|---|---|---|---|
| **H CC** | F | 7 | 0.89 | 0.525 | 0.364 to 0.758 | 3.78 | 0.02 | 0.07 |
| **▲/ ▭** | PN | 13 | 0.96 | 0.423 | 0.373 to 0.480 | 4.39 | <0.01 | 0.06 |
| **H ML** | F | 7 | 0.96 | 0.442 | 0.350 to 0.557 | 5.05 | 0.03 | 0.13 |
| **— / ▭** | PN | 13 | 0.92 | 0.379 | 0.315 to 0.456 | 5.21 | 0.16 | 0.91 |
| **H circ** | F | 7 | 0.99 | 0.414 | 0.364 to 0.471 | 18.2 | 0.01 | 0.10 |
| **▲/ ▭** | PN | 16 | 0.97 | 0.386 | 0.348 to 0.427 | 16.3 | 0.01 | 0.56 |
| **R CC** | F | 7 | 0.99 | 0.421 | 0.374 to 0.473 | 4.60 | <0.01 | 0.05 |
| **—** | PN | 13 | 0.97 | 0.309 | 0.274 to 0.348 | 6.49 | 0.19 | <0.01 |
| **R ML** | F | 7 | 0.99 | 0.460 | 0.381 to 0.556 | 4.48 | <0.01 | 0.04 |
| **— / ▭** | PN | 13 | 0.98 | 0.371 | 0.337 to 0.407 | 5.37 | 0.03 | 0.78 |
| **R circ** | F | 7 | 0.97 | 0.389 | 0.319 to 0.474 | 18.8 | 0.10 | 0.67 |
| **—** | PN | 16 | 0.98 | 0.337 | 0.308 to 0.369 | 20.1 | 0.80 | 0.02 |
| **Mc CC** | F | 7 | 0.97 | 0.479 | 0.333 to 0.689 | 3.56 | 0.01 | 0.15 |
| **▼** | PN | 24 | 0.95 | 0.286 | 0.258 to 0.318 | 7.03 | 0.01 | <0.01 |
| **Mc ML** | F | 7 | 0.90 | 0.502 | 0.345to 0.730 | 3.60 | 0.05 | 0.10 |
| **— / ▭** | PN | 24 | 0.96 | 0.331 | 0.302 to 0.363 | 5.70 | 0.90 | 0.01 |
| **Mc circ** | F | 7 | 0.99 | 0.413 | 0.371 to 0.460 | 16.5 | <0.01 | 0.07 |
| **▼** | PN | 31 | 0.95 | 0.301 | 0.277 to 0.327 | 22.8 | 0.02 | <0.01 |
| **F CC** | F | 7 | 0.90 | 0.453 | 0.315 to 0.652 | 5.02 | 0.08 | 0.25 |
| **—** | PN | 13 | 0.97 | 0.311 | 0.280 to 0.346 | 7.85 | 0.19 | <0.01 |
| **F ML** | F | 7 | 0.86 | 0.484 | 0.317 to 0.739 | 4.22 | 0.07 | 0.19 |
| **—** | PN | 13 | 0.98 | 0.306 | 0.280 to 0.335 | 6.89 | 0.06 | <0.01 |
| **F circ** | F | 7 | 0.94 | 0.371 | 0.281 to 0.490 | 21.4 | 0.37 | 0.92 |
| **▼** | PN | 16 | 0.97 | 0.293 | 0.266 to 0.324 | 25.7 | 0.02 | <0.01 |
| **T CC** | F | 7 | 0.90 | 0.464 | 0.324 to 0.665 | 3.86 | 0.07 | 0.19 |
| **—** | PN | 13 | 0.91 | 0.296 | 0.244 to 0.359 | 6.82 | 0.21 | 0.02 |
| **T ML** | F | 7 | 0.77 | 0.429 | 0.254 to 0.724 | 5.53 | 0.28 | 0.56 |
| **— / ▭** | PN | 13 | 0.98 | 0.335 | 0.301 to 0.372 | 7.11 | 0.93 | 0.04 |
| **T circ** | F | 7 | 0.94 | 0.338 | 0.253 to 0.451 | 23.9 | 0.91 | 0.40 |
| **—** | PN | 16 | 0.98 | 0.308 | 0.282 to 0.337 | 24.0 | 0.08 | <0.01 |
| **Mt CC** | F | 7 | 0.97 | 0.454 | 0.368 to 0.561 | 3.74 | 0.01 | 0.07 |
| **—** | PN | 24 | 0.94 | 0.296 | 0.266 to 0.330 | 6.69 | 0.03 | <0.01 |
| **Mt ML** | F | 7 | 0.94 | 0.435 | 0.331 to 0.572 | 4.35 | 0.05 | 0.23 |
| **— / ▭** | PN | 24 | 0.93 | 0.350 | 0.312 to 0.392 | 4.71 | 0.38 | 0.22 |
| **Mt circ** | F | 7 | 0.93 | 0.384 | 0.285 to 0.518 | 2.88 | 0.28 | 0.84 |
| **▼** | PN | 31 | 0.93 | 0.299 | 0.270 to 0.330 | 3.11 | 0.04 | <0.01 |

*Note: In all cases the underlying regressions were significant (i.e. p<0.05). The last two columns indicate the probability of the exponent (b) being geometrically similar (0.333) or elastically similar (0.375). The significance level for each test was adjusted according to the sequential Bonferroni technique (Rice, 1989). Postnatal bone growth patterns are highlighted with a key: — geometric similarity, ▱ elastic similarity, ▲ positive allometry, ▼ negative allometry. In cases where growth could not be distinguished from either geometric similarity or elastic similarity, or where allometries were both positive and elastically similar, two keys are shown [were indicated]. n = number of animals sampled, CI = confidence interval, F = fetus, PN = postnatal animal, CC = cranio-caudal diameter, ML = medio-lateral diameter, circ = circumference, H = Humerus, R = Radius, Mc = Metacarpus, F = Femur, T = Tibia, Mt = Metatarsus.*

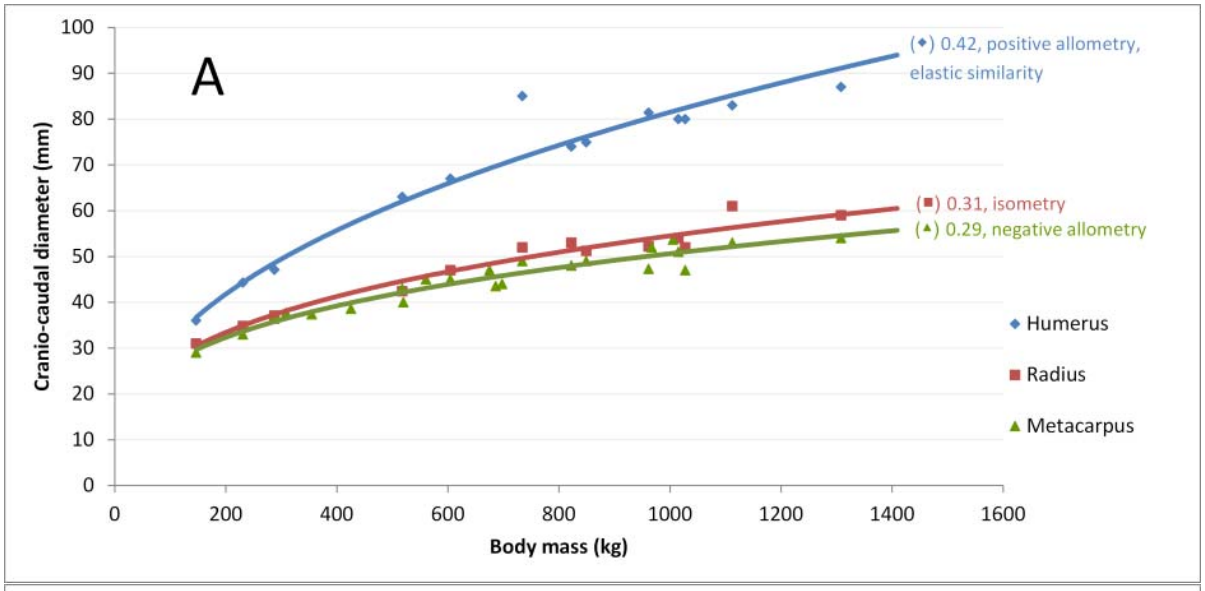


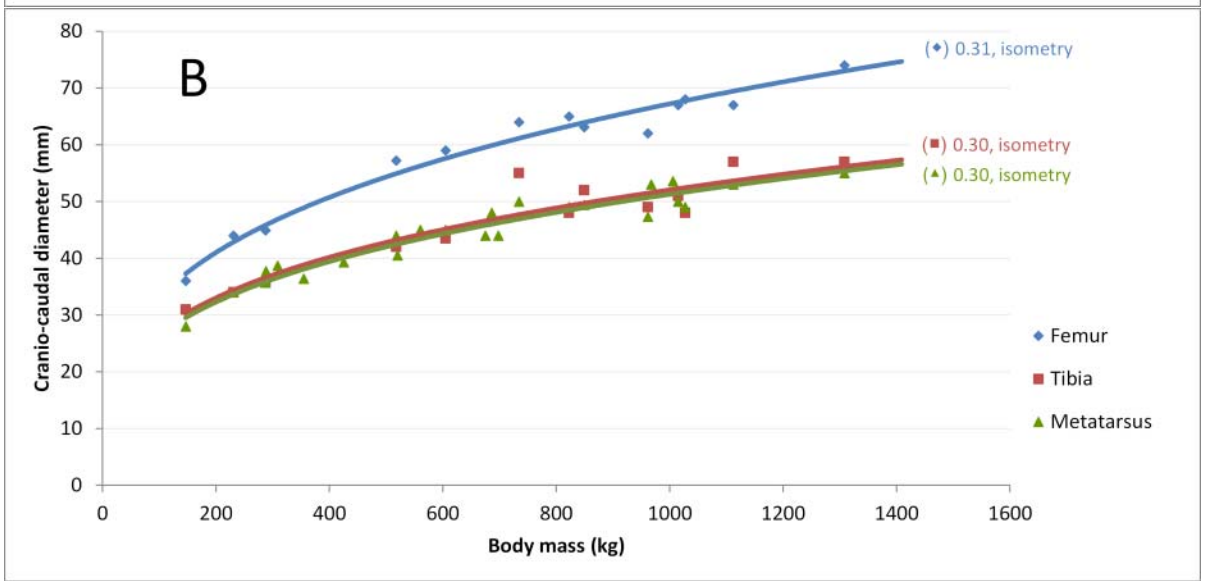

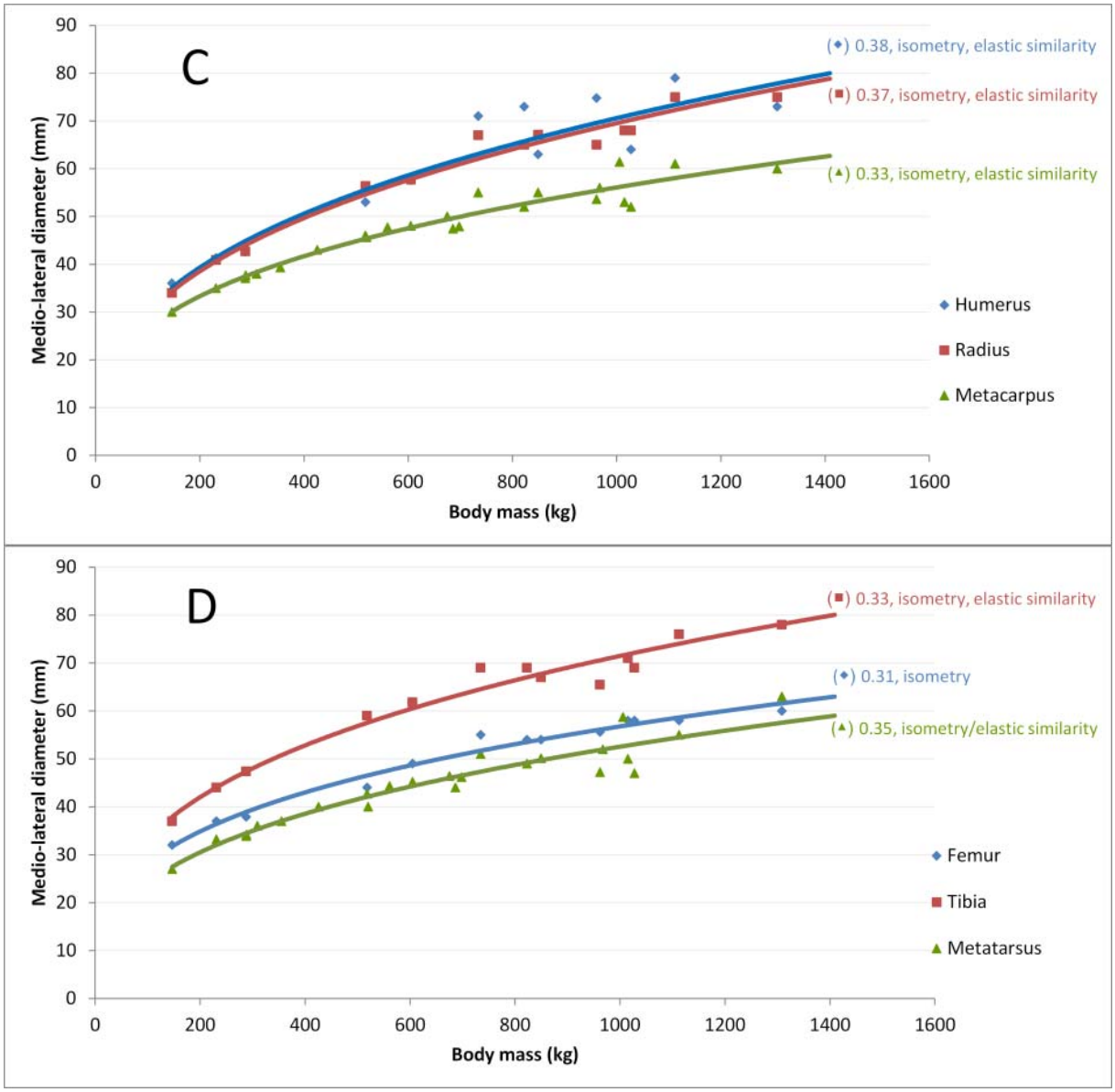


***Figure 3.3 Diameters of the long bones of the postnatal appendicular skeleton with regard to body mass. CC diameters are indicated in parts (A) and (B) and ML diameters in parts (C and D). Note the positively allometric and elastically similar growth of the humerus in CC diameter. The only bones to grow with significant negative allometry were the metacarpals in CC diameter. None of the other bone diameters could be discerned from isometry with enough statistical certainty. The allometric exponent and its classification are indicated next to each curve.***

In postnatal animals the humerus CC (0.42, positive allometry) and metacarpus CC (0.29, negative allometry) exponents were significantly different from isometry ($p_{(H0:k = 0.333)}$ = 0.002 and 0.006 respectively). The humerus CC was the only exponent not significantly different from elastic similarity ($P_{(H0:b=0.375)}$ = 0.06). None of the ML slopes were significantly different from isometry. However it is important to consider that, apart from the femur ML ($P_{(H0:b=0.375)}$ < 0.001), none of the ML slopes were significantly different from elastic similarity either. This indicates that confidence intervals for ML exponents are too wide to detect significant differences from either isometry or negative allometry. The probability for elastic similarity is however greater than isometry in the humerus and radius ML diameter:

$P_{(H0:b=0.375)}$ = 0.91 (humerus) and 0.78 (radius); $P_{(H0:k = 0.333)}$ = 0.16 (humerus) and 0.03 (radius).

Increases in circumference followed the same general pattern as diameter. In the foetus, neither null model (elastic or geometric similarity) could be rejected for hindlimb circumferences (Table 3.5). In the frontlimb, geometric similarity could be rejected for the humerus and metacarpus. The difference between the mean foetal (0.38 ± 0.03) and postnatal (0.32 ± 0.04) exponents was significant (*p<0.01*). Changes in postnatal circumference were positively allometric in the humerus (exponent = 0.39), negatively allometric in the femur (exponent = 0.29) and metapodials (both exponents = 0.30), and isometric in the radius (exponent = 0.33) and tibia (exponent = 0.31). Only the humerus increased in circumference according to elastic similarity.

In the postnatal forelimb absolute circumference decreased from proximal to distal bones. The circumference of the humerus increased more (2.7-fold) than that of the radius (2.4-fold) or metacarpus (2.2-fold) from birth to adult. In the hind limb the increase in tibial circumference was the greatest. As would be expected from the circumferential growth exponents, hind limb bone thicknesses stayed fairly constant relative to each other: the diameters increased from 2.1 (femur) to 2.2-fold (tibia and metatarsus) from neonate to adult.

*3.3.3.2.2 Increase in diameters and circumference with bone length as covariate*

A one way ANOVA was conducted to test for differences in the mean foetal and postnatal diameter vs. bone length slopes. A significant difference was found ($F_{(3, 20)}$ = 4.09, $P$ = 0.02) amongst foetal CC (1.29±0.14), ML (1.27 ± 0.11), postnatal CC (1.05 ±0.21) and ML (1.13 ± 0.08) slopes. Nevertheless, post hoc t-tests using the sequential Bonferroni technique could not show a difference between corresponding foetal and postnatal groups ($P_{(CC\ foetal = postnatal)}$ = 0.04, $P_{(ML\ foetal = postnatal)}$ = 0.03. Similarly, when individual dimensions were compared across these age groups, only the radial diameters (CC and ML) and the metatarsus CC diameter could be shown as significantly different (radius $CC_{foetus\ slope}$ = 1.24 compared with $CC_{postnatal\ slope}$ = 0.88, $P_{(H0:\ foetus\ slope = postnatal\ slope)}$ = 0.002; radius $ML_{foetus\ slope}$ = 1.35 compared with $ML_{postnatal\ slope}$ = 1.06, $P_{(H0:\ foetus\ slope = postnatal\ slope)}$ = 0.034); metatarsus $CC_{foetus\ slope}$ = 1.48 compared with $CC_{postnatal\ slope}$ = 0.96, $P_{(H0:\ foetus\ slope = postnatal\ slope)}$ = 0.004). This was because the small foetal sample sizes caused much wider confidence intervals for the exponents, decreasing the power to detect differences from post natal samples.

For the same reason many of the foetal exponents could not be distinguished from isometry despite being large. The humeral CC exponent was positively allometric (1.41) but its ML exponent was still isometric (1.18), similar to both femoral diameters (CC = 1.11 and ML = 1.18). Radial exponents increased with significant positive allometry in both diameters ($CC_{foetus\ slope}$ = 1.24, $ML_{foetus\ slope}$ = 1.35). Neither of the tibial diameters could be distinguished from isometry ($CC_{foetus\ slope}$ = 1.26, $ML_{foetus\ slope}$ = 1.09). Similarly, the

metacarpal exponents could not be shown different from isometry despite being large ($CC_{foetal\ slope}$ = 1.26, $ML_{foetal\ slope}$ = 1.32), whereas the metatarsals could ($CC_{foetal\ slope}$ = 1.48, $ML_{foetal\ slope}$ = 1.42).

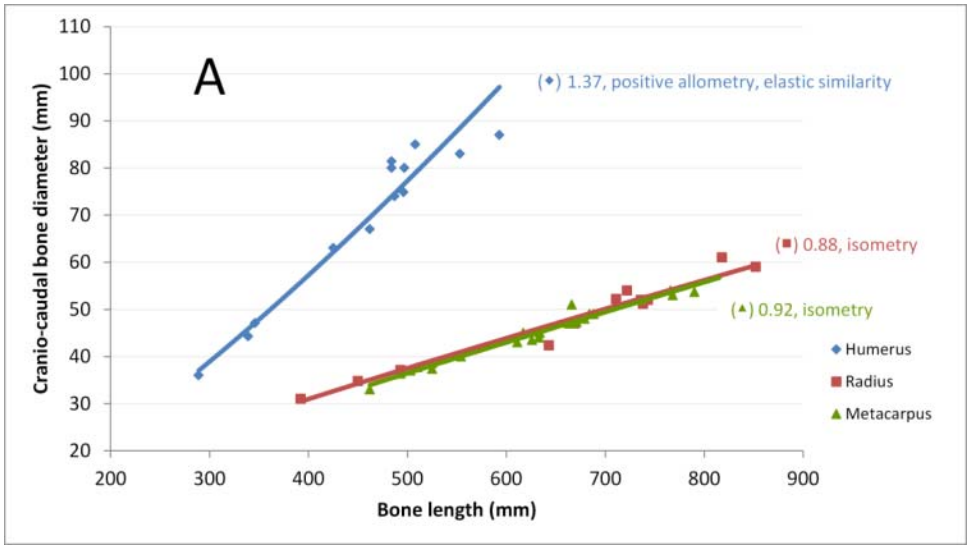


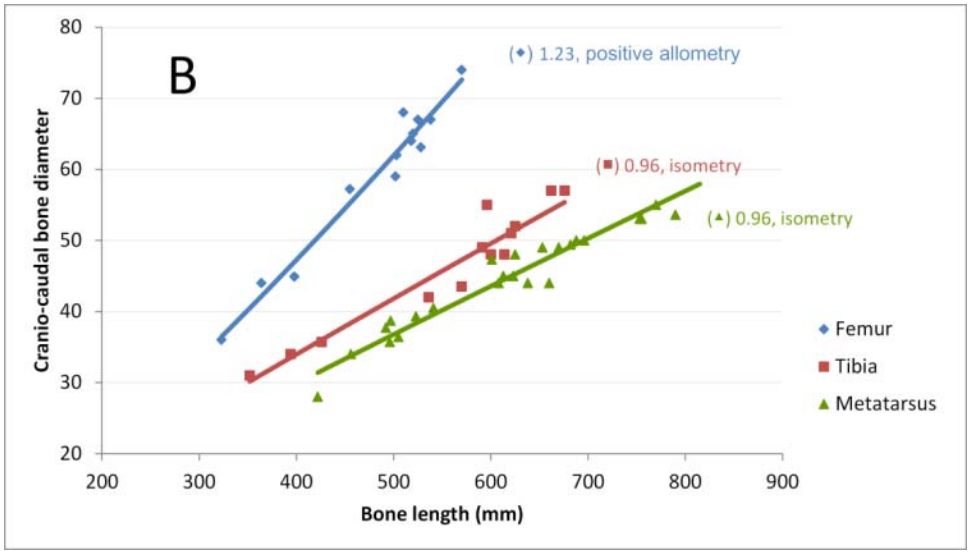


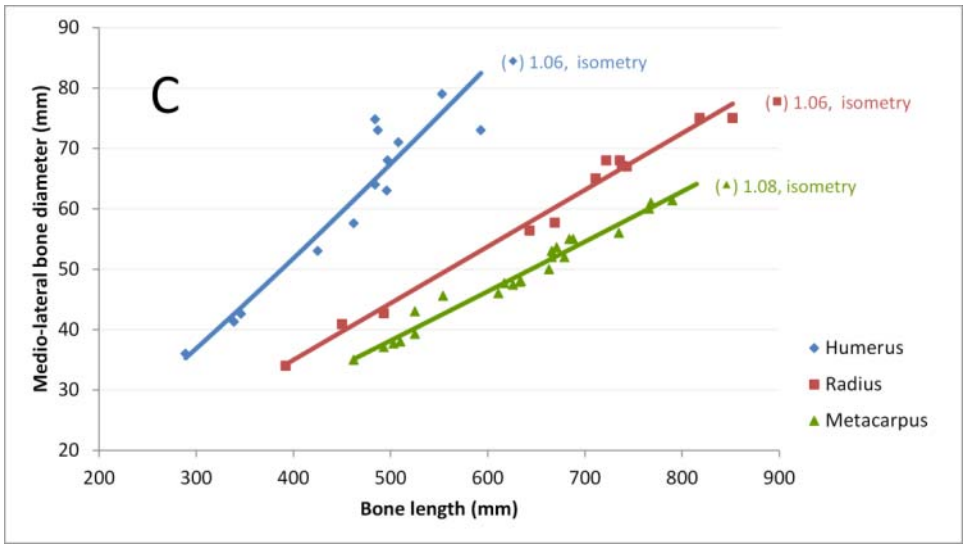

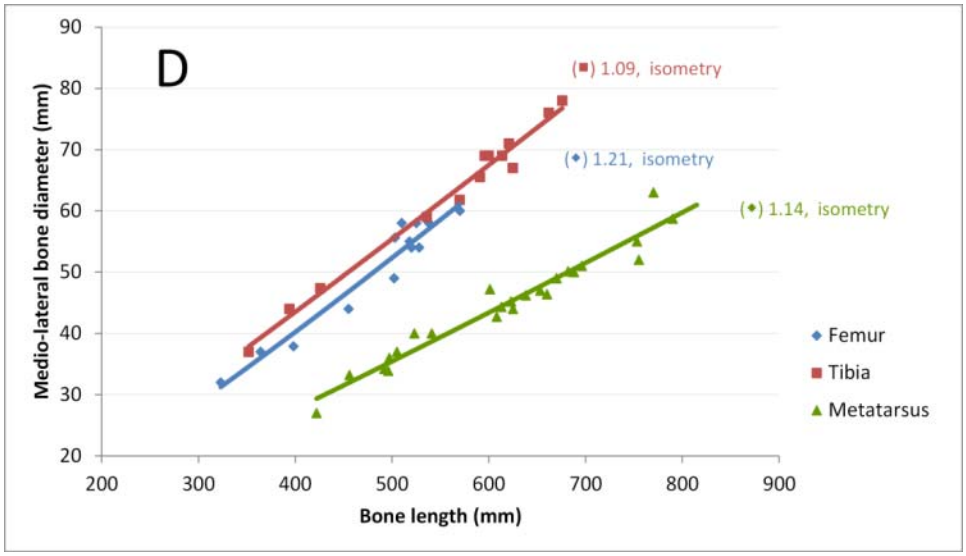


***Figure 3.4 Diameter versus length plots in post natal animals. CC diameters are indicated in (A) and (B) and ML diameters in (C) and (D). Note the positive allometric scaling of the humerus and femur in both diameters. The allometric exponent and its classification are indicated next to each curve.***

Figure 3.4 illustrates the relationship between bone diameter and bone length in postnatal giraffes during growth. During this phase both CC diameters of the humerus ($CC_{postnatal\ slope}$ = 1.37) and femur ($CC_{postnatal\ slope}$ = 1.23) increased with positive allometry relative to increases in bone length (for both bones $P_{(H0:\ slope = 1.00)} \leq 0.002$). The craniocaudal exponent of the humerus was not significantly different from elastic similarity (viz., 1.5), the only diameter to increase in this way out of all postnatal bones (for all other bones $p_{(H0:\ slope =1.5)} \leq 0.003$). Diameters of long bones below the elbow and knee did not grow significantly different from isometry (note that the sequential Bonferroni technique was applied to post hoc comparisons, with $k_t = 4$, and therefore certain p-values ≤0.05 were still considered non-significant.) In the bones below the elbow and knee the ML diameter exponents were significantly greater than the CC exponents ($P_{(H0:\ CC = ML\ slope)} \leq 0.023$), except in the tibia.

When considering increases in bone circumference with regard to increases in bone length, a significant difference between the mean foetal and postnatal slopes could not be detected (mean exponent = 1.07 for both). The diameters of the humerus (exponent = 1.27) and femur (exponent = 1.18) in postnatal giraffes increased positively allometric with regard to bone length ($p_{(H0:\ slope = 1.00)} \leq 0.006$), while those in all the other bones increased isometrically (exponents range from 0.97 to 1.02).

In summary, foetal diameter and circumference vs. bone length slopes could not be shown significantly higher than postnatal slopes. Postnatal humeral and femoral diameters and circumferences increased relatively faster than length. Craniocaudal diameters increased relatively slower than that of mediolateral diameters in the bones below the humerus, to the extent that the distal front leg bones become relatively more slender in the cranio-caudal plane as the animal matures.

Comparing the bone length: circumference ratio gives a measure of how robust bones are. The mean ratio (from neonate to adult) for the humerus is 2.3 which is more robust than

that of the femur (ratio = 2.8, t-test, p<0.001). However, the opposite is true for the radius and tibia—the radius's mean ratio was 3.7, significantly less robust (p<0.001) than the mean tibia ratio (3.1). The mean metatarsal ratio (4.0) is slightly albeit significantly greater than the metacarpal ratio (3.9, p=0.017). These ratios also illustrate that the metapodials are far more gracile than other limb bones.

*Changes in cross sectional area with body mass and bone length as covariates*

Relative to increases in body mass the mean foetal (0.91 ± 0.03) and postnatal (0.66 ± 0.07) exponents were significantly different (p<0.01).

In postnatal animals, none of the CSA versus body mass slopes were significantly different from isometry ($p \geq 0.018$, using sequential Bonferroni technique). Nevertheless, unlike the other bones ($p \leq 0.013$), the humerus and radius CSA slopes were also not significantly different from elastic similarity ($Bm^{0.80}$, $P_{(H0: slope = 0.75)} = 0.36$ and $Bm^{0.68,}$ $P_{(H0: slope = 0.75)} = 0.03$ respectively, sequential Bonferroni technique). The radius CSA slope has a much higher probability (p = 0.81) of being similar to isometry however, and its non-significant difference to the elastic similarity exponent was probably brought about by loss of power by the Bonferroni technique (Figure 3.5 A and B). The mean foetal CSA versus bone length slope was significantly higher (mean = 2.52 ± 0.22, isometry = 2.00) from the postnatal mean (2.17 ± 0.28; $p<0.05$). During postnatal growth only the humerus and femur could be shown to have a CSA growth pattern that was significantly and positively allometric relative to increases in length ($p \leq 0.004$; Figure 3.5 C and D).

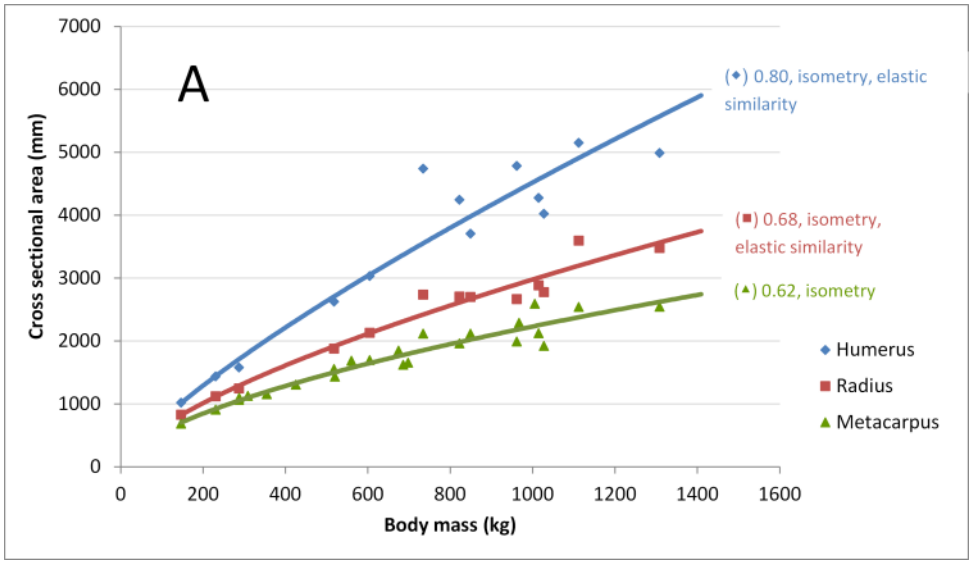


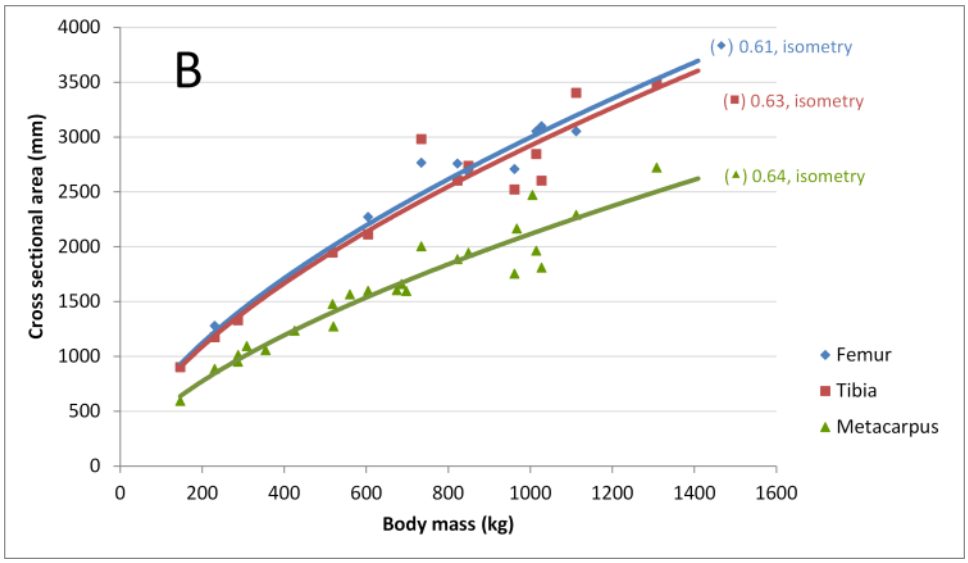


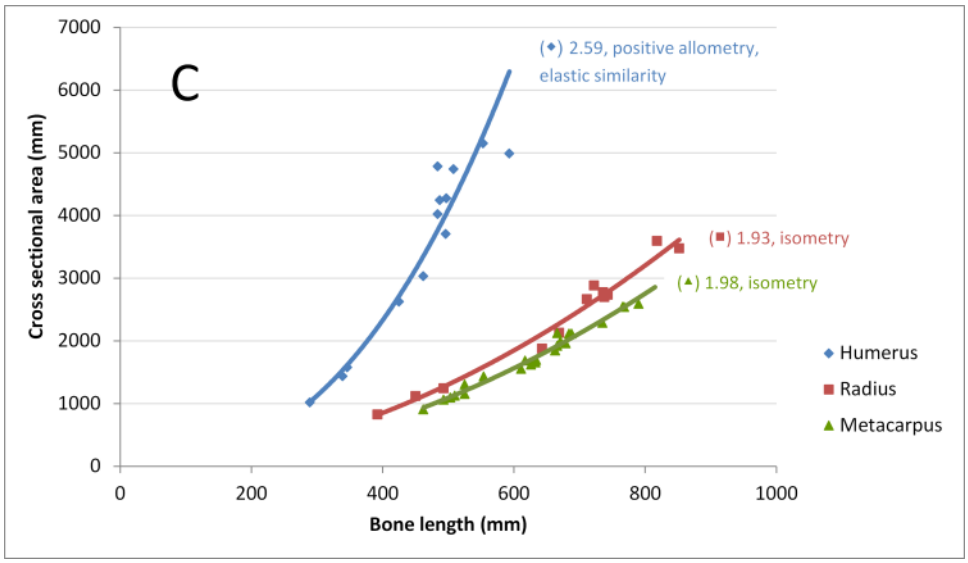

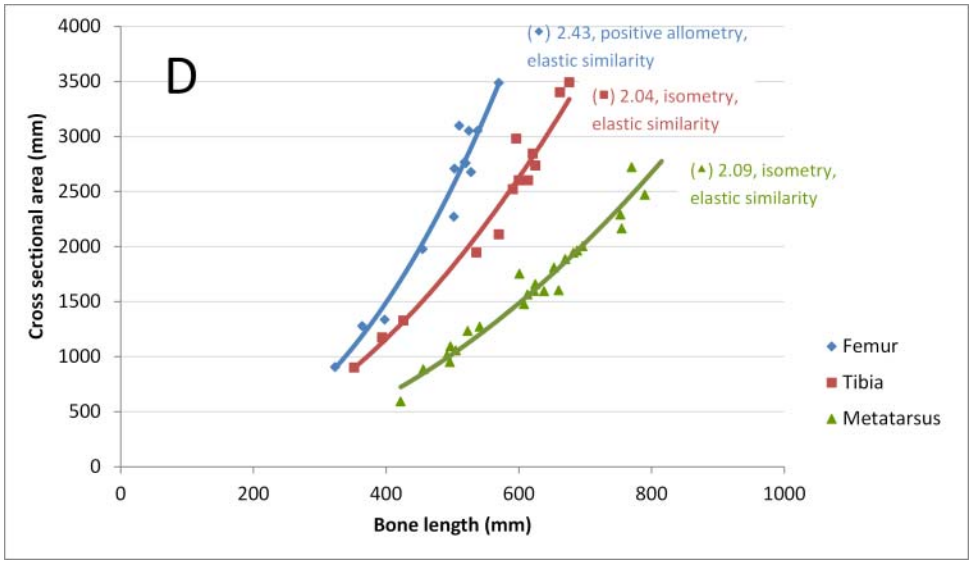


***Figure 3.5 Growth in CSA with regard to body mass and bone length. Growth with regard to body mass is indicated by parts (A) and (B) while (C) and (D) indicates growth with regard to bone length. When compared to body mass, none of the exponents could be shown different from isometry, despite some (humerus and radius) also being equal to elastic similarity. When compared to bone length, however, both the humerus and femur increase with positive allometry. The allometric exponent and its classification are indicated next to each curve.***

## 3.4 Discussion

### 3.4.1 Pre- and postnatal growth differences

This study has illustrated that, as expected, there are significant differences between pre- and postnatal limb bone development in giraffes. Although the foetal skeleton is shaped through epigenetic as well as genetic factors (Carter *et al.* 1996), it nevertheless does not have to support weight. The postnatal skeleton on the other hand has to respond to stresses and strains imposed by an increasing body mass and movement, and shapes itself to incorporate the necessary safety factors against failure.

The transition from a life *in utero* to that outside of it will therefore only be successful if certain 'day one' skeletal competencies have been established before birth. It follows that these competencies are almost wholly genetically dependent. In this chapter it was demonstrated that in the prenatal skeleton, where the effects of gravity are countered by the buoyancy inside the uterus, growth proceeds in length and width positively allometrically with regard to body mass. Postnatally however, this positive allometric trend does not continue and could have at least four explanations: It is not possible genetically, not possible biomechanically or too costly in terms of anatomical and physiological requirements. A fourth scenario might be that there was no drive for further increases in length and that adaptation in this regard remained 'neutral'.

### 3.4.2 Sexual dimorphism

At the onset of the study, sexual dimorphism was not expected between equivalent body mass giraffes—a supposition that turned out to be correct. Our expectation was based on the lack of dimorphism in giraffe neck length and cervical vertebrae growth patterns (Mitchell *et al.* 2009a, 2013a; Van Sittert *et al.* 2010). The results reported here further confirm that sexual selection has not played a major (if any) role in the evolution of tallness in giraffes.

### 3.4.3 Long bone length vs. body mass

Long bone length growth relative to body mass does not give an indication of the slenderness of the bone, but does highlight whether the limb bones lengthen faster than body size or not. The lack of significant pre– and postnatal differences could mean that the long bones grew at a similar rate pre– and postnatally (probably radius and metatarsus) or that confidence intervals were too wide to detect a difference (probably humerus and tibia). Although limb bones lengthened with positive allometry *in utero*, it was not foreseen that none of the giraffe limb bones would grow with positive allometry after birth, given the remarkable length of the legs. In fact, compared to other animals studied, giraffes do not seem to have uniquely high postnatal limb lengthening exponents at all (Figure 3.6A). This finding begs further data on ontogenetic limb lengthening in other species, especially artiodactyls.

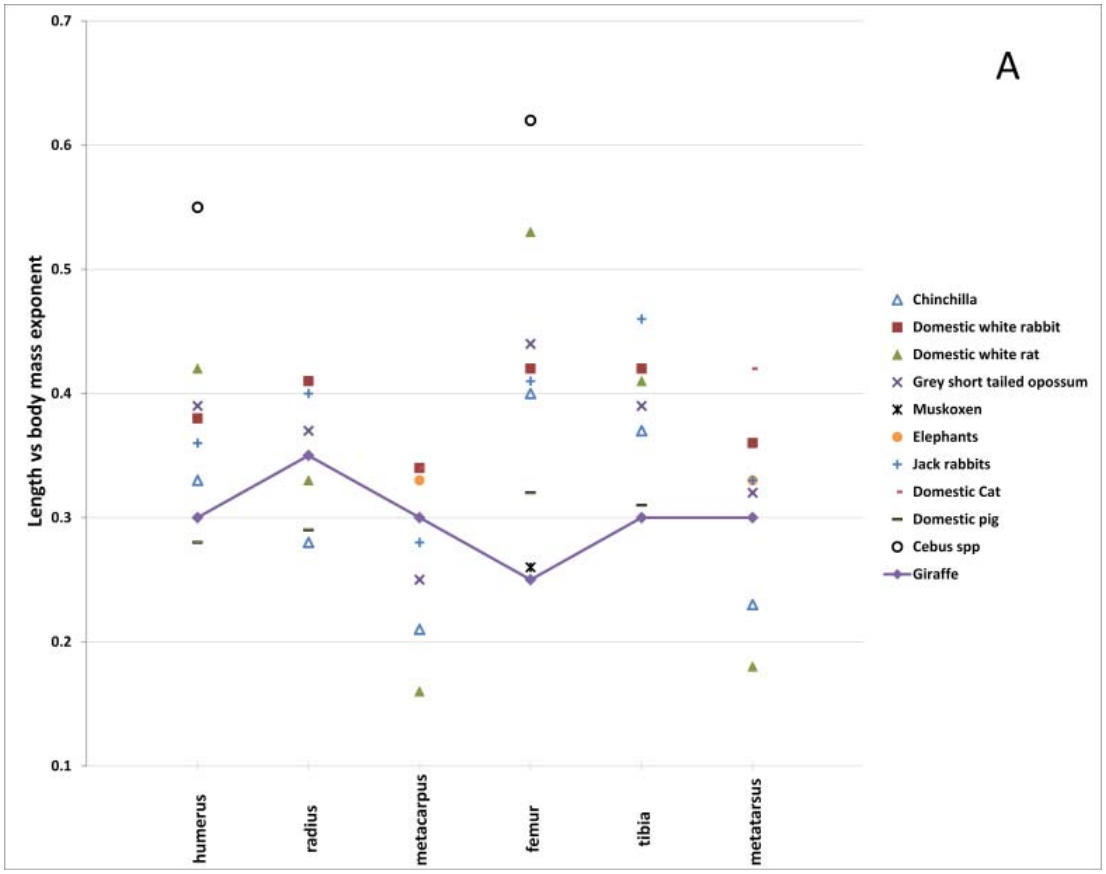


***Figure 3.6A's caption continued below.***

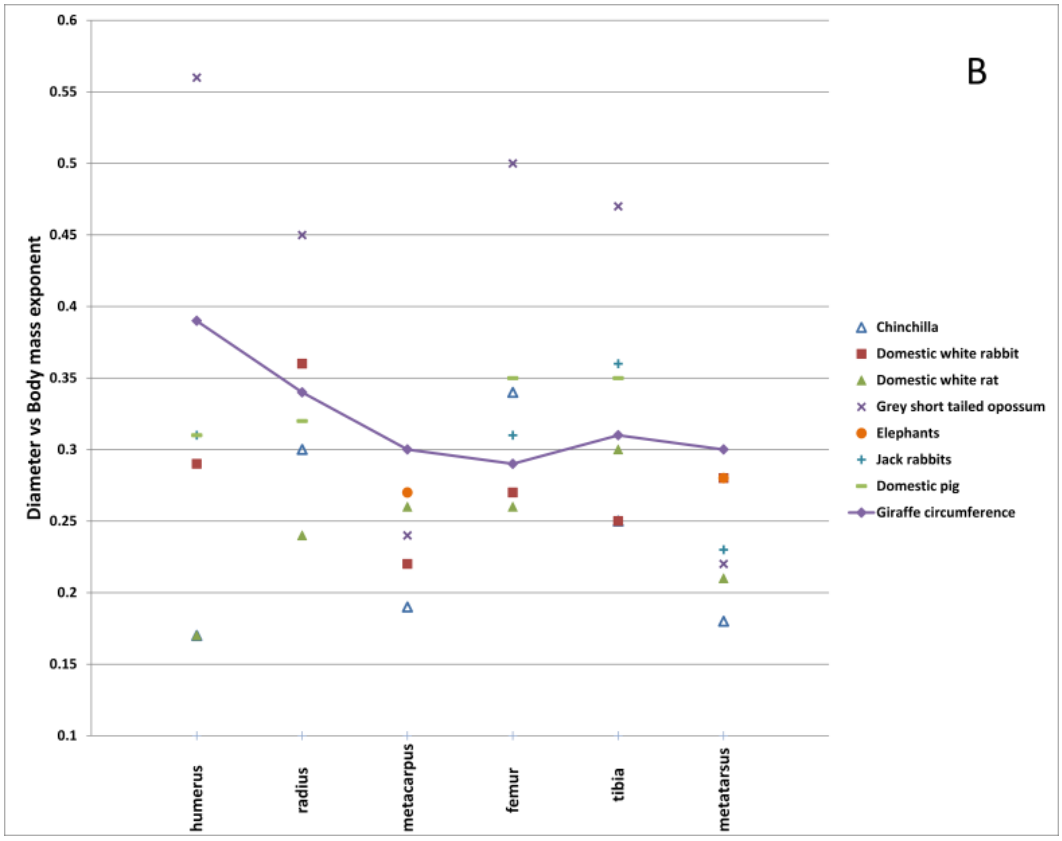


***Figure 3.6 Length and diameter vs body mass ontogenetic exponents of previously described mammalian species. (A) Length versus body mass ontogenetic exponents of previously described species. Note that giraffe exponents are within the range of previously described exponents, except in the femur and tibia where it is, surprisingly, slightly lower than previously described exponents. (B) Diameter versus body mass exponents of previously described species. Because two giraffe diameters were taken in this study, the circumference exponent was chosen to represent average diameter growth. Giraffes do seem to have higher metapodial exponents, but note that there are no artiodactyls in the metapodial samples. Furthermore, data on artiodactyls comparable to this study are still very scant, and conclusion should be drawn with caution. Data from Carrier (1983); Heinrich et al. (1999); Lammers & German (2002); Liu et al. (1999); Miller et al. (2008); Young(2008)***

The postnatal negatively allometric/isometric lengthening of limb bones contrasts with the positively allometric lengthening of the C2-C7 cervical vertebrae (mean cervical scaling exponent = 0.41 ± 0.01), and is also less than the more isometric T2-T14 and L1 to L5 vertebrae (both 0.34 ±0.01; Van Sittert *et al.* 2010). The fastest growth in leg length occurred in the first year of life with the final limb length of mature animals being approximately twice their length at birth compared to a three-fold increase in neck length (Mitchell *et al.* 2009a). Giraffes thus have relatively longer limbs and shorter necks per unit body mass as juveniles, and the remarkable length of limb bones per body mass seems to be established *in utero* already. Note that it is not unusual for a precocial species to have relatively longer legs as juveniles, where the animal needs to be mobile within hours after birth, and needs to take advantage of longer legs to increase speed and stride length (Carrier 1983; Grossi & Canals 2010; Heinrich *et al.* 1999). Furthermore, giraffe ontogenetic limb proportions do not seem to differ much from proportions known in other artiodactyls. For example, giraffe front limb proportions are in agreement with cervid proportions at birth, while hind limb proportions are only slightly different: giraffes have higher femoral (30%, cervid range 28-29%), lower tibial (32%, cervid range 36-38%) and higher metatarsal

(38%, cervid range 33-36%) proportions (Van der Geer *et al.* 2006). Adult giraffe limb bone proportions similarly fit within described cervid ranges in the front limb but were lower in the femur and tibia and higher in the metatarsus. Interestingly, cervid radii start out shorter but end up longer than the metacarpus, similar to giraffes.

The sum of the lengths of the three main bones of the front legs of giraffes is slightly longer than that of the hind legs (from about 40 mm in a neonate to 140 mm in an adult 1300 kg giraffe; Table 3.3). This finding supports an observation by Colbert in 1938 that, in contrast to other ruminants, the front legs of giraffe are longer than the back legs and thereby contribute to the appearance of a sloping back. It should be clarified, however, that, a) the sum of long bone lengths is not the same as leg length as the *manus* and *pes* is excluded, and b) contrary to what Colbert noted, neither the total front leg nor any of its constituent long bones lengthen significantly more than those of the hind legs. Rather, the radius starts out longer than the tibia at birth, with their relative growth rates staying fairly similar during postnatal ontogeny. Surprisingly, the longest bone in the giraffe limb was the radius and not the metacarpus. The appearance of a longer metacarpus is therefore probably an optical illusion caused by its remarkable slenderness and verticality, and the contrast with thicker limb diameter at the region of the radius. In the hindlimb however, the metatarsus is indeed longer than the tibia throughout growth.

### 3.4.4 Increase in diameter and circumference with regard to body mass

Giraffe long bones all increase in diameter and circumference *in utero* at a rate faster than increases in body mass. Conversely, postnatal diameters increase iso- or negatively allometric to body mass, except the humeral CC ($Bm^{0.42}$) and radial ML ($Bm^{0.37}$) diameters. In addition, although the humeral ML diameter could not be shown significantly different from isometry, the exponent is still high ($Bm^{0.38}$).

It may seem superfluous to report both diameter and circumferential measurements. However, bone circumference can be regarded as a summary of the two diameters and helps clarify patterns seen. For example, in postnatal giraffes only the humerus had a positive allometric change in circumference with regard to body mass, and thereby supports our conclusion that this bone becomes increasingly robust relative to body mass. The positive allometry of radial ML diameter are offset by the lower isometric CC increase resulting in an overall isometric increase in radial circumference. On the other hand femoral and metapodial circumferential growth does not keep up with increases in body mass. A second reason for including both circumferential and diameter data is to facilitate comparison with past and future studies, where often only one or the other is reported. Note as an example that metapodial circumferences, although increasing with negative allometry to body mass, still have higher exponents than other species previously reported (Figure 3.6B).

Counterintuitively, limb diameters and circumferences do not increase at a faster rate than body mass to compensate for the larger loads upon it, not even in the direction of limb

movement viz. craniocaudal diameter. This phenomenon is however not uncommon. Younger animals have 'overbuilt' bones to compensate for reduced bone stiffness and locomotor ability, causing long bones to become more gracile in ontogeny. Nevertheless, the fact that the giraffe humerus and radius (ML diameter) become more robust relative to body mass does seem to be an exception given the morphology of other giraffe long bones, and is almost certainly related to the positively allometric increase in neck mass during growth (Mitchell *et al.* 2013a; Mitchell & Skinner 2009). However, it is known that quadrupedal mammals typically support 60% of their body weight in the front limbs and it remains to be tested whether giraffes differ from other mammals in this regard. The relatively faster increase in ML diameters compared to CC diameters may be a requirement of weight support in limb design, but may also be related to safety factors required for when the giraffe drinks water and the front legs are splayed apart, putting more stress and strain on the mediolateral aspects of the bones. Other possible correlates to this effect such as mating behaviour, neck length and general artiodactyl traits need to be borne in mind and further data is needed before further conclusions can be reached.

### 3.4.5 Diameter and circumference vs. length

In this type of analysis, isometry denotes a bone that increases in length and diameter at the same rate.

Individual foetal and postnatal slopes could not be distinguished because of wide confidence intervals for foetal exponents. Whereas the stylopodial (humerus and femur) bones grew robust in both directions, the trend for zeugopodial and metapodial bones was to grow more robust in mediolateral direction than in craniocaudal direction. The greater robusticity of the humerus could indicate that the humerus carries more weight than the femur. On the other hand the tibia is probably exposed to higher stresses and strains than the radius especially in the CC direction. Interestingly, the femur becomes more robust with regard to its own length, but not with regard to body mass. It is proposed that this growth pattern reflects the larger proportion of the body mass that is carried in the neck and therefore front limb. Unfortunately, comparative ontogenetic data in the literature could not be found, and this proposition cannot be tested until further data becomes available. Nevertheless, this finding stresses the importance of interpreting changes in bone cross sectional area in terms of bone length as well as with regard to body mass.

This study found no long bone circumference to grow according to McMahon's (1975) elastic similarity model. This is perhaps not surprising in the light of Kilbourne and Makovicky's (2012) findings that showed elastic similarity (Length (L) $\propto$ Circumference (C)$^{0.67}$ or C $\propto$ L$^{1.5}$) to be the exception rather than the rule in ontogeny of mammals. Kilbourne and Makovicky also demonstrated that cetartiodactyl limb bones generally become more robust during ontogeny (i.e. L$\propto$C$<^{1.00}$). However, an interesting exception to this pattern was the okapi (*O. johnstoni*), in which the bone length to circumference exponents were >1.00 – that is, bones became increasingly slender during growth. As okapis represent the ancestral

morphology of giraffe (Mitchell & Skinner 2003) and both giraffes and okapis have slender legs compared to other ungulates (Kilbourne & Makovicky 2012; McMahon 1975; Scott 1990), it would not have been unreasonable to expect that giraffe legs would grow more gracile throughout ontogeny as well. Contrarily, this study has demonstrated that giraffes are born with such slender legs that they are either not capable of decreasing or that it would be of no benefit to decrease in relative circumference any further. This appears to us to be a classic example of ontogeny revealing key milestones in phylogeny as proposed by Pincher (1949). Pincher suggested that the evolution of neck elongation in giraffes was a secondary response to leg elongation, in order for the animal to reach the ground to drink. The problem with Pincher's hypothesis is, as shown in this study, that neck elongation proceeds disproportionately faster than leg elongation and does not simply 'trail' the elongating limbs. In other words, if long legs prevented the giraffe to drink water the giraffe would be disadvantaged throughout most of ontogeny before the neck finally 'caught up'. Leg elongation on the other hand may have been accompanied by increases in body mass which will have required more browsing strata from which to feed (Jarman-Bell Principle; Du Toit 2005), in turn necessitating disproportionate neck length increase. This idea is supported by studies that showed that giraffes utilise various feeding strata in trees (Cameron & Du Toit 2007) and even graze (Seeber *et al.* 2012). The neck therefore is not only advantageous during a dearth as proposed by Darwin (1888), but essential throughout all seasons.

### 3.4.6 Cross sectional area

Although it has been shown that long bone periosteal contours correlate highly with cross sectional properties in adult human populations, this does not necessarily hold for individuals, subadults nor for other species (Sparacello & Pearson 2010). In addition, cortical thickness has been shown to be significantly greater in giraffes compared to buffaloes (Van Schalkwyk *et al.* 2004). In order to see if the medullary cavity could have an influence on the findings made in this chapter, an estimate of endosteal area was subtracted from periosteal area, using cortical thickness measurements. However, the findings remained similar even when estimating cross sectional area without a medullary cavity. This is arguably a very rough estimate and more accurate measures of CSA as well as second moment of area are needed in future.

Goat and elephant CSA's become more gracile with body mass during growth: both scaling as $Bm^{0.53}$ (Main & Biewener 2004; Miller *et al.* 2008). Because this causes increased strain and reduced resistance to bending, it was proposed that younger animals have overbuilt bones to compensate for less stiff bones. The findings in this thesis that giraffe limb bones do not grow more gracile during growth mean either that giraffe calves do not have overbuild bones or that the long neck prohibits bones from becoming more gracile.

### 3.4.7 Practical application of giraffe allometric equations

Previous authors proposed the giraffe metapodials to be the seat of limb propulsion and elongation (Colbert 1938; McMahon 1975; Thompson 1917). Additionally, in proficient runners elongated distal elements are more energy efficient and increase stride length (Carrier 1983; Christiansen 2002; Lammers & German 2002; Young *et al.* 2014). The data presented in this study show however that the metapodials of giraffes do not elongate more than other limb bones over their lifetime. The lengths of the radius and tibia increase about 2.3 fold between birth and maturity while the length of the metapodials increases only 1.95 fold. Thus, although greatly elongated, the specialisation of the most distal limb segments in giraffes does not seem to be an adaptation to increase locomotor efficacy as one of the principle functions (Pincher 1949).

## 3.5 Conclusion

This study is set apart by the quality of its sampling base—a broad range of bone parameters were measured, body mass was measured (not inferred) and a broad population of wild (not zoo) giraffes was available. It was found that the giraffe appendicular skeleton does not elongate in the dramatic way the neck does. Limbs at birth, after lengthening with positive allometry *in utero*, are already elongated and slender in shape and a further increase in the gracility of the bones is probably not possible or not desirable. The humerus is the only bone that becomes increasingly robust with regard to body mass *and* bone length, suggesting a functional response to increasingly high loads and/or bending moments, which may be caused by the neck mass which increases with positive allometry and the need for giraffe forelimbs to bend at the carpus and splay during drinking. It may also be related to the orientation of the humerus to the ground, but this needs to be substantiated by further study. Indeed, a broader range of species (in particular artiodactyls) and their body mass through ontogeny needs to be sampled before definitive conclusions can be reached. Further clues regarding the functionally of the giraffe's slender bones will also lie in the cross sectional distribution of bone around the centroid, whole bone geometry and bone curvature.

# Chapter 4
# On reconstructing *Giraffa sivalensis*, an extinct giraffid from the Siwalik Hills, India

*This chapter is adapted from the publication by SJ van Sittert and G Mitchell entitled: 'On reconstructing Giraffa sivalensis, an extinct giraffid from the Siwalik Hills, India', published in PeerJ 2015; 3:e1135. The paragraphs on G. sivalensis palaeoart are additional and were not included in the original paper.*

**Abstract**

*Giraffa sivalensis* occurred during the Plio-Pleistocene period and probably represents the terminal species of the genus in Southern Asia. The holotype is an almost perfectly preserved cervical vertebra of disputed anatomical location. Although there is also uncertainty regarding this animal's size, other specimens that have been assigned to this species include fragments of two *Humeri*, a radius, *Metacarpi* and teeth. In this chapter the neck length, leg length and body mass is estimated using interspecific and, unusually, ontogenetic allometry of extant giraffe skeletal parameters. The appropriateness of each equation to estimate body mass was evaluated by calculating the prediction error incurred in both extant giraffes (*G. camelopardalis*) and okapis (*Okapia johnstoni*). It followed that the equations with the lowest prediction error in both species were considered robust enough to use in *G. sivalensis*. The size of *G. sivalensis*, based on the holotype, is proposed as 400 kg (range 228 kg–575 kg), with a neck length of approximately 147 cm and a height of 390 cm. The molar lengths of tooth specimens considered agree with this size estimate. The humerus was the most appropriate long bone to establish body mass, which estimates a heavier animal of ca 790 kg. The discrepancy with the vertebral body weight estimate might indicate sexual dimorphism. Radial and metacarpal specimens estimate G. Sivalensis to be as heavy as extant giraffes. This may indicate that the radius and metacarpus are unsuitable for body mass predictions in *Giraffa spp*. Alternatively, certain long bones may have belonged to another long legged giraffid that occurred during the same period and locality as *G. sivalensis*. It was concluded that if sexual dimorphism was present then males would have been about twice the size of females. If sexual dimorphism was not present and all bones were correctly attributed to this species, then *G. sivalensis* had a slender neck with a relatively stocky body.

## 4.1 Introduction

*Giraffa sivalensis* (Falconer & Cautley 1843) was the first extinct *Giraffa* species to be discovered, yet neither a complete skull nor specimens related to the holotype vertebra have been found. Notwithstanding this limitation, many fossil specimens have been assigned as belonging to this species, without adequate consideration of its size or without explicitly citing the stratigraphic horizon of discovery (Appendix 2). In addition, many of the discovered specimens have only been described in the Fauna Antiqua Sivalensis, which is a collection of Falconer's publications and unpublished notes (Falconer 1868c). Although all the plates (notably plate E) within the Fauna Antiqua Sivalensis are well described (Falconer 1868b), many of them have never been published.

*History of G. sivalensis discovery*

In 1838 Cautley briefly described the discovery of a remarkable vertebra in the Siwalik Hills in India. He reported the specimen to be very similar to that of extant giraffes—a significant statement, because up until that time no other *Giraffa* species were known. Falconer & Cautley (1843) subsequently named the species *Camelopardalis sivalensis* and assigned the fossil, which was to become the holotype (Badam 1979), as a third cervical vertebra. However, Lydekker (1885a) disputed this and proposed that the holotype was in actual fact a fifth cervical vertebra of a 'very small individual'. Since Cautley's discovery, other *Giraffa*-like fossils have also been found in Asia, Europe and Africa, subsequently leading to proposals for species such as *G. priscilla*, *G. jumae*, *G. stillei*, *G. gracilis*, *G. pygmaea* and *G. punjabiensis.* The references to these fossil specimens are extensive, incomplete and confusing as can be seen by the references to *G. sivalensis* alone in Appendix 2**.**

*Geographic and stratigraphic distribution of fossils*

Matthew (1929) placed the upper Siwalik deposits, where *G. sivalensis* fossils and nearly all Siwalik fauna discovered by early writers, such as Falconer, have been found (Lydekker 1876), as part of the Pinjor zone (Akhtar *et al.* 1991; Bhatti 2004; Gaur *et al.* 1985; Nanda 2002, 2008). The Pinjor zone dates to roughly 2.58 to 0.6 million years ago, placing the fauna discovered in this site as originating during the late Pliocene / early Pleistocene (Nanda 2008). The site of discovery of the holotype for *G. sivalensis* was presented by Falconer and Cautley (1843) only as 'the Sewalik range to the west of the river Jumna' (currently the Yamuna river). Although Spamer *et al.* (1995) described the locality as 'Siwalik Hills, near Hardwar, Uttar Pradesh', this is unlikely as Hardwar is east of the Yamuna. It is therefore proposed that the locality where *G. sivalensis'* holotype was found was in the vicinity of the current Shivalik fossil park, Saketi, Himachal Pradesh, India (Figure 1**)**.


***Figure 4.1 A map indicating the probable vicinity of G. sivalensis fossil discoveries. The marker indicates the location of the Shivalik Fossil Park in the Siwalik Hills, a subHimalayan mountain range. This is most probably the area "west to the river Jumna" (currently Yamuna River) to which Falconer & Cautley (1843) referred. Map data: AutoNavi, Google.***

*Size estimates and controversy*

Size estimates of *G. sivalensis* have been inadequate or contradictory. For example, it has been proposed that *G. sivalensis* was about 'one third shorter' with a neck about 'one tenth more slender' than extant giraffes (Falconer & Cautley 1843), and that the holotype belonged to a very small individual (Lydekker 1885a), that it had the same sized cranium as extant giraffes but with a shorter neck (Lydekker 1876), that it was a large species but smaller than extant giraffes (Bhatti 2004, p. 155), that it was of comparable size to modern giraffes (Bhatti 2004, p. 255), that it was larger than extant giraffes (Mitchell & Skinner 2003) and that certain proportions of the species' neck were larger than extant giraffes (Lydekker 1876, p. 105). Additional fossil specimens originally thought to belong to a separate species, *G. affinis* (Falconer & Cautley 1843), were subsequently shown to belong to *G. sivalensis* and are currently interpreted as a larger individual of the species (Bhatti 2004, p. 140; Lydekker 1876, p. 105). Table 4.1 summarises previous size estimates for *G. sivalensis*. In this chapter the relevant information regarding *G. sivalensis* and its remains will be clarified. In addition, the size of this animal will be allometrically estimated.

***Table 4.1 Previous size estimates of G sivalensis***

| Size estimate | Author | Relevant specimens/ comments |
|---|---|---|
| 'One third shorter' with a neck 'one tenth more slender' as extant giraffes. | Falconer & Cautley, 1843; Lydekker, 1876 (p.105) | Holotype vertebra, OR39747 |
| Large species but smaller than extant giraffes | Bhatti 2004, p. 155 | No specimen referred to. |
| Of comparable size to modern giraffes | Bhatti 2004, p.225 | No specimen referred to. |
| Similar head size to extant giraffes but with a shorter neck. | Lydekker, 1876, p.105 | OR39747. Lydekker noted that the areas of the zygoapophyses are 'considerably larger' than in those of extant giraffes, making the neck 'at least equally strong' as that that of extant giraffes. The larger cranial and caudal articular surfaces were also noted by Falconer & Cautley 1843. |
| Similar in size to extant giraffes | Lydekker 1883 | Cervical vertebra similar in size as that of *G. camelopardalis.* Referring to an imperfect 'first' cervical vertebra, later catalogued as a 'third' cervical, BM39746 (Lydekker 1885a). |
| Slightly larger than extant giraffes. | Falconer 1868c, p.207 | Right humerus. Museum of the Asiatic Society of Bengal no 43, Natural History Museum no 39749. Exact form to that of extant giraffes, but a little larger (Falconer 1868a). Lydekker (1885a) however mentions that this fossil bone originated from a 'small individual'. |
| Similar in size to extant giraffes | Falconer 1868c, p.206 | Left radius. Asiatic Museum of Bengal no 690. Nearly equal in dimensions to existing giraffes. |
| Similar in size to extant giraffes | Falconer 1868c, p.207 | Left metacarpus. Asiatic Museum of Bengal no 52. Of the size of existing giraffe. |
| Similar in size to extant giraffes | Lydekker 1885a | Phalangeals, no 17131a. Almost indistinguishable from the corresponding bones of extant giraffes. |
| Similar in size to extant female giraffes | Falconer & Cautley 1843 | Fragments from upper and lower jaws. Falconer originally ascribed these specimens to *G. affinis*. Lydekker (1876) however refuted this species and proposed that it in actual fact *G. sivalensis*. |
| Larger than extant giraffes with smaller teeth than extant giraffes | Mitchell & Skinner, 2003 | Review of literature |

## 4.2 Materials and methods

### 4.2.1 Studied material and dimensions measured

All postcranial specimens assigned to *G. sivalensis* that were available at the Natural History Museum in London were studied. From these specimens, body and neck size estimates were calculated using giraffe ontogenetic or available interspecific allometric equations. The only vertebra measured was the holotype (OR39747, Figure 4.2), a cervical which had been extensively described by Falconer and Cautley (1843). A caudal fragment of a 'fourth' cervical (OR39748; Lydekker 1885a), also described as a second cervical by Falconer (1845), as well as a caudal part of a 'third' cervical (OR39746; Lydekker (1885a) were missing from the Siwalik collection at the Natural History Museum. Dimensions were measured with a vernier calliper and included: vertebral body length, cranial vertebral body height, cranial vertebral body width, caudal vertebral body height, caudal vertebral body width and spinous process length (Figure 2.1 and Figure 4.2).

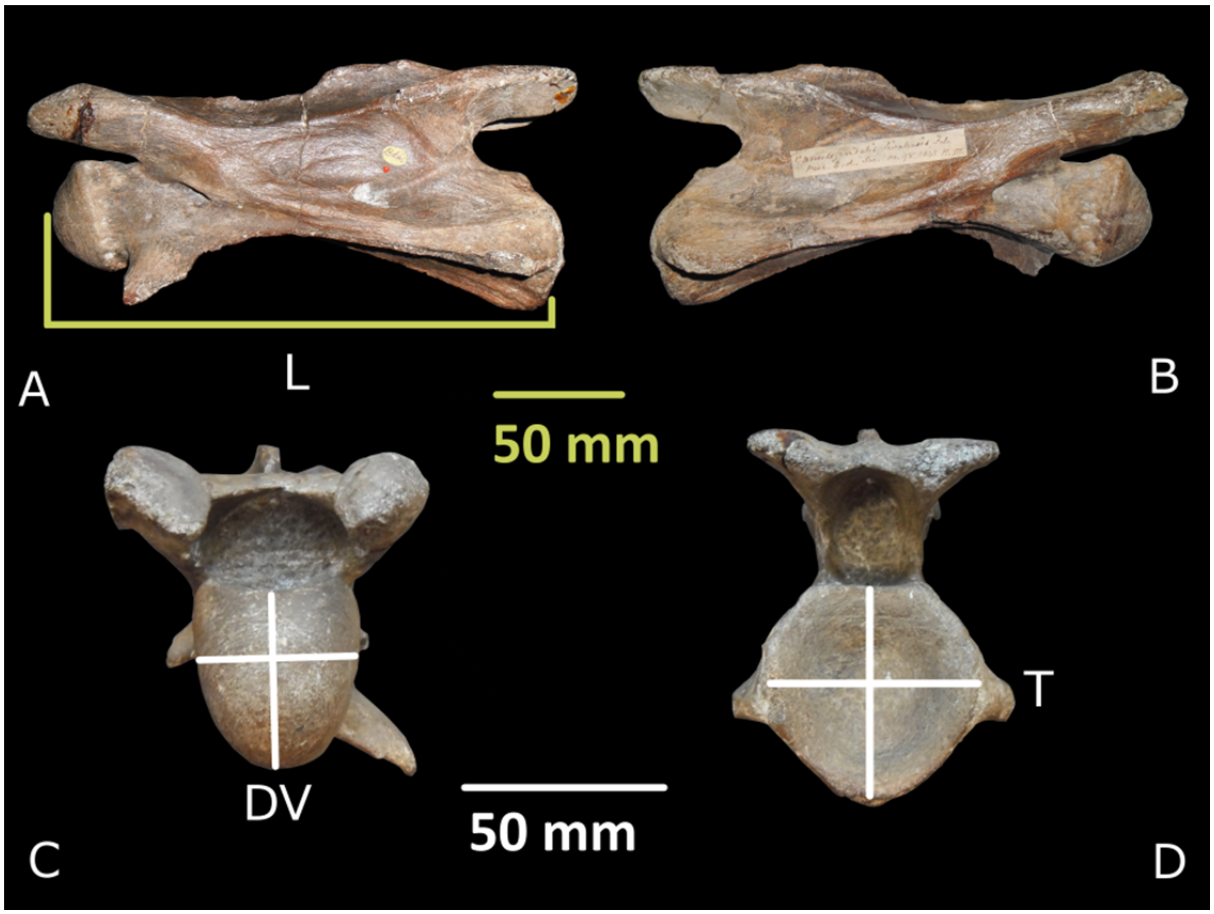


***Figure 4.2 Giraffa sivalensis holotype, specimen OR39747. Presented, from left to right, in left lateral (A), right lateral (B), cranial (C) and caudal (D) views. On left lateral view the line indicates the landmarks for the vertebral body length (L) measurement. On cranial and caudal views the vertical lines indicate the height (dorsoventral, DV) while the horizontal lines indicate the width (transverse, T) measurements.***

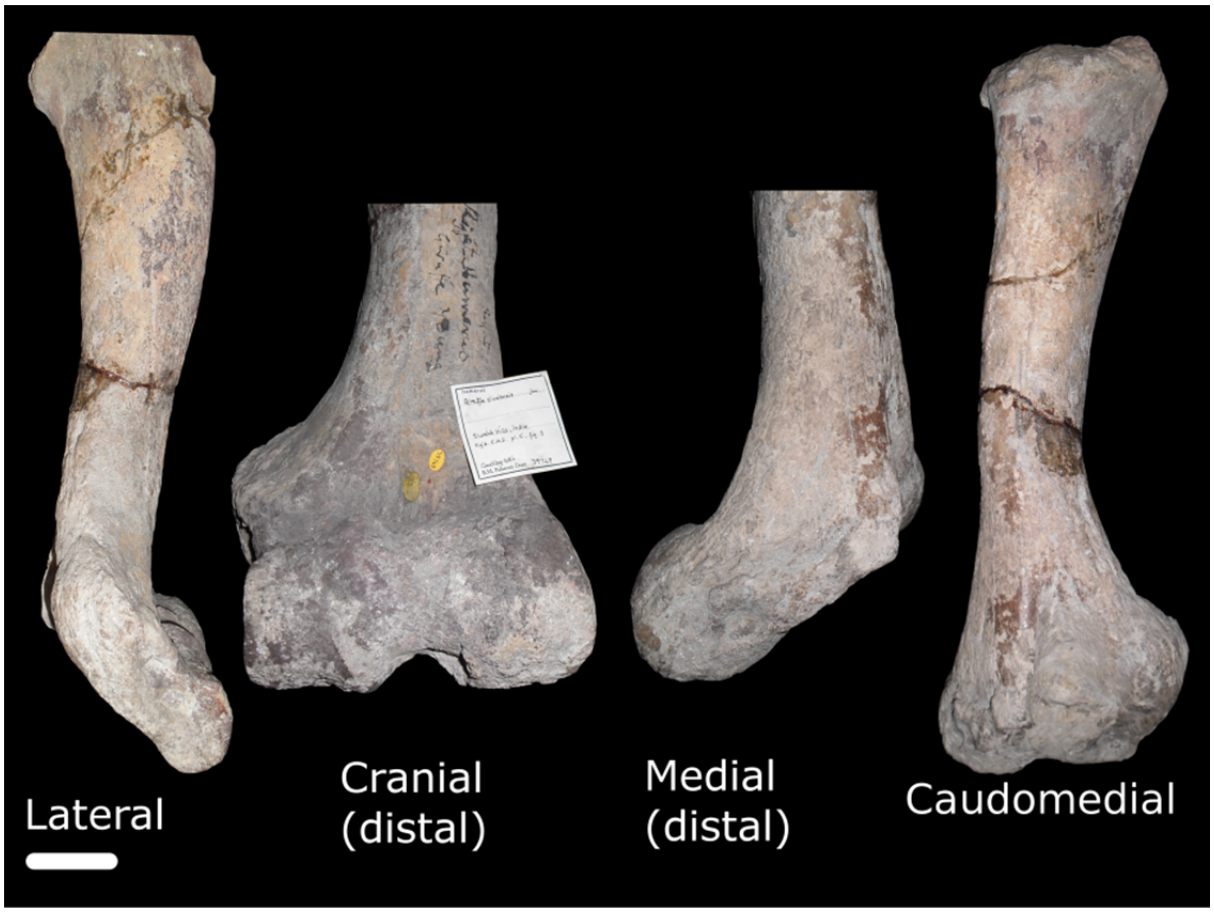


***Figure 4.3 Specimen OR39749. This image represents different views of a right humerus that has been assigned to G. sivalensis. The different views are not to scale; where only distal parts of the bone are shown, these have been enlarged relative to images of the specimen in toto. The scale bar indicates 50 mm and pertains to the lateral view only.***

Additional postcranial specimens assigned to *G. sivalensis* held at the Natural History Museum include fragments of two humeri (OR39749 and OR17136; Figure 4.3 and Figure 4.4 respectively), a fragment of a radius/ ulna (OR17130) and various fragments of metacarpi and phalanges. All metacarpal specimens except OR39750 were avoided due to the unclear numbering of specimens and deformation of the fossils. Measurements of the long bones included length, midshaft circumference and midshaft diameter in craniocaudal and transverse planes. The length and circumference measurements were done with a measuring tape, while the cross sectional diameters were done with a vernier calliper.

Because there is no complete *G. sivalensis* skeleton, its shape needs to be inferred as analogous to the only other extant *Giraffa: G. camelopardalis*. One of the methods of inferring body size from a model animal or animals requires that regression equations in the form $y=bx^k$ (Huxley 1932) be constructed. These regression equations can be based on data from different species (interspecific allometry), within the growth phase of a single animal (ontogenetic allometry) or amongst adult animals of different size but within the same species (static allometry). Ontogenetic as well as interspecific allometric equations were applied to predict body mass in this case.

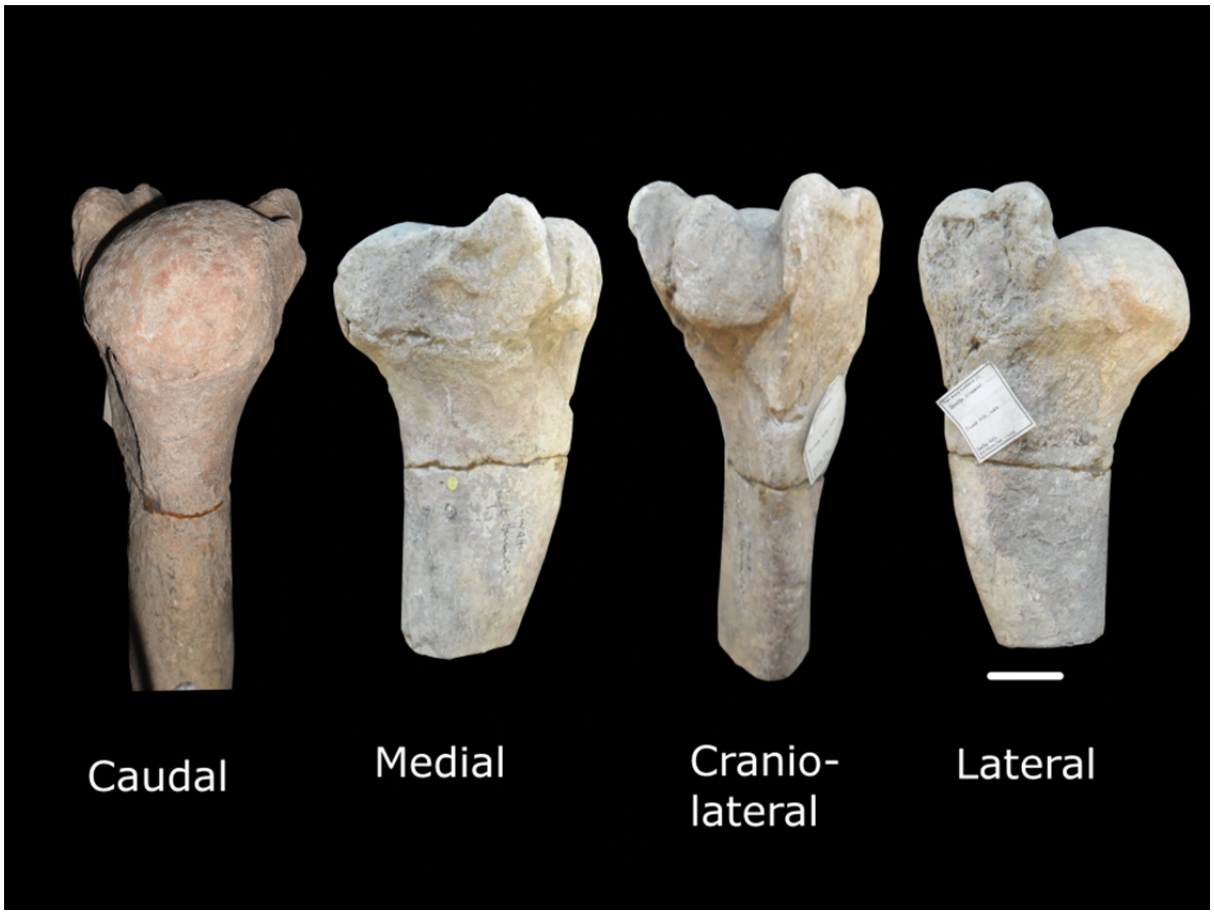


***Figure 4.4 Specimen OR17136. This represents different views of the proximal part of a left humerus that has been assigned to G. sivalensis. The scale bar indicates 50 mm and pertains to the lateral view only as the different views are not drawn to scale.***

Ontogenetic data were obtained from previous studies by the author and others (Mitchell *et al.* 2009a; Van Sittert *et al.* 2010, 2015). These data were used to construct allometric equations to describe body mass or body dimensions. The dimensions used from ontogenetic vertebral data are summarised in Table 4.2. Interspecific regression equations were sourced from previously published work (Anderson *et al.* 1985; Campione & Evans 2012; Roth 1990; Scott 1990). The dimensions measured for the long bone ontogenetic data are summarised in Table 4.3.

*Table 4.2 Dimensions for the G sivalensis holotype; a well preserved C3 cervical vertebra (specimen OR39747)*

| Dimension and description | (Falconer & Cautley 1843)'s terminology | Present study's measurement (± 95% confidence interval for three measurements) (mm) | (Falconer & Cautley 1843)) measurement (mm) |
|---|---|---|---|
| **Vertebral body length**: Longitudinal axis of the vertebral body, from the most cranial curvature of the cranial extremity to the most caudal part of the caudal extremity | Length of the body of the vertebrae between articulating heads | 200.2 ± 0.7 | 198.1 |
| **Cranial vertebral body height:** Greatest dorsoventral height of cranial extremity | Vertical height articulating head? | 42.9 ± 1.4 | 25.4 |
| | Antero-posterior diameter articulating head? | | 48.3 |
| **Cranial vertebral body width:** Greatest transverse width of cranial extremity | Greatest diameter at articulating head | 36.2±2.8 | 35.6 |
| **Caudal Vertebral body height:** Greatest dorsoventral height of caudal extremity | Vertical diameter, articular cup, posterior end | 53.1±0.3 | 50.8 |
| **Caudal vertebral body width:** Greatest transverse width of caudal extremity | Transverse diameter, articular cup, posterior end | 53.4±0.3 | 50.8 |
| **Spinous process length:** From roof of the vertebral foramen to the highest point of the spinous process, perpendicular to the long axis of the vertebral body | | 21.8±2.6 | |

*Note: All values in mm. Nomenclature is based on the Nomina Anatomica Veterinaria (International Committee on Veterinary Gross Anatomical Nomenclature 2012)*

*Table 4.3 Dimensions for long bone specimens marked as belonging to G. sivalensis. All values in mm*

| Specimen no | HL | HCirc | HCr | HTr | RL | RCirc | RCr | RTr | McL | MCirc | McCr | McTr |
|---|---|---|---|---|---|---|---|---|---|---|---|---|
| OR39750* | | | | | | | | | 389 | 186 | 53 | 60 |
| OR17130† | | | | | 220 | 217 | 53 | 71 | | | | |
| OR39749‡ | 453 | 212 | 66 | 66 | | | | | | | | |
| OR17136* | 279 | 216 | 76 | 57 | | | | | | | | |

*Abbreviations: H, Humerus; R, Radius; Mc, Metacarpus; L, Length; Circ, Midshaft circumference; Cr, midshaft craniocaudal diameter; Tr, midshaft transverse diameter. * distal proportion lacking. † only diaphysis. ‡ proximal metaphysis missing. OR39749 is marked as a juvenile.*

***Table 4.4 Summary of fossil teeth assigned to G affinis by Falconer and Cautley (1843), and subsequently assigned to G sivalensis.***

| Fossil specimens | Museum no | References to specimen | Dimensions | Relevant regression equation (reference) | Body mass prediction |
|---|---|---|---|---|---|
| Fragment of left maxilla including two rear molars. The 'back part of the maxillary, beyond the teeth, is attached'. | 39756 a (Lydekker 1885a) | Figured in Plate 2 fig. 3a and 3b of (Falconer & Cautley 1843)). | Joint length of two back molars, maxilla =2.5 in = 63.5mm | | |
| | | | Greatest with of last molar = 1.4 in = 35.56 mm | 38.02xTUMW$^{2.77}$ (all ungulates) | 752 kg |
| | | | | 32.36 x TUMW$^{2.87}$ (all selenodonts) | 945 kg |
| | | | | 17.78 x TUMW$^{2.97}$ (selenodont browsers) | 718 kg |
| | | | Greatest with of penultimate molar = 1.45 in = 36.83 mm | 32.36xSUMW$^{2.78}$ (all ungulates) | 731 kg |
| | | | | 22.91 x SUMW$^{2.96}$ (all selenodonts) | 991 kg |
| | | | | 12.02 x SUMW$^{3.08}$ (selondont browsers) | 801 kg |
| | | | **Average of width measurements (SD)** | | **823 (117) kg** |
| Rear molar of right maxilla | 39756 (Lydekker 1885a) | Figured in Plate 2 fig. 4 of Falconer and Cautley (1843). | Length = 1.2 in = 30.48 mm<br>* it is not sure whether this is the greatest dimensions or occlusal surface. | 19.50 xTUML$^{2.81}$ (all ungulates) | 288 kg |
| | | | | 8.71 x TUML$^{3.12}$ (all selenodonts) | 372 kg |
| | | | | 6.31 x TUML$^{3.29}$ (selenodont browsers) | 481 kg |
| | | | **Average of length measurements (SD)** | | **380 (97) kg** |

| Fossil specimens | Museum no | References to specimen | Dimensions | Relevant regression equation (reference) | Body mass prediction |
|---|---|---|---|---|---|
| | | | Width = 1.4 in = 35.56 mm * it is not sure whether this is the greatest dimensions or occlusal surface. | 38.02xTUMW$^{2.77}$ (all ungulates) | 752 kg |
| | | | | 32.36 x TUMW$^{2.87}$ (all selenodonts) | 915 kg |
| | | | | 17.78 x TUMW$^{2.97}$ (selenodont browsers) | 718 kg |
| | | | **Average of width measurements (SD)** | | **795 (105) kg** |
| Fragment of left mandible containing the third molar | 39755 (Lydekker 1885a) | Figured in plate 2 figure 5a and 5b of (Falconer & Cautley 1843)). | Length = 1.7 in =43.18 mm | 6.31 xTLML$^{2.99}$ (all ungulates) | 489 kg |
| | | | | 3.24 x TLML$^{3.19}$ (all selenodonts) | 533 kg |
| | | | | 2.24 x TLML$^{3.35}$ (selenodont browsers) | 673 kg |
| | | | **Average of length measurements (SD)** | | **565 (96) kg** |
| | | | Greatest width = 1.0 in = 25.4 mm | 109.64xTLMW$^{2.73}$ (all ungulates) | 750 kg |
| | | | | 77.62 x TLMW$^{2.93}$ (all selenodonts) | 1014 kg |
| | | | | 64.56x TLMW$^{2.88}$ (selenodont browsers) | 718 kg |
| | | | **Average of width measurements (SD)** | | **827 (162) kg** |
| Third premolar of the left mandible, detached. | 39757 (Lydekker 1885a) | Figured in Plate 2 figure 6 of (Falconer & Cautley 1843)). | Length = 1.0 in = 25.4 mm | 79.43xTLPL$^{2.76}$ (all ungulates) | 599 kg |
| | | | | 61.66xTLPL$^{2.92}$ (all selenodonts) | 780 kg |
| | | | | 20.42x TLPL$^{3.19}$ (selenodont browsers) | 618 kg |
| | | | **Average of length measurements (SD)** | | **666 (99) kg** |
| | | | Width = 0.9 in = 22.86 mm | 524.81xTLPW$^{2.45}$ (all ungulates) | 1121 kg |
| | | | | 524.81x TLPW$^{2.53}$ (all selenodonts) | 1440 kg |
| | | | | 398.11x TLPW$^{2.49}$ (selenodont browsers) | 964 kg |
| | | | **Average of width measurements (SD)** | | **1175 (243) kg** |
| Second premolar of right maxilla | | Figured in Plate 2 figure 7 of (Falconer & | Length = 1.0 in = 25.4 mm | 169.82xSUPL$^{2.51}$ (all ungulates) | 570 kg |

| Fossil specimens | Museum no | References to specimen | Dimensions | Relevant regression equation (reference) | Body mass prediction |
|---|---|---|---|---|---|
| | | Cautley 1843)). | | 141.25xSUPL$^{2.65}$ (all selenodonts) | 746 kg |
| | | | | 20.41xSUPL$^{3.26}$ (selenodont browsers) | 776 kg |
| | | | **Average of length measurements (SD)** | | **697 (111) kg** |
| | | | Width = 1.12 in = 28.45 mm | 380.19xSUPW$^{2.3}$ (all ungulates) | 840 kg |
| | | | | 416.87xSUPW$^{2.31}$ (all selenodonts) | 953 kg |
| | | | | 208.93x SUPW$^{2.44}$ (selenodont browsers) | 738 kg |
| | | | **Average of width measurements (SD)** | | **843 (108) kg** |

*Abbreviations: TUML = third upper molar length, TUMW = third upper molar width, SUMW = second upper molar width, TLML = third lower molar length, TLMW = third lower molar width, TLPL = third lower premolar length, TLPW = third lower premolar width, SUPL = second upper premolar length, SUPW = second upper premolar width, SD = sample standard deviation*

There are inherent problems associated with using dental measurements as body size predictors, especially when only a single tooth is used (Damuth 1990; Fortelius 1990; Janis 1990). Nevertheless, size were estimated from teeth originally measured by Falconer & Cautley (1843), even though these teeth were initially assigned to a new species *G. affinis,* a species that was eventually abandoned (Lydekker 1883). Uncertainty regarding these teeth specimens persisted until recent times (Spamer *et al.* 1995). Teeth specimens described by authors other than Falconer and Cautley which are noted in Appendix 2 were not evaluated further as there was either uncertainty regarding the authors' species association (Lydekker 1876), or the teeth specimens were not necessarily collected in the vicinity or stratigraphical layer of fossils described by Falconer and Cautley (Lydekker 1878), or because certain specimens were deciduous. Table 4.4 presents dental specimens as well as dimensions as measured by Falconer and Cautley (1843). Body masses were estimated from regression equations established by Damuth (1990).

### 4.2.2 Statistical analyses

Allometric equations were generated from bivariate data through ordinary least squares regression. To facilitate this, measurements were logarithmically transformed to base *e* prior to analyses. According to Warton *et al.* (2006), ordinary least squares regression is appropriate when one wishes to predict y from x, even when x contains measurement error, as long as the results are interpreted in the context of 'predicting y from x measured with error'. It is worth noting that there is controversy regarding the practice of logarithmically transforming data in scaling studies (Cawley & Janacek 2010; Packard 2013; Packard *et al.* 2009, 2010). The main argument is whether error becomes larger as body mass increases (multiplicative error), in which case logarithmic transformation is appropriate, or whether there is no correlation between error and body mass, in which case logarithmic transformation is not appropriate (Glazier 2013). The debate is ongoing and will not be reviewed here. In this study the method of log-transformation of data were selected as it enables more convenient comparison among similar datasets.

Because body dimensions (especially body masses) can be predicted by different equations and by different fossil specimens, the predictions need to be validated. If regression equations had reasonable power in estimating body mass in both extant giraffids (*G. camelopardalis* and *O. johnstoni*), then they were regarded as robust enough to extrapolate to *G. sivalensis* as well. Therefore, dimensions of 10 okapi skeletons were recorded in addition to data obtained from *G. camelopardalis*. The okapi skeletons were housed in various museums and were recorded as the opportunities presented themselves (Table 4.5). Adult okapi specimens were assumed to have weighed 250 kg, with a range of 200 kg to 300 kg (Lindsey & Bennett 1999; Stuart & Stuart 2006). The mature okapi specimens were identified through additional data associated with each museum specimen as well as by the degree of fusion of the epiphyses. The robustness of giraffe ontogenetic as well as interspecific equations to predict body mass in both adult giraffes and adult okapis correctly were assessed through the percent prediction error, calculated according to Smith (1984) and Van Valkenburgh (1990):

$$\frac{(\text{Observed value} - \text{Predicted value})}{\text{Predicted value}} \times 100$$

### 4.2.3 Assumptions made

One of the major assumptions of this study is that *G. sivalensis* dimensions can be modelled from *G. camelopardalis* ontogeny. Although it is unusual to model an animal from the ontogeny of a different species it is not unique (an example is Roth 1990). In assigning the holotype to a specific vertebra, it was also assumed that there would be broad similarity in shape between the cervical vertebrae of *G. sivalensis* and *G. camelopardalis*. Falconer and

Cautley (1843) illustrated this assumption to be the case for many but not all features of the holotype vertebra.

Another assumption was that the specimens used came from the same *Giraffa* species. An attempt was made to use only those specimens that were clearly attributable to the Plio-Pleistocene and to the vicinity of the holotype discovery (Figure 4.1), in order to limit possible confusion with other *Giraffa* species like *G. punjabiensis*. However, in some instances these criteria were not clear due to the lack of other samples or information, as in the discussion of vertebrae OR39746 and OR39748. Lastly, in terms of estimating body proportions in adult animals based on vertebral length, similarity in shape to *G. camelopardalis* was assumed.

*Table 4.5 The studied okapi specimens and their dimensions used in determining the appropriateness of allometric equations in determining body size and shape estimates in G. sivalensis*

| Specimen no | Museum | OTVL | OVNL | OVNL-1 | C3VBL | OFL | N:FL | PVNL | Predicted vertebral neck length regression equation | %PE |
|---|---|---|---|---|---|---|---|---|---|---|
| az2348 | DMNH | 1259 | 557 | 522 | 85 | 932 | 0.60 | 586 | | 0.05 |
| az2440 | DMNH | 1392 | 567 | 531 | 83 | | | 574 | | 0.01 |
| 1973-178 | MNHN | 722 | 273 | 260 | 42 | 752 | 0.36 | 310 | | 0.14 |
| 1961-131 | MNHN | 400 | 149 | 137 | 22.1 | 553 | 0.27 | 174 | | 0.17 |
| 1984-56 | MNHN | | 459 | 428 | 73.5 | | | 514 | $PVNL=10.65*C3VBL^{0.902}$ | 0.12 |
| 1996-102 | MNHN | 1529 | 632 | 600 | 96.9 | 1018 | 0.62 | 660 | | 0.04 |
| 27194 | SM | 1442 | 621 | 589 | 106 | 1018 | 0.61 | 715 | | 0.15 |
| 73224 | SM | 1521 | 647 | 613 | 107 | 993 | 0.65 | 722 | | 0.12 |
| 56346 | SM | 1458 | 630 | 599 | 102 | 998 | 0.63 | 691 | | 0.10 |
| 92290 | SM | | | 142 | 22 | 534 | | | | |

*Abbreviations: DMNH, Ditsong National Museum of Natural History (Formerly Transvaal Museum), Pretoria; MNHN, Museum National d'Histoire Naturelle, Paris; SM, Senckenberg Naturmuseum, Frankfurt; OTVL, observed total vertebral length; ONL, observed neck length; ONL-1, observed neck length minus C1; OTL, observed trunk length; OFL, observed front limb long bone lengths; OHL, observed hind limb long bone lengths; N:FL, neck length to foreleg length ratio; PVNL, predicted vertebral neck length; % PE, percent prediction error for vertebral length based on giraffe ontogenetic allometry; VBL, vertebral body length*

## 4.3 Results

### 4.3.1 Dimensions measured

The OR39747 and long bone dimensions measured are summarised in Table 4.2 and Table 4.3 respectively, and where applicable the dimensions contain the equivalent measured values according to Falconer and Cautley (1843). Except for the cranial vertebral body height, our measurements on OR39747 are within 1% to 5% of that reported by Falconer and Cautley. Dimensions measured from okapi skeletons are presented in Table 4.5. Table 4.5 also contains predictions and prediction errors for okapi vertebral neck length based on *G. camelopardalis* ontogenetic data.

### 4.3.2 Predictions based on vertebra OR39747

Based on *G. camelopardalis* ontogenetic data, the average of dorsal and ventral neck length including soft tissue in *G. sivalensis* was 1467 mm ($y = 1.55\ x^{0.859}$), the vertebral neck length excluding soft tissue was 1270 mm ($y = 10.66\ x^{0.902}$) and the foreleg (hoof to withers) height in the living *G. sivalensis* adult was 2540 mm ($y = 7.61x^{0.663}$, Table 4.6). This would mean that the reaching height of *G. sivalensis* was around 3.9m.

The different vertebral dimensions predict the body mass to be within a range of 228 kg to 575 kg, with an average of 373 kg (Table 4.7, 95% Confidence interval (CI) ±168 kg). The dimensions that could predict body mass accurately across species were identified by calculating prediction errors when applying the *G. camelopardalis* regression equations to both extant giraffes and okapis. Naturally, because the predictions were done using *G. camelopardalis* ontogenetic allometry, the *G. camelopardalis* prediction errors were lowest (8% to 50%, depending on the measurement used for prediction). Predictions for okapi body mass, however, ranged from 17% to 99%. The only variable which provided relatively low body mass prediction errors in both okapi (17%) and *G. camelopardalis* (25%) was the caudal vertebral body dorsoventral height. This dimension predicts a body mass of 390 kg in *G. sivalensis* if OR39747 is considered as a third cervical. If OR39747 was considered a fourth or fifth cervical, body mass predictions will be 274 kg ($y= 0.0011x^{\wedge 3.128}$) or 187 kg ($y = 0.0004x^{\wedge 3.285}$) respectively (Table 4.7).

*Table 4.6 Power functions, their origin and predicted values for linear dimensions of G. sivalensis*

| Dimension predicted for *G. sivalensis* (dependent (y) variable) | Prediction based on (independent (x) variable) | Equation generated from | Equation, Slope Confidence interval, $R^2$ | Prediction |
|---|---|---|---|---|
| Vertebral neck length (C1 to C7 | OR39747 (C3) vertebral body length | *G. camelopardalis* ontogenetic data | $y = 10.66\ x^{0.902}$ CI = 0.874 – 0.930 $R^2 = 0.99$ | 1270 mm |
| Vertebral neck length (C2 to C7) | OR39747 (C3) vertebral body length | *G. camelopardalis* ontogenetic data | $y = 9.708x^{\wedge 0.908}$ CI = 0.881 – 0.936 $R^2 = 0.99$ | 1195 mm |
| Vertebral neck length (C2 to C7) | OR39747 (C3) vertebral body length | Various ungulates, data from (Badlangana *et al.* 2009) | $y = 5.023\ x^{1.025}$ CI = 0.977 – 1.614 $R^2 = 0.99$ | 1148 mm |
| Dorsal neck length (occipital crest to withers) | OR39747 (C3) vertebral body length | *G. camelopardalis* ontogenetic data | $y = 1.694\ x^{0.822}$ CI = 0.716 – 0.928 $R^2 = 0.87$ | 1321 mm |
| Ventral neck length (angle of jaw to acromion) | OR39747 (C3) vertebral body length | *G. camelopardalis* ontogenetic data | $y = 1.442\ x^{0.890}$ CI = 0.765 – 1.014 $R^2 = 0.85$ | 1608 mm |
| Average neck length (of dorsal and ventral neck length) | OR39747 (C3) vertebral body length | *G. camelopardalis* ontogenetic data | $y = 1.55\ x^{0.859}$ CI = 0.767 – 0.951 $R^2 = 0.91$ | 1467 mm |
| Front leg length (humerus+ radius+ metacarpus long bones) | OR39747 (C3) vertebral body length | *G. camelopardalis* ontogenetic data | $y = 70.2x^{0.598}$ CI = 0.332 – 0.8642 $R^2 = 0.87$ | 1668 mm |
| Foreleg withers height | OR39747 (C3) vertebral body length | *G. camelopardalis* ontogenetic data | $y = 7.61x^{0.663}$ CI = 0.586 – 0.741 $R^2 = 0.92$ | 2558 mm |
| Approximate reaching height (hoof to occipital crest) | OR39747 (C3) vertebral body length | *G. camelopardalis* ontogenetic data | $y = 7.600x^{0.742}$ CI = 0.678-0.806 $R^2 = 0.95$ | 3880 mm |

### 4.3.3 Predictions based on long bone dimensions

All of the *G. sivalensis* long bone specimens available at the Natural History Museum were incomplete proximally and/or distally. It was clear, nevertheless, that the bones had a similar slender appearance of extant giraffes and were elongated. Humeral specimen OR39749 was almost complete except for the proximal metaphysis, which has clearly broken off at the physeal line of a subadult animal. Regarding the radius/ ulna specimen, the bones' fusion at the midshaft was not complete as in modern giraffes, where the two bones are indistinguishable at midshaft in adults. The metacarpus specimen included in the study had the same caudal 'columns' or caudal groove as those evident in the extant giraffe (Solounias 1999; Van Schalkwyk 2004; Van Schalkwyk *et al.* 2004) as well as in those of the okapi (own observation).

***Table 4.7 Functions for the prediction of body mass based on various G. sivalensis specimens***

| **Independent(x) variable** | **Model sample** | **Model r2** | **Allometric equation** | **Body mass prediction (kg)** | **Body mass PE% confidence intervals in kg (based on prediction errors when applied to *G. camelopardalis data*)** | **Body mass confidence intervals in kg (based on prediction errors when applied to *O. johnstoni data*** |
|---|---|---|---|---|---|---|
| OR39747 (C3) vertebral body length | *G. camelopardalis* ontogenetic data | 0.91 | $y = 0.022*x^{1.919}$ | 575 | 8% PE (529-612) | 81% PE (109-1041) |
| OR39747 (C3) cr dv | *G. camelopardalis* ontogenetic data | 0.77 | $y = 0.0023*x^{3.21}$ | 400 | 18% PE (328-472) | 87% PE (52-748) |
| OR39747 (C3) cr tr | *G. camelopardalis* ontogenetic data | 0.84 | $y= 0.0054*x^{2.967}$ | 228 | 14% PE (196-260) | 99% PE (2-454) |
| OR39747 (C3) cd dv | *G. camelopardalis* ontogenetic data | 0.69 | $y= 0.0048*x^{2.847}$ | **390** | **25% PE (293-487)** | **17% PE (323-456)** |
| OR39747 (C3) cd tr | *G. camelopardalis* ontogenetic data | 0.57 | $y= 0.0227*x^{2.360}$ | 271 | 50% PE (136-407) | 21% PE (214-328) |
| Average of OR39747 vertebral dimensions (SD) | | | | **373 (135)** | | |
| OR39748 (C3) cd dv | *G. camelopardalis* ontogenetic data | 0.69 | $y= 0.0048*x^{2.847}$ | 394 | 25% PE (296-493) | 17% PE (327-462) |
| OR39747 (C4) cd dv | *G. camelopardalis* ontogenetic data | 0.69 | $y= 0.0011*x^{3.128}$ | 274 | | |
| OR39747 (C5) cd dv | *G. camelopardalis* ontogenetic data | 0.69 | $Y = 0.0004*x^{3.285}$ | 187 | | |
| Humerus midshaft circumference (OR17136) | *G. camelopardalis* ontogenetic data | 0.98 | $y = 8.96*10^{-4}\ x^{2.55}$ | 809 | 5% PE (767-851) | 5%PE (766-852) |
| Humerus midshaft circumference (OR39749) | *G. camelopardalis* ontogenetic data | | | 772 | 5% PE (732-812) | 5%PE (731-813) |
| average of humeral circumferences (SD) | | | | 791 (26) | | |
| Humerus midshaft craniocaudal diameter (OR17136) | *G. camelopardalis* ontogenetic data | 0.98 | $y = 3.59*10^{-2}\ x^{2.32}$ | 834 | 11% PE (743-925) | 13%PE (723-945) |
| Humerus midshaft craniocaudal diameter (OR39749) | *G. camelopardalis* ontogenetic data | | y = 3.59*10-2 $x^{2.32}$ | 602 | 11% PE (537-667) | 13%PE (522-682) |
| Humerus midshaft transverse diameter (OR17136) | *G. camelopardalis* ontogenetic data | 0.96 | y = 2.00*10-2 $x^{2.53}$ | 561 | 24% PE (429-693) | 22%PE (438-684) |
| Humerus midshaft transverse diameter (OR39749) | *G. camelopardalis* ontogenetic data | | y = 2.00*10-2 $x^{2.53}$ | 813 | 24% PE (622-1004) | 22%PE (635-991) |
| Average humeral craniocaudal and transverse (SD) | | | | 703 (141) | | |

| **Independent(x) variable** | **Model sample** | **Model r2** | **Allometric equation** | **Body mass prediction (kg)** | **Body mass PE% confidence intervals in kg (based on prediction errors when applied to *G. camelopardalis data*)** | **Body mass confidence intervals in kg (based on prediction errors when applied to *O. johnstoni data*** |
|---|---|---|---|---|---|---|
| All humeral ontogenetic average (SD) | | | | **732 (119)** | | |
| Radius midshaft circumference (OR17130) | *G. camelopardalis* ontogenetic data | 0.99 | $y = 1.65*10\text{-}4\ x^{2.93}$ | 1179 | 10%PE (1064-1294) | 31%PE (726-1390) |
| Radius midshaft craniocaudal diameter (OR17130) | *G. camelopardalis* ontogenetic data | 0.98 | $y = 2.89*10\text{-}3\ x^{3.19}$ | 847 | 12%PE (746-948) | 62%PE (416-1780) |
| Radius midshaft transverse diameter (OR17130) | *G. camelopardalis* ontogenetic data | 0.99 | $y = 1.18*10\text{-}2\ x^{2.67}$ | 1047 | 9%PE (948-1146) | 19%PE (943-1387) |
| Radius ontogenetic average (SD) | | | | 1024 (167) | | |
| Metacarpal midshaft circumference (OR39750) | *G. camelopardalis* ontogenetic data | 0.96 | $y = 4.70*10\text{-}5\ x^{3.24}$ | 1058 | 11%PE (942-1174) | 31%PE (726-1390) |
| Metacarpal midshaft craniocaudal diameter (OR39750) | *G. camelopardalis* ontogenetic data | 0.97 | $y = 1.59*10\text{-}3\ x^{3.40}$ | 1098 | 21%PE (867-1329) | 62%PE (416-1780) |
| Metacarpal midshaft transverse diameter (OR39750) | *G. camelopardalis* ontogenetic data | 0.98 | $y = 6.71*10\text{-}3\ x^{2.95}$ | 1165 | 20%PE (932-1398) | 19%PE (943-1387) |
| Average metacarpus | | | | 1107 (54) | | |
| Humerus midshaft craniocaudal diameter (OR17136) | Artiodactyl interspecific allometry (Scott 1990) | 0.94 | $y = 7.63\ x^{2.455}$ | 1106 | 18%PE (906-1305) | 24%PE (844-1368) |
| Humerus midshaft craniocaudal diameter (OR39749) | Artiodactyl interspecific allometry (Scott 1990) | | | 793 | 18%PE (650-936) | 24%PE (605-981) |
| Humerus midshaft transverse diameter (OR17136) | Artiodactyl static interspecific (Scott 1990) | 0.95 | $y = 12.4\ x^{2.46}$ | 900 | 26%PE (662-1138) | 52%PE (428-1372) |
| Humerus midshaft transverse diameter (OR39749) | Artiodactyl interspecific allometry (Scott 1990) | | | 1268 | 26%PE (822-1518) | 52% (603-1933) |

| **Independent(x) variable** | **Model sample** | **Model r2** | **Allometric equation** | **Body mass prediction (kg)** | **Body mass PE% confidence intervals in kg (based on prediction errors when applied to *G. camelopardalis* data)** | **Body mass confidence intervals in kg (based on prediction errors when applied to *O. johnstoni* data** |
|---|---|---|---|---|---|---|
| Humerus midshaft circumference (OR17136) | Various mammalian taxa (Roth 1990) | 0.99 | $y = 9.45*10^{-4} x^{2.61}$ | 1170 | 30%PE (822-1518) | 29%PE (831-1509) |
| Humerus midshaft circumference (OR39749) | Various mammalian taxa (Roth 1990) | | | 1115 | 30%PE (784-1446) | 29%PE (792-1438) |
| Humerus midshaft circumference (OR17136) | Various mammalian taxa (Anderson *et al.* 1985) | 0.99 | $0.0009 x^{2.6392}$ | 1304 | 37%PE (819-1789) | 35%PE (842-1766) |
| Humerus midshaft circumference (OR39749) | Various mammalian taxa (Anderson *et al.* 1985) | | | 1241 | 37%PE (780-1702) | 35%PE (801-1681) |
| Humerus midshaft circumference (OR17136) | Ungulates (Campione & Evans 2012) | 0.95 | $y = 1.469 x^{2.5273}$ | 1167 | 29%PE (831-1503) | 31%PE (800-1534) |
| Humerus midshaft circumference (OR39749) | Ungulates (Campione & Evans 2012) | | | 1113 | 29%PE (792-1433) | 31%PE (763-1463) |
| All humeral interspecific average (SD) | | | | 1112 (180) | | |
| Radius midshaft craniocaudal diameter (OR 17130) | Artiodactyl static allometry (Scott 1990) | 0.93 | $y =29.2 x^{2.51}$ | 1891 | 50%PE 946-2837 | 54%PE 870-2911 |
| Radius midshaft transverse diameter (OR 17130) | Artiodactyl static allometry (Scott 1990) | 0.91 | $y = 8.19 x^{2.555}$ | 1238 | 11%PE 1102-1374 | 43%PE (711-1765) |
| Radial interspecific average (SD) | | | | 1565 (462) | | |

*SD, Standard deviation; PE, Prediction error; cr dv, cranial dorsoventral diameter; cr tr, cranial transverse diameter; cd dv, caudal dorsoventral diameter; cd tr, caudal transverse diameter. * indicates multiplied, and is used in this instance to avoid confusion with the x variable. The body weights in bold indicate the body weight predictions considered most accurate in reconstructing G. sivalensis.*

As no bones were complete length wise, bone length could not be used as a predictor for body mass which, in any case, has been shown to be a poor estimator of body mass in other taxa (Scott 1990). Based on circumferences of the humeri (OR39749 and OR17136) and using *G. camelopardalis* ontogenetic data these specimens may have belonged to animals with body weight in the range of 770 kg to 810 kg. An extant giraffe of this body mass would have a humerus length of about 477 mm to 484 mm ($y=63.2M_b^{0.304}$), which is just slightly longer than the 453 mm measured on OR39749 that lacked a distal metaphysis. The predictors based on radial and metacarpal cross sectional dimensions offered much higher

body mass estimates, with averages of 1024 kg and 1107 kg respectively. In addition to employing ontogenetic data to generate allometric equations, previously published interspecific studies were also referred to (Anderson *et al.* 1985; Campione & Evans 2012; Roth 1990; Scott 1990). Interspecific equations tended to predict heavier body masses than ontogenetic equations, especially so in the distal long bone samples.

### 4.3.4 Predictions based on dental dimensions

Four molars and two premolars were used for size predictions (Table 4.4), using equations developed by Damuth (1990). Body mass predictions based on tooth length (average = 577 kg, standard deviation = 155 kg) tended to be smaller than the predictions based on tooth width (average = 881 kg, standard deviation = 188 kg, $t_{(27)} = 4.83, p < 0.01$). Predictions from molar length dimensions also tended to be lower than those from premolar lengths (average from molar lengths = 473 kg, average from premolar lengths = 682 kg, $t_{(9)} = -3.12, p < 0.05$).

## 4.4 Discussion

### 4.4.1 Vertebral identity of OR39747

The anatomical identity of OR39747 was disputed by Lydekker (1885a). He showed that Falconer was in a habit of not counting the atlas and axis as cervical vertebrae—which often meant that the start of the numbering of vertebra commenced at the third or occasionally the second postcranial vertebra. Mammalian C3 to C5 forms a repetitive series and often does not have the distinguishing characteristics present in the other cervical vertebrae (Solounias 1999). It is therefore indeed challenging to assign OR39747 to a specific vertebra. However, if approximate similarity in shape between *G. sivalensis* and *G. camelopardalis* were assumed, there are clues in the extent to which the cranial articular processes (*Proc. articularis cranialis)* extend beyond the body or centrum of the vertebra (*Corpus vertebrae*, Figure 4.5 and Figure 4.6). In the *G. camelopardalis* C3, this process extends well beyond the cranial extremity of the vertebral body, but ends before or approximately at the same dorsoventral plane as the vertebral body in C4 and C5. Judging then by the extent of the articular processes of OR39747, it is a third, fourth or fifth cervical in decreasing order of likelihood. Falconer was therefore correct in assigning this vertebra as a third cervical, albeit fortuitously so.

***Figure 4.5 The C3's (centre of image) of different size giraffes. Note the extent to which the cranial articular process extends beyond the cranial extremity of the vertebral body***

***Figure 4.6 The C4's (centre of image) of different sized giraffes. Note the extent of the cranial articular processes.***

### 4.4.2 Ontogenetic and interspecific scaling models

It is unusual although not unique to use ontogenetic allometry to predict an extinct animal's size. For instance, Roth (1990) proposed that smaller animals of a species with distinctive morphologies (be they juvenile or adult) may still be better analogues than other taxa, at least in some aspects. In the current study, this view is warranted, as no extant species has such an extreme shape as *G. camelopardalis.* Predicting fossil masses from interspecific equations are further complicated by the decision of which taxa to include in regressions. For example, it is not clear whether predictions generated from interspecific allometric data are more accurate when based on closely related taxa with similar locomotor habits (Janis *et al.* 2002; Runestad 1994) or when using a wider sampling base (De Esteban-Trivigno *et al.* 2008). Other factors that may influence precision of body mass predictions in interspecific studies are body mass estimations (instead of body mass measurements), small intrataxa sample sizes, and overrepresentation of animals of one sex or of exaggerated proportions. To overcome these problems, it was investigated which ontogenetic scaling parameters, if any, might be suitable and robust enough for predictions amongst extant Giraffidae. It is possible that giraffe ontogenetic equations are also acceptable for comparison not just amongst the Giraffidae but amongst, for example, extant camelids with similar gaits. However, okapis were considered as an adequate reference in this case as they are closest to giraffes phylogenetically and because it has been shown that the ontogenetic scaling of their long bones are indeed unusual amongst the cetartiodactyla (Kilbourne & Makovicky 2012). Nevertheless, it was borne in mind that ontogenetic and interspecific scaling exponents are generally not interchangeable (Gould 1966; Pélabon *et al.* 2013) and that it

would only be the case under certain assumptions. In this case the assumption was that *G. sivalensis* had a similar body plan as juvenile extant giraffes. With the above limitations in mind, it was thus found reasonable to test the feasibility of both types of allometry in describing the proportions of *G.* sivalensis. It was further realised that neither of these methods may be appropriate for each and every dimension measured.

### 4.4.3 Neck length and reaching height

Badlangana *et al.* (2009) presented interspecific predictions for vertebral neck length based on vertebral body length. Using their data (presented in Table 1 of their 2009 paper), the vertebral neck length of *G.* sivalensis C2–C7 could be estimated as 1150 mm (Table 4.6), slightly shorter (45 mm or 4%) than vertebral neck length calculated from the ontogenetic data presented in this study. There are therefore reasonable grounds to conclude that our estimated neck length based on ontogenetic data is valid, or at least close to interspecific curves. Further support for this rationale can be seen where the *G. camelopardalis* ontogenetic curve gives appropriate predictions for vertebral neck length in both the extant giraffe and okapi (Figure 4.7). Extant adult giraffes have an average external neck length of about 2013 mm in males (1000 kg and above) and 1832 mm in females (800 kg and above) (Mitchell *et al.* 2009a). Assuming the same body plan for *G. sivalensis* as for *G. camelopardalis*, then *G. sivalensis* had around 350 mm (20%) to 550 mm (27%) shorter necks than modern giraffes, depending on whether OR39747 came from a female or male animal. This is a slightly longer neck length than Falconer & Cautley's (1943) estimated neck length for *G. sivalensis,* which is approximately a third shorter than extant giraffes.

### 4.4.4 Body mass

The body mass predictions for *G. sivalensis* are wide (Figure 4.8). Possible reasons for the large range of predictions are that certain fossils were erroneously attributed to *G. sivalensis* and/or that certain specimens and allometric equations are inadequate for body mass predictions. Before decisions could be made regarding the validity of attributing a fossil to *G. sivalensis*, the equations that were robust enough to predict body mass accurately across species were ascertained.

#### 4.4.4.1 Vertebra OR39747 body mass estimates

It is unconventional to use vertebrae as proxies for body mass, although due to the lack of other samples it has been done before (see for instance Taylor 2007; Taylor & Naish 2007). As OR39747 is the holotype, it necessitates that body mass estimates are made from it if other *Giraffa spp.* specimens are to be attributed to it. Although vertebral body length has higher $R^2$ values than cross sectional vertebral properties (Table 4.7, Van Sittert *et al.* 2010), cross sectional properties are still preferable predictors of body mass in this case. The first reason is that $R^2$ value is inferior to percent prediction error (%PE) and percent standard error of the estimate when assessing reliability of body mass predictions through regressions (Smith 1984). Secondly, vertebral cross sectional properties are subjected to the

stresses and strains within the neck (Slijper 1946) and therefore are a much better indicator of head and neck mass and by implication body mass. Conversely, vertebral body length is influenced by factors other than body mass such as the number of vertebrae in an anatomical area (compare birds and mammals' cervical region) or the lifestyle of the animal. Caudal vertebral height (dorsoventral diameter) had the lowest %PE (25% and 17%) when predicting body mass in both extant giraffes and okapis respectively (Table 4.7, Figure 4.9), and therefore considered this dimension to be most robust for body mass predictions across giraffids. No other published material could be found regarding interspecific regression equations using vertebral dimensions for the prediction of body mass in ungulates. The caudal vertebral height predicts a body mass of 390 kg in *G. sivalensis*. Interestingly, the average body mass prediction from the remaining vertebral regression equations (C3 vertebral body length, cranial height, cranial width and caudal width, Table 4.7) is fairly similar—368 kg. The only body mass prediction to fall outside the 95% confidence interval based on all vertebral dimensions including vertebral height (373 kg ± 119 kg) is vertebral body length, predicting a mass of 575 kg.

Nevertheless, the body mass prediction from caudal vertebral height could be either an over or underestimate. Considering it as an overestimate would mean that this animal had a relatively heavy neck and head complex but a slender or lightweight body. This is unlikely as a larger head and neck complex is unsupportable unless accompanied by a larger total body size (Taylor & Wedel 2013b). Conversely an underestimate would mean a slender neck and head complex but a relatively stocky body. This is a more plausible scenario and if indeed it is the case, it might explain the discrepancy between vertebral and dental body mass predictions when compared to those of limb bones.

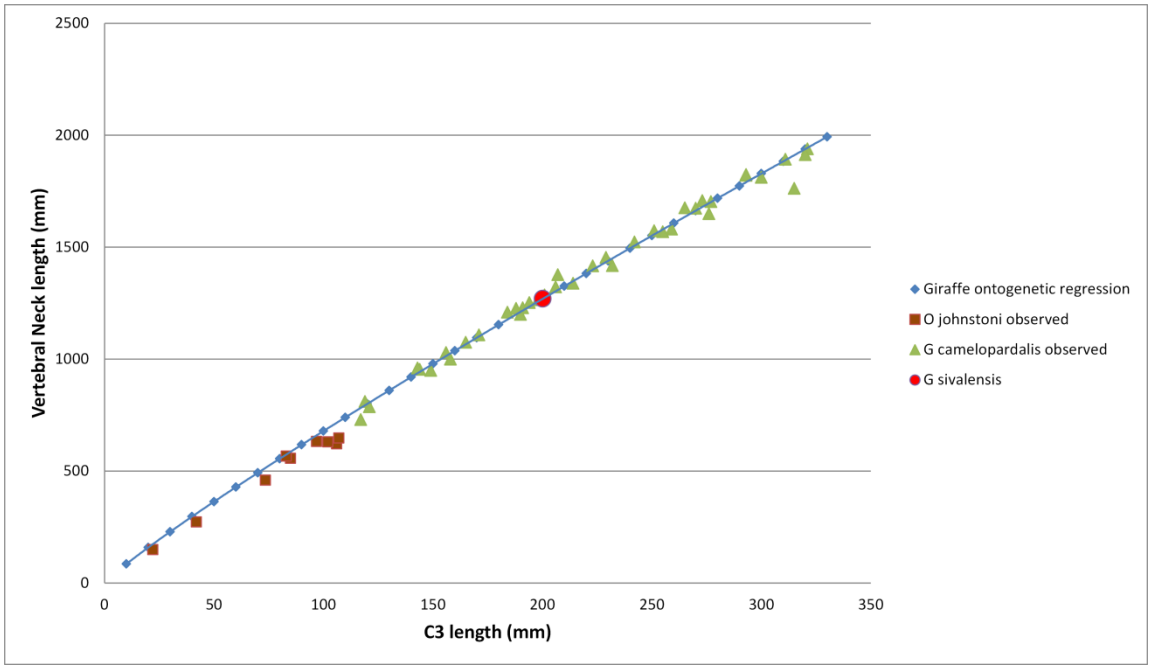


***Figure 4.7 The relationship between neck length and C3 vertebral length throughout ontogeny in giraffes and okapis. A regression line is based on the giraffe ontogenetic series and is extrapolated to the okapi range. The use of a regression line for ontogenetic and phylogenetic allometry seems to be appropriate in this case, supporting the use of a giraffe ontogenetic regression line to predict a neck length value for G. sivalensis.***

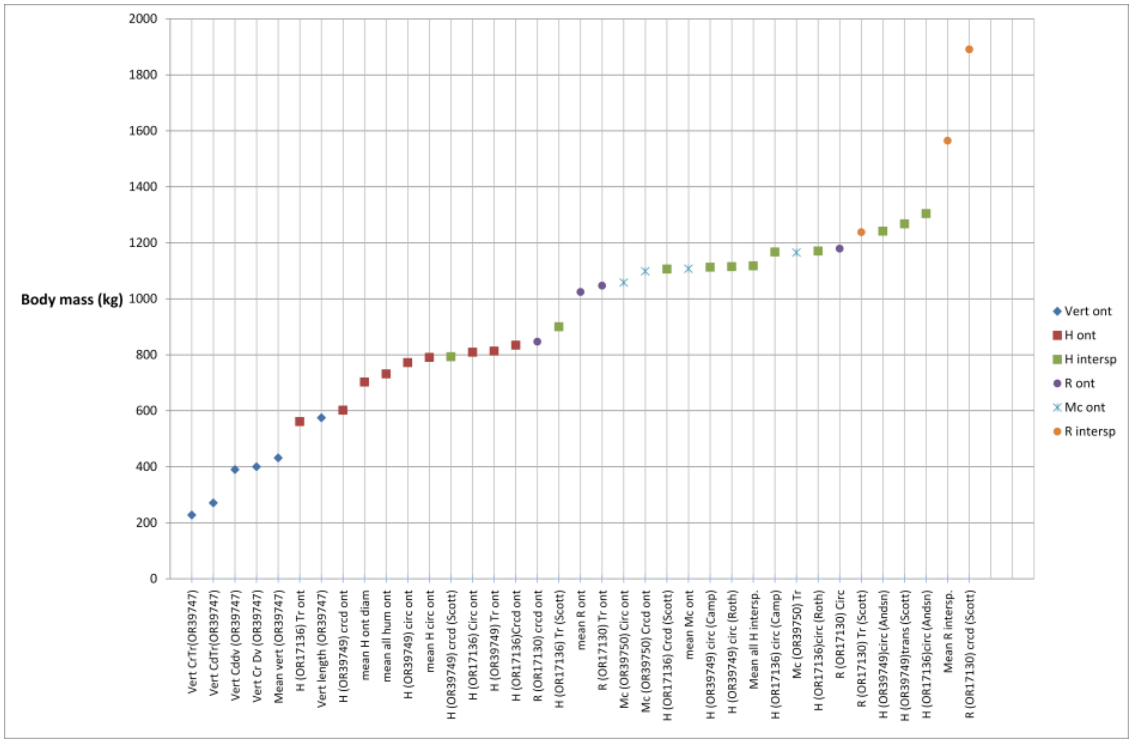


***Figure 4.8 Body mass predictions for G. sivalensis based on various fossil specimens. The labels are divided into predictions from vertebral dimensions (diamond shapes), humeral dimensions (squares), radial dimensions (circles) and metacarpal dimensions (crosses). The humeral and radial dimensions are further subdivided into those originating from ontogenetic allometric equations (red and purple, respectively) and those from interspecific equations (green and orange, respectively). Note that the interspecific predictions generally provide heavier estimates of body mass than predictions based on ontogenetic data. Furthermore, the distal bones tend to predict higher values than the proximal (humerus) bone predictions. Vertebral predictions give the lightest body mass estimates. Abbreviations: Vert, Vertebral body; H, Humerus; R, Radius; Mc, Metacarpus; Cr, Cranial; Cd, Caudal; CrTr, Cranial Transverse Diameter; CrDv, Cranial Dorsoventral Diameter; CdTr, Caudal Transverse Diameter; CdDv, Caudal Dorsoventral Diameter; CrCd, Craniocaudal Midshaft Diameter; Tr, Transverse Midshaft Diameter; Circ, Midshaft Circumference; ont, ontogenetic sample; inters, interspecific sample; Sc, (Scott, 1990); Ro, (Roth, 1990); An, (Anderson, Hall-Martin & Russell, 1985).***

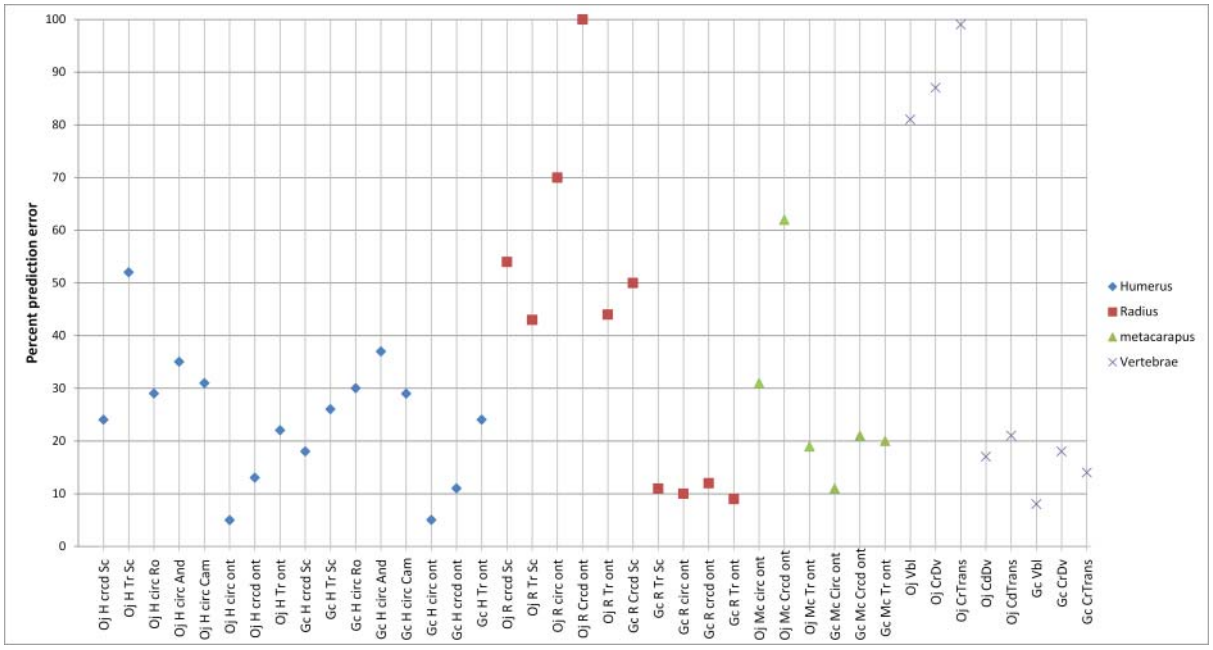


***Figure 4.9 The body mass prediction errors (absolute values) associated with various dimensions in Okapia johnstoni and Giraffa camelopardalis. Of the available regressions and variables measured, it would appear that humeral circumference and craniocaudal diameter (using G. camelopardalis ontogenetic regression) is best suited for body mass predictions, both in giraffes and okapis, and therefore also likely to be useful for body mass predictions in G. sivalensis. Vertebral caudal dorsoventral diameter represents an acceptable variable should estimates only be based on the holotype, with prediction errors of 17% and 25% in giraffes and okapis respectively. Different shapes indicate different bones used for body mass predictions. Note that for clarity of the graph, the maximum indicated prediction error is 100%. Abbreviations: Oj, Okapia johnstoni; Gc, Giraffa camelopardalis; other abbreviations as listed for Figure 4.2***

4.4.4.2 Limb bone body mass estimates

Interspecific long bone cross sectional properties, although probably more closely related to body mass than any other variable, have nevertheless been found to be poor predictors of body mass in giraffes and in some cases, okapis (Anderson *et al.* 1985; Janis *et al.* 2002; McMahon 1975; Scott 1990), although it should be noted that a recent interspecific study has shown giraffes to be more amenable to interspecific equation predictions (Campione & Evans 2012). Similarly, there were higher prediction errors with interspecific equations compared to *G. camelopardalis* ontogenetic curves, with a 5% prediction error based on humeral ontogenetic data (Figure 4.9). Errors were inflated when using more distal bones. Therefore, the most appropriate long bone variable useful for *G. sivalensis* body mass determination is very likely humeral cross sectional properties, using our ontogenetic *G. camelopardalis* sample.

The average body mass estimated from humeral ontogenetic analysis is 732 kg. Interestingly, this body mass is about 150 kg more than would be indicated by a *G. camelopardalis* of similar neck length, and 342 kg more than the mass predicted from OR39747 cross sectional properties. This could mean that either the humeral fossil specimens were incorrectly assigned to *G. sivalensis,* that *G. sivalensis* had a relatively stockier body and thinner neck than *G. camelopardalis* or that the holotype vertebra came from a female and the humeral specimens from large males.

Unfortunately, none of the other long bone dimensions seem to be reliable predictors of body mass across extant giraffids. The best non-humerus candidate using interspecific scaling seems to be the radius transverse diameter with a 43% and 11% prediction error in okapis and giraffes respectively. This dimension predicts that the specimen belonged to an animal of approximately 1238 kg, which suggests this animal might have been heavier than *G. sivalensis*. Interspecific equations for metacarpi could not be found. Therefore, only ontogenetic equations could be applied to the measurements made. Yet, similar to the radial prediction, the metacarpal transverse diameter predicts a body mass of 1165 with around 20% prediction error. The inflated prediction errors could be because humeri and femora are generally more suitable for body mass predictions than more distal bones, especially in giraffes (McMahon 1975). It is also possible that the fossil long bones were incorrectly assigned to *G. sivalensis* and perhaps belonged to another similar species existing at the same time and location.

#### 4.4.4.3 Dental body mass estimates

There have been numerous dental specimens ascribed to *G. sivalensis* (Appendix 2). Unfortunately, not all of these specimens are from the same locality and are probably from different stratigraphic zones. Subsequently, there appeared to be uncertainty regarding the correct species allocation of these fossils (see especially Lydekker 1876). A discussion on the morphology and correct species classification of teeth specimens assigned to *G. sivalensis* were not considered as part of this study, and only those teeth mentioned by Falconer and Cautley (1843) were used. These specimens were originally assigned to the species *G. affinis*—a classification later abandoned by Falconer himself and also disputed by Lydekker (1883), who re-assigned the fossils to *G. sivalensis*. As the specimens originated from the same area and strata as the holotype OR39747, which is the Pliocene of the Siwaliks (Lydekker 1885a), it is reasonable to consider them as truly *G. sivalensis* teeth until further evidence emerges.

Molar length measurements are more reliable indicators of body mass than molar width or area (Damuth 1990; Fortelius 1990; Janis 1990). Furthermore, Janis (1990) found that premolar row length is a poorer correlates than molar row length. Molar lengths predict an animal within the range of 288 kg to 673 kg, which is similar to OR39747's caudal vertebral height body mass prediction of 390 kg.

#### 4.4.4.4 Combined size estimates

Lydekker's (1885a) suggestion that OR39747 belonged to a small individual could have meant that the animal was still immature, that the animal was a relatively small individual of the species or that the species itself was small within the genus. It is unlikely that Lydekker meant an immature animal as the fusion of the epiphyses to the body of the vertebra is complete and clear definitions of bony ridges and muscular depressions indicate a mature animal (Falconer & Cautley 1843). (Lydekker 1885a) might have based his idea of a small individual on two larger vertebrae assigned to *G. sivalensis*—a proximal part of a 'third' and

distal part of a 'fourth' cervical, OR39746 and OR39748 respectively (Lydekker 1885a), Appendix 2). Unfortunately, these vertebrae were not locatable within the Siwalik collection at the time of this study (Personal communication, P Brewer, Curator of fossil mammals, Natural History Museum, 2013), and it could subsequently not be measured. Nevertheless, Falconer (1845) reported OR39748 to be 2.1 inch (53.3 mm) in height and width at the caudal extremity, which is only 0.2 mm greater and 0.1 mm less than our respective measurements of OR39747 (Table 4.2). Based on ontogenetic allometry for caudal vertebral body height, OR39748 came from an animal weighing 394 kg or 277 kg, depending on whether it was a C3 or C4 vertebra respectively (Table 4.7). Therefore, the animal from which the holotype vertebrae originated was not relatively small compared to the size estimated from specimen OR39748. It is possible though, especially considering body mass estimates from the humerus, that there might have been sexual size dimorphism present in *G. sivalensis*. If that is indeed the case, OR39747 and OR39748 would have been females about half the size of fully grown male animals, a possibility also supported by the fossil teeth considered in body mass estimates.

### 4.4.5 *G. sivalensis* palaeoart— notes on palaeoenvironment, body shape and skin colour

An artist was approached with the task of illustrating the reconstructed *G. sivalensis* and its palaeoenvironment. The tasks involved three general steps: Scaling the animal to known proportions, proposing a skin colour and pattern and researching the Siwalik palaeoenvironment and contemporary fauna and flora.

#### 4.4.5.1 Scaling the artwork to known proportions

The proportions of *G. sivalensis* were discussed in the previous paragraphs and only the salient features will be highlighted here. Based on the holotype, the animal weighed approximately 400 kg with a range of 228–575 kg. However, based on the fossil limb bone dimensions, *G. sivalensis* weighed around 800 kg, which means either that it had a stocky body with a slender neck, exhibited sexual dimorphism in body size or perhaps some combination of the two. In the artwork depicted here, a body form that was both stockier in the male (around 800 kg) as well as more gracile in the female was depicted. The dorsal neck length and shoulder height was around 1.3 m and 2.5 m respectively, which makes dorsal neck length about a third of total length (Figure 4.10). As this animal was part of the giraffa genus the general shape of the modern giraffe was maintained, with the neck 'inserting' behind the shoulder (Solounias 1999) and a prominent withers area, albeit to a lesser extent. *G. sivalensis* was endowed with larger ears than contemporary giraffes, similar to that seen in the okapi (Figure 1.1), to reflect its forest environment (see below). Additionally, although no proof of such structures have been found in *G. sivalensis*, three ossicones which included a relatively prominent median horn were added.

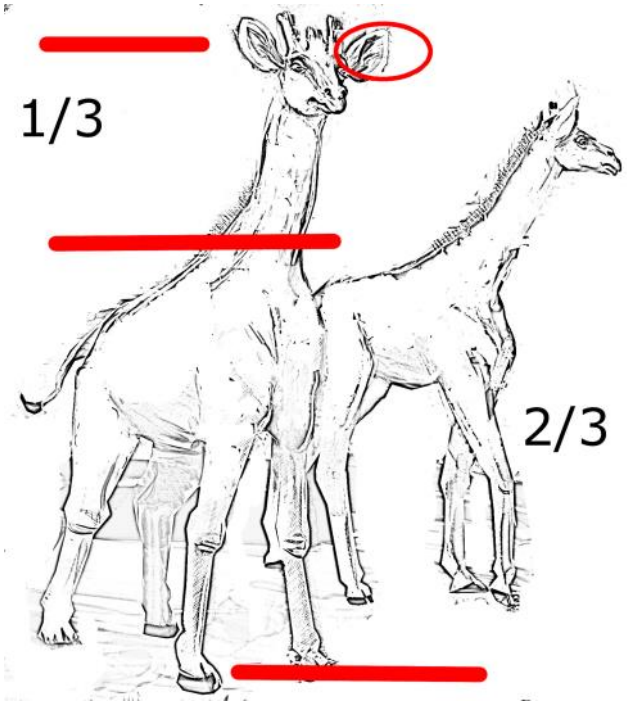


***Figure 4.10 G. sivalensis outline and proportions. On the left is a bull, with a more slender, younger female next to it. The dorsal neck length occupies about a third of total length. The circled area emphasises the ears, which were made larger than modern giraffes in order to reflect a forest dweller.***

### 4.4.5.2 Proposing a skin pattern and colour

Probably the first study to theorise on the adaptive advantages of giraffe coat patterns was that of Trouessart in 1908. In this paper Trouessart argued that the skin pattern of 'polygonal patches' is related to the way in which light penetrates the branches of Acacia trees, which itself is polygonal in shape (Figure 4.11).

***Figure 4.11 Trouessart's (1908) depiction of polygonal shapes in the giraffe's background environment.***

Theories on the evolution of mammalian coat patterns, especially in ungulates, remained essentially stagnant over the past century (Caro 2005). What is known is that there is a

broad range of factors that may act singularly or in combination to produce a species' coat pattern. In the vast majority of cases, the resultant coat pattern should offer some sort of advantage to the wearer. Seen from another angle: Coat patterns that disadvantage an animal are expected to be eliminated from the population rapidly. Beneficial coat patterning may aid an animal through concealment, communication and/ or thermoregulatory processes. Concealment can occur through crypsis (matching background colour), pattern blending, disruptive colouration (by breaking the body outline) or through counter colouration (light ventral and dark dorsal surfaces). Communicative colouration can be intraspecific (parent-offspring; intraspecies aggression or sexual suitability) or be directed to predators, such as warning signals, signals that a predator has been spotted or signals that may confuse predators (Caro 2005, 2009; Stoner *et al.* 2003). In some cases, communicative patterning may even be directed towards parasites: Zebra patterns, for example, may discourage biting insects from landing on an animal (Caro 2009; Caro & Stankowich 2015). Physiological reasons for patterning predominantly has some thermoregulatory process tied to it. Concealment, communication and thermoregulation need not influence coat pattern in a mutually exclusive manner either. In the case of the okapi, for example, the rump pattern has been hypothesised to function as communicative signals (conspecifics and predators) and as a thermoregulatory aid.

Notwithstanding the broad range of influences on coat pattern, there are general trends observable in artiodactyls. Concealment, it seems, remains the greatest influencer of coat colour and pattern in this order. Darker colours tend to be associated with animals that live in the tropics (Gloger's rule, Stoner *et al.* 2003) although, interestingly, environments (e.g. forest, grassland or woodland) are not as well associated with animal colour. That being said, the tropics do tend to facilitate closed forest canopies and in that way many forest dwellers may be darker in colour. Striped coats in adults are associated with concealment, whereas spotted coats in adults are generally not. White faces are associated with being diurnal and living in open environments, while darker faces are correlated with social grouping and being pursued by coursers. Leg markings are associated with open habitats (the okapi being an exception) and probably has communicative functions. As can be seen, deviations from common trends in artiodactyl coat colour and patterning are common. Nevertheless, one of the more robust trends is a darker coat colour which are associated with animals occurring in the tropics. Given *G. sivalensis's* still rather tropical surroundings at the turn of the Pliocene (see below), it would be a fair assumption that this animal would have been darker in colour as well.

The giraffe, with is dappled or spotted coat, is a peculiar deviation from the trend that spotted coats in ungulates are not well correlated with concealment (Stoner *et al.* 2003). In addition and quite importantly, Stoner *et al.* found that spotted species tend to be closely related, particularly in cervids. This explained their finding that certain spotted species of deer occurred in areas other than grasslands and forest environments. It would be particularly useful if further research could investigate correlations between coat patterns

and related ungulate species, and to what extent animals need to be related for correlations to hold. In this study it was found reasonable to assume that some baseline pattern would have been shared by all *Giraffa spp*. However, the forests and woodlands of India were more of a broad-leaved type than the environments of current giraffes. The patterning of *G. sivalensis* might therefore have reflected smaller specs of light reaching the ground, rather than the larger polygonal shapes mentioned by Trouessart. In other words, *G. sivalensis* probably still had a 'blotchy' spotted pattern, but with much smaller spots, perhaps almost leopard like. The spots may have been closer together and even coalescing on the dorsum, to a create a darker coat colour which would have been befitting to an animal living in a tropical environment.

***Figure 4.12 G. sivalensis coat pattern. The blotches are smaller and closer together than that of modern giraffes. Blotches on the dorsum coalesce to create a generally darker coat pattern.***

4.4.5.3 On the palaeoenvironment and contemporary fauna and flora

As early as 1876 Lydekker proposed a detailed view of what the Siwaliks looked like a few million years ago. He did not find it strange that so few of the genera that occured there during the Plio-Pleistocene epochs (e.g. *Elephas*, *Camelus*, *Giraffa*, *Equus*, *Sivatherium*, *Hippopotamus* and *Rhinoceros*) remained up until modern times. With the Pliocene Siwaliks being flatter than now, Lydekker saw conditions suitable for slow river flows with extensive marshes and pans, similar to the habitats currently found in Assam in Northeast India. Therefore, given its late Pliocene (or perhaps even earlier) origins, *G. sivalensis* probably also preferred forests type ecologies. Much more recently, Badam (1979) presented a similar view. He judged the presence of fossil reptiles such as *Crocodylus spp.*, *Megalochelys (=Colossochelys) atlas*, *Geoclemys sivalensis* and *Gavialis browni* to mean that the Plio-Pleistocene Siwaliks had an abundance of lakes and swamps and experienced seasonal

flooding. The fossil bovids, equids and cervids on the other hand indicated areas of drier land with lush vegetation interspersed between the wetlands.

The orogeny of the Himalayas started to change the climate of the region. Rising mountains meant cooler and subsequently drier environments. In addition, as the Siwalik and Himalayan mountains increased in height, river flow started to accelerate which further drained water from the area. Tropical wet evergreen and temperate forests were slowly being replaced by steppe biomes with patches of forest remaining interspersed. These changes probably did not occur linearly and the intervening warming and cooling periods will have caused the forest and steppe biomes to alternately expand and contract. The presence of *Rhinoceros spp.* and *Chilotherium intermedium* indicates that the wetlands were indeed starting to dry up, with plains starting to dominate (Badam 1979). It was the gradual environmental cooling, encroachment of grassland and decline of forests that would ultimately lead to the demise of the giraffids and many other Pleistocene species in India. In the artwork, a patch of remaining wetland and forest is depicted, at the edge of which stands *G. sivalensis*. In the background the rising Siwaliks, and further back, Himalayas, are visible. The clearing of forests and replacement by grasses is depicted behind the foreground forest. According to Singh & Singh (1987), remaining and interspersed forests were not homogenous and consisted of the following dominating forest types: *Quercus/ Carya spp*, *Larix-Quercus spp*, *Engelhardia*, *Quercus-Alnus spp* and *Pinus roxburghii*. The steppe consisted mostly of grasses (Poaceae) with or without *Chenopodium/ Amaranthus* and *Artemisia*. By the end of the Pliocene, tropical African elements, such as *Ziziphus mauritiana* had also reached the lower slopes of the western Himalaya. The artwork also includes the broad outlines of these tree types.

Nanda (2008) reviewed and listed Pinjor mammalian fauna occurring in the Indo-Pakistan region. The following species were subsequently included as contemporary mammal species on the artwork: *Anancus sivalensis*, *Rhinoceros sp.*, *Sivatherium giganteum*, *Bubalis sp.*, *Histrix spp.* and a *Cervus* species. In addition a reptilian contemporary in *Megalochelys atlas* (Badam 1979) was also added in the foreground Figure 4.13.

Fossilisation in the Plio-Pleistocene Siwaliks occurred in a relatively high energy environment, where many skeletons were transported, scattered and fragmented before preservation. Therefore, no articulating individual skeletons have yet been found (Badam 1979). Given the circumstances for fossilisation and the lack of teeth in birds, it is perhaps not surprising that bird fossils are rare in the area (Lydekker 1884). Nevertheless, the following bird genera and species have been described (Lydekker 1884; Patnaik & Sahni 1994; Stidham *et al.* 2014): *Pelecanus* (*Pelecanus cautleyi* and *Pelecanus sivalensis*), *Phalacrocorax, Leptoptilos spp.*, *Mergus spp.*, *Struthio asiaticus*, *Dromaius* and a member of the Strigidae. Because swamp-like environmental conditions were perhaps more conducive to fossil making, the majority of smaller bird fossils were waterbirds, which were also depicted on the artwork (Figure 4.13). The final artwork is presented in Figure 4.14.

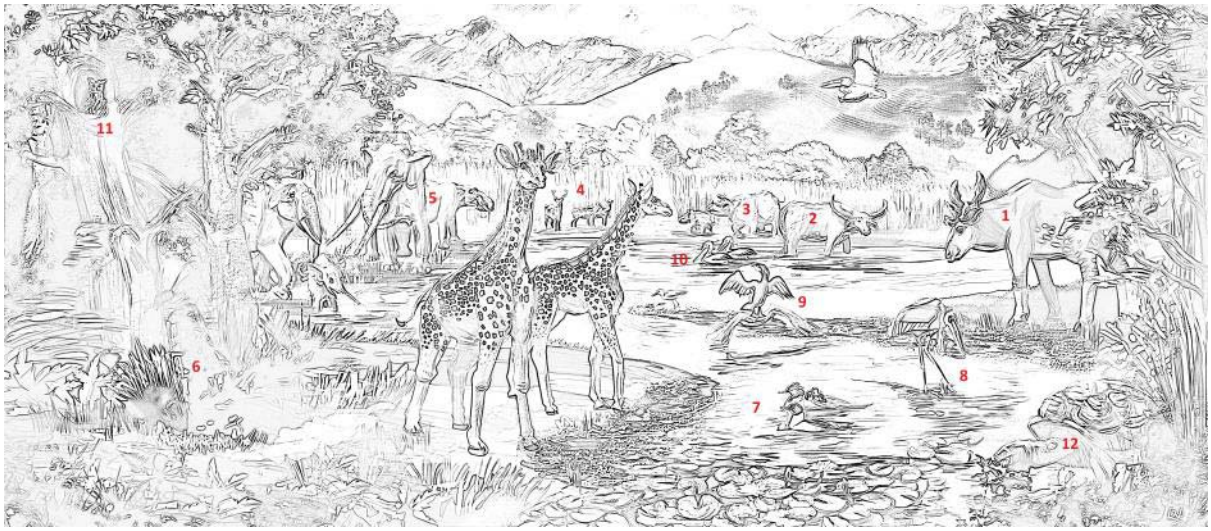


***Figure 4.13 G. sivalensis' palaeoenvironment. The environment shows the edge of a remaining forested area with the Siwaliks and Himalayas in the far background. Note: The form of animals in the background has not been reviewed in depth will be based on prior depictions or extrapolations. Key: 1.Sivatherium giganteum, showing its older 'moose-like' body form; 2. Bubalis sp.; 3. Rhinoceros sp .; 4. Cervus sp.; 5. Ananchus sivalensis; 6.Hystrix sp.7) Mergus sp.; 8. Leptoptilos sp.; 9. Phalacrocorax sp.; 10. Pelecanus sp.; 11. Member of the Stigidae; 12. Megalochelys atlas.***

## 4.5 Conclusion

The considered opinion that emerged out of this thesis is that *G. sivalensis,* from which the holotype cervical vertebra originated, weighed approximately 400 kg, had a neck length of about 1.47 m and a reaching height of 3.9 m. There is a possibility that it displayed sexual dimorphism, in which case male animals would have been a little less than twice the size of females and both would have had a similar morphology. If sexual dimorphism was not present and all bones were correctly attributed to this species, then the animal had a slender neck with a relatively stocky body, a shape that is not unrealistic to imagine.

*Figure 4.14 The final palaeoart in colour.Artist: Gina Viglietti.*

# Chapter 5
# General discussion

## 5.1 Introduction and salient findings

The principle aim of this study was to describe how the giraffe's extraordinary shape is reached throughout its life history. Accordingly, the growth of the postcranial skeleton was studied in a cross sectional sample of giraffes, spanning foetuses through to adults. Specifically, a description of the increase in length, diameters and cross sectional area of vertebrae and long bones were allometrically related to increases in body mass or increases in other dimensions. Finally, the regression equations obtained were applied in the reconstruction of *G. sivalensis*, an extinct giraffid that occurred in the Plio-Pleistocene epoch in Southern Asia.

The following salient findings regarding the growth patterns were made:

- There are no significant differences in the lengthening rates of individual cervical vertebrae (C2 to C7) with regard to body mass.
- Cervical vertebral lengthening with regard to body mass changes from isometric in the foetus to positively allometric in the postnatal animal.
- Long bone lengthening and thickening with regard to body mass changes from positively allometric in the foetus to isometric or negatively allometric after birth. With regard to length, long bones also do not become increasingly robust or increasingly slender.
- In addition to previously described morphological adaptations, T1 seems 'cervicalised'. It remains, however, significantly shorter than the rest of cervical vertebral bodies.
- Spinous processes scale with larger allometric exponents in the caudal cervical and cranial thoracic region, and reflect a response to the increasing weight of the neck.
- There is no sexual dimorphism regarding the lengthening of vertebra with regard to body mass.
- There is no sexual dimorphism regarding the lengthening of long bones with regard to body mass.

## 5.2 Research questions

The salient findings above are related to the research questions which were addressed as follows:

Question one addressed patterns of ontogenetic allometry in the vertebral skeleton. The following conclusions were made:

a) The hypothesis that sex does not play a role in the lengthening of the vertebral column sections could not be rejected. In particular, it was interesting to note that the cervical vertebral elongation did not display significant sexual dimorphism.

b) The hypothesis that lengthening exponents in vertebral regions are equal to 0.333 was rejected for the cervical vertebral region, but not for the thoracic and lumbar regions. In other words, the cervical vertebral column grows with positive allometry in postnatal animals.

c) Lengthening rates were not similar pre- and postnatally in the cervical region and therefore this hypothesis were rejected. In the thoracic and lumbar region however, this hypothesis could not be rejected.

Question two addressed patterns of ontogenetic allometry in the appendicular skeleton. The following conclusions were made:

a) The long bones did not elongate with regard to body mass in a significantly different way between the sexes.

b) Isometric lengthening and widening with regard to body mass were detected in many of the long bones:

   i) Isometric growth could not be rejected in the humerus, radius, metacarpus, tibia and metatarsus. However, isometry was rejected in the case of the femur, where the slope was negatively allometric.

   ii) The hypothesis that long bones widen (circumference) isometrically with regard to body mass could not be rejected in the case of the radius and tibia, but was rejected in the case of the humerus (positively allometric), metacarpus (negatively allometric), femur (negatively allometric) and metatarsus (negatively allometric).

c) The hypothesis that long bones do not become more robust or gracile relative to their length was not rejected in the case of the Zeugopodial and Metapodial bones of the front and hindlimb. For both the front and hind stylopodial bones however, the hypothesis was rejected as the bones become increasing robust with regard to length throughout growth

d) The hypotheses that long bones lengthen similarly pre-and-postnatally could be rejected for total leg length, metacarpus and femur. There were however no

significant differences in the pre-and postnatal lengthening of the humerus, Radius, tibia, and metatarsus. Long bones widened relatively faster in foetuses than postnatally.

The third question attempts to summarise the findings of the previous two questions by comparing them. Cervical vertebral and appendicular lengthening seems to follow opposite trends throughout ontogeny. In the cervical skeleton, the lengthening occurred isometric in the foetus but positively allometric in the postnatal animal. In the appendicular skeleton, the growth is positively allometric or isometric in the foetus and isometric after birth.

The fourth question aims to establish the significance of this thesis' findings in evolutionary terms. The lack of sexual dimorphism in lengthening with regard to body mass lends evidence against the 'necks for sex' hypothesis that emerged or re-emerged recently (Simmons & Scheepers 1996). In addition, this study proposes that as the evolutionary advantages of the long neck in the giraffe needs to be viewed from the perspective of a large body mass. Increasing body mass in an obligate browser demands increased levels of browse (during all seasons and browse availability), which in turn required neck length increase, with increases in leg length following suit. This study therefore casts doubt on the proposal of Pincher (1949), that neck elongation was a response to leg elongation. That being said, it also has to be considered that very few (if any) studies ever truly considered a multifactorial facet as an evolutionary drive for the giraffe shape. Under this framework, evolution of giraffe shape might have been driven (or maintained) by more than one potential advantage, simultaneously or separated temporally. If such a scenario was indeed the case, obviously more than one of the above theories might be plausible, either currently (i.e. maintaining the shape) or in the past.

Question five aims to ascertain the significance of this thesis' findings in biomechanical rather than evolutionary terms. It was proposed that the cross sectional properties of caudal cervical and cranial thoracic vertebrae, as well as the length of the spinous processes indicate a response to to increasing loads. The humerus and radius, in mediolateral diameter at least, may also reflect a response to increasing neck mass as well as behaviours such as splaying the legs while drinking. However, these proposals were not tested explicitly and further investigations would be needed to confirm or refute them.

Lastly, question six established whether the data obtained in this thesis could be used practically in palaeontology, specifically in an extinct member of the genus. The study showed that it was indeed feasible and, in certain cases, perhaps even desirable to reconstruct *G. sivalensis* from fossil remains using giraffe ontogenetic allometry. This animal weighed approximately 400 kg, had a neck length of about 1.47 m and a reaching height of 3.9 m. In addition, there is a possibility of sexual dimorphism in this species.

## 5.3 Value of study

Other morphometric studies on giraffes and ontogenetic studies in general were often limited in in sample size and variation. With large animals in particular, direct body mass measurements are often lacking and are estimated or taken from the literature. In addition, many of the specimens used in studies of the sort tend to originate from museums, which can carry the danger of being overrepresented in sex or animals of exaggerated proportions. In this study these limitation are overcome through the availability of an unprecedented sample size of giraffe vertebrae and long bones of which the body masses were known.

### 5.3.1 Perspective on the evolution of the giraffe

In recent times a theory of sexual selection as a driver for the long neck of the giraffe (Simmons & Scheepers 1996) has become well known and even popular. The theory has subsequently also been applied to sauropod necks (Senter 2007). One of the major contributions of the current study, building on the work of Mitchell *et al.* (2009a), was to show that sexual dimorphism, in terms of bone length vs. body mass, is not present in giraffes. This finding therefore disputes sexual selection as a sole driver for the elongation of the giraffe. In addition to morphometric data, behavioural data also do not seem to support sexual selection as a driver for elongation. Although Pratt & Anderson's (1985, 1982) studies have been used as evidence in favour of sexual selection (Simmons & Altwegg 2010; Simmons & Scheepers 1996), their data actually point to the opposite. It would seem that hierarchy establishment and male-male contests generally occur before the final, 'more advantageous' size for sexual selection is reached. In addition, after 3264 hours of behavioural observation in two parks, Pratt & Anderson (1985) witnessed only two real fighting events. Sparring behaviour were more frequent than 'real' contests, but sparring is usually initiated by younger bulls and even females—older, bigger bulls did not seem to partake in this activity. It is therefore suggested that necking behaviour in giraffes originated as a by-product of neck elongation and was not the cause of it. This scenario would be a good example of Gould's (1966) argument that shape change permits new functions. However, if however one assumes that necking behaviour was indeed established in certain short necked giraffid predecessors (although necking behaviour has not been observed directly in okapi, Kingdon & Hoffmann 2013), it could also be argued that necking is a form of combat utilised in giraffids with limited cranial armoury. In this case increasing the neck length would seem a rather costly exercise rather than elaborating on the existing cranial appendages, as was the case in other giraffids like *Sivatherium giganteum*.

### 5.3.2 Size estimates for *G. sivalensis*

Specimen OR39747 is among the best preserved fossil specimens of an extinct giraffe. It was found in a highly fossiliferous area, but one in which *complete* skeletal and fossil remains are exquisitely rare. OR39747 therefore merits in depth investigation. In addition, as it represents the terminal species of the genus in India it provides a size estimate where,

survival was not possible anymore, given climate changes or changes in interspecies competition. It therefore represents, for future studies, an interesting inference onto the ecology and body size requirements in the middle to late Pleistocene. Lastly, this study showed that, in the case of the Giraffinae at least, ontogenetic allometry of certain body dimensions might be a more accurate estimate than interspecific data.

### 5.3.3 Determining the population structure of giraffes that succumbed during a drought

The data presented this study has potential for use in retrospective ecological and epidemiological studies. As an example, Mitchell *et al.* 2010 used vertebral data to estimate the proportions of giraffe body weight groups that died during a drought. The study suggested that large males and juveniles were most susceptible to food shortages. This finding casted doubt on Darwin's (1888) suggestion that taller animals would survive droughts better than shorter animals, a view that has persistent till current times. Rather, as noted in the chapter on the appendicular skeleton, it is plausible that giraffe neck length evolved to support a large body mass of an obligate browser which facilitate multistrata browsing, during times of both plenty and scarcity.

## 5.4 Limitations of study

### 5.4.1 Small foetal sample sizes

Although a welcome addition to the field of allometry, the foetal sample size is still relatively small, and inferences regarding foetal growth remains with some hesitation. With small sample sizes distinction between isometry and departures from it becomes hazy, and isometric results in these cases can become meaningless (Brown & Vavrek 2015).

### 5.4.2 Lack of data on other taxa

Perhaps because of difficulty in collecting similar data in other large bodied mammals, species for comparison with giraffe data remain scarce. Similar data on other long necked or long limbed animals as well as okapis will provide additional evidence whether some patterns seen in this study are truly unique to giraffes.

### 5.4.3 Lack of certainty regarding the origin of fossil specimens of *G. sivalensis*

Many early palaeontologists were not in the habit of recording the localities of their finds with precision. Lydekker (1876) vented his frustration in this regard: “In the early part of the present year I made a journey to Attock for the purpose of re-discovering the beds from which these fossils had been obtained; unfortunately I had not been correctly informed as to the precise locality at which the fossils had been found, and I was consequently unsuccessful in the main object of my journey.” This results in uncertainty as to whether fossil specimens did indeed arise from similar strata or from a similar species. In the case of this study, if indeed localities had been incorrectly recorded, this could have led to erroneous assumptions on aspects of sexual dimorphism, for example.

### 5.4.4 Cross sectional areas

Long bone cross sectional second moments of area are more accurate determinants of long bone breaking strength. In this study, due to limited acquisition of periosteal and endosteal contours and cortical thickness, this was not possible.

### 5.4.5 The effect of soft tissues or cartilage loss

The effects of changes in cartilage proportions during vertebral growth have not been quantified in this study. Its effects may very well be significant; for example, Taylor & Wedel (2013a) has shown this to be the case regarding assumptions of neutral neck posture. Nevertheless, cartilage loss was minimised during the course of the study, and where it did occur during the boiling process of certain bones, it was replaced in situ as a reasonable approximate for the cartilage pre-dislodgement.

## 5.5 Possible avenues for future research

There is a dearth of similar data from larger species, and this study’s findings need to be validated against such data as it becomes available. Specifically, it would interesting to

determine if positively allometric neck growth combined with isometric leg growth is found in other mammalian species. It would be fascinating to compare the giraffe's early foetal growth, specifically body segmentation and vertebral growth, to the findings from late foetal growth reported in this study.

Although neck and head mass data have been collected as part of this study, it still needs to be analysed and interpreted in terms of limb bone growth, spinous process growth and cross sectional vertebral growth. In addition, the strengths of giraffe long bones and vertebrae need to be investigated with more accuracy using images of the cross sectional areas to determine parameters like second moment of area. Lastly, further palaeontological studies on other giraffid sizes are necessary to validate the current and future interpretations of fossil giraffid findings.

# References

Akhtar, M., Sarwar, M., Saeed, M. & Khan, A.A., 1991, 'Vertical distribution of Siwalik giraffids', *Acta Scientia* 1, 145–152.

Alexander, R., 1977, 'Allometry of the limbs of antelopes (Bovidae)*', *Journal of Zoology* 183, 125–146.

Alexander, R., Jayes, A.S., Maloiy, G.M.O. & Wathuta, E.M., 1979, 'Allometry of the limb bones of mammals from shrews (*Sorex) to elephant (*Loxodonta)', *Journal of Zoology* 189, 305–314.

Anderson, J.F., Hall-Martin, A. & Russell, D.A., 1985, 'Long-bone circumference and weight in mammals, birds and dinosaurs', *Journal of Zoology* 207, 53–61.

Angermeyer, M., 1966, 'Zur kenntnis der Halsmuskeln und Halsnerven von *Giraffa camelopardalis* (L.)', *Zoologischer Anzeiger* 177, 188–200.

Badam, G.L., 1979, *Pleistocene Fauna of India with special reference to the Siwaliks*, 1st ed., Deccan College Postgraduate and Research Institute, Pune, India.

Badlangana, N.L., Adams, J.W. & Manger, P.R., 2011, 'A Comparative Assessment of the Size of the Frontal Air Sinus in the Giraffe (*Giraffa camelopardalis*)', *Anatomical Record* 294, 931–940.

Badlangana, N.L., Adams, J.W. & Manger, P.R., 2009, 'The giraffe (*Giraffa camelopardalis*) cervical vertebral column: a heuristic example in understanding evolutionary processes?', *Zoological Journal of the Linnean Society* 155, 736–757.

Badlangana, N.L., Bhagwandin, A., Fuxe, K. & Manger, P.R., 2007, 'Observations on the giraffe central nervous system related to the corticospinal tract, motor cortex and spinal cord: What difference does a long neck make?', *Neuroscience* 148, 522–534.

Bertram, J.E. & Biewener, A.A., 1990, 'Differential scaling of the long bones in the terrestrial Carnivora and other mammals', *Journal of Morphology* 204, 157–169.

Bhatti, Z.H., 2004, 'Taxonomy, evolutionary history and biogeography of the Siwalik giraffids', Ph.D. Thesis, University of the Punjab, Lahore.

Biewener, A.A., 1983, 'Allometry of quadrupedal locomotion: the scaling of duty factor, bone curvature and limb orientation to body size', *Journal of Experimental Biology* 105, 147–171.

Biewener, A.A., 1982, 'Bone strength in small mammals and bipedal birds: do safety factors change with body size?', *Journal of Experimental Biology* 98, 289–301.

Biewener, A.A., 1989, 'Scaling body support in mammals: limb posture and muscle mechanics', *Science* 245, 45–48.

Bou, J., Casinos, A. & Ocana, J., 1987, 'Allometry of the limb long bones of insectivores and rodents', *Journal of Morphology* 192, 113–123.

Brear, K., Currey, J.D. & Pond, C.M., 1990, 'Ontogenetic changes in the mechanical properties of the femur of the polar bear *Ursus maritimus*', *Journal of Zoology* 222, 49–58.

Bredin, I.P., Skinner, J.D. & Mitchell, G., 2008, 'Can osteophagia provide giraffes with phosphorus and calcium?', *Onderstepoort Journal of Veterinary Research* 75, 1–9.

Brown, C.M. & Vavrek, M.J., 2015, 'Small sample sizes in the study of ontogenetic allometry; implications for palaeobiology', *PeerJ* 3, e818.

Brown, D.M., Brenneman, R.A., Koepfli, K.-P., Pollinger, J.P., Milá, B., Georgiadis, N.J., *et al.*, 2007, 'Extensive population genetic structure in the giraffe', *BMC Biology* 5, 57.

Brownlee, A., 1963, 'Evolution of the giraffe.', *Nature* 200, 1022.

Buchholtz, E.A. & Stepien, C.C., 2009, 'Anatomical transformation in mammals: developmental origin of aberrant cervical anatomy in tree sloths', *Evolution & Development* 11, 69–79.

Burke, A.C., Nelson, C.E., Morgan, B.A. & Tabin, C., 1995, 'Hox genes and the evolution of vertebrate axial morphology', *Development* 121, 333–346.

Calder, W.A., 1984, *Size, Function, and Life History*, Courier Corporation.

Cameron, E.T. & Du Toit, J.T., 2007, 'Winning by a Neck: Tall Giraffes Avoid Competing with Shorter Browsers', *American Naturalist* 169, 130–135.

Campione, N.E. & Evans, D.C., 2012, 'A universal scaling relationship between body mass and proximal limb bone dimensions in quadrupedal terrestrial tetrapods', *BMC Biology* 10, 60.

Caro, T.M., 2009, 'Contrasting coloration in terrestrial mammals', *Philosophical Transactions of the Royal Society of London B: Biological Sciences* 364, 537–548.

Caro, T.M., 2005, 'The Adaptive Significance of Coloration in Mammals', *BioScience* 55, 125–136.

Caro, T.M. & Stankowich, T., 2015, 'Concordance on zebra stripes: a comment on Larison et al. (2015)', *Royal Society Open Science* 2, 150323.

Carrier, D. & Leon, L.R., 1990, 'Skeletal growth and function in the California gull (*Larus californicus*)', *Journal of Zoology* 222, 375–389.

Carrier, D.R., 1996, 'Ontogenetic limits on locomotor performance', *Physiological zoology* 69, 467–488.

Carrier, D.R., 1983, 'Postnatal ontogeny of the musculo-skeletal system in the Black- tailed jack rabbit (*Lepus californicus*)', *Journal of Zoology (London)* 201, 27–55.

Carter, D.R., Van Der Meulen, M.C. & Beaupré, G.S., 1996, 'Mechanical factors in bone growth and development', *Bone* 18, 5S–10S.

Cautley, P.T., 1838, 'Note on a fossil ruminant genus allied to Giraffidae, in the Siwalik Hills.', *Journal of the Asiatic Society of Bengal* 7, 658–660.

Cawley, G.C. & Janacek, G.J., 2010, 'On allometric equations for predicting body mass of dinosaurs', *Journal of Zoology* 280, 355–361.

Christiansen, P., 2007, 'Long-bone geometry in columnar-limbed animals: allometry of the proboscidean appendicular skeleton', *Zoological Journal of the Linnean Society* 149, 423–436.

Christiansen, P., 1999, 'Scaling of the limb long bones to body mass in terrestrial mammals', *Journal of Morphology* 239, 167–190.

Christiansen, P.E.R., 2002, 'Locomotion in terrestrial mammals: the influence of body mass, limb length and bone proportions on speed', *Zoological Journal of the Linnean Society* 136, 685–714.

Colbert, E.H., 1938, 'The relationships of the okapi', *Journal of Mammology* 19, 47–64.

Currey, J.D., 2002, *Bones: Structure and Mechanics*, Princeton University Press, New Jersey.

Currey, J.D., 2003, 'The many adaptations of bone', *Journal of Biomechanics* 36, 1487–1495.

Currey, J.D. & Alexander, R.M., 1985, 'The thickness of the walls of tubular bones', *Journal of Zoology* 206, 453–468.

Dagg, A.I., 2014, *Giraffe: Biology, Behaviour and Conservation*, Cambridge University Press, Cambridge.

Dagg, A.I., 1962, 'The Subspeciation of the Giraffe', *Journal of Mammalogy* 43, 550–552.

Dagg, A.I. & Foster, J.B., 1976, *The giraffe: Its biology, behaviour, and ecology.*, Van Nostrand Reinhold Company, New York.

Damkjær, M., Wang, T., Brøndum, E., Østergaard, K.H., Baandrup, U., Hørlyck, A., *et al.*, 2015, 'The giraffe kidney tolerates high arterial blood pressure by high renal interstitial pressure and low glomerular filtration rate', *Acta Physiologica* 214, 497–510.

Damuth, J., 1990, 'Problems in estimating body masses of archaic ungulates using dental measurements', in J. D. Damuth & B. J. MacFadden (eds.) *Body Size in Mammalian Paleobiology: Estimation and Biological Implications*, pp. 229–253, Cambridge University Press, Cambridge.

Darwin, C.R., 1888, 'The origin of species: By means of natural selection, the preservation of favoured races in the struggle for life', in p. 177, John Murray, London.

De Esteban-Trivigno, S., Mendoza, M. & De Renzi, M., 2008, 'Body mass estimation in Xenarthra: a predictive equation suitable for all quadrupedal terrestrial placentals?', *Journal of morphology* 269, 1276–1293.

Dequéant, M.-L. & Pourquié, O., 2008, 'Segmental patterning of the vertebrate embryonic axis', *Nature Reviews Genetics* 9, 370–382.

Du Toit, J.T., 2005, 'Sex differences in the foraging ecology of large mammalian herbivores', in K. Ruckstuhl & P. Neuhaus (eds.) *Sexual Segregation in Vertebrates*, pp. 35–52, Cambridge University Press, Cambridge.

Dzemski, G., 2005, 'Funktionsmorpholgische Betrachtungen der Halsstellung bei Zoogiraffen', *Zoologische Garten* 75, 189.

Eberhard, W.G., 2009, 'Static Allometry and Animal Genitalia', *Evolution* 63, 48–66.

Economos, A.C., 1983, 'Elastic and/or geometric similarity in mammalian design?', *Journal of Theoretical Biology* 103, 167–172.

Endo, H., Yamagiwa, D., Fujisawa, M., Kimura, J., Kurohmaru, M. & Hayashi, Y., 1997, 'Modified neck muscular system of the giraffe (*Giraffa camelopardalis*)', *Annals of Anatomy-Anatomischer Anzeiger* 179, 481–485.

Falconer, H., 1868a, 'Description by Dr. Falconer of fossil remains of Giraffe in the museum of Asiatic Society of Bengal', in C. Murchison (ed.) *Palaeontological memoirs and notes of the late Hugh Falconer. Fauna Antiqua Sivalensis*, pp. 206–207, R. Hardwicke, London.

Falconer, H., 1845, 'Description of some fossil remains of Dinotherium, Giraffe, and other mammalia, from the Gulf of Cambay, western coast of India, chiefly from the collection presented by Captain Fulljames, of the Bombay Engineers, to the Museum of the Geological Society', *Quarterly Journal of the Geological Society* 1, 356–372.

Falconer, H., 1868b, *Description of the plates of the Fauna Antiqua Sivalensis*, C. Murchison (ed.), R. Hardwicke, London, viewed 8 November 2014, from http://archive.org/details/descriptionofpla00falc.

Falconer, H., 1868c, *Palæontological Memoirs and Notes of the Late Hugh Falconer: With a Biographical Sketch of the Author*, C. Murchison (ed.), R. Hardwicke, London.

Falconer, H. & Cautley, P.T., 1843, 'On some fossil remains of Anoplotherium and Giraffe, from the Sewalik Hills, in the north of India.', *Proceedings of the Geological Society of London* 4, 235–249.

Falster, D.S., Warton, D.I. & Wright, I.J., 2006, *SMATR: Standardised Major Axis and Routines Ver. 2*, from http://www.bio.mq.edu.au/ecology/SMATR/.

Flower, W.H., 1885, *An introduction to the osteology of the Mammalia*, Macmillan and Company, London.

Fortelius, M., 1990, 'Problems with sing fossil teeth to estimate body sizes of extinct mammals', in J. Damuth & B. J. MacFadden (eds.) *Body Size in Mammalian Paleobiology: Estimation and Biological Implications*, Cambridge University Press, Cambridge.

Fraser, F.C., 1951, 'Vestigial metapodials in the Okapi and Giraffe.', *Proceedings of the Zoological Society of London* 121, 315–317.

Galilei, G., 1638, *Dialogues concerning two new sciences*, The MacMillan Company, New York.

Galis, F., 1999, 'Why do almost all mammals have seven cervical vertebrae? Developmental constraints, Hox genes, and cancer', *Journal of Experimental Zoology* 285, 19–26.

Garcia, G.J. & da Silva, J.K., 2004, 'On the scaling of mammalian long bones', *Journal of experimental biology* 207, 1577–1584.

Garcia, G.J. & da Silva, J.K.L., 2006, 'Interspecific allometry of bone dimensions: A review of the theoretical models', *Physics of life reviews* 3, 188–209.

Gaunt, S.J., 1994, 'Conservation in the Hox code during morphological evolution.', *The International journal of developmental biology* 38, 549–552.

Gaur, R., Vasishat, N. & Chopra, S.R.K., 1985, 'New and some additional fossil mammals from the Siwaliks exposed at Nurpur, Kangra district, H.P.', *Journal of the palaeontological society of India* 30, 42–48.

Gayon, J., 2000, 'History of the Concept of Allometry', *American Zoologist* 40, 748–758.

Ghazi, S.R. & Gholami, S., 1994, 'Allometric growth of the spinal cord in relation to the vertebral column during prenatal and postnatal life in the sheep (Ovis aries).', *Journal of anatomy* 185, 427.

Giffin, E.B. & Gillett, M., 1996, 'Neurological and osteological definitions of cervical vertebrae in mammals', *Brain, behavior and evolution* 47, 214–218.

Glazier, D.S., 2013, 'Log-transformation is useful for examining proportional relationships in allometric scaling', *Journal of theoretical biology* 334, 200–203.

Goetz, R.H. & Keen, E.N., 1957, 'Some aspects of the cardiovascular system in the giraffe', *Angiology* 8, 542–564.

Gould, S.J., 1966, 'Allometry and size in ontogeny and phylogeny.', *Biological reviews of the Cambridge Philosophical Society* 41, 587–640.

Gould, S.J., 1971, 'Geometric similarity in allometric growth: a contribution to the problem of scaling in the evolution of size.', *The American Naturalist* 105, 113–136.

Grossi, B. & Canals, M., 2010, 'Comparison of the morphology of the limbs of juvenile and adult horses (Equus caballus) and their implications on the locomotor biomechanics', *Journal of Experimental Zoology Part A: Ecological Genetics and Physiology* 313, 292–300.

Hall-Martin, A.J., 1975, 'Studies on the biology and productivity of the Giraffe *Giraffa camelopardalis*', DSc. Thesis, University of Pretoria, Pretoria.

Hargens, A.R., Millard, R.W., Pettersson, K. & Johansen, K., 1987, 'Gravitational haemodynamics and oedema prevention in the giraffe', *Nature* 329, 59–60.

Hassanin, A., Ropiquet, A., Gourmand, A.L., Chardonnet, B. & Rigoulet, J., 2007, 'Variabilite de l'ADN mitochondrial chez *Giraffa camelopardalis* : consequences pour la taxinornie, la phylogeographie et la conservation des girafes en Afrique de l'Ouest et centrale. Mitochondrial DNA variability in Giraffa camelopardalis: consequences for taxonomy, phylogeography and conservation of giraffes in West and central Africa', *Comptes Rendus Biologies* 330, 265–274.

Heinrich, R.E., Ruff, C.B. & Adamczewski, J.Z., 1999, 'Ontogenetic changes in mineralization and bone geometry in the femur of muskoxen (*Ovibos moschatus*)', *Journal of zoology* 247, 215–223.

Henderson, D.M. & Naish, D., 2010, 'Predicting the buoyancy, equilibrium and potential swimming ability of giraffes by computational analysis', *Journal of theoretical biology* 265, 151–159.

Hernández Fernández, M. & Vrba, E.S., 2005, 'A complete estimate of the phylogenetic relationships in Ruminantia: A dated species-level supertree of the extant ruminants', *Biological Reviews of the Cambridge Philosophical Society* 80, 269–302.

Huxley, J.S., 1924, 'Constant differential growth-ratios and their significance', *Nature* 114, 895–896.

Huxley, J.S., 1932, *Problems of relative growth.*, The dial press, New York.

International Committee on Veterinary Gross Anatomical Nomenclature, 2012, *Nomina Anatomica Veterinaria (N.A.V.)*, Editorial Committee, World Assosiation of Veterinary Anatomists, Hannover (Germany), Columbia (USA), Ghent (Belgium), Sapporo (Japan).

Janis, C.M., 1990, 'Correlation of cranial and dental variables with body size in ungulates and macropodoids', in J. Damuth & B. J. MacFadden (eds.) *Body size in mammalian paleobiology: estimation and biological implications*, Cambridge University Press, Cambridge.

Janis, C.M. & Scott, K.M., 1987, 'The interrelationships of higher ruminant families: with special emphasis on the members of the Cervoidea. American Museum novitates; no. 2893', *American Museum Noviates* 2893, 1–85.

Janis, C.M. & Scott, K.M., 1988, 'The phylogeny of the Ruminantia (Artiodactyla, Mammalia)', in *The phylogeny and classification of the tetrapods*, pp. 273–282, Clarendon Press., viewed 3 October 2015, from http://scholar.google.com/scholar?cluster=7500604023270201065&hl=en&oi=scholarr.

Janis, C.M. & Theodor, J.M., 2014, 'Cranial and postcranial morphological data in ruminant phylogenetics', *Zitteliana*, 15–31.

Janis, C.M., Theodor, J.M. & Boisvert, B., 2002, 'Locomotor evolution in camels revisited: a quantitative analysis of pedal anatomy and the acquisition of the pacing gait', *Journal of vertebrate paleontology* 22, 110–121.

Kerkhoff, A.J. & Enquist, B.J., 2009, 'Multiplicative by nature: why logarithmic transformation is necessary in allometry', *Journal of Theoretical Biology* 257, 519–521.

Kilbourne, B.M. & Makovicky, P.J., 2012, 'Postnatal long bone growth in terrestrial placental mammals: Allometry, life history, and organismal traits', *Journal of Morphology* 273, 1111–1126.

Kingdon, J. & Hoffmann, M. (eds.), 2013, 'Family Giraffidae', in *Mammals of Africa*, pp. 95–115, Bloomsbury Publishing, London.

Kokshenev, V.B., Silva, J.K.L. & Garcia, G.J.M., 2003, 'Long-bone allometry of terrestrial mammals and the geometric-shape and elastic-force constraints of bone evolution', *Journal of Theoretical Biology* 224, 551–556.

Lammers, A.R. & German, R.Z., 2002, 'Ontogenetic allometry in the locomotor skeleton of specialized half-bounding mammals', *Journal of zoology* 258, 485–495.

Lankester, R., 1908, 'On certain points in the structure of the cervical vertebrae of the okapi and the giraffe.', *Proceedings of the Zoological Society of London* 1908, 320–334.

Leppänen, O., 2009, 'Postnatal Bone Ontogeny', Ph.D. Thesis, University of Tampere, Tampere, viewed 15 January 2014, from http://tampub.uta.fi/handle/10024/66429.

Lindsey, S.L. & Bennett, C.L., 1999, *The Okapi: Mysterious Animal of Congo-Zaire*, University of Texas Press, Austin.

Liu, M.F., He, P., Aherne, F.X. & Berg, R.T., 1999, 'Postnatal limb bone growth in relation to live weight in pigs from birth to 84 days of age.', *Journal of Animal Science* 77, 1693–1701.

Lydekker, R., 1885a, *Catalogue of fossil mammalia. Part ii. Containing the order Ungulata, suborder Artiodactyla*, Taylor and Francis. Printed by order of the Trustees, London.

Lydekker, R., 1885b, *Catalogue of the remains of Siwalik vertebrata contained in the geological department of the Indian museum, Calcutta: Mammalia*, Superintendent of Government Printing, Calcutta.

Lydekker, R., 1883, 'Indian Tertiary and post Tertiary vertebrata: Siwalik Camelopardalidae', in *Memoirs of the Geological survey of India: Palaeontologica Indica, Being Figures and Descriptions of the Organic Remains Procured During the Progress of the Geological Survey of India*, pp. 99–142, Geological survey of India, by order of the Governor-General of India, Calcutta., viewed 28 January 2015, from http://www.europeana.eu/portal/record/9200143/BibliographicResource_2000069323222.html.

Lydekker, R., 1876, 'Notes on the fossil mammalian faunae of India and Burma', in *Records of the Geological Survey of India*, pp. 86–105, Trübner and Co., London.

Lydekker, R., 1878, 'Notices of Siwalik Mammals', in *Records of the Geological Survey of India*, pp. 83–95, Trübner and Co., London.

Lydekker, R., 1904, 'On the subspecies of *Giraffa camelopardalis*', *Proceedings of the Zoological Society of London* 1904:v.1 (Jan.-Apr.), 202–227.

Lydekker, R., 1884, 'Siwalik birds', in *Memoirs of the Geological survey of India: Palaeontologica Indica, Being Figures and Descriptions of the Organic Remains Procured During the Progress of the Geological Survey of India*, Indian Tertiary and Post Tertiary Vertebrata. Geological Survey Office [etc.], Calcutta., viewed 7 October 2015, from https://dds.crl.edu/crldelivery/20072.

Main, R.P., 2007, 'Ontogenetic relationships between in vivo strain environment, bone histomorphometry and growth in the goat radius', *Journal of anatomy* 210, 272–293.

Main, R.P. & Biewener, A.A., 2006, 'In vivo bone strain and ontogenetic growth patterns in relation to life-history strategies and performance in two vertebrate taxa: goats and emu', *Physiological and biochemical zoology: PBZ* 79, 57–72.

Main, R.P. & Biewener, A.A., 2004, 'Ontogenetic patterns of limb loading, in vivo bone strains and growth in the goat radius', *The Journal of Experimental Zoology* 207, 2577–2588.

Main, R.P., Lynch, M.E. & van der Meulen, M.C.H., 2010, 'In vivo tibial stiffness is maintained by whole bone morphology and cross-sectional geometry in growing female mice', *Journal of Biomechanics* 43, 2689–2694.

Maluf, N.S.R., 2002, 'Kidney of giraffes', *Anatomical Record* 267, 94–111.

Matthew, W.D., 1929, 'Critical observations upon Siwalik mammals (exclusive of Proboscidea)', *Bulletin of the American Museum of Natural History* 56, 437–560.

McGowan, C., 1999, *A practical guide to vertebral mechanics.*, Cambridge University Press, Cambridge.

McMahon, T.A., 1975, 'Allometry and Biomechanics: Limb Bones in Adult Ungulates', *The American Naturalist* 109, 547–563.

McMahon, T.A., 1973, 'Size and shape in biology.', *Science* 179, 1201–1204.

Miller, C.E., Basu, C., Fritsch, G., Hildebrandt, T. & Hutchinson, J.R., 2008, 'Ontogenetic scaling of foot musculoskeletal anatomy in elephants', *Journal of the Royal Society Interface* 5, 465–475.

Mitchell, G., 2009, 'The origins of the scientific study and classification of giraffes', *Transactions of the Royal Society of South Africa* 64, 1–13.

Mitchell, G. & Lust, A., 2008, 'The carotid rete and artiodactyl success', *Biology letters* 4, 415–418.

Mitchell, G., Roberts, D.G., Van Sittert, S.J. & Skinner, J.D., 2013a, 'Growth patterns and masses of the heads and necks of male and female giraffes', *Journal of Zoology* 290, 49–57.

Mitchell, G., Roberts, D.G., Van Sittert, S.J. & Skinner, J.D., 2013b, 'Orbit orientation and eye morphometrics in giraffes (*Giraffa camelopardalis*)', *African Zoology* 48, 333–339.

Mitchell, G. & Skinner, J.D., 2009, 'An allometric analysis of the giraffe cardiovascular system', *Comparative Biochemistry and Physiology - A Molecular and Integrative Physiology* 154, 523–529.

Mitchell, G. & Skinner, J.D., 2004, 'Giraffe thermoregulation: a review', *Transactions of the Royal Society of South Africa* 59, 109–118.

Mitchell, G. & Skinner, J.D., 1993, 'How giraffe adapt to their extraordinary shape', *Transactions of the Royal Society of South Africa* 48, 207–218.

Mitchell, G. & Skinner, J.D., 2011, 'Lung volumes in giraffes, *Giraffa camelopardalis*', *Comparative biochemistry and physiology. Part A, Molecular & integrative physiology* 158, 72–78.

Mitchell, G. & Skinner, J.D., 2003, 'On the origin, evolution and phylogeny of giraffes *Giraffa camelopardalis*.', *Transactions of the Royal Society of South Africa* 58, 51–73.

Mitchell, G., Van Sittert, S.J. & Skinner, J.D., 2009a, 'Sexual selection is not the origin of long necks in giraffes', *Journal of Zoology (London)* 278, 281–286.

Mitchell, G., Van Sittert, S.J. & Skinner, J.D., 2010, 'The demography of giraffe deaths in a drought', *Transactions of the Royal Society of South Africa* 65, 165–168.

Mitchell, G., Van Sittert, S.J. & Skinner, J.D., 2009b, 'The structure and function of giraffe jugular vein valves', *South African Journal of Wildlife Research* 39, 175–180.

Montgelard, C., Catzeflis, F.M. & Douzery, E., 1997, 'Phylogenetic relationships of artiodactyls and cetaceans as deduced from the comparison of cytochrome b and 12S rRNA mitochondrial sequences.', *Molecular Biology and Evolution* 14, 550–559.

Murie, J., 1872, 'On the horns, viscera, and muscles of the giraffe; with a record of the post mortem examination of two specimens killed by a fire', *The annals and magazine of natural history, including zoology, botany and geology* 9, 177.

Nanda, A.C., 2008, 'Comments on the Pinjor Mammalian Fauna of the Siwalik Group in relation to the post-Siwalik faunas of Peninsular India and Indo-Gangetic Plain', *Quaternary International* 192, 6–13.

Nanda, A.C., 2002, 'Upper Siwalik mammalian faunas of India and associated events', *Journal of Asian Earth Sciences* 21, 47–58.

Narita, Y. & Kuratani, S., 2005, 'Evolution of the vertbral formulae in mammals: a perspective on developmental constraints.', *Journal of Experimental Zoology Part B Molecular and Developmental Evolution* 304B, 91–106.

Nishida, F., Andrés, J.B., Barbeito, C.G. & Portiansky, E.L., 2014, 'Is the vertebral canal prepared to host the aged spinal cord? A morphometric assessment', *Zoomorphology* 133, 219–225.

Norberg, R.Å. & Aldrin, B.S.W., 2010, 'Scaling for stress similarity and distorted-shape similarity in bending and torsion under maximal muscle forces concurs with geometric similarity among different-sized animals', *Journal of Experimental Biology* 213, 2873–2888.

O'Brien, H.D. & Bourke, J., 2015, 'Physical and computational fluid dynamics models for the hemodynamics of the artiodactyl carotid rete', *Journal of Theoretical Biology* 386, 122–131.

Owen, R., 1838, 'Notes on the Anatomy of the Nubian Giraffe', *Transactions of the Zoological Society (London)* 2, 217–248.

Owen, R., 1850, 'On the anatomy of the Indian Rhinoceros', *Transactions of the Zoological Society (London)* 4, 31–58.

Packard, G.C., 2013, 'Is logarithmic transformation necessary in allometry?', *Biological Journal of the Linnean Society* 109, 476–486.

Packard, G.C., 2009, 'On the use of logarithmic transformations in allometric analyses', *Journal of Theoretical Biology* 257, 515–518.

Packard, G.C. & Birchard, G.F., 2008, 'Traditional allometric analysis fails to provide a valid predictive model for mammalian metabolic rates', *Journal of Experimental Biology* 211, 3581–3587.

Packard, G.C. & Boardman, T.J., 2008, 'Model selection and logarithmic transformation in allometric analysis', *Physiological and Biochemical Zoology* 81, 496–507.

Packard, G.C., Boardman, T.J. & Birchard, G.F., 2009, 'Allometric equations for predicting body mass of dinosaurs', *Journal of Zoology* 279, 102–110.

Packard, G.C., Boardman, T.J. & Birchard, G.F., 2010, 'Allometric equations for predicting body mass of dinosaurs: a comment on Cawley & Janacek (2010)', *Journal of Zoology* 282, 221–222.

Patnaik, R. & Sahni, A., 1994, 'Record of a bird humerus from Upper Pleistocene Narmada valley sediments', *J. Palaeontol. Soc. India* 39, 77–79.

Pedley, T.J., 1987, 'How giraffes prevent oedema', *Nature* 329, 13–14.

Pélabon, C., Bolstad, G.H., Egset, C.K., Cheverud, J.M., Pavlicev, M. & Rosenqvist, G., 2013, 'On the relationship between ontogenetic and static allometry', *The American naturalist* 181, 195–212.

Pincher, C., 1949, 'Evolution of the giraffe', *Nature* 164, 29–30.

Pratt, D.M. & Anderson, V.H., 1985, 'Giraffe social behaviour', *Journal of Natural History* 19, 771–781.

Pratt, D.M. & Anderson, V.H., 1982, 'Population, distribution, and behaviour of giraffe in the Arusha National Park, Tanzania', *Journal of Natural History* 16, 481–489.

Rice, W.R., 1989, 'Analyzing tables of statistical tests', *Evolution* 43, 223–225.

Roth, V.L., 1990, 'Insular dwarf elephants: a case study in body mass estimation and ecological inference.', in J. D. Damuth & B. J. MacFadden (eds.) *Body Size in Mammalian Paleobiology: Estimation and Biological Implications*, pp. 151–179, Cambridge University Press, Cambridge.

Runestad, J.A., 1994, 'Humeral and Femoral Diaphyseal Cross-sectional Geometry and Articular Dimensions in Prosimii and Platyrrhini (primates) with Application for Reconstruction of Body Mass and Locomotor Behavior in Adapidae (primates: Eocene)', Ph.D. Thesis, Johns Hopkins University, Baltimore.

Sakamoto, J., Arihara, K., Tai, H. & Yamazaki, T., 2011, 'A study on cervical spine of giraffe to consider its mechanical adaptation', in International Society of Biomechanics Congress xxiii. Brussels., from https://isbweb.org/images/conf/2011/ScientificProgram/ISB2011_ScientificProgram_files/1085.pdf.

Sathar, F., Badlangana, N.L. & Manger, P.R., 2010, 'Variations in the thickness and composition of the skin of the giraffe', *Anatomical Record* 293, 1615–1627.

Scott, K.M., 1990, 'Postcranial dimensions of ungulates as predictors of body mass', in J. Damuth & B. J. MacFadden (eds.) *Body size in mammalian paleobiology*, Cambridge University Press, Cambridge.

Seeber, P.A., Ndlovu, H.T., Duncan, P. & Ganswindt, A., 2012, 'Grazing behaviour of the giraffe in Hwange National Park, Zimbabwe', *African Journal of Ecology* 50, 247–250.

Selker, F. & Carter, D.R., 1989, 'Scaling of long bone fracture strength with animal mass', *Journal of biomechanics* 22, 1175–1183.

Senter, P., 2007, 'Necks for sex: sexual selection as an explanation for sauropod dinosaur neck elongation', *Journal of Zoology (London)* 271, 45–53.

Seymour, R., 2001, 'Patterns of subspecies diversity in the giraffe, Giraffa camelopardalis (L. 1758) : comparison of systematic methods and their implications for conservation policy', Ph.D. Thesis, University of Kent at Canterbury, Canterbury, viewed 8 July 2015, from http://ethos.bl.uk/OrderDetails.do?uin=uk.bl.ethos.275008.

Seymour, R., 2012, 'The taxonomic history of the giraffe', *Giraffa* 6, 5–9.

Shortridge, G.C., 1934, *The mammals of South West Africa*, Heinemann, London, viewed 4 October 2015, from http://www.rhinoresourcecenter.com/pdf_files/127/1276554135.pdf.

Simmons, R.E. & Altwegg, R., 2010, 'Necks-for-sex or competing browsers? A critique of ideas on the evolution of giraffe', *Journal of zoology* 282, 6–12.

Simmons, R.E. & Scheepers, L., 1996, 'Winning by a neck: Sexual selection in the evolution of giraffe', *The American Naturalist* 148, 771–786.

Simpson, G.G., 1945, 'The principles of classification and a classification of mammals.', *Bulletin of the American Museum of Natural History* 85, xvi+350.

Singh, J.S. & Singh, S.P., 1987, 'Forest vegetation of the Himalaya', *The Botanical Review* 53, 80–192.

Skinner, J.D. & Chimimba, C.T., 2005, 'Family Giraffidae Gray 1821', in The mammals of the Southern African Subregion. pp. 616–620, Cambridge University Press, Cambridge.

Skinner, J.D. & Hall-Martin, A.J., 1975, 'A note on foetal growth and development of the giraffe *Giraffa camelopardalis giraffa*', *Journal of Zoology (London)* 177, 73–79.

Slijper, E.J., 1946, 'Comparative biologic-anatomical investigations on the vertebral column and spinal musculature of mammals', *Verhandelingen der Koninklijke Nederlandsche Akademie van Wetenschappen Afdeling Natuurkunde* 42, 1–128.

Smith, R.J., 1984, 'Allometric scaling in comparative biology: problems of concept and method', *American Journal of Physiology-Regulatory, Integrative and Comparative Physiology* 246, R152–R160.

Solounias, N., 2007, 'Family Giraffidae', in D. R. Prothero & S. E. Foss (eds.) *The Evolution of Artiodactyls*, Johns Hopkins University Press, Baltimore.

Solounias, N., 1999, 'The remarkable anatomy of the giraffe's neck', *Journal of Zoology (London)* 247, 257–268.

Solounias, N. & Tang, N., 1990, 'The two types of cranial appendages in *Giraffa camelopardalis* (Mammalia, Artiodactyla)', *Journal of Zoology* 222, 293–302.

Spamer, E.E., Daeschler, E. & Vostreys-Shapiro, L.G., 1995, *A Study of Fossil Vertebrate Types in the Academy of Natural Sciences of Philadelphia: Taxonomic, Systematic, and Historical Perspectives*, Academy of Natural Sciences, Philadelphia, U.S.A.

Sparacello, V.S. & Pearson, O.M., 2010, 'The importance of accounting for the area of the medullary cavity in cross-sectional geometry: A test based on the femoral midshaft', *American Journal of Physical Anthropology* 143, 612–624.

Spinage, C.A., 1993, 'The median ossicone of Giraffa camelopardalis', *Journal of Zoology* 230, 1–5.

Stidham, T.A., Krishan, K., Singh, B., Ghosh, A. & Patnaik, R., 2014, 'A Pelican Tarsometatarsus (Aves: Pelecanidae) from the Latest Pliocene Siwaliks of India', *PLoS ONE* 9, e111210.

Stoner, C.J., Caro, T.M. & Graham, C.M., 2003, 'Ecological and behavioral correlates of coloration in artiodactyls: systematic analyses of conventional hypotheses', *Behavioral Ecology* 14, 823–840.

Stuart, C. & Stuart, M., 2006, *Field Guide to Larger Mammals of Africa*, Third Edition., Struik Publishers, Cape Town.

Taylor, M.P., 2007, 'Xenoposeidon week, day 4: the question everyone is asking … how big was it?', *Sauropod Vertebra Picture of the Week*, viewed 27 May 2015, from http://svpow.com/2007/11/18/xenoposeidon-week-day-4-the-question-everyone-is-asking-how-big-was-it/.

Taylor, M.P. & Naish, D., 2007, 'An Unusual New Neosauropod Dinosaur from the Lower Cretaceous Hastings Beds Group of East Sussex, England', *Palaeontology* 50, 1547–1564.

Taylor, M.P. & Wedel, M.J., 2013a, 'The Effect of Intervertebral Cartilage on Neutral Posture and Range of Motion in the Necks of Sauropod Dinosaurs', *PLoS ONE* 8, e78214.

Taylor, M.P. & Wedel, M.J., 2013b, 'Why sauropods had long necks; and why giraffes have short necks', *PeerJ* 1, e36.

Thomas, O., 1901, 'On the five-horned giraffe obtained by Sir Harry Johnston near Mount Elgon', *Proceedings of the Zoological Society of London* 2, 474–483.

Thompson, D.W., 1917, *On growth and form*, Cambridge University Press, Cambridge, viewed 30 May 2013, from http://archive.org/details/ongrowthform1917thom.

Torzilli, P.A., Takebe, K., Burstein, A.H. & Heiple, K.G., 1981, 'Structural properties of immature canine bone.', *Journal of biomechanical engineering* 103, 232.

Torzilli, P.A., Takebe, K., Burstein, A.H., Zika, J.M. & Heiple, K.G., 1982, 'The material properties of immature bone.', *Journal of biomechanical engineering* 104, 12.

Trouessart, E., 1908, 'La nouvelle girafe du Muséum et les différentes variétés de l'espèce', *La Nature. Revue des sciences et de leurs applications aux arts et à l'industrie.* 36, 339–342.

Turner, H.N., 1847, 'Observations on the distinction between the cervical and dorsal vertebrae in the class Mammalia', *Proceedings of the Zoological Society of London* 15, 110–114.

Van Citters, R.L., Franklin, D.L., Vatner, S.F., Patrick, T. & Warren, J.V., 1969, 'Cerebral hemodynamics in the giraffe.', *Transactions of the Association of American Physicians* 82, 293.

Van Citters, R.L., Kemper, W.. & Franklin, D.., 1968, 'Blood flow and pressure in the giraffe carotid artery', *Comparative biochemistry and physiology* 24, 1035–1042.

Van der Geer, A., Dermitzakis, M. & De Vos, J., 2006, 'Relative growth of the metapodals in a juvenile island deer: Candiacervus (Mammalia, Cervidae) from the Pleistocene of Crete', *Hellenic J Geosci* 41, 119–125.

Van Schalkwyk, O.L., 2004, 'Bone density and calcium and phosphorous content of the giraffe (*Giraffa camelopardalis*) and African buffalo (*Syncerus caffer*) skeletons', MSc Dissertation, University of Pretoria, Pretoria, from http://upetd.up.ac.za/UPeTD.htm.

Van Schalkwyk, O.L., Skinner, J.D. & Mitchell, G., 2004, 'A comparison of the bone density and morphology of giraffe (*Giraffa camelopardalis*) and buffalo (*Syncerus caffer*) skeletons', *Journal of zoology* 264, 307–315.

Van Sittert, S.J., Skinner, J.D. & Mitchell, G., 2010, 'From fetus to adult - an allometric analysis of the giraffe vertebral column', *Journal of Experimental Zoology Part B Molecular and Developmental Evolution* 314B, 469–479.

Van Sittert, S.J., Skinner, J.D. & Mitchell, G., 2015, 'Scaling of the appendicular skeleton of the giraffe (*Giraffa camelopardalis*)', *Journal of Morphology* 276, 503–516.

Van Valkenburgh, B., 1990, 'Skeletal and dental predictors of body mass in carnivores', in J. Damuth & B. J. MacFadden (eds.) *Body size in mammalian paleobiology*, Cambridge University Press, Cambridge.

Warton, D.I., Wright, I.J., Falster, D.S. & Westoby, M., 2006, 'Bivariate line-fitting methods for allometry', *Biological reviews of the Cambridge Philosophical Society* 81, 259–291.

White, J.F. & Gould, S.J., 1965, 'Interpretation of the coefficient in the allometric equation', *American Naturalist*, 5–18.

Young, J.W., 2008, 'Ontogeny of Locomotion in Saimiri boliviensis and Callithrix jacchus: Implications for Primate Locomotor Ecology and Evolution', Ph.D. Thesis, Stony Brook University, Stony Brook, NY., viewed 26 January 2014, from http://dspace.sunyconnect.suny.edu/handle/1951/45380.

Young, J.W., Danczak, R., Russo, G.A. & Fellmann, C.D., 2014, 'Limb bone morphology, bone strength, and cursoriality in lagomorphs', *Journal of anatomy* 225, 403–418.

Zar, J.H., 2010, *Biostatistical Analysis*, 5th ed., Prentice Hall, New Jersey, USA.

Zar, J.H., 1968, 'Calculation and miscalculation of the allometric equation as a model in biological data', *Bioscience* 18, 1118–1120.

# Appendices

***Appendix 1 The allometric equations for the determination of caudal dorsoventral diameter, caudal lateral diameter and spinous process length (in mm) from body mass.***

| Vertebra | n† | Allometric equation † | r2 † | n ‡ | Allometric equation ‡ | r2 ‡ | N § | Allometric equation§¶ | r2§ |
|---|---|---|---|---|---|---|---|---|---|
| C2 | 39 | $9.07 \times M_b^{0.280\ (0.235\text{-}0.333)}$ | 0.73 | 39 | $7.37 \times M_b^{0.358\ (0.284\text{-}0.452)}$ | 0.5 | 33 | $4.98 \times M_b^{0.319\ (0.265\text{-}0.383)}$ | 0.75 |
| C3 | 39 | $9.55 \times M_b^{0.292\ (0.243\text{-}0.351)}$ | 0.69 | 39 | $9.76 \times M_b^{0.320\ (0.257\text{-}0.397)}$ | 0.57 | 38 | $3.65 \times M_b^{0.371\ (0.303\text{-}0.453)}$ | 0.64 |
| C4 | 39 | $12.50 \times M_b^{0.266\ (0.221\text{-}0.320)}$ | 0.69 | 39 | $11.78 \times M_b^{0.296\ (0.243\text{-}0.361)}$ | 0.64 | 38 | $4.68 \times M_b^{0.335\ (0.269\text{-}0.417)}$ | 0.58 |
| C5 | 39 | $14.35 \times M_b^{0.261\ (0.220\text{-}0.309)}$ | 0.73 | 39 | $12.48 \times M_b^{0.300\ (0.245\text{-}0.367)}$ | 0.62 | 38 | $2.55 \times M_b^{0.434\ (0.372\text{-}0.507)}$ | 0.79 |
| C6 | 39 | $14.32 \times M_b^{0.272\ (0.233\text{-}0.318)}$ | 0.78 | 39 | $15.38 \times M_b^{0.277\ (0.229\text{-}0.336)}$ | 0.67 | 37 | $1.40 \times M_b^{0.536\ (0.462\text{-}0.622)}$ | 0.81 |
| C7 | 39 | $13.96 \times M_b^{0.271\ (0.228\text{-}0.323)}$ | 0.73 | 39 | $15.12 \times M_b^{0.274\ (0.224\text{-}0.335)}$ | 0.63 | 38 | $1.16 \times M_b^{0.613\ (0.557\text{-}0.674)}$ | 0.92 |
| T1 | 37 | $12.30 \times M_b^{0.274\ (0.229\text{-}0.329)}$ | 0.72 | 37 | $14.15 \times M_b^{0.256\ (0.214\text{-}0.308)}$ | 0.72 | 36 | $3.38 \times M_b^{0.582\ (0.510\text{-}0.665)}$ | 0.85 |
| T2 | 35 | $10.97 \times M_b^{0.282\ (0.236\text{-}0.337)}$ | 0.75 | 35 | $12.57 \times M_b^{0.269\ (0.221\text{-}0.327)}$ | 0.69 | 34 | $4.68 \times M_b^{0.582\ (0.524\text{-}0.646)}$ | 0.92 |
| T3 | 31 | $9.48 \times M_b^{0.291\ (0.232\text{-}0.365)}$ | 0.64 | 31 | $11.6 \times M_b^{0.265\ (0.202\text{-}0.347)}$ | 0.47 | 30 | $7.03 \times M_b^{0.541\ (0.497\text{-}0.590)}$ | 0.95 |
| T4 | 30 | $8.16 \times M_b^{0.306\ (0.245\text{-}0.382)}$ | 0.67 | 30 | $12.18 \times M_b^{0.25\ (0.192\text{-}0.326)}$ | 0.52 | 29 | $8.51 \times M_b^{0.514\ (0.466\text{-}0.566)}$ | 0.94 |
| T5 | 31 | $8.12 \times M_b^{0.296\ (0.235\text{-}0.372)}$ | 0.63 | 31 | $9.63 \times M_b^{0.281\ (0.213\text{-}0.371)}$ | 0.46 | 30 | $10.25 \times M_b^{0.482\ (0.435\text{-}0.534)}$ | 0.93 |
| T6 | 31 | $7.06 \times M_b^{0.306\ (0.246\text{-}0.380)}$ | 0.67 | 31 | $8.22 \times M_b^{0.301\ (0.233\text{-}0.39)}$ | 0.53 | 30 | $10.76 \times M_b^{0.468\ (0.425\text{-}0.515)}$ | 0.94 |
| T7 | 31 | $8.46 \times M_b^{0.269\ (0.218\text{-}0.333)}$ | 0.68 | 31 | $9.63 \times M_b^{0.275\ (0.218\text{-}0.346)}$ | 0.63 | 30 | $9.46 \times M_b^{0.476\ (0.433\text{-}0.524)}$ | 0.94 |
| T8 | 30 | $8.04 \times M_b^{0.267\ (0.209\text{-}0.341)}$ | 0.59 | 30 | $8.21 \times M_b^{0.290\ (0.224\text{-}0.377)}$ | 0.54 | 30 | $9.15 \times M_b^{0.465\ (0.424\text{-}0.511)}$ | 0.94 |
| T9 | 30 | $7.33 \times M_b^{0.274\ (0.216\text{-}0.348)}$ | 0.61 | 30 | $8.88 \times M_b^{0.275\ (0.213\text{-}0.356)}$ | 0.55 | 30 | $8.28 \times M_b^{0.457\ (0.398\text{-}0.524)}$ | 0.87 |
| T10 | 30 | $8.60 \times M_b^{0.249\ (0.204\text{-}0.303)}$ | 0.74 | 30 | $9.91 \times M_b^{0.262\ (0.205\text{-}0.336)}$ | 0.58 | 30 | $7.89 \times M_b^{0.443\ (0.376\text{-}0.522)}$ | 0.82 |

| | | | | | | | | | |
|---|---|---|---|---|---|---|---|---|---|
| T11 | 29 | $8.58 \times M_b^{0.248\ (0.198\text{-}0.311)}$ | 0.67 | 29 | $12.52 \times M_b^{0.232\ (0.185\text{-}0.292)}$ | 0.66 | 29 | $4.00 \times M_b^{0.522\ (0.46\text{-}0.592)}$ | 0.9 |
| T12 | 30 | $8.97 \times M_b^{0.241\ (0.196\text{-}0.298)}$ | 0.7 | 30 | $10.55 \times M_b^{0.26\ (0.205\text{-}0.331)}$ | 0.61 | 30 | $4.49 \times M_b^{0.48\ (0.423\text{-}0.544)}$ | 0.89 |
| T13 | 30 | $8.63 \times M_b^{0.246\ (0.201\text{-}0.302)}$ | 0.72 | 30 | $11.51 \times M_b^{0.251\ (0.204\text{-}0.31)}$ | 0.7 | 30 | $4.26 \times M_b^{0.464\ (0.411\text{-}0.524)}$ | 0.9 |
| T14 | 30 | $10.34 \times M_b^{0.223\ (0.184\text{-}0.269)}$ | 0.76 | 30 | $11.18 \times M_b^{0.251\ (0.214\text{-}0.296)}$ | 0.82 | 31 | $4.24 \times M_b^{0.45\ (0.395\text{-}0.514)}$ | 0.88 |
| L1 | 30 | $9.31 \times M_b^{0.242\ (0.198\text{-}0.296)}$ | 0.73 | 30 | $10.35 \times M_b^{0.269\ (0.219\text{-}0.331)}$ | 0.72 | 30 | $3.97 \times M_b^{0.447\ (0.392\text{-}0.509)}$ | 0.89 |
| L2 | 30 | $7.93 \times M_b^{0.265\ (0.210\text{-}0.335)}$ | 0.63 | 30 | $9.03 \times M_b^{0.290\ (0.232\text{-}0.362)}$ | 0.67 | 30 | $3.54 \times M_b^{0.457\ (0.412\text{-}0.507)}$ | 0.93 |
| L3 | 27 | $10.7 \times M_b^{0.22\ (0.171\text{-}0.281)}$ | 0.63 | 27 | $11.98 \times M_b^{0.256\ (0.192\text{-}0.342)}$ | 0.5 | 27 | $2.49 \times M_b^{0.512\ (0.454\text{-}0.576)}$ | 0.92 |
| L4 | 25 | $9.36 \times M_b^{0.24\ (0.177\text{-}0.325)}$ | 0.48 | 25 | $13.78 \times M_b^{0.245\ (0.185\text{-}0.325)}$ | 0.56 | 24 | $2.39 \times M_b^{0.513\ (0.446\text{-}0.59)}$ | 0.9 |
| L5 | 17 | $7.85 \times M_b^{0.266\ (0.191\text{-}0.369)}$ | 0.63 | 17 | $8.41 \times M_b^{0.341\ (0.239\text{-}0.487)}$ | 0.56 | 17 | $4.28 \times M_b^{0.412\ (0.336\text{-}0.505)}$ | 0.86 |

*Note: † Vertebral body-caudal extremity, dorsoventral (height). ‡ Vertebral body-caudal extremity, transverse (width). § Spinous process. $M_b$= Body mass (kg). The brackets contain the upper and lower 95% confidence interval for the scaling exponent. In all cases the underlying regressions were significant (i.e. $p<0.05$).*

***Appendix 2 Fossil discoveries which have been assigned to Giraffa sivalensis***

| Named species | Fossil specimen | Museum no | Origin | References to specimen | Paper summary or highlights |
|---|---|---|---|---|---|
| ***G sivalensis*** | Cervical vertebra, complete, well preserved, holotype. 'Third' (Falconer & Cautley 1843) or 'Fifth' (Lydekker 1883) cervical. | | Siwalik hills, India | Cautley, 1838 | Dimensions of vertebra given - postulated to be Giraffid in origin. |
| ***G sivalensis*** | | | | Falconer & Cautley, 1843 | Detailed description of vertebra and assigned the name *Camelopardalis sivalensis*. Postulated that these animals were in length about a third shorter than modern giraffes. |
| ***G sivalensis*** | | | | Falconer 1868b, (Unpublished plate E, Fig. 1) | Third cervical vertebra of fossil giraffe, from the Siwalik hills. The elongated character of the vertebra shows that the animal had a columnar neck, and the fact that the transverse processes are provided with foramina for the vertebral arteries shows that it was not a camel. The complete synostosis of the upper and lower articulating surfaces, the strong relief of the ridges, and the depth of the muscular depressions, indicate that the animal was an adult, which had long attained its full size. |
| ***G sivalensis*** | | | | Lydekker, 1876 | Found that there was not much difference in the dimensions of *G. sivalensis* vertebra and modern giraffes, and that some of the diameter measurements were even larger. *G. sivalensis* had similar molar teeth as extant giraffes, but with a neck about one third shorter. |

| Named species | Fossil specimen | Museum no | Origin | References to specimen | Paper summary or highlights |
|---|---|---|---|---|---|
| ***G sivalensis*** | | | | Lydekker, 1883 | Lydekker corrected his previous postulates, saying that the extant giraffe used for comparison was immature and that comparisons were therefore invalid. Mentioned that the holotype was actually a 'fifth' cervical. |
| ***G sivalensis*** | | 39747 | | Lydekker 1885a | Described *G. sivalensis* as a very small individual. |
| ***G sivalensis*** | | B187 | | Lydekker 1885b | Mentioned a cast of the 'fifth' cervical vertebra located in the Indian Museum. |
| ***G sivalensis*** | Second or third dorsal vertebra | 60 | Perim Island (referring most probably to Piram Bet Island, Gulf of Khambat | Falconer, 1868 | Second or third dorsal vertebra of giraffe, concave and convex articular surfaces present. Apophyses wanting. |
| ***G sivalensis*** | | | | Lydekker, 1883 | Referred to plate e of Fauna Antiqua Sivalensis. |
| ***G sivalensis*** | Caudal fragment of "second" cervical vertebra | | Perim Island (referring most probably to Piram Bet Island, Gulf of Khambat | Falconer 1845 | Adult. Well marked longitudinal ridge along middle, corresponding to the 'third' cervical. Same 'lateral ridges' which are different to extant giraffes. Ventral curve similar to C3 dimensions given. |

| Named species | Fossil specimen | Museum no | Origin | References to specimen | Paper summary or highlights |
|---|---|---|---|---|---|
| ***G sivalensis*** | | | | Lydekker, 1883 | Lydekker called this specimen an imperfect fourth cervical vertebra. Also mentioned in the Palaeontological memoirs (Murchison, 1868b) p.391. May be the 'larger incomplete third cervical' from the Siwalik hills to which Lydekker referred (see below). |
| ***G sivalensis*** | | 39748 | | Falconer 1868b, plate E, Fig. 2) | Fragment of second cervical vertebra of *Giraffa (Camelopardalis) sivalensis*, from Perim Island. The right margin of the drawing shows the mesial longitudinal ridge under the side of the body, and the left margin is the ridge of the spinous process. The process pointing downwards on the left side is the inferior oblique process. The cup shaped articulating surface for the head of the third cervical vertebra is well seen. This specimen was in the collection of fossils brought from Perim Island by Captain Fulljames. Length of fragment, 4.9". Height of body posteriorly, 2.5". Greatest breadth posteriorly between remains of transverse processes, 3.1". Height of the spinal canal, 1.4". Height of the broken surface of the spine above inferior margin of body, 5.4". Vertical diameter of articulating cup, 2.1". Transverse diameter of articulating cup, 2.1" |
| ***G sivalensis*** | | | | Lydekker, 1883 | Referred to as the second specimen published in Falconer, 1845. |
| ***G sivalensis*** | | | | Lydekker 1885a | Posterior part of a much battered fourth (?) cervical vertebra, intermediate in size between specimen 39746 and 39747. From the Siwaliks of 'Perim Island in the Gulf of Cambay'. Cautley collection 1842. |

| Named species | Fossil specimen | Museum no | Origin | References to specimen | Paper summary or highlights |
|---|---|---|---|---|---|
| ***G sivalensis*** | Larger incomplete 'third' cervical | | Siwalik Hills, India | Lydekker, 1883 | Mentioned that this specimen had not been described yet by Messrs Falconer and Cautley. |
| ***G sivalensis*** | 'First' or 'third' cervical vertebra, imperfect | | Siwalik hills, India | Falconer 1868c, Unpublished plate E, Fig. 11 | Dimensions given. |
| ***G sivalensis*** | | | | Lydekker, 1883 | Seemingly as large as the corresponding bone of *G. camelopardalis*. Regarding the description of this specimen in the plates of the Fauna Antiqua Sivalensis (Murchison, 1868a), Lydekker mentioned that these measurements were probably erroneous. It is also noted that Falconer at this stage abandoned the distinction between *G. sivalensis* and *G. affinis.* |
| ***G sivalensis*** | | BM39746 | | Lydekker 1885a | Posterior moiety of the 'third' cervical vertebra of a full sized individual. Pliocene. Cautley collection 1842. |
| ***G sivalensis*** | Humerus, Right, two fragments | 43 | Perim Island (referring most probably to Piram Bet Island, Gulf of Khambat | Falconer 1868a | From Perim Island. Lower articulating surface perfect, upper broken off immediately below the head. Exact form to that of the giraffe, but little larger. |
| ***G sivalensis*** | | 39749 | Siwalik hills, India | Lydekker 1885a | Right humerus without proximal extremity of a small individual, thought to be from the Pliocene of the Siwaliks. |

| Named species | Fossil specimen | Museum no | Origin | References to specimen | Paper summary or highlights |
|---|---|---|---|---|---|
| ***G sivalensis*** | | BM 37749 | | Falconer 1868b (unpublished plate E) | |
| ***G sivalensis*** | | | | Lydekker, 1883 | |
| ***G sivalensis*** | | B363 | | Lydekker 1885b | Cast of the greater portion of the right humerus. Original is from 'Siwalik hills' and is figured in The Fauna Antiqua Sivalensis (Murchison, 1868a) (unpublished plate E, Fig. 3). British museum no 39749. |
| ***G sivalensis*** | Humerus, Left, proximal third | 17136 | Siwalik hills | Lydekker 1885a | Proximal third of left humerus, from the Pliocene of the Siwalik hills. |
| ***G sivalensis*** | Radius, Left, Upper portion | 690 | Siwalik | Falconer, 1868 | Bone much flattened, outer border considerable curve, abrupt expansion of the articulating head and sudden contraction of shaft. Nearly equal in dimensions to existing giraffe, but flattened. Greyish appearance due to sandstone matrix. |
| ***G sivalensis*** | | | | Lydekker, 1883 | |

| Named species | Fossil specimen | Museum no | Origin | References to specimen | Paper summary or highlights |
|---|---|---|---|---|---|
| ***G sivalensis*** | Radius and ulna, Left, Shaft only | 17130 | Siwalik | Lydekker 1885a | From the Pliocene. Figured in Murchison (1868a) (Unpublished Plate E, Fig. 4) |
| ***G sivalensis*** | | BM 17130 | | Murchison, 1868a (Unpublished plate E, Figs 4a and 4b) | Fragment of shaft of left radius and ulna<br>Length of fragment, 8.5 inch *(215.9 mm)*<br>Greatest diameter 3'' *(76.2 mm)*<br>Smaller diameter 2.1'' *(53.34 mm)*<br>Great diameter of ulna at upper extremity = 7'' *(177.8 mm)*<br>thickness of ulna at upper extremity = 5'' *(127 mm)* |
| ***G sivalensis*** | Radius and ulna, restored | | | Falconer & Murchison (1867) (Unpublished plate E, Figs 5a and 5b) | No other info given |
| ***G sivalensis*** | Metacarpus, L, lower end, with articulating surfaces | 52 | Perim Island (referring most probably to Piram Bet Island, Gulf of Khambat | Falconer, 1868 | Of the size of existing giraffe. |

| Named species | Fossil specimen | Museum no | Origin | References to specimen | Paper summary or highlights |
|---|---|---|---|---|---|
| ***G sivalensis*** | Metacarpus, fragment including upper end | BM39750 | | Murchison, 1868a (plate E, Fig. 6) | Metacarpal bone, Fragment including upper end.<br>Length of fragment 18.7'' *(474.98 mm)*<br>Transverse diameter of upper extremity = 3.7'' *(93.98 mm)*<br>Antero-posterior diameter of upper extremity = 2.3'' *(58.42 mm)*<br>Transverse diameter of centre shaft = 2.4'' *(60.96 mm)*<br>Antero posterior diameter of centre shaft = 1.8'' *(45.72 mm)* |
| ***G sivalensis*** | | | Siwalik Hills | Lydekker 1885a | Proximal half of left metacarpus, from the Pliocene. Presented 1842. |
| ***G sivalensis*** | Metacarpus, fragment of shaft | BM17129 | | Murchison, 1868a, (Unpublished plate E, Fig. 8) | Fragment of shaft of metacarpal bone<br>Length of fragment 6.8'' *(172.72mm).* |
| ***G sivalensis*** | | | | Lydekker 1885a | From the Pliocene of the Siwaliks. |

| Named species | Fossil specimen | Museum no | Origin | References to specimen | Paper summary or highlights |
|---|---|---|---|---|---|
| ***G sivalensis*** | Metacarpus, fragment of shaft near lower end | BM17131 | | Murchison, 1868a (Unpublished plate E, Fig. 9) | Fragment of shaft of metacarpal bone, near lower end<br>Length of fragment = 3.9'' *(99.06mm),*<br>Transverse diameter of shaft at lower extremity = 2.8'' *(71.12mm),*<br>Anterioposterior diameter of shaft at upper extremity = 1.5'' *(38.1mm)* |
| ***G sivalensis*** | | | | Lydekker 1885a | |
| ***G sivalensis*** | Metacarpus, entire bone restored | | | Murchison, 1868a (Unpublished plate E, Figs 10a and 10b) | No other info provided. |
| ***G sivalensis*** | Metacarpus, fragment of shaft | 39751 | Siwalik hills | Lydekker 1885a | From the Pliocene. Cautley collection, presented in 1842. |
| ***G sivalensis*** | | | | Murchison, 1868a (Unpublished plate E Fig.7) | |
| ***G sivalensis*** | Phalangeals, proximal, two | 17131a | Siwalik hills | Lydekker 1885a | These bones are almost indistinguishable from the corresponding bones of *G. camelopardalis*. Cautley collection 1842. |

| Named species | Fossil specimen | Museum no | Origin | References to specimen | Paper summary or highlights |
|---|---|---|---|---|---|
| ***G sivalensis*** | Phalangeal, proximal. | 17131b | Siwalik hills | Lydekker 1885a | Closely resembling phalangeals marked 17131a, from the Pliocene. Cautley collection 1842. |
| ***G sivalensis*** | Proximal anterior phalangeal | B362 | Punjab | Lydekker 1885b | |
| ***G sivalensis*** | Proximal posterior phalangeal | B368 | Punjab | Lydekker 1885b | |
| ***G sivalensis*** | Distal portion of tarsus metatarsus (imperfect inferiorly). And the first phalangeal | B186 | Punjab | Lydekker 1885b | |
| ***G sivalensis*** | All *G. affinis* fossils | | | Lydekker, 1876 | Lydekker concluded that *G. sivalensis* and *G. affinis* are actually the same species, based on the characteristics of the fossil teeth on which *G. affinis* was founded. |
| ***G sivalensis*** | Upper extremity of right metacarpus | 405 | Siwalik | Falconer, 1868 | Probably giraffe. Siwalik hills near Nahun (Nahan) |

| Named species | Fossil specimen | Museum no | Origin | References to specimen | Paper summary or highlights |
|---|---|---|---|---|---|
| ***G sivalensis*** | Portion of L Maxilla with 3 molars | | | Lydekker, 1878, 1883 | The majority of these specimens do not differ in character from the corresponding teeth of the extant giraffe. Lydekker postulates that only *G. sivalensis* true upper molars are represent in this *Giraffa* molar catalogue. Nevertheless, he is open to the idea that there might have been a second or third species, based on the lower molars and premolars. All these specimens were assigned to *G. sivalensis* and 'some other species'. |
| ***G sivalensis*** | Portion of R Maxilla containing the two last premolars (same individual as above?) | | | | Lydekker (1883) expressed greater certainty that this and above specimens are part of the same animal. |
| ***G sivalensis*** | Two detached penultimate molars | | | | |
| ***G sivalensis*** | Two last right upper molars | | | | |
| ***G sivalensis*** | Two penultimate upper molars | | | | |
| ***G sivalensis*** | Last right upper premolar | | | | |

| Named species | Fossil specimen | Museum no | Origin | References to specimen | Paper summary or highlights |
|---|---|---|---|---|---|
| ***G sivalensis*** | Portion of R Maxilla containing the two last milk molars and first permanent molar | | | | |
| ***G sivalensis*** | Fragment of left ramus of mandible containing the two last permanent molars | | | | |
| ***G sivalensis*** | Another fragment of the right mandible containing the last tooth | | | | |
| ***G sivalensis*** | First right mandibular molar | | | | |
| ***G sivalensis*** | Last right mandibular premolar (large) | | | | |
| ***G sivalensis*** | Penultimate left mandibular premolar | | | | |

| Named species | Fossil specimen | Museum no | Origin | References to specimen | Paper summary or highlights |
|---|---|---|---|---|---|
| ***G sivalensis*** | Fragment of right ramus of mandible containing two anterior premolars | | | | |
| ***G sivalensis*** | Last left mandibular molar | | | | Last molar only is too small for *G. sivalensis*, and probably belonged to another species. |
| ***G sivalensis*** | Two last maxillary molars | | | | These teeth had been collected, figured and described on plate 16 of Murchison, 1868b |
| ***G sivalensis*** | Penultimate maxillary premolar | | | | |
| ***G sivalensis*** | Three mandibular molars | | | | |
| ***G sivalensis*** | Last mandibular premolar | | | | |

| Named species | Fossil specimen | Museum no | Origin | References to specimen | Paper summary or highlights |
|---|---|---|---|---|---|
| ***G sivalensis*** | Right ramus of the mandible with last premolar and the first and second true molars of a Siwalik giraffe | | | Lydekker, 1883 | |
| ***G sivalensis*** | | | | | In summary, up until Lydekker's (1883) publication: six mandibular specimens of Siwalik giraffes, of which five contained the last lower true molars and two contained both the second and first true molars and last premolar. Specimens are B179 (pl 16 Fig. 6), B179A; B178, Falconer's specimens, B173 (pl 16 Fig. 5), living giraffe, B1 (vol. 1 pl. 7 Fig. 14 and 16) |
| ***G sivalensis*** | Lower jaw, right, three milk molars in site and first molar germ in jaw. Two posterior premolars. | 560 | Siwalik hills | Falconer, 1868 | There is netted rugosity of enamel – Therefore *Giraffa* and not Sivatherium or Bramatherium. (*Note however that Lydekker (1885a) proposed that a rugose enamel is a characteristic of the Giraffidae (which included the Sivatheres).* |
| ***G sivalensis*** | | | | Lydekker, 1883 | Lower jaws of a 'ruminant'. |
| ***G sivalensis*** | Lower jaw, left, three milk molars | 561 | Siwalik hills | Falconer, 1868 | Enamel surface also shows rugose netting, but not clear enough to be confident. |
| ***G sivalensis*** | | | | Lydekker, 1883 | Two lower jaws of 'a ruminant'. |

| Named species | Fossil specimen | Museum no | Origin | References to specimen | Paper summary or highlights |
|---|---|---|---|---|---|
| ***G sivalensis*** | Part of lower jaw | | | Lydekker, 1876 | |
| ***G sivalensis*** | Molars | s560 & s561 | | Falconer, 1868 | |
| ***G sivalensis*** | | | | Lydekker, 1876 | These teeth are actually from a *Bos spp.* |
| ***G sivalensis*** | Portions of the associated right and left maxillae, showing last 4 teeth | B184 | Asnot, Punjab | Lydekker 1885b | Figured in Lydekker (1883) in plate xvi: "Collected by Mr Theobald in the Siwaliks of the Punjab". |
| ***G sivalensis*** | Part of the maxilla with mm (milk molar?) 3, 4 and molar 1. | B177 | Potwar district, Punjab | | Collected by Mr Theobald |
| ***G sivalensis*** | Part of the right maxilla with m2, m 3 | B180 | Potwar district, Punjab | | Collected by Mr Theobald. |

| Named species | Fossil specimen | Museum no | Origin | References to specimen | Paper summary or highlights |
|---|---|---|---|---|---|
| ***G sivalensis*** | Three detached maxillary true molars | B181 | Punjab | | Collected by Mr Theobald. |
| ***G sivalensis*** | Two detached maxillary premolars | B182 | Punjab | | Collected by Mr Theobald. |
| ***G sivalensis*** | Casts of the last maxillary and mandibular true molars | B183 | Siwalik hills | | Originals are figured in Falconer & Cautley (1843) plate 2 Figs 4, 5 and in Murchison (1868b) pl. 16 Fig. 6 and 7. Originals in the British museum as 39756 and 39755 |
| ***G sivalensis*** | Third left mandibular molar (?) | B346 | ? | | |
| ***G sivalensis*** | Upper molar | B406 | Punjab | | |
| ***G sivalensis*** | Part of right ramus of mandible | B173 | Niki, Punjab | | Figured in Lydekker (1883) plate 16 Fig. 5. |

| Named species | Fossil specimen | Museum no | Origin | References to specimen | Paper summary or highlights |
|---|---|---|---|---|---|
| ***G sivalensis*** | Part of the right ramus of the mandible | B174 | Padri | | Figured in Lydekker (1883) plate 7 Fig. 14. |
| ***G sivalensis*** | Part of the left ramus of the mandible, with m2 and m3 | B178 | Potwar district, Punjab | | |
| ***G sivalensis*** | Three specimens of the last mandibular true molars | B179 | Potwar district, Punjab | | One of these is of very small size, and is figured in the Lydekker (1883) plate 16 Fig. 6. The author does not rule out the probability that this specimen really belonged to Palaeomeryx. |
| ***G sivalensis*** | last left mandibular premolar | B185 | Asnot, Punjab | | |
| ***G sivalensis*** | Cast of the last left mandibular premolar | B185a | Siwalik hills | | Figured in Falconer & Cautley (1843) plate 2 Fig. 6 and in Murchison (1868b) Plate 16 Fig. 8, 9. |
| ***G sivalensis*** | The last right mandibular milk molar | B175 | Asnot, Punjab | | Figured in Lydekker (1883) plate 16 Fig. 8. |

| Named species | Fossil specimen | Museum no | Origin | References to specimen | Paper summary or highlights |
|---|---|---|---|---|---|
| **Originally ascribed to *G. affinis* however, was later synonymised with *G sivalensis*** | Fragment of left maxilla including two rear molars. The 'back part of the maxillary, beyond the teeth, is attached'. | | Siwalik Hills. Described as a 'soft fossil' having been embedded in clay. | Falconer & Cautley, 1843 | Figured in Plate 2 fig. 3a and 3b of Falconer and Cautley (1843). Belonged to fully-grown individual. Specimen agrees almost exactly to that of an adult female giraffe. Dimensions:<br>• Joint length of two back molars, maxilla =2.5 inches.<br>• Greatest with of last molar = 1.4 inches.<br>• Greatest with of penultimate molar = 1.45 inches. |
| **Originally ascribed to *G. affinis* however, was later synonymised with *G sivalensis*** | | 39756 a | Siwalik Hills | Lydekker 1885a | From the Pliocene. Left maxilla containing m2 and m3. Figured in Falconer & Cautley (1843) (above) and in Murchison (1868b) plate 16 Fig. 5. Cautley collection |
| **Originally ascribed to *G. affinis* however, was later synonymised with *G sivalensis*** | Rear molar of right maxilla | | Siwalik Hills. Described as a 'soft fossil' having been embedded in clay. | Falconer & Cautley, 1843 | Same form as left side (of 39756a?), but more worn - different individual? Figured in Plate 2 Fig 4 of Falconer & Cautley (1843). 'The agreement extends down to the small cone of enamel at the base of the hollow between the barrels on the inside' Dimensions:<br>• Length = 1.2 inch.<br>• Width = 1.4 inch. |
| **Originally ascribed to *G. affinis* however, was later synonymised with *G sivalensis*** | | 39756 | Siwalik Hills | Lydekker 1885a | 'Third right upper true molar'. From the Pliocene of the Siwalik Hills. Figured in Falconer and Cautley, (1843) (above) and in Falconer and Murchison (1868b) vol 1 plate 16 Fig 6. Cautley collection. |
| **Originally ascribed to *G. affinis* however, was later synonymised with *G sivalensis*** | | | | Murchison, 1868b | Described as in Plate 16 fig 6 as 'last upper molar, right side, one half of natural size'. |

| Named species | Fossil specimen | Museum no | Origin | References to specimen | Paper summary or highlights |
|---|---|---|---|---|---|
| **Originally ascribed to *G. affinis* however, was later synonymised with *G sivalensis*** | Fragment of left mandible containing the last molar | | Siwalik Hills. Described as a 'soft fossil' having been embedded in clay. | Falconer & Cautley, 1843 | Same form and proportions of an extant female giraffe specimen observed by Falconer and Cautley (1843). Figured in plate 2 Fig 5a and 5b of Falconer and Cautley (1843). Dimensions of tooth:<br>• Length = 1.7 inch.<br>• Greatest width = 1.0 inch. |
| **Originally ascribed to *G. affinis* however, was later synonymised with *G sivalensis*** | | 39755 | Siwalik Hills | Lydekker 1885a | Described as a 'third left lower true molar, in an early condition of wear'. From the Pliocene epoch. No mention is made of the 'fragment of the left lower jaw' noted by Falconer & Cautley (1843). |
| **Originally ascribed to *G. affinis* however, was later synonymised with *G sivalensis*** | | | | Murchison, 1868b | Volume 1 plate 16 figure 7. Described as last lower molar, left side. |
| **Originally ascribed to *G. affinis* however, was later synonymised with *G sivalensis*** | Last premolar ('false molar') of the left mandible, detached. | | Siwalik Hills. Described as a 'soft fossil' having been embedded in clay. | Falconer & Cautley, 1843 | Agrees closely with corresponding tooth in an extant female giraffe specimen observed by Falconer & Cautley. The specific tooth is noted to be 'thicker' in proportion to its length in giraffes compared to other ruminants. Figured in Plate 2 Fig 6 of Falconer & Cautley (1843). Dimensions:<br>• Length = 1.0 inches.<br>• Width = 0.9 inches. |
| **Originally ascribed to *G. affinis* however, was later synonymised with *G sivalensis*** | | 39757 | Siwalik Hills | Lydekker 1885a | Lydekker (1885a) assigned this specimen as a 'right lower premolar', as opposed to Falconer and Cautley (1843) who considered it a 'left' premolar. From the Pliocene epoch. |

| Named species | Fossil specimen | Museum no | Origin | References to specimen | Paper summary or highlights |
|---|---|---|---|---|---|
| **Originally ascribed to *G. affinis* however, was later synonymised with *G sivalensis*** | | | | Murchison, 1868b | Volume 1 plate 16 Fig 8. |
| **Originally ascribed to *G. affinis* however, was later synonymised with *G sivalensis*** | Penultimate premolar of right maxilla | | Siwalik Hills. Described as a 'soft fossil' having been embedded in clay. | Falconer & Cautley, 1843 | Described as a 'false molar'. Except for 'three tubercles at the inside of the base' the tooth has the same size and form as the corresponding tooth in an extant female giraffe specimen observed by Falconer and Cautley. Figured in Plate 2 Fig 7 of Falconer and Cautley (1843), described here as: 'second false molar; upper jaw, right side'. Dimensions given as:<br>• Length = 1.0 inch.<br>• Breadth = 1.12 inch. |
| **Originally ascribed to *G. affinis* however, was later synonymised with *G sivalensis*** | | | | Murchison, 1868b | Plate 16, Fig 9. |
| **Originally ascribed to *G. affinis* however, was later synonymised with *G sivalensis*** | First false molar of right maxilla | | | Falconer and Cautley, 1843 | Not figured in the referring text. Dimensions not given. |
| **Originally ascribed to *G. affinis* however, was later synonymised with *G sivalensis*** | | | | Lydekker, 1876 | Stated that based on erroneous teeth allocation by Falconer, there was probably not a *G. affinis* species. Appears to have been founded by mistake. |

UNIVERSITEIT VAN PRETORIA
UNIVERSITY OF PRETORIA
YUNIBESITHI YA PRETORIA

# Animal Ethics Committee

| | |
|---|---|
| PROJECT TITLE | **Ontogenetic allometry / growth patterns of the giraffe skeleton** |
| PROJECT NUMBER | **V043-08** |
| RESEARCHER/PRINCIPAL INVESTIGATOR | **Dr. SJ van Sittert** |

| | |
|---|---|
| STUDENT NUMBER (where applicable) | **22042629** |
| DISSERTATION/THESIS SUBMITTED FOR | **PhD** |

| | | |
|---|---|---|
| ANIMAL SPECIES | ***Giraffa camelopardalis*** | |
| NUMBER OF ANIMALS | **Depends on availability** | |
| Approval period to use animals for research/testing purposes | | **2008–December 2013** |
| SUPERVISOR | **Prof. G Mitchell** | |

*KINDLY NOTE:*

Should there be a change in the species or number of animal/s required, or the experimental procedure/s - please submit an amendment form to the UP Animal Ethics Committee for approval before commencing with the experiment

| | |
|---|---|
| **APPROVED** | Date **18 March 2013** |
| CHAIRMAN: UP Animal Ethics Committee | Signature |